

Piecing the puzzle together

A MULTIDISCIPLINARY EXPLORATION INTO
THE CONSEQUENCES OF RADIOTHERAPY
IN PATIENTS WITH BRAIN METASTASES



UMC Utrecht BrainCenter

Eva Elisabeth van Ghinsven

Piecing the puzzle together

A multidisciplinary exploration into the
consequences of radiotherapy in patients with
brain metastases

Eva Elisabeth van Grinsven

Cover description

Exploring the mountainous landscape of the consequences of brain radiotherapy, together.

Piecing the puzzle together

PhD Thesis, Utrecht University, The Netherlands

Provided by thesis specialist Ridderprint, ridderprint.nl

Printing: Ridderprint

Layout and design: Annemarie van Amerongen, persoonlijkproefschrift.nl

Artwork: Evelien Jagtman & Mariska Offerman

© evelienjagtman.com

ISBN: 978-94-6483-766-7

DOI: 10.33540/1053

© Eva van Grinsven, 2023. All rights reserved. No part of this thesis may be reproduced, stored or transmitted in any way or by any means without the prior permission from the author. The copyright of papers that have been published or have been accepted for publication has been transferred to the respective journals.

Part of the research described in this thesis was financially supported by the Koningin Wilhelmina Fonds voor de Nederlandse Kankerbestrijding (KWF, grant number 11110).

Piecing the puzzle together

A multidisciplinary exploration into the
consequences of radiotherapy in patients with brain
metastases

Samen de puzzelstukjes leggen

Een multidisciplinaire zoektocht naar de gevolgen van radiotherapie bij
patiënten met hersenmetastasen

(met een samenvatting in het Nederlands)

Proefschrift

ter verkrijging van de graad van doctor aan de
Universiteit Utrecht
op gezag van de
rector magnificus, prof. dr. H.R.B.M. Kummeling,
ingevolge het besluit van het college voor promoties
in het openbaar te verdedigen op

donderdag 11 april 2024 des middags te 4.15 uur

door

Eva Elisabeth van Grinsven

geboren op 8 mei 1994
te Enkhuizen

Promotoren:

Prof. dr. M.J.E. Van Zandvoort

Dr. ir. M.E.P. Philippens

Copromotoren:

Prof. dr. J.J.C. Verhoeff

Dr. A. Bhogal

Beoordelingscommissie:

Prof. dr. G.J. Biessels (voorzitter)

Dr. S. Deprez

Prof. dr. J. Hendrikse

Prof. dr. S.B. Schagen

Prof. dr. H.M. Verkooijen

TABLE OF CONTENTS

Chapter 1	General introduction and thesis outline	7
Part I: Neurocognitive functioning in patients with brain metastases		
Chapter 2	The impact of stereotactic or whole brain radiotherapy on neurocognitive functioning in adult patients with brain metastases – A systematic review & meta-analysis	25
Chapter 3	Different profiles of neurocognitive functioning in patients with brain metastases prior to brain radiotherapy	57
Chapter 4	Individualized trajectories in post-radiotherapy neurocognitive functioning of patients with brain metastases	79
Part II: Using imaging techniques to understand neurocognitive functioning		
Chapter 5	The impact of etiology in lesion-symptom mapping – A direct comparison between tumor and stroke	105
Chapter 6	Hemodynamic imaging parameters in brain metastases patients – Agreement between multi-delay ASL and hypercapnic BOLD	145
Chapter 7	Evaluating physiological MRI biomarkers and cognitive performance in patients with brain metastases after stereotactic radiosurgery - a preliminary analysis and case-report	171
Summary and Discussion		
Chapter 8	Summary	203
Chapter 9	Discussion	211
Chapter 10	Summary in Dutch (Nederlandstalige samenvatting)	235
Appendices	List of publications	246
	Educational portfolio	250
	Dankwoord (Acknowledgements)	252
	About the author	262





1

General Introduction

Brain metastases (BMs) are a significant neurological consequence of cancer that occurs when cancer cells from a solid tumor elsewhere in the body migrate to the brain. The most common primary tumors that metastasize to the brain are lung, breast, and melanoma.¹ BMs affect a substantial proportion of adult patients with cancer with estimates ranging from 10 to 30%.²⁻⁴ Despite improvements in medical treatments, the median overall survival of patients remains limited, ranging from 3 to 47 months.^{5,6} Various factors influence survival, including age, Karnofsky performance status (KPS), extent of extracranial disease, number of BMs, and histological and molecular features of the primary tumor.⁵⁻⁹ Currently, treatment options for BMs include surgery, chemotherapy, immunotherapy, and radiotherapy, typically given in a combination. The population of patients with BMs is expected to grow in the coming years due to advancements in medical treatments improving survival of cancer patients and enhanced imaging techniques allowing for earlier detection of BMs.¹⁰⁻¹² Consequently, patients with BMs are now living longer with cancer. In this context, patient-centered treatment is increasingly focused on not only extending the life span, but especially on maintaining or even improving quality of life (QoL).

RADIOTHERAPY FOR BRAIN METASTASES

Radiotherapy is a cornerstone of medical treatment for BMs. It is a non-invasive technique in which ionizing radiation is delivered to the affected areas. By damaging the DNA within cancerous cells, radiation therapy can lead to senescence and ultimately cell death. The two prominent strategies for radiotherapy in BMs are stereotactic radiosurgery (SRS) and whole-brain radiotherapy (WBRT; **Figure 1**). Traditionally, WBRT was the standard treatment for BMs. Stereotactic treatment can be delivered using either a gamma knife or a conventional linear accelerator. Both apply a steep dose gradient by allowing overdosage up to 130 percent inside the tumor. Due to advances in these techniques, SRS has now been established as an optimal option for patients with one up to ten BMs, with a total volume of ≤ 30 cc.¹³⁻¹⁵ With SRS, the radiation dose to the target is divided over multiple arc beams delivered from different angles to accumulate a high-precision localized dose in the BMs while reducing the dose to the surrounding healthy brain tissue. The prescribed physical dose to the BMs usually varies between 15 and 24 Gray (Gy), dependent on the size of the lesion. WBRT is typically advised to patients with more than ten BMs to ensure coverage of all brain tissue and to sterilize not-yet visible BMs.^{16,17} WBRT is either delivered in five fractions of 4 Gy or ten fractions of 3 Gy: a much lower biological dose to prevent immediate whole brain damage. To decrease radiation

dose to organs at risk, like the hippocampus, and thereby reduce the risk of cognitive decline, hippocampal avoidance (HA-WBRT) is preferred over WBRT when possible.

A challenge in radiotherapy treatment, as in any treatment, is achieving the optimal balance between maximizing anti-tumor effects and minimizing adverse side-effects. This balance is constrained by the underlying physics and limitations of the radiotherapy technique employed. To ensure adequate tumor coverage with appropriate safety margins, two treatment volumes are defined for SRS: 1) gross tumor volume (GTV) and 2) planning treatment volume (PTV). The GTV represents the total volume of the BMS as seen on imaging (**Figure 2**). The GTV is typically identified based on the hyperintense region in a T1-weighted MRI scans after gadolinium injection. The PTV includes the volume of the GTV plus a 1-3 mm margin, depending on the radiotherapy equipment.¹⁸ This so-called error margin is necessary to achieve the desired therapeutic effect while taking into account patient set-up variation and the motion within the radiation positioning mask. Even with high dose fall-off at tumor borders, such as in SRS, some dose gradient will fall outside the tumor, possibly leading to radiation-induced brain injury in the surrounding healthy brain tissue.

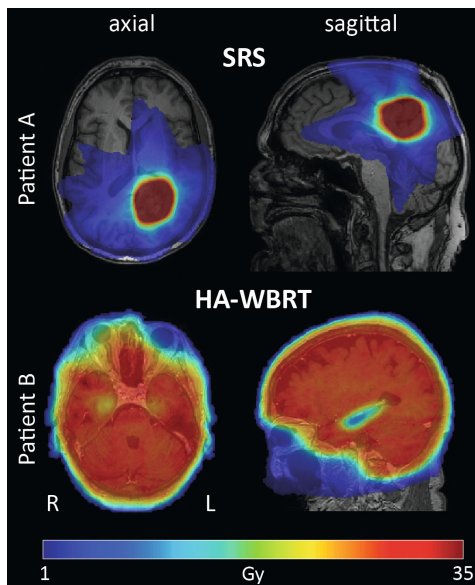


Figure 1. Biological dose (EQD2) distribution in stereotactic radiosurgery (SRS) and hippocampal avoidance whole-brain radiotherapy (HA-WBRT) shown on a T1-weighted MRI in axial and sagittal view (radiological orientation). Patient A was treated with 1 fraction of 15 Gy and had a single BMS in the left parietal lobe. Patient B was treated with 5 fractions of 4 Gy and had multiple BMS throughout the brain.

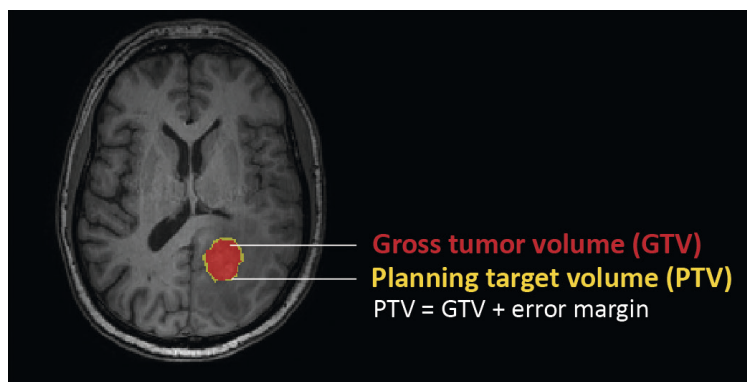


Figure 2. Treatment volumes for SRS overlaid on a T1-weighted MRI.

COGNITIVE PERFORMANCE

In the context of prolonged life expectancy, potential treatment-related cognitive impairment has become an increasingly important topic. Especially since nearly 50% of patients with BMs already have cognitive deficits prior to radiotherapy.^{19–21} The acute radiation-induced injury that occurs in the first weeks is typically transient.^{22,23} However, delayed brain toxicity has been shown following radiation, leading to irreversible cognitive deterioration.^{22–24} Cognitive difficulties can have far-reaching impacts on various aspects of life such as work, relationships, and leisure activities.²⁵ In fact, the impact of cognitive impairment on an individuals' QoL has now been recognized as second only to survival in clinical trials.²⁶ Importantly, not only severe cognitive impairment (e.g. dementia) can impact QoL, but mild cognitive changes are also perceived as a significant burden to both patients and caregivers.²⁵ This highlights the importance of not only assessing objective cognitive functioning, but also subjective cognitive performance. Regrettably, a significant drawback of previous research is the reliance on cognitive screenings tests like the Mini-Mental Status Examination (MMSE), which cannot accurately detect these subtle, but burdensome, cognitive impairments. Additionally, studies have predominantly used group-level analyses and/or employed a focused, and thereby restricted, range of cognitive tests, thus limiting our understanding of the extent of cognitive difficulties and their full impact on individuals' daily life.

EFFECT OF BRAIN METASTASES ON THE BRAIN

As briefly mentioned previously, approximately half of the patients with BMs already have cognitive problems before radiotherapy due to negative effects of

the presence of BMs themselves, and due to previous systemic treatments.²⁷⁻³⁰ The extent and type of preradiotherapy cognitive impairment can vary depending on the lesion location. Lesion studies have demonstrated the topological organization of the brain, with different areas of the brain responsible for different cognitive processes such as memory, attention, language, and executive function.³¹ Most of the research has focused on patients with ischemic stroke. This population has become the gold standard in this field due to the acute and focal nature of the lesions that are well-defined on imaging. Moreover, as stroke is a relatively common medical condition³², this allows for the required large patient samples in lesion-symptom mapping studies. The reliance on this population, however, raises concerns regarding the applicability of these findings to other populations, such as those with BMs. Behavioral consequences of a lesion may vary as a result of how the brain is affected by the lesion.^{31,33} For example, lesion distributions differ between etiologies, with certain brain areas more likely to be damaged than others, thereby affecting the spatial accuracy of lesion-symptom analyses. BMs mostly affect the cortex and subcortical white matter areas corresponding to watershed areas of large arteries³⁴, while a stroke most often occurs in subcortical areas in the territory of the middle cerebral artery.³⁵⁻³⁷ Moreover, the mechanism of injury could vary; where an ischemic stroke leads to cell death due to a lack of oxygen and nutrients from the blood, BMs form tumor cells within the brain.

MRI BIOMARKERS FOR RADIOTHERAPY-EFFECTS

Although advancements have been made to limit the radiation dose to surrounding brain tissue, it is currently impossible to entirely avoid it due to the physical limitations of the photon radiotherapy technique. Consequently, cranial irradiation can potentially lead to encephalopathy, a complex phenomenon which is influenced by both the dose and time since exposure to radiation.³⁸ The dose- and time-dependency of this process is attributed to the differential radiosensitivity of the various components of the brain tissue and the blood vessels. Cranial irradiation can lead to various sequelae, including changes to the neuronal architecture, suppression of neurogenesis, neuroinflammation and autoimmune responses.^{23,38,39} Considering this, the underlying cause of radiation-induced cognitive decline is most likely multifaceted. In this thesis I mostly focused on the vascular component of the radiation effect. Animal experiments have revealed widespread vascular changes following cranial radiotherapy, including reduced vessel density and destabilization of the vascular endothelium.^{22,40-43} Microvascular damage resulting in reduced blood perfusion has already been reported in brain areas exposed to low doses of 10-15 Gy.^{44,45} Moreover, age-related vascular changes have been linked to cognitive

performance in healthy individuals.⁴⁶ Thereby, parallels have been drawn between the pathogenesis underlying vascular cognitive impairment (e.g. vascular dementia) and radiation-induced brain injury.^{47,48}

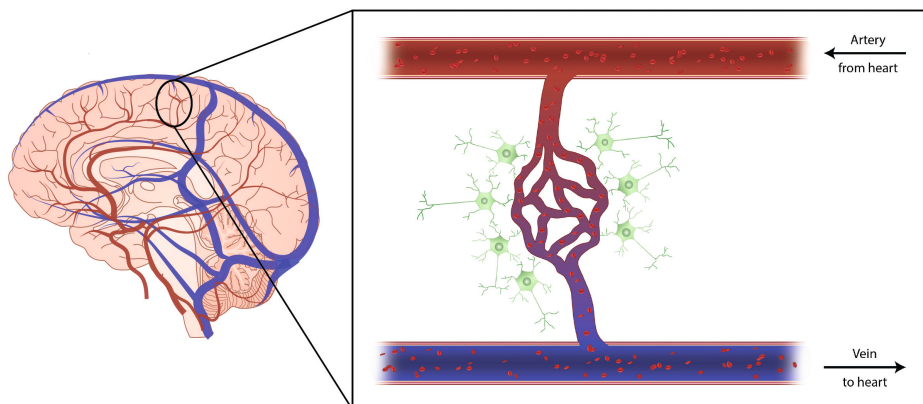


Figure 3. Simplified illustration of brain metabolism. Oxygenated red blood cells travel from the heart through the arteries (red), to the arterioles in the brain where they deliver oxygen and nutrients to the neurons (green cells), before the deoxygenated blood returns to the heart through the veins (blue) for renewed circulation.

The brain has an intricate network of blood vessels in order to meet its high oxygen and glucose demands (**Figure 3**). MRI is a non-invasive method that can be used to detect subtle vascular changes throughout the brain. Cerebral blood flow (CBF) indicates the amount of blood flowing to the brain through the arteries and can be measured using arterial spin labelling (ASL) MRI.⁴⁹⁻⁵¹ To guarantee healthy functioning, CBF to the brain must remain relatively constant in response to changes in perfusion pressure or other hemodynamic events. Cerebrovascular reactivity (CVR) plays an important role in maintaining optimal CBF by regulating the diameter of cerebral vessels in response to changes in blood pressure and CO_2 levels.⁵²⁻⁵⁴ For example, increased CO_2 , a metabolic waste product, acts as a signal for heightened brain activity. In response, arterial blood vessels in these active regions dilate, facilitating increased blood flow to help remove excess CO_2 and deliver oxygen-rich blood to this tissue (**Figure 4**). This dynamic control, facilitated by smooth-muscle cells, also serves as a significant compensatory mechanism when cerebral hemodynamics are compromised by disease (e.g. narrowing of blood vessels). The CVR response can be assessed and spatially mapped using Blood Oxygenation Level-Dependent (BOLD) MRI in combination with controlled hypercapnic stimuli, like inhalation of CO_2 . When the brain's metabolic demand is not (fully) met by blood flow compensation through CVR, the Oxygen Extraction Fraction (OEF) serves as an

additional regulatory mechanism. OEF reflects the amount of oxygen extracted from the brain's arterial supply and is closely linked to oxygen usage and metabolism in the brain. Using innovative imaging techniques, OEF can be mapped by combining Quantitative Susceptibility Mapping (QSM) with quantitative BOLD (qBOLD). The cerebral metabolic rate of oxygen ($CMRO_2$), is calculated by multiplying CBF and OEF, and thus reflects the balance between the two. As the brain heavily relies on oxygen-dependent glucose metabolism for energy production, $CMRO_2$ serves as a key indicator for energy homeostasis and brain health.⁵⁵ To illustrate, in a healthy brain CBF typically increases more than the oxygen metabolism, leading to a decrease in OEF and consequently a relatively steady $CMRO_2$.⁵⁶

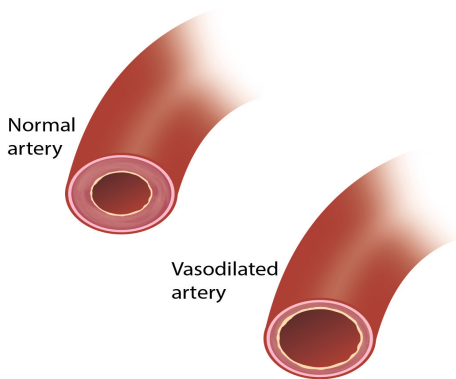


Figure 4. Illustration of vasodilation in arterial blood vessels, for example in response to increased CO_2 levels in the blood.

These different parameters thus reflect various aspects of the brain's vascular reserve capacity, working together to ensure a continuous and sufficient supply of oxygen and nutrients.^{57,58} Disruptions to this hemodynamic balance, such as those caused by tumor growth or cranial irradiation, could result in altered blood vessel structure and function. While previous animal studies have shown radiation-induced vascular damage in surrounding healthy brain tissue, research on hemodynamic changes after cranial irradiation in humans is scarce. However, the field is continuously evolving and advances in imaging techniques now allow non-invasive MRI measurements of cerebral hemodynamics. Hypothetically, in humans vascular damage following cranial irradiation could impact the ability of blood vessels to constrict and dilate (i.e. CVR), reducing the capacity to modulate CBF to meet tissue needs. When blood flow compensation through CVR is insufficient,

the brain could subsequently increase the OEF to maintain sufficient CMRO₂. At the same time, previous studies have demonstrated extensive structural brain changes after radiotherapy, including cortical thinning⁵⁹, grey and white matter volume loss^{60,61}, and changes in white matter microstructure⁶²⁻⁶⁸. Following this research, it could be hypothesized that these structural changes lead to a decreased number of neurons and synapses and reduced neural communication, causing decreased brain metabolism and subsequently lower OEF. Interestingly, such a differential effect on OEF has already been illustrated in previous dementia research, whereby the effect on OEF varied depending on the type of dementia.⁶⁹ In patients with vascular cognitive impairment, OEF was increased as a consequence of the vascular damage, while OEF was reduced in patient with Alzheimer's Dementia most likely due to reduced brain metabolism. This underscores the importance of investigating these hemodynamic brain measures in parallel, as it provides insights into the underlying mechanism of the changes. However, these hemodynamic MRI measures have not yet been assessed in patients with BMs undergoing radiotherapy. As a result, it is still unclear whether and how these measures are influenced by either the presence of the BMs themselves or the subsequent cranial radiotherapy.

THESIS OUTLINE

In the pursuit of providing optimal care that considers both survival and quality of life, an integrative and multidisciplinary approach is not only essential in clinical practice, but also in research. To ensure patient-centered care, including treatment-shared decision making, thorough research is crucial to pinpoint the frequently occurring side-effects, accurately predict their occurrence in individual patients, and explore various avenues to proactively prevent them. This thesis aims to set the first steps by using a multidisciplinary approach to study radiation-induced brain injury. By simultaneously exploring neurocognitive functioning and the potential value of several potential MRI-biomarkers, this research can advance our understanding and pave the way for improved patient outcomes in the field of BMs radiotherapy.

Part I: Neurocognitive functioning in patients with brain metastases

The first part of this thesis will investigate neurocognitive functioning in patients with BMs both before and after radiotherapy. The aim is to provide comprehensive individual and group-level results that can deepen our understanding of this impact. By addressing these issues in detail, the hope is to offer insights that can subsequently be used in treatment-shared decision making in this population.

To provide a thorough overview of the current knowledge in the field, **Chapter 2** summarizes and compares the available literature on the effect of either SRS or WBRT on neurocognitive performance in patients with BMs. Since SRS is increasingly being favored over WBRT in current practice, this review aimed to gain insight on whether current evidence regarding cognitive side-effects substantiate contemporary shifts in treatment preference. Moreover, this chapter offers insights into potential gaps in knowledge, which can serve as a foundation for future studies.

Chapter 3 offers a detailed description of the cognitive performance, both subjectively and objectively, of patients with BMs before they begin radiotherapy. Examination of clusters of cognitive deficits enabled a deeper understanding of how different aspects of cognitive function may relate to one another. This chapter provides a thorough understanding of the patients who will be the topic of investigation in this thesis and their presentation to the radiotherapy clinic. It thereby provides important context within which the post-radiotherapy cognitive changes should be evaluated.

Chapter 4 evaluates the short- and long-term changes in both subjective and objective cognitive performance in patients with BMs after radiotherapy. It provides insight into the multifaceted nature of changes and highlights opportunities for interventions (e.g. patient-tailored psycho-education, cognitive strategy training) in this specific group of patients. Individual trajectories of cognitive function are assessed to gain a clearer understanding of the cognitive impact of radiotherapy on the individuals comprising this patient group.

Part II: Using imaging techniques to understand neurocognitive functioning

To aid in understanding of the pathophysiology underlying the cognitive difficulties described in part I, the second part of this thesis focuses on the use of various imaging techniques. The aim is two-fold. First, I determined the generalizability of insights from other imaging studies to different patient populations. Next, the use of physiological MRI biomarkers within the BMs population was assessed.

As researching lesion-behavior patterns in large populations of patients with BMs is challenging due to their limited life expectancy and diversity of lesion locations, we sought to gain insights from other diseases affecting the central nervous system, like ischemic stroke. In **Chapter 5** we examined whether damage to the same brain regions cause by either a stroke or primary brain tumor resulted in similar or different sets of cognitive outcomes. This aids in understanding the generalizability of findings from one patient population to others.

It is crucial to not only capture, but also comprehend the nature of post-radiotherapy changes on physiological imaging. **Chapter 6** describes how imaging parameters derived from BOLD imaging and ASL measures were compared in patients with BMs before undergoing cranial radiotherapy. The study aimed to improve our understanding of the relationship between these two imaging techniques and their respective value in the BMs population.

Building on the findings from the previous chapters, **Chapter 7** provides preliminary evidence for the added value of several physiological MRI biomarkers in detecting changes after radiotherapy. Through a case-report the potential of these MRI biomarkers and their link to cognitive performance are described.

A summary of the main findings and implications of all chapters within this doctoral thesis are discussed in **Chapter 8** and **9**, respectively.

REFERENCES

1. Cagney DN, Martin AM, Catalano PJ, et al. Incidence and prognosis of patients with brain metastases at diagnosis of systemic malignancy: a population-based study. *Neuro Oncol* 2017; 19: 1511–1521.
2. Barnholtz-Sloan JS, Yu C, Sloan AE, et al. A nomogram for individualized estimation of survival among patients with brain metastasis. *Neuro Oncol* 2012; 14: 910–918.
3. Barnholtz-Sloan JS, Sloan AE, Davis FG, et al. Incidence proportions of brain metastases in patients diagnosed (1973 to 2001) in the Metropolitan Detroit Cancer Surveillance System. *Journal of Clinical Oncology* 2004; 22: 2865–2872.
4. Achrol AS, Rennert RC, Anders C, et al. Brain metastases. *Nat Rev Dis Primers*; 5. Epub ahead of print 2019. DOI: 10.1038/s41572-018-0055-y.
5. Gaspar L, Scott C, Rotman M, et al. Recursive partitioning analysis (RPA) of prognostic factors in three Radiation Therapy Oncology Group (RTOG) brain metastases trials. *Int J Radiat Oncol Biol Phys* 1997; 37: 745–751.
6. Sperduto PW, Chao ST, Sneed PK, et al. Diagnosis-specific prognostic factors, indexes, and treatment outcomes for patients with newly diagnosed brain metastases: a multi-institutional analysis of 4,259 patients. *Int J Radiat Oncol Biol Phys* 2010; 77: 655–661.
7. Oken MM, Creech RH, Tormey DC, et al. Toxicity and response criteria of the Eastern Cooperative Oncology Group. *American Journal of Clinical Oncology: Cancer Clinical Trials* 1982; 5: 649–656.
8. Sperduto PW, Kased N, Roberge D, et al. Summary report on the graded prognostic assessment: An accurate and facile diagnosis-specific tool to estimate survival for patients with brain metastases. *Journal of Clinical Oncology* 2012; 30: 419–425.
9. Gilbride L, Siker M, Bovi J, et al. Current predictive indices and nomograms to enable personalization of radiation therapy for patients with secondary malignant neoplasms of the central nervous system: A review. *Neurosurgery* 2018; 82: 595–603.
10. Nieder C, Spanne O, Mehta MP, et al. Presentation, patterns of care, and survival in patients with brain metastases: What has changed in the last 20 years? *Cancer* 2011; 117: 2505–2512.
11. Lanier CM, Hughes R, Ahmed T, et al. Immunotherapy is associated with improved survival and decreased neurologic death after SRS for brain metastases from lung and melanoma primaries. *Neurooncol Pract* 2019; 6: 402–409.
12. Nayak L, Lee EQ, Wen PY. Epidemiology of brain metastases. *Curr Oncol Rep* 2012; 14: 48–54.
13. Pinkham MB, Whitfield GA, Brada M. New developments in intracranial stereotactic radiotherapy for metastases. *Clin Oncol* 2015; 27: 316–323.
14. Yamamoto M, Serizawa T, Shuto T, et al. Stereotactic radiosurgery for patients with multiple brain metastases (JLGK0901): A multi-institutional prospective observational study. *Lancet Oncol* 2014; 15: 387–395.
15. Soliman H, Das S, Larson DA, et al. Stereotactic radiosurgery (SRS) in the modern management of patients with brain metastases. *Oncotarget* 2016; 7: 12318–12330.

16. Khuntia D, Brown P, Li J, et al. Whole-brain radiotherapy in the management of brain metastasis. *Journal of Clinical Oncology* 2006; 24: 1295–1304.
17. Mehta MP. The controversy surrounding the use of whole-brain radiotherapy in brain metastases patients. *Neuro Oncol* 2015; 17: 919–923.
18. Wilke L, Andratschke N, Blanck O, et al. ICRU report 91 on prescribing, recording, and reporting of stereotactic treatments with small photon beams. *Strahlentherapie und Onkologie* 2019; 195: 193–198.
19. Grosshans DR, Meyers CA, Allen PK, et al. Neurocognitive function in patients with small cell lung cancer: effect of prophylactic cranial irradiation. *Cancer* 2008; 112: 589–595.
20. Vardy J, Dhillon HM, Pond GR, et al. Cognitive function and fatigue after diagnosis of colorectal cancer. *Annals of Oncology* 2014; 25: 2404–2412.
21. Mitchell T, Turton P. 'Chemobrain': Concentration and memory effects in people receiving chemotherapy - a descriptive phenomenological study. *Eur J Cancer Care (Engl)* 2011; 20: 539–548.
22. Makale MT, McDonald CR, Hattangadi-Gluth JA, et al. Mechanisms of radiotherapy-associated cognitive disability in patients with brain tumours. *Nat Rev Neurol* 2017; 13: 52–64.
23. Greene-Schloesser D, Robbins ME, Peiffer AM, et al. Radiation-induced brain injury: A review. *Front Oncol* 2012; 2 JUL: 1–18.
24. Duffau H. Why brain radiation therapy should take account of the individual structural and functional connectivity: Toward an irradiation "à la carte". *Crit Rev Oncol Hematol*; 154. Epub ahead of print 2020. DOI: 10.1016/j.critrevonc.2020.103073.
25. Mitchell AJ, Kemp S, Benito-León J, et al. The influence of cognitive impairment on health-related quality of life in neurological disease. *Acta Neuropsychiatr* 2010; 22: 2–13.
26. Frost MH, Sloan JA. Quality of life measurements: A soft outcome - Or is it? *American Journal of Managed Care* 2002; 8: 574–579.
27. Hodgson KD, Hutchinson AD, Wilson CJ, et al. A meta-analysis of the effects of chemotherapy on cognition in patients with cancer. *Cancer Treat Rev* 2013; 39: 297–304.
28. Joly F, Castel H, Tron L, et al. Potential effect of immunotherapy agents on cognitive function in cancer patients. *J Natl Cancer Inst* 2020; 112: 123–127.
29. Wefel JS, Schagen SB. Chemotherapy-related cognitive dysfunction. *Curr Neurol Neurosci Rep* 2012; 12: 267–275.
30. Schagen SB, Tsvetkov AS, Compter A, et al. Cognitive adverse effects of chemotherapy and immunotherapy: are interventions within reach? *Nat Rev Neurol* 2022; 18: 173–185.
31. Karnath HO, Sperber C, Rorden C. Mapping human brain lesions and their functional consequences. *Neuroimage* 2018; 165: 180–189.
32. Vaartjes I, Reitsma JB, De Bruin A, et al. Nationwide incidence of first stroke and TIA in the Netherlands. *Eur J Neurol* 2008; 15: 1315–1323.
33. Karnath HO, Berger MF, Küker W, et al. The anatomy of spatial neglect based on voxelwise statistical analysis: A study of 140 patients. *Cerebral Cortex* 2004; 14: 1164–1172.
34. Akeret K, Staartjes VE, Vasella F, et al. Distinct topographic-anatomical patterns in primary and secondary brain tumors and their therapeutic potential. *J Neurooncol* 2020; 149: 73–85.

35. Sperber C, Karnath HO. Topography of acute stroke in a sample of 439 right brain damaged patients. *Neuroimage Clin* 2016; 10: 124–128.
36. Corbetta M, Ramsey L, Callejas A, et al. Common behavioral clusters and subcortical anatomy in stroke. *Neuron* 2015; 85: 927–941.
37. Phan TG, Donnan GA, Wright PM, et al. A digital map of middle cerebral artery infarcts associated with middle cerebral artery trunk and branch occlusion. *Stroke* 2005; 36: 986–991.
38. Gorbunov N V., Kiang JG. Brain Damage and Patterns of Neurovascular Disorder after Ionizing Irradiation. Complications in Radiotherapy and Radiation Combined Injury. *Radiat Res* 2021; 196: 1–16.
39. Katsura M, Sato J, Akahane M, et al. Recognizing radiation-induced changes in the central nervous system: Where to look and what to look for. *Radiographics* 2021; 41: 224–248.
40. Brown WR, Blair RM, Moody DM, et al. Capillary loss precedes the cognitive impairment induced by fractionated whole-brain irradiation: A potential rat model of vascular dementia. *J Neurol Sci* 2007; 257: 67–71.
41. Price RE, Langford LA, Jackson EF, et al. Radiation-induced morphologic changes in the rhesus monkey (*Macaca mulatta*) brain. *J Med Primatol* 2001; 30: 81–87.
42. Peña LA, Fuks Z, Kolesnick RN. Radiation-induced apoptosis of endothelial cells in the murine central nervous system: Protection by fibroblast growth factor and sphingomyelinase deficiency. *Cancer Res* 2000; 60: 321–327.
43. Li YQ, Chen P, Haimovitz-Friedman A, et al. Endothelial apoptosis initiates acute blood-brain barrier disruption after ionizing radiation. *Cancer Res* 2003; 63: 5950–5956.
44. Park HJ, Griffin RJ, Hui S, et al. Radiation-induced vascular damage in tumors: Implications of vascular damage in ablative hypofractionated radiotherapy (SBRT and SRS). *Radiat Res* 2012; 177: 311–327.
45. Hou C, Gong G, Wang L, et al. The Study of Cerebral Blood Flow Variations during Brain Metastases Radiotherapy. *Oncol Res Treat* 2022; 45: 130–137.
46. Peng SL, Chen X, Li Y, et al. Age-related changes in cerebrovascular reactivity and their relationship to cognition: A four-year longitudinal study. *Neuroimage* 2018; 174: 257–262.
47. Román GC. Vascular dementia revisited: Diagnosis, pathogenesis, treatment, and prevention. *Medical Clinics of North America* 2002; 86: 477–499.
48. Jellinger KA. Pathology and pathogenesis of vascular cognitive impairment—a critical update. *Front Aging Neurosci* 2013; 5: 1–19.
49. Alsop DC, Detre JA, Golay X, et al. Recommended Implementation of Arterial Spin Labeled Perfusion MRI for Clinical Applications: A consensus of the ISMRM Perfusion Study Group and the European Consortium for ASL in Dementia. *Magn Reson Med* 2015; 73: 102–116.
50. Detre JA, Rao H, Wang DJJ, et al. Applications of arterial spin labeled MRI in the brain. *Journal of Magnetic Resonance Imaging* 2012; 35: 1026–1037.
51. Telischak NA, Detre JA, Zaharchuk G. Arterial spin labeling MRI: Clinical applications in the brain. *Journal of Magnetic Resonance Imaging* 2015; 41: 1165–1180.
52. Markus HS. Cerebral perfusion and stroke. *J Neurol Neurosurg Psychiatry* 2004; 75: 353–361.
53. Sebök M, Niftrik CHB Van, Wegener S, et al. Agreement of Novel Hemodynamic Imaging Parameters for the Acute and Chronic Stages of Ischemic Stroke: A Matched-pair Cohort Study. *Neurosurg Focus* 2021; 51: 1–8.

54. Václavů L, Meynart BN, Mutsaerts HJMM, et al. Hemodynamic provocation with acetazolamide shows impaired cerebrovascular reserve in adults with sickle cell disease. *Haematologica* 2019; 104: 690–699.
55. Rodgers ZB, Detre JA, Wehrli FW. MRI-based methods for quantification of the cerebral metabolic rate of oxygen. *Journal of Cerebral Blood Flow and Metabolism* 2016; 36: 1165–1185.
56. Angleys H, Jespersen SN, Østergaard L. The effects of capillary transit time heterogeneity on the BOLD signal. *Hum Brain Mapp* 2018; 39: 2329–2352.
57. Fantini S, Sassaroli A, Tgavalekos KT, et al. Cerebral blood flow and autoregulation: current measurement techniques and prospects for noninvasive optical methods. *Neurophotonics* 2016; 3: 031411.
58. Murkin JM. Cerebral autoregulation: The role of CO₂ in metabolic homeostasis. *Semin Cardiothorac Vasc Anesth* 2007; 11: 269–273.
59. Nagtegaal SHJ, David S, Snijders TJ, et al. Effect of radiation therapy on cerebral cortical thickness in glioma patients: Treatment-induced thinning of the healthy cortex. *Neuro-Oncology Advances*; 2. Epub ahead of print 2020. DOI: 10.1093/naajnl/vdaa060.
60. Nagtegaal SHJ, David S, Philippens MEP, et al. Dose-dependent volume loss in subcortical deep grey matter structures after cranial radiotherapy. *Clin Transl Radiat Oncol* 2021; 26: 35–41.
61. Nagtegaal SHJ, David S, van Grinsven EE, et al. Morphological changes after cranial fractionated photon radiotherapy: Localized loss of white matter and grey matter volume with increasing dose. *Clin Transl Radiat Oncol* 2021; 31: 14–20.
62. Nazem-Zadeh MR, Chapman CH, Lawrence TL, et al. Radiation therapy effects on white matter fiber tracts of the limbic circuit. *Med Phys* 2012; 39: 5603–5613.
63. Zhu T, Chapman CH, Tsien C, et al. Effect of the Maximum Dose on White Matter Fiber Bundles Using Longitudinal Diffusion Tensor Imaging. *Int J Radiat Oncol Biol Phys* 2016; 96: 696–705.
64. Connor M, Karunamuni R, McDonald C, et al. Regional susceptibility to dose-dependent white matter damage after brain radiotherapy. *Radiotherapy and Oncology* 2017; 123: 209–217.
65. Tibbs MD, Huynh-Le MP, Karunamuni R, et al. Microstructural Injury to Left-Sided Perisylvian White Matter Predicts Language Decline After Brain Radiation Therapy. *Int J Radiat Oncol Biol Phys* 2020; 108: 1218–1228.
66. Chapman CH, Zhu T, Nazem-Zadeh M, et al. Diffusion tensor imaging predicts cognitive function change following partial brain radiotherapy for low-grade and benign tumors. *Radiotherapy and Oncology* 2016; 120: 234–240.
67. Chapman CH, Nagesh V, Sundgren PC, et al. Diffusion tensor imaging of normal-appearing white matter as biomarker for radiation-induced late delayed cognitive decline. *Int J Radiat Oncol Biol Phys* 2012; 82: 2033–2040.
68. Huynh-Le MP, Tibbs MD, Karunamuni R, et al. Microstructural Injury to Corpus Callosum and Intrahemispheric White Matter Tracts Correlate With Attention and Processing Speed Decline After Brain Radiation. *Int J Radiat Oncol Biol Phys* 2021; 110: 337–347.
69. Jiang D, Lin Z, Liu P, et al. Brain Oxygen Extraction Is Differentially Altered by Alzheimer’s and Vascular Diseases. *Journal of Magnetic Resonance Imaging* 2020; 52: 1829–1837.





Part I

Neurocognitive functioning in patients
with brain metastases



2

The impact of stereotactic or whole brain radiotherapy on neurocognitive functioning in adult patients with brain metastases – A systematic review & meta-analysis

Eva E. van Grinsven, Steven H. J. Nagtegaal, Joost J. C. Verhoeff,
& Martine J. E. van Zandvoort

Oncology Research and Treatment (2021)

ABSTRACT

Background & Objectives

Radiotherapy is standard treatment for patients with brain metastases (BMs), although it may lead to radiation-induced cognitive impairment. This review explores the impact of whole brain radiotherapy (WBRT) or stereotactic radiosurgery (SRS) on cognition.

Methods

The PRISMA-guidelines were used to identify manuscripts on PubMed and EmBase reporting on objective assessment of cognition before, and at least once after radiotherapy, in adult patients with non-resected BMs.

Results

Of the 867 records screened, twenty manuscripts (14 unique studies) were included. WBRT lead to decline in cognitive performance, which stabilized or returned to baseline in patients with survival of at least 9-15 months. For SRS, a decline in cognitive performance was sometimes observed shortly after treatment, but the majority of patients returned to or remained at baseline until a year after treatment.

Conclusions

These findings suggest that after WBRT patients can experience deterioration over a longer period of time. The cognitive side-effects of SRS are transient. Therefore this review advices to choose SRS, as this will result in lowest risks for cognitive adverse side-effects, irrespective of predicted survival. In an already cognitively vulnerable patient population with limited survival, this information can be used in communicating risks and aid in making educated decisions.

INTRODUCTION

Local and systemic treatment for extracranial cancers is improving, leading to longer life expectancy. New challenges arise due to increased survival rates including the development of brain metastases (BMs). BMs occur in at least 10% of patients diagnosed with cancer and this incidence continues to rise.^{1,2} BMs are difficult to treat systemically because chemotherapeutic agents barely pass the blood-brain barrier. Median overall survival, despite systemic and focal treatment, is limited spanning months to several years, depending on factors such as lesion number, Karnofsky performance status and the primary cancer as reflected in GPA calculators.^{3,4} Treatment (shared) decisions in this vulnerable patient population are tailored towards gaining the best disease control while maintaining adequate quality of life (QoL) during the remaining life span.

Treatment for BMs consists of different (palliative) options, including surgery, chemotherapy, immunotherapy and radiotherapy.⁵ One of the concerns with radiotherapy treatment is how to achieve the optimal balance between maximizing anti-tumor effects and minimizing possible adverse side-effects. The two prominent strategies for radiotherapy in BMs are whole-brain radiotherapy (WBRT) and stereotactic radiosurgery (SRS). WBRT is typically advised for patients with more than three BMs since treatment covers all brain tissue and has the advantage of sterilizing not-yet visible BMs.^{6,7} The main disadvantage is that WBRT can lead to radiation-induced tissue damage across the entire brain. SRS has mainly been applied in selected patients with one to three BMs and a favorable prognosis.⁸ During SRS, high precision localized irradiation is delivered to the BMs in a single fraction to maximize local tumor control and minimize the dose to the surrounding, healthy brain tissue.

Patients with BMs compose a vulnerable patient group, since a high percentage of patients already experience cognitive impairment before starting radiotherapy, as a direct result of BMs but also due to previous cancer treatments.⁹⁻¹¹ Deteriorated cognitive functions have been related to impaired financial, work and social activities, which are all important in maintaining good QoL and autonomy.^{12,13} Although literature on the cognitive changes after radiotherapy has been reviewed both for WBRT and SRS separately^{14,15}, to date no publication exists comparing WBRT with SRS in relation to the cognitive outcome after treatment. Since SRS is increasingly being favored over WBRT in current practice¹⁶, we performed a systematic review on changes in cognitive functioning provoked by either WBRT or SRS in adult patients

with non-resected BMs to gain insight on whether current evidence regarding cognitive side-effects substantiate contemporary shifts in treatment preference.

METHODS

Search Strategy

The Preferred Reporting Items for Systematic Reviews and Meta-Analyses (PRISMA) guidelines were used in conducting and reporting this systematic review.¹⁷ We reviewed all published manuscripts on the neurocognitive effects of WBRT or SRS in adult patients with BMs from 1-1-1950 until 4-1-2021. The search strategy combined terms for BMs, radiotherapy and cognition, and was developed for PubMed and adapted for Embase. The complete search strings can be found in the **Supplementary Materials**. Additionally, reference lists were manually screened for potentially relevant studies. Manuscripts were screened by two researchers (EEvG & SHJN) and disagreement was resolved through consensus meetings. The screening of the studies was facilitated by Covidence systematic review software (Veritas Health Innovation, Melbourne, Australia). Reasons for exclusion were documented for each paper.

Eligibility

The search was confined to manuscripts in English and Dutch. Studies were selected in which objective neurocognitive assessment was performed at baseline (defined as any time point between presentation of the BMs and start of radiotherapy), and at least once after radiotherapy, in adult patients with BMs. Only objective cognitive measurements were included since self-reports may be biased due to impairments caused by the BMs and (previous) cancer treatments.¹⁸ Moreover, subjective cognitive complaints do not represent underlying cognitive deficits per se and may be more indicative of psychological distress than actual cognitive impairment.^{19,20} Studies solely utilizing short neurocognitive-screening tools, such as the Mini-Mental Status Examination (MMSE), were excluded since these tests lack the sensitivity to detect subtle changes in cognitive functioning expected to be present after radiotherapy.²¹⁻²³ Furthermore, all papers including patients with resected BMs were excluded since co-acting cortical tissue damage adjacent to the resection site can influence cognitive performance. Studies investigating the influence of treatments concurrent to radiotherapy (e.g. memantine) that did not report on a radiotherapy-only control group were also excluded. Case reports, reviews, commentaries, editorials and protocols were excluded. If multiple papers reported on the same dataset, the results were combined and reviewed as one cohort.

Data extraction and analysis

The follow-up time points were converted to units of 'months after radiotherapy'. To aid comparability across studies and following the classification used in previous studies, time points were clustered: *short-term follow-up* 1 to 4 months after radiotherapy, *mid-term follow-up* 5 to 8 months after radiotherapy, and *long-term follow-up* 9 to 15 months after radiotherapy. Baseline measurements always refer to the assessment before start of radiotherapy treatment. Additionally, neuropsychological tests were attributed to cognitive constructs in a data-driven classification, based on the subdivision as reported in the majority of the included studies (**Supplementary Materials**). Data was collected from text, tables and figures from the manuscripts and then tabulated. Missing data points were excluded from analyses and changes in sample size due to attrition were considered. For meta-analysis of the incidence of cognitive decline compared to baseline performance, we used the inverse variance method in a DerSimonian-Laird random effects model. For individual studies Clopper-Pearson confidence intervals were calculated. Heterogeneity between studies was assessed using Cochran's Q test and the I² statistic. Statistical analyses were performed with R 3.5.1 open-source software with the 'meta' package (<http://www.R-project.org>).

Data quality

A critical appraisal of the included studies was performed to assess data quality as reported in the manuscripts, for which a checklist consisting of 7 criteria was constructed (shown in **Table 1**). One point was awarded if the criterion was met and zero points if not, or if it was unclear based on the available information. A maximum score of 7 points could be obtained. A score between 5 and 7 indicates good to high quality, 3 and 4 medium quality and scores below 2 indicate low quality.

RESULTS

Study inclusion

The initial search yielded 867 unique manuscripts. After applying the in- and exclusion criteria, 20 manuscripts reporting on 14 original datasets were included in this review (**Figure 1**). The majority of these studies were rated a *good to high quality* (**Table 2**). The one study rated as low quality was excluded from further analysis.²⁴ Study and baseline patient characteristics and the main conclusions of the selected papers are shown in **Table 3** and **Table 4** respectively. Patient numbers varied considerably across studies with a median sample size of 81 (range: 20-208) and 35 (range: 7-111) at baseline for the WBRT and SRS studies, respectively. In total, 751 WBRT patients were included and 300 SRS patients. Since data on the incidence

of cognitive decline was absent in some manuscripts, the meta-analysis could only be performed for those studies that reported on this data.

Table 1. Criteria for assessing the quality of the data of the manuscripts for the review, including reasons for assessing these criteria.

Criteria	Reason
Inclusion of >20 patients at baseline	(avoid type II errors for baseline data)
≥50% of patients available for first follow-up measurements	(avoid type II errors for follow-up data)
Neurocognitive performance scores corrected to norms for age, sex and education when appropriate	(bias by demographical variables)
Definition of change in cognitive performance was provided	(bias by definition of change)
Cognitive performance at follow-up time points were adjusted for baseline performance	(bias by differences in baseline performance)
Use of parallel versions of neuropsychological tests for retesting procedures was stated in the manuscript	(bias by learning effects due to repeated administration)
Diversity of neurocognitive assessment, assessed by fulfilling (1/2 point each): ≥3 different neuropsychological tests used AND ≥3 cognitive constructs assessed with test battery	(quality of cognitive testing procedures)

Baseline cognitive performance

Data on baseline cognitive performance before WBRT was solely explicitly reported for the Mehta et al. study ($N = 208$).¹⁸ The other included studies reported relative scores to an unreported baseline. Before starting WBRT 91% of the patients displayed cognitive impairment (Z -score ≤ 1.5) on ≥ 1 neuropsychological test and 42% on ≥ 4 neuropsychological tests. Fine motor coordination was impaired in 63-65%, learning and memory (L&M) in 21-60%, executive function (EF) in 44% and verbal fluency in 33%. Lower baseline cognitive performance correlated with higher total BMs volume at baseline, but not with number of BMs.^{18,25} On the contrary, in another study neither the volume of BMs nor volume of white matter injury correlated with L&M performance before radiotherapy in a subset of patients.^{26,27} Patients with a KPS of ≥ 80 and patients ≤ 65 years performed better at baseline on subtests of L&M.²⁸

Data on the incidence of baseline cognitive impairment before SRS was explicitly reported for the pilot-study by Chang et al. ($N = 15$) and by Habets et al. ($N = 77$).^{29,30} Pre-radiotherapy 53-67% of patients had cognitive impairment (Z-score ≤ 1.5 SD) on ≥ 1 neuropsychological test. At baseline, EF was impaired in 47% of the patients, fine motor coordination in 40%, L&M in 31%, visual memory and visuoconstruction in 22%, information processing speed in 10% and verbal fluency in 7%. Before SRS the mean z-scores of both the Chang et al. ($N = 30$) and the Brown et al. cohort ($N = 111$) were impaired.^{31,32} Worst group performance was observed on tasks for EF and information processing speed. Patients with a baseline BMs volume of >3 cc performed worse on attention than those with smaller lesion volumes.²⁹ Similarly, Onodera et al. reported higher total lesion volume, but not number of BMs at baseline corresponded with worse cognitive performance, while Habets et al. reported no significant association with BMs volume.^{25,30}

Post-radiotherapy cognitive performance

At short-term follow-up (1-4 months) the majority of the WBRT studies ($N = 455$ patients) found consistent declines in cognitive performance on most cognitive constructs.^{18,25,26,28,33-40} Overall, between 19-37% of the patients deteriorated regarding L&M performance. Gondi et al. found that patients treated with hippocampal avoidance WBRT (HA-WBRT) had significantly less mean relative decline in L&M performance compared to the patients of Mehta et al. who received conventional WBRT (7% vs 30%, respectively).^{18,26} The change in L&M performance was correlated to pre-treatment BMs volume, age and the volume of white matter injuries.²⁷ Other impaired cognitive constructs in the WBRT studies were EF (29-38%), fine motor coordination (31%), information processing speed (28%) and verbal fluency (7-32%). Even though Westover et al. observed a decline in 17% of their patients ($N = 18$) regarding L&M performance, on the group level no significant changes from baseline were found for the other cognitive constructs.⁴¹ Nevertheless, large variations in mean relative change were found for all cognitive constructs (L&M, information processing speed, EF, verbal fluency).

At mid-term follow-up (5-8 months) the results were more variable. The 29 patients who received HA-WBRT had a mere relative decline of 0-3% on multiple tests for L&M at mid-term follow-up compared to baseline.^{26,33} Similarly, patients who survived more than 6 months after HA-WBRT with simultaneous integrated boost recovered to baseline scores regarding L&M performance.⁴² On the contrary, performance on most cognitive tasks declined in at least 114 patients who received conventional WBRT.^{35,39,40} L&M performance was most often affected, with 53% of the patients showing decline.³⁵ Moreover, the percentage of patients with declined performance

increased from 19% at short-term to 35% at mid-term follow-up.³⁹ Although group performance declined compared to both baseline and short-term follow-up when considering all 17 patients in the Onodera et al. cohort, improvements were observed in a subgroup of patients with a baseline BMs volume of <4.0 cc and in BMs patients surviving at least 12 months.²⁵ A similar trend was reported by Saito et al., where the subgroup surviving at least 8 months ($N = 19$) had stable L&M performance over time.²⁸ Thus, most patients further decreased in cognitive performance at mid-term follow-up, but in a subgroup of patients stable or improved cognitive performance was observed over time.

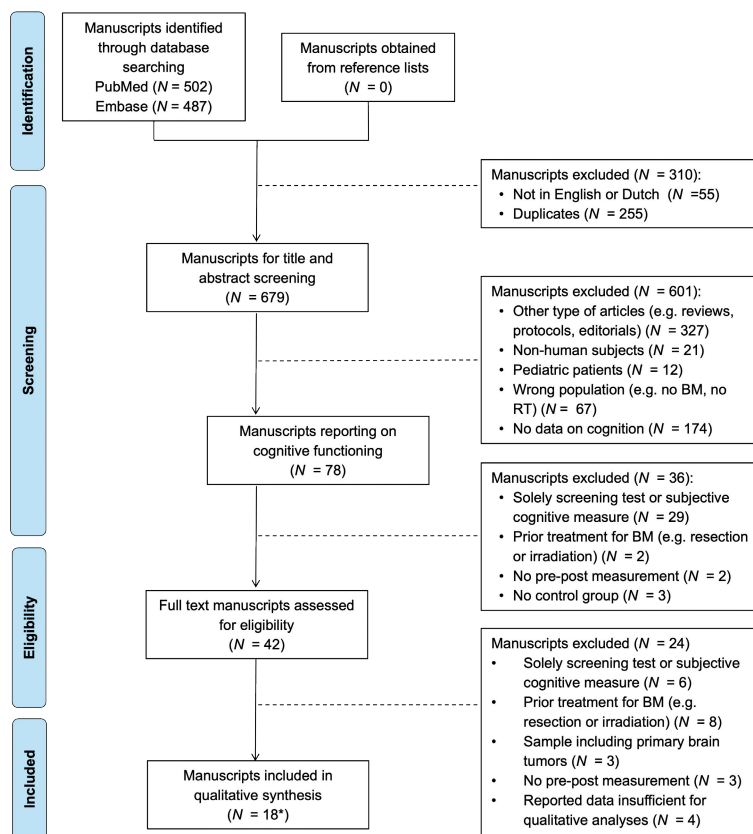


Figure 1. PRISMA flow chart illustrating the systematic review process conducted to identify the articles in this review. *14 original datasets

Table 2. Assessment of data quality for each included study listed from highest to lowest quality. + indicates 1 point awarded for that criterion, - indicates no points and +/- 0.5 points.

Authors	≥20 patients	≥50% at first follow-up	Corrected to norms	Definition provided	Adjusted for baseline	Parallel tests	Diversity NCA	Overall quality
Mehta et al., 2003 ^{18,36-38}	+	+	+	+	+	-	+	6 good
Gondi et al., 2014 ^{26,27,33}	+	+	-	+	+	+	+/-	5.5 good
Westover et al., 2020 ⁴¹	+	+	-	+/-	+	+	+	5.5 good
Saito et al., 2016 ²⁸	+	+	-	+	+	+	-	5 good
Deng et al., 2017 ³⁵	+	+	-	+	+	-	+	5 good
Zhu et al., 2018 ⁴⁰	+	+	-	+	+	-	+	5 good
Zhan et al., 2018 ³⁹	+	+	-	+	+	-	-	4 medium
Onodera et al., 2014 ²⁵	+	+	+	-	-	-	+	4 medium
Cheng et al., 2018 ³⁴	+	+	-	-	-	-	+	3 medium
Chang et al., 2007 ²⁹	-	+	+	+	+	+	+	6 good
Brown et al., 2016 ³²	+	+	+	+	+	-	+	6 good
Chang et al., 2009 ³¹	+	+	-	+	+	-	+	5 good
Habets et al., 2016 ^{30,43}	+	-	+	+	+	-	+	5 good
Minniti et al., 2020 ⁴⁴	+	+	-	+	+	+	-	5 good
Onodera et al., 2014 ²⁵	-	+	+	-	-	-	+	3 medium
Kirkpatrick et al., 2015 ²⁴	+	-	-	-	-	-	+/-	1.5 low

Abbreviations: NCA, neurocognitive assessment; RT, radiotherapy; SRS, stereotactic radiosurgery; WBRT, whole-brain radiotherapy.

At long-term follow-up (9-15 months) performance on most cognitive constructs either returned to baseline values or remained stable compared to mid-term follow-up. Mehta et al. found slight improvements or stable functioning ($N = 9$) regarding verbal fluency, information processing speed and fine motor coordination compared to baseline.¹⁸ In the Zhu et al. cohort ($N = 22$) 48% of the patients had deteriorated on L&M performance, which is comparable to the 50% at mid-term follow-up, suggesting most patients had stable cognitive performance from mid- to long-term follow-up.⁴⁰ Similarly, for the 9 patients in the Onodera et al. study performance on tests for verbal fluency and information processing speed remained stable over the entire study L&M performance (delayed recognition) significantly declined compared to both baseline and mid-term follow-up and a similar trend was seen for EF.²⁵ Forest plots of the incidence of patients with cognitive decline for each construct at each time point are presented in the **Supplementary Materials**. The analyses indicated significant heterogeneity between studies for L&M at mid-term follow-up. The meta-analysis suggests an increase in the number of patients with cognitive decline over time until mid-term follow-up, with a (relatively) stable or even lower incidence was found at long-term (**Figure 2a**).

In accordance with the results described above, Gondi et al. reported a trend towards deteriorated performance on L&M tasks 1 month after WBRT, which stabilized and reverted back to baseline values after that time point.²⁶ In the Mehta et al. cohort time to neurocognitive deterioration was on average shortest for fine motor coordination, L&M and EF.¹⁸ Additionally, they found that time to neurocognitive deterioration significantly differed between patients showing a volume reduction below or above 45% after 2 months, with patients with more volume reduction (classified as good responders) having a longer time to deterioration on fine motor coordination.

At short-term follow-up (1-4 months) after SRS the majority of studies reported a decline in cognitive performance when compared to baseline. Overall, declined performance was most common regarding L&M (23-54%) and fine motor coordination (35-46%).^{29,31,32} Similarly, between 13-19% of the patients in the Minniti et al. cohort ($N = 32$) showed a mean decline of 10-14% from baseline.⁴⁴ For the other assessed cognitive constructs (verbal fluency, attention, information processing speed and EF) the amount of patients in the Chang et al. study that had deteriorated were balanced out by the patients that had improved.²⁹ Contrarily, 18% showed a decline in EF in the other study by Chang et al. ($N = 20$) and 17% on information processing speed in the study by Brown et al. ($N = 60$).^{31,32} Both studies found least deterioration on tasks for attention (6%) and verbal fluency (2%). The two other

studies assessing short-term cognitive performance found no change in cognition compared to baseline.^{25,30} For example, it was reported that 78-100% of the patients ($N = 19$) had stable performance regarding the different cognitive constructs, where the small percentage of patients that showed declined cognitive performance on the different tests (3-8%) was balanced by those that improved (3-17%).³⁰ At both mid-term (5-8 months) and long-term follow-up (9-12 months) all studies reported either stable or slightly improved cognitive performance compared to baseline performance.^{25,29-32,44,45} To illustrate, the percentage of patients with declined performance on L&M decreased at both mid- and long-term follow-up compared to short-term.⁴⁴ Additionally, the mean decline reduced to 2-5% at long-term follow-up compared to 10-14% at short-term, suggesting that both the number of patients as well as the severity of the cognitive decline decreased.

Forest plots of the incidence of patients with cognitive decline for each construct at each time point are presented in the **Supplementary Materials**. There was no significant heterogeneity between studies for any cognitive construct at any time point for the SRS studies. The meta-analysis suggests a relatively constant number of patients experiencing cognitive decline over time after SRS, albeit with large confidence intervals (**Figure 2b**).

Table 3: Study characteristics and baseline patient characteristics categorized by type of radiotherapy

RT type	Authors and year of publication	Study type	Radiation schedule	N	Sex (M:F)	Median age in years (range or N of patients)	KPS (N of patients)	Number of BMs (N of patients)	Median total volume of BMs in cc	Median overall survival in months	Primary tumor location (N of patients)
WBRT	Mehta et al., 2003 ^{18,36-38}	Phase III RCT	WBRT 30 Gy/10 fr	208	90:118	58 (N.A.)	70 (43) 80 (55) 90 (77) 100 (33)	1 (41) 2-3 (69) 4-6 (41) >6 (53)	N.A.	4.9	Lung (128) Breast (42) Other (38)
	Gondi et al., 2014 ^{26,27,33}	Phase II trial	HA-WBRT 30 Gy/10 fr	100	N.A.	61 (28-83)	70 (19) 80 (17) 90 (39) 100: 25	N.A.	6.7	6.8	Lung (56) Breast (15) Other (29)
	Saito et al., 2016 ²⁸	Prospective trial	WBRT 30 Gy/10 fr	18	21:13	65.5 (39-86)	≤70 (22) ≥80 (12)	N.A.	N.A.	N.A.	Lung (20) Breast (7) Other (7)
			WBRT 35 Gy/14 fr	16							
	Deng et al., 2017 ³⁵	Retrospective trial	WBRT 30 Gy/10 fr	109	67:42	≤60 (38) >60 (71)	N.A.	≤3 (32) >3 (77)	N.A.	7.3	Lung (109)
	Cheng et al., 2018 ⁴⁶	Prospective trial	WBRT 40 Gy/20 fr	81	48:33	<65 (39) ≥65 (42)	≥80 (81)	<3 (54) ≥3 (23)	N.A.	7.5	Lung (49) Other (32)
	Zhan et al., 2018 ³⁹	RCT	WBRT 30 Gy/15 fr	117	68:49	≤60 (51) >60 (66)	<70 (85) ≥70 (32)	≤2 (94) >2 (23)	N.A.	6.5	N.A.
	Zhu et al., 2018 ⁴⁰	Retrospective trial	WBRT 40 Gy/20 fr	33	18:15	≤61 (14) >61 (19)	N.A.	≥4 (33)	N.A.	7.5	Lung (33)
	Westover et al., 2020 ⁴¹	Phase II trial	HA-WBRT + SIB + 40 Gy/10 fr	49	24:25	60 (54-65)	≥70 (49)	1-3 (19) 4-6 (20) 7-8 (10)	0.8	9.0	Lung (39) Breast (5) Other (5)
	Onodera et al., 2014 ²⁵	Non-randomized pilot study	WBRT 35 Gy/14 fr	20	11:9	62.6 (N.A.)	70 (1) 80 (2) 90 (17)	<3 (6) ≥3 (14)	6.7	N.A.	Lung (17) Breast (1) Other (2)

Table 3: Study characteristics and baseline patient characteristics categorized by type of radiotherapy (continued)

RT type	Authors and year of publication	Study type	Radiation schedule	N	Sex (M:F)	Median age in years (range or N of patients)	KPS (N of patients)	Number of BMs (N of patients)	Median total volume of BMs in cc	Median overall survival in months	Primary tumor location (N of patients)
SRS			SRS 25 Gy/1 fr or 28-35 Gy/4 fr	7	2:5	56.3 (N.A.)	70 (1) 80 (1) 90 (5)	1 (7)	2.8	N.A.	Lung (6) Breast (0) Other (1)
	Chang et al., 2007 ²⁹	Prospective pilot study	SRS median 20 Gy (14-21 Gy)	15	5:10	64.9 (31.5-77)	70 (1) 80 (2) 90 (8) 100 (4)	1 (11) 2-3 (4)	1.8	7.2	Lung (8) Renal (3) Melanoma (4)
	Chang et al., 2009 ³¹	RCT	SRS median 19 Gy (15-20 Gy)	30	12:18	63 (35-82)	≥80 (30)	1 (18) 2-3 (12)	1.4	15.2	Lung (16) Breast (4) Renal (2) Melanoma (4) Other (4)
	Brown et al., 2016 ³²	RCT	SRS median 20 Gy (14-21 Gy)	111	54:57	<60 (53) ≥60 (58)	N.A.	1 (55) 2 (39) 3 (17)	N.A.	10.4	Lung (80) Breast (11) Melanoma (3) Other (17)
SRS	Habetts et al., 2016 ^{30,43}	Prospective trial	SRS median 19 Gy (15-20 Gy)	97	46:51	63 (33-82)	60-80 (62) ≥90 (35)	1 (43) 2 (31) 3 (18) 4 (5)	7.8	7.7	Lung (48) Breast (8) Melanoma (9) Other (32)
	Minniti et al., 2020 ⁴⁴	Prospective trial	SRS 22 Gy (<2cm lesion) 16-18 Gy (≥2cm lesion)	40	23:17	57 (37-74)	≥60 (40)	10-14 (32) 15-21 (8)	4.7	14.1	Lung (17) Breast (7) Melanoma (10) Kidney (6)

Abbreviations: BMs, brain metastases; Fr, fractions; Gy, RT dose in Gray; HA-WBRT, hippocampal avoidance whole-brain radiotherapy; KPS, Karnofsky Performance Status; N, number of patients; N.A., not available; RCT, randomized controlled trial; RT, radiotherapy; SIB, simultaneous integrated boost; SRS, stereotactic radiosurgery; WBRT, whole-brain radiotherapy; N.A. not available

Table 4: Main message of the studies categorized by type of radiotherapy. T = time point in months after radiotherapy.

RT type	Authors and year of publication	Number of patients	Time points NCF assessed in months after RT	Definition of cognitive change	Main message
WBRT	Mehta et al., 2003 ^{18,36-38}	208	T0	≤2 SD change in average Z-score	Most patients deteriorate on fine motor coordination and least patients on verbal fluency.
			T1		
			T2		
			T3		
			T4		
			T5		
			T6		
			T9		
			T12		
			T15		
	T18				
	Gondi et al., 2014 ^{26,27,33}	100 53 42 29	T0	RCI	7-18% mean decline from T0 in learning and memory performance.
			T2		
			T4		
			T6		
T6					
Saito et al., 2016 ²⁸	34 34 19	T0	RCI	Learning and memory deteriorated significantly compared to T0 in those who only completed T0 and T4 assessments. In total 27-33% of the patients had deteriorated.	
		T4			
		T8			
		T8			
					T8: On average stable cognitive performance was observed on learning and memory in subgroup completing assessments at all 3 time points. Of this subgroup, 11-26% had deteriorated learning and memory performance compared to baseline.

Table 4: Main message of the studies categorized by type of radiotherapy. T = time point in months after radiotherapy. (continued)

RT type	Authors and year of publication	Number of patients	Time points NCF assessed in months after RT	Definition of cognitive change	Main message
WBRT	Deng et al., 2017 ³⁵	109	T0	RCI	T3: 22-38% of the patients deteriorated on overall cognitive performance, with greatest deterioration on learning and memory (22-37%), executive function (38%) and verbal fluency (32%)
		87-89*	T3		
		61-64*	T5		
	Cheng et al., 2018 ⁴⁶	81	T0	N.A.	T5: 40-55% of the patients deteriorated on at least one cognitive task, with greatest deterioration on learning and memory (52-55%) and verbal fluency (53%)
		81	T1		
	Zhan et al., 2018 ³⁹	117	T0	RCI	T7: 47-61% of the patients deteriorated on at least one cognitive task, with greatest deterioration on executive function (61%) and verbal fluency (59%).
91		T1	T1: Significantly decreased performance compared to T0 on global cognitive performance, attention, verbal fluency and event-based prospective memory. Stable performance on time-based prospective memory.		
		T2			
54		T3	T3: 19% of the patients deteriorated on learning and memory performance.		
	T4	T6: 35% of the patients deteriorated on learning and memory performance.			
		T5			
		T6			

Table 4: Main message of the studies categorized by type of radiotherapy. T = time point in months after radiotherapy. (continued)

RT type	Authors and year of publication	Number of patients	Time points NCF assessed in months after RT	Definition of cognitive change	Main message	
WBRT	Zhu et al., 2018 ⁴⁰	33	T0	RCI	T3: Deteriorated cognitive performance was found on learning and memory, executive function and verbal fluency in 19%, 29% and 28% of the patients, respectively.	
		29-31*	T3			
		26-29*	T6			
	Westover et al., 2020 ⁴¹	47	T0			T6: Deteriorated cognitive performance was found on learning and memory, executive function and verbal fluency in 48%, 48% and 50% of the patients, respectively.
			T3			
		18	T6			T9: Deteriorated cognitive performance was found on learning and memory, executive function and verbal fluency in 50%, 58% and 57% of the patients, respectively.
		8	T9			
		5	T12			T3: Compared to T0 learning & memory performance declined in 17% of the patients on delayed recall with a mean decline of 11%. No significant changes were found on the other cognitive tasks, but there were large variations.
	Onodera et al., 2014 ²⁵	20	T0			T6: Mean learning & memory performance (delayed recall) recovered to pre-treatment values.
			T4			
17		T8			T4: Patients receiving WBRT deteriorated significantly compared to T0 on learning and memory (delayed recall). Additional analysis showed only patients with a brain edema volume ≥ 16.8 cc. decreased on learning and memory (delayed recall) and executive function.	
14		T12			T8: Patients receiving WBRT deteriorated significantly compared to T0 and T4 on learning and memory (immediate recall). Improvements in immediate and delayed recall at T8 compared to T4 were only observed in patients with a <4.0 cc total volume of BM at T0.	

Table 4: Main message of the studies categorized by type of radiotherapy. T = time point in months after radiotherapy. (continued)

RT type	Authors and year of publication	Number of patients	Time points NCF assessed in months after RT	Definition of cognitive change	Main message
WBRT	Onodera et al., 2014 ²⁵	20 17 14 9	T0 T4 T8 T12	N.A.	T12: In the subgroup of patients followed for at least 12 months, learning and memory (delayed recognition) had significantly declined compared to T0 at both T4 and T12. This subgroup also had significantly declined executive function at T4 compared to T0, with a similar trend at T12. Additionally, learning and memory (immediate recall) had returned to baseline values at T12 after a significant improvement at T8.
					No changes in verbal fluency, information processing speed or on cognitive screening measure at any time point.
SRS		7 5 5 4	T0 T4 T8 T12	N.A.	T4-12 SRS group had no change in cognitive performance for any tested cognitive construct over the entire study period.
	Chang et al., 2007 ²⁹	15 13 5	T0 T1 T2 T3 T4 T5 T7-9 T10-12	RCI	T1: All patients declined on ≥ 1 neuropsychological test and 54% on ≥ 2 tests, with decline in learning and memory (54%) and fine motor coordination (46%) most common. Improvements were also observed, mostly on executive function (38%), verbal fluency (15%), fine motor coordination (15%) and information processing speed (15%). T7-9: Stable or improved cognitive performance was found for 80% of the patients for learning and memory, 60.0% for executive function and fine motor coordination.

Table 4: Main message of the studies categorized by type of radiotherapy. T = time point in months after radiotherapy. (continued)

RT type	Authors and year of publication	Number of patients	Time points NCF assessed in months after RT	Definition of cognitive change	Main message
	Chang et al., 2009 ³¹	30	T0 T1 T2 T4 T6 T12 T15 T18	RCI	T4: Most cognitive decline on tests for learning and memory (20% of the patients on total recall). The mean posterior probability of decline was 24% for total recall, 6% for delayed recall and 0% for delayed recognition. Analyses were also performed for other cognitive tests, but might have been underpowered since the trial was stopped prematurely due to significant larger probability of decline on learning and memory (total recall) after 4 months in the SRS+WBRT versus the SRS alone group.
		20			T6: The mean posterior probability of decline on total recall was 8%.
SRS	Brown et al., 2016 ³²	111	T0 T1.5 T3 T6 T9 T12	≥1 SD	T3: 64% of the patients showed cognitive deterioration on ≥1 test compared to T=0. Most patients deteriorated on learning and memory (recognition) performance (23%) and information processing speed (19%) and least on verbal fluency (2%).
		63			T6: In those patients surviving at least 12 months 50% deteriorated on at least 1 test compared to T=0. Most patients deteriorated on learning and memory (delayed recall) performance (33%) and none deteriorated on information processing speed.
		10-12*			T9: In those patients surviving at least 12 months 50% deteriorated on at least 1 test compared to T=0. Most patients deteriorated on learning and memory (delayed recall and discrimination index) performance (both 23%) and none on verbal fluency.
		12-14*			
		9-10*			

Table 4: Main message of the studies categorized by type of radiotherapy. T = time point in months after radiotherapy. (continued)

RT type	Authors and year of publication	Number of patients	Time points NCF assessed in months after RT	Definition of cognitive change	Main message
SRS	Habets et al., 2016 ^{30,45}	97	T0	≤1.5 SD mean of healthy controls	T12: In those patients surviving at least 12 months 60% deteriorated on at least 1 test compared to T=0. Most deteriorated on learning and memory (delayed recall) performance (20%) and none on verbal fluency.
		39	T3		
		29	T6		
	Minniti et al., 2020 ⁴⁴	38	T0	RCI	T6: The majority of the patients maintained their pre-treatment levels of cognitive performance over the entire study period. Only verbal fluency performance showed trend towards improvement.
		32	T3		
		26	T6		
21	T12	T3: Compared to T0 learning & memory performance declined in 13%, 16% and 19% of the patients on immediate recall, recognition and delayed recall. The mean decline varied between 10-14%.			
T6:	T6:	T6:	T6:	T6:	Compared to T0 learning & memory performance declined in 12%, 15% and 15% of the patients on immediate recall, recognition and delayed recall. The mean decline varied between 5-9%.
					T12:

Abbreviations: N.A., not available; NCF, neurocognitive functioning; RCI, reliable change index; RT, radiotherapy; SD, standard deviations; SRS, stereotactic radiosurgery; WBRT, whole-brain radiotherapy; * ranges in patient numbers are caused by different numbers of patients completing the different cognitive tests during the study-procedures.

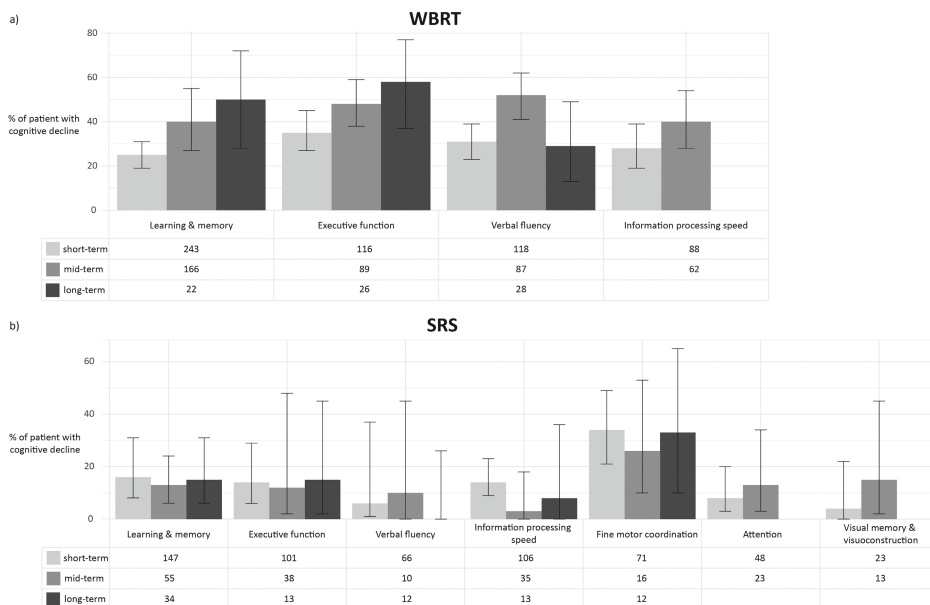


Figure 2. Bar charts illustrating the pooled incidence of declined cognitive performance compared to baseline on the different cognitive constructs at different time points (a) WBRT and (b) SRS. The error bars display the 95% CIs. The table below the chart displays the number of patients for whom these data were available.

Abbreviations: CIs, confidence intervals.

DISCUSSION

The aim of this study was to systematically assess the current evidence on the cognitive changes across different cognitive constructs after either WBRT or SRS in adult patients with non-resected BMs with objective neurocognitive assessments performed at baseline and after treatment. Our meta-analysis indicates that after WBRT the majority of patients show a decline in cognitive performance until mid-term follow-up (5-8 months), whereas a subset of patients with relatively good outcome shows stable cognitive performance in the long-term (9-15 months). For SRS, an initial dip (1-4 months) in cognitive performance in patients was observed by half of the studies, whereas at mid- and long-term follow-up all studies reported that the majority of the patients performed at pre-treatment levels. Since cognitive decline was assessed relative to baseline performance, differences in cognitive performance prior to radiotherapy were accounted for and thus cannot explain the differences between WBRT and SRS. This suggests that while the cognitive side-effects of SRS are transient, after WBRT patients can experience deterioration over a

longer period of time. This especially holds for those patients with shorter survival. Thereby, this review points towards SRS resulting in lowest risks for cognitive adverse side-effects in this already cognitively vulnerable patient population with limited survival. Since WBRT and SRS have resulted in comparable survival rates in selected groups of patients, it could even be suggested to totally abstain from WBRT in patients with a limited number of BMs.⁴⁷ However, sometimes WBRT is inevitable due to high number of metastases and current technical capabilities. The information provided by this review can be used in communicating risks to patients and aid patients in making educated (shared) treatment decisions towards maintaining optimal QoL.

A high percentage of patients already experience cognitive problems before starting radiotherapy treatment, with at least one out of every two patients with BMs demonstrating cognitive impairment on minimally one cognitive construct.^{18,29,30} Baseline cognitive impairment was only significantly predicted by larger baseline BMs volume, even when considering other factors such as the number of previous chemotherapy regimens.³⁸ Thus, not only previous cancer treatments, but also the BMs themselves exert a significant burden on cognitive functioning. This indicates, once again, that patients with BMs represent a vulnerable patient group in which further cognitive decline should be minimized when possible.

The majority of WBRT studies found a consistent decline in cognitive performance from baseline to short-term follow-up with a further decrease in performance at mid-term, with verbal L&M, EF and verbal fluency most often affected.^{18,25,26,28,33-40} However, in a subgroup of patients with a better outcome (lower baseline BMs volume, long-term BMs survivors) stable or improved cognitive performance was observed at mid-term.^{25,28} Additionally, patients receiving HA-WBRT showed less cognitive decline than those receiving conventional WBRT with even stable performance on some cognitive constructs.^{26,33,41} At long-term follow-up (9-15 months) cognitive performance either remained stable compared to mid-term follow-up or returned to baseline values for most cognitive constructs.^{18,25,40} Our meta-analysis confirmed these results; at short- and mid-term follow-up an increase in the incidence of WBRT patients with cognitive impairment was found, while a (relatively) stable or even lower incidence was found in the long-term. This suggests that while some patients show a decline in cognitive performance up until mid-term follow-up after WBRT, a (relatively) good outcome is often accompanied by stable cognitive performance over time. To illustrate, stronger reduction in tumor volume four months after WBRT was related to better preservation of cognitive performance over time.^{18,36-38} It is unclear whether the observed decline in cognitive

performance is characteristic of the worse responders (i.e. patients with less tumor shrinkage), or that the good responders survive long enough to recover from this dip in performance. Nonetheless, the data suggest that for patients with a longer survival (at least 9-15 months) the benefits of WBRT radiotherapy outweigh the costs in the long-term. Currently the majority of patients do not (yet) survive long-term, despite improvements in life expectancy with the introduction of immunotherapies and targeted therapies.⁴⁸⁻⁵⁰ While early delayed effects (1-4 months after WBRT) are generally considered to be transient, the cognitive decline traditionally characterized as a late delayed effect (5-9 months after WBRT) is thought to be progressive and irreversible.⁵¹ Therefore, the cognitive decline found at short- and mid-term should not be discounted against the possible stable long-term cognitive performance in those with a good survival and should be discussed with BMs patients during shared decision making. However, better discernment of short and long survival should be included in evaluating this.

Results regarding cognitive performance after SRS at short-term follow-up (1-4 months) were variable; approximately half of the included studies observed cognitive deterioration, most frequently for verbal L&M, fine motor coordination and EF.^{29,31,32,44} The other studies found no changes in cognition compared to baseline.^{25,30,45} At both mid-term (5-8 months) and long-term follow-up (9-12 months) all studies reported either stable or (slightly) improved cognitive performance compared to baseline.^{25,29-32,44,45} The meta-analysis largely confirms these results; a relatively stable incidence of patients with cognitive decline from baseline was observed up until long-term follow-up, albeit with large confidence intervals. The initial dip in cognitive performance in some of the patients could be attributed to an increase in peri-lesional edema which is sometimes observed shortly after SRS, but is often resolved six months later.⁵² Moreover, adjuvant systemic treatment will often be (re-)initialized shortly after SRS. The short-term side-effects of systemic treatments could therefore be the cause of this initial dip, rather than the radiotherapy treatment. Conclusively, after SRS an initial, transient dip in cognitive performance can occur, but at mid- and long-term the majority of patients will have returned to or remained at pre-radiotherapy cognitive levels.

Looking in more detail at the affected cognitive constructs, not one is specifically affected by WBRT or SRS. Rather, change in cognitive performance was observed across several cognitive constructs, including, but not limited to verbal L&M, EF, information processing speed, and fine motor coordination, which have been linked to a wide range of neuroanatomical substrates involving both cortical areas and white matter networks.⁵³⁻⁵⁷ This is supported by previous research indicating

morphological changes after brain irradiation in both cortical structures (cortical thickness, grey matter volume, grey matter density) as well as white matter networks.⁵⁸⁻⁶⁴ Additionally, the amount of microstructural damage to white matter fibers has been shown to be directly associated with cognitive deterioration in cancer patients.⁶⁵

Strengths and Limitations

Cognitive functioning after cranial radiotherapy has been gaining research interest, as reflected by the included studies (published between 2003 and 2020), with most (9/14) published over the last five years. Nonetheless, studying cognitive changes after radiotherapy in patients with BMs remains challenging for multiple reasons. Firstly, different factors could influence cognitive functioning over the follow-up period, including tumor progression, adjuvant systemic treatment or changes in mood. Additionally, a substantial number of patients drop out during the study period, most often due to high disease burden. Especially in the long-term, results are therefore based on the small numbers of patients that are fit enough to stay compliant. Unfortunately, this is inevitable in this vulnerable patient population with limited overall survival.

Additionally, numerous challenges hinder in-depth comparison across studies, including differences in patient characteristics (e.g. age), disease characteristics (e.g. primary tumor type) and treatment characteristics (radiotherapy schedule) of the study populations. For example, two studies investigated HA-WBRT ($N = 149$), while all others investigated conventional WBRT. We chose not to exclude these, since during HA-WBRT less brain tissue is irradiated and including this in the review would lead to an underrepresentation rather than an overrepresentation of the cognitive damage to be expected after WBRT compared to SRS. Also, there was much heterogeneity across studies regarding both the methodology (e.g. definition for cognitive impairment and decline, timing of cognitive testing) and reported data (e.g. baseline cognitive data). To illustrate, most studies did not control for practice effects due to repeated testing over time and only five out of fourteen studies reported using parallel test for the repeated neuropsychological testing, even though cognitive assessment was repeated up to nine times within a one-year period in some studies. These methodological shortcomings could have led to an underestimation of the cognitive changes after radiotherapy as cognitive problems might be masked by repeated testing effects. In order to aid comparability across studies, we chose to cluster the follow-up time points according to classifications used in previous studies. However, the subtle dynamics of cognitive change may not be ideally assessed by this classification. To illustrate, a difference in cognitive-

deterioration-free survival of merely 0.7 months was found in favor of patients with resected BMs who received SRS (3.7 months) compared to WBRT (3 months).⁶⁶ Thus, the time point clustering used in this study could have masked slight differences that are present between the SRS and WBRT patient groups.

The heterogeneity between studies was also reflected by our meta-analysis on the incidence of cognitive decline over time; the meta-analysis indicated significant heterogeneity between studies regarding the reported incidence of cognitive decline for L&M at mid-term for the WBRT studies. This could be explained by the fact that the definition used to assess cognitive change varied greatly between studies and, moreover, was not always reported. Additionally, the meta-analysis shows relatively broad confidence intervals, due to the low number of patients for whom the data was available. Nonetheless, even with a small number of studies reporting the incidence of patients with cognitive decline, the meta-analysis indicated significant heterogeneity only for one type of radiotherapy, at one time-point and for one cognitive construct.

In this review, 20 manuscripts reporting on 14 original datasets were included. We chose to include all 20 manuscripts since they answered different questions regarding cognitive functioning, thus did not present overlap. Results were summarized together per dataset to avoid overrepresentation of the same patients in this review. Strict inclusion criteria were used to minimize the potential confounding effects on cognitive performance (e.g. no resected BMs were included). Additionally, a critical appraisal was performed to ensure the quality of the data as reported in the manuscript, which indicated that the majority of the included studies (75%) was of good to high-quality. Therefore, we believe our conclusions are warranted.

Future directions

Currently, multiple single center trials are collecting and analyzing prospective data that will hopefully further improve our understanding of cognitive impairment after brain irradiation ^{e.g. 67-70}. Ideally, all future studies should at minimum use the neuropsychological tests recommended by the International Cancer and Cognition Task Force, since these tests have been proven to be sensitive to the neurotoxic effects of cancer treatment.⁷¹ A valuable line of research is to explore possible additional therapeutic strategies that could reduce treatment toxicity. As the mechanisms leading to radiation-induced cognitive impairment are multifactorial, several strategies, each addressing different mechanisms, have been proposed to potentially reduce the neurocognitive toxicity of radiation.^{72,73} For example,

avoiding high dose radiation on hippocampi and adding synthetic metallophthalocyanine or memantine to WBRT have shown encouraging, but mixed results.^{53,54,74-79} These strategies provide promising prospects for the future, but do require further research.

CONCLUSION

This review indicates that after treatment with WBRT, most patients show declined cognitive performance until at least eight months after treatment, after which those with a longer overall survival show stable cognitive performance. A proportion of SRS-treated patients first show a decline in cognitive performance, but the majority of the patients return to pre-treatment levels already five months after SRS and continue to display stable cognitive performance up until one year after SRS. It remains challenging to disentangle the effects of radiotherapy on cognitive functioning from the possible deleterious effects of systemic treatments, the effects of BMs themselves and patient's psychological state. Nonetheless, this current review indicates that while the cognitive side-effects of SRS are transient, after WBRT patients can experience deterioration over a longer period of time. Thus, SRS will result in lowest risks for cognitive adverse side-effects in this already (cognitively) vulnerable patient population with limited survival. This information can be used in communicating risks to patients and aid in making educated (shared) treatment decisions towards maintaining optimal QoL.

SUPPLEMENTARY MATERIALS



REFERENCES

1. Barnholtz-Sloan JS, Yu C, Sloan AE, et al. A nomogram for individualized estimation of survival among patients with brain metastasis. *Neuro Oncol* 2012; 14: 910–918.
2. Barnholtz-Sloan JS, Sloan AE, Davis FG, et al. Incidence proportions of brain metastases in patients diagnosed (1973 to 2001) in the Metropolitan Detroit Cancer Surveillance System. *Journal of Clinical Oncology* 2004; 22: 2865–2872.
3. Gaspar L, Scott C, Rotman M, et al. Recursive partitioning analysis (RPA) of prognostic factors in three Radiation Therapy Oncology Group (RTOG) brain metastases trials. *Int J Radiat Oncol Biol Phys* 1997; 37: 745–751.
4. Sperduto PW, Chao ST, Sneed PK, et al. Diagnosis-specific prognostic factors, indexes, and treatment outcomes for patients with newly diagnosed brain metastases: a multi-institutional analysis of 4,259 patients. *Int J Radiat Oncol Biol Phys* 2010; 77: 655–661.
5. Eichler AF, Loeffler JS. Multidisciplinary management of brain metastases. *Oncologist* 2007; 12: 884–898.
6. Khuntia D, Brown P, Li J, et al. Whole-brain radiotherapy in the management of brain metastasis. *Journal of Clinical Oncology* 2006; 24: 1295–1304.
7. Mehta MP. The controversy surrounding the use of whole-brain radiotherapy in brain metastases patients. *Neuro Oncol* 2015; 17: 919–923.
8. Pinkham MB, Whitfield GA, Brada M. New developments in intracranial stereotactic radiotherapy for metastases. *Clin Oncol* 2015; 27: 316–323.
9. Grosshans DR, Meyers CA, Allen PK, et al. Neurocognitive function in patients with small cell lung cancer: effect of prophylactic cranial irradiation. *Cancer* 2008; 112: 589–595.
10. Vardy J, Dhillon HM, Pond GR, et al. Cognitive function and fatigue after diagnosis of colorectal cancer. *Annals of Oncology* 2014; 25: 2404–2412.
11. Mitchell T, Turton P. ‘Chemobrain’: Concentration and memory effects in people receiving chemotherapy - a descriptive phenomenological study. *Eur J Cancer Care (Engl)* 2011; 20: 539–548.
12. Reid-Arndt SA, Yee A, Perry MC, et al. Cognitive and psychological factors associated with early posttreatment functional outcomes in breast cancer survivors. *J Psychosoc Oncol* 2009; 27: 415–434.
13. Griffith HR, Belue K, Sicola A, et al. Impaired financial abilities in mild cognitive impairment: a direct assessment approach. *Neurology* 2003; 60: 449–457.
14. Schimmel WCM, Gehring K, Eekers DBP, et al. Cognitive effects of stereotactic radiosurgery in adult patients with brain metastases: A systematic review. *Adv Radiat Oncol* 2018; 3: 568–581.
15. Tallet A V, Azria D, Barlesi F, et al. Neurocognitive function impairment after whole brain radiotherapy for brain metastases: actual assessment. *Radiation oncology* 2012; 7: 77.
16. Tsao MN, Rades D, Wirth A, et al. Radiotherapeutic and surgical management for newly diagnosed brain metastasis(es): An American Society for Radiation Oncology evidence-based guideline. *Pract Radiat Oncol* 2012; 2: 210–225.
17. Moher D, Shamseer L, Clarke M, et al. Preferred reporting items for systematic review and meta-analysis protocols (prisma-p) 2015 statement. *Syst Rev* 2015; 4: 1–9.

18. Mehta MP, Rodrigus P, Terhaard CHJ, et al. Survival and neurologic outcomes in a randomized trial of motexafin gadolinium and whole-brain radiation therapy in brain metastases. *Journal of Clinical Oncology* 2003; 21: 2529–2536.
19. Bray VJ, Dhillon HM, Vardy JL. Systematic review of self-reported cognitive function in cancer patients following chemotherapy treatment. *Journal of Cancer Survivorship* 2018; 12: 537–559.
20. Hutchinson AD, Hosking JR, Kichenadasse G, et al. Objective and subjective cognitive impairment following chemotherapy for cancer: A systematic review. *Cancer Treat Rev* 2012; 38: 926–934.
21. Lin NU, Wefel JS, Lee EQ, et al. Challenges relating to solid tumour brain metastases in clinical trials, part 2: neurocognitive, neurological, and quality-of-life outcomes. A report from the RANO group. *Lancet Oncol* 2013; 14: e407-16.
22. Meyers CA, Rock EP, Fine HA. Refining endpoints in brain tumor clinical trials. *J Neurooncol* 2012; 108: 227–230.
23. Meyers CA, Wefel JS. The use of the mini-mental state examination to assess cognitive functioning in cancer trials: no ifs, ands, buts, or sensitivity. *Journal of Clinical Oncology* 2003; 21: 3557–3558.
24. Kirkpatrick JP, Wang Z, Sampson JH, et al. Defining the optimal planning target volume in image-guided stereotactic radiosurgery of brain metastases: Results of a randomized trial. *Int J Radiat Oncol Biol Phys* 2015; 91: 100–108.
25. Onodera S, Aoyama H, Tha KK, et al. The value of 4-month neurocognitive function as an endpoint in brain metastases trials. *J Neurooncol* 2014; 120: 311–319.
26. Gondi V, Pugh SL, Tome WA, et al. Preservation of memory with conformal avoidance of the hippocampal neural stem-cell compartment during whole-brain radiotherapy for brain metastases (RTOG 0933): A phase II multi-institutional trial. *Journal of Clinical Oncology* 2014; 32: 3810–3816.
27. Bovi JA, Pugh SL, Sabsevitz D, et al. Pretreatment Volume of MRI-Determined White Matter Injury Predicts Neurocognitive Decline After Hippocampal Avoidant Whole-Brain Radiation Therapy for Brain Metastases: Secondary Analysis of NRG Oncology Radiation Therapy Oncology Group 0933. *Adv Radiat Oncol* 2019; 4: 579–586.
28. Saito H, Tanaka K, Kanemoto A, et al. Factors affecting the baseline and post-treatment scores on the hopkins verbal learning test-revised Japanese version before and after whole-brain radiation therapy. *Int J Mol Sci* 2016; 17: 1834.
29. Chang EL, Wefel JS, Maor MH, et al. A pilot study of neurocognitive function in patients with one to three new brain metastases initially treated with stereotactic radiosurgery alone. *Neurosurgery* 2007; 60: 277–283.
30. Habets EJJ, Dirven L, Wiggeraad RG, et al. Neurocognitive functioning and health-related quality of life in patients treated with stereotactic radiotherapy for brain metastases: A prospective study. *Neuro Oncol* 2016; 18: 435–444.
31. Chang EL, Wefel JS, Hess KR, et al. Neurocognition in patients with brain metastases treated with radiosurgery or radiosurgery plus whole-brain irradiation: a randomised controlled trial. *Lancet Oncol* 2009; 10: 1037–1044.
32. Brown PD, Jaeckle K, Ballman K V., et al. Effect of radiosurgery alone vs radiosurgery with whole brain radiation therapy on cognitive function in patients with 1 to 3 brain metastases a randomized clinical trial. *JAMA* 2016; 316: 401–409.

33. Caine C, Deshmukh S, Gondi V, et al. CogState computerized memory tests in patients with brain metastases: Secondary endpoint results of NRG oncology RTOG 0933. *J Neurooncol* 2016; 126: 327–336.
34. Cheng H, Chen H, Lv Y, et al. Prospective memory impairment following whole brain radiotherapy in patients with metastatic brain cancer. *Cancer Med*. Epub ahead of print 2018. DOI: 10.1002/cam4.1784.
35. Deng X, Zheng Z, Lin B, et al. The efficacy and roles of combining temozolomide with whole brain radiotherapy in protection neurocognitive function and improvement quality of life of non-small-cell lung cancer patients with brain metastases. *BMC Cancer* 2017; 17: 42.
36. Li J, Bentzen SM, Li J, et al. Relationship Between Neurocognitive Function and Quality of Life After Whole-Brain Radiotherapy in Patients With Brain Metastasis. *Int J Radiat Oncol Biol Phys* 2008; 71: 64–70.
37. Li J, Bentzen SM, Renschler M, et al. Regression after whole-brain radiation therapy for brain metastases correlates with survival and improved neurocognitive function. *Journal of Clinical Oncology* 2007; 25: 1260–1266.
38. Meyers CA, Smith JA, Bejjani A, et al. Neurocognitive function and progression in patients with brain metastases treated with whole-brain radiation and motexafin gadolinium: results of a randomized phase III trial. *Journal of Clinical Oncology* 2004; 22: 157–165.
39. Zhan Y, Jiang X. Concomitant treatment of brain metastases with whole brain radiotherapy and temozolomide protects neurocognitive function and improve quality of life. *Tropical Journal of Pharmaceutical Research* 2018; 17: 1209–1213.
40. Zhu Y, Fu L, Jing W, et al. Effectiveness of temozolomide combined with whole brain radiotherapy for non-small cell lung cancer brain metastases. *Thorac Cancer* 2018; 9: 1121–1128.
41. Westover KD, Mendel JT, Dan T, et al. Phase II trial of hippocampal-sparing whole brain irradiation with simultaneous integrated boost for metastatic cancer. *Neuro Oncol* 2020; 22: 1831–1839.
42. Westover KD, Mendel JT, Dan T, et al. Phase II trial of hippocampal-sparing whole brain irradiation with simultaneous integrated boost for metastatic cancer. *Neuro Oncol* 2020; 22: 1831–1839.
43. van der Meer PB, Habets EJJ, Wiggenraad RG, et al. Individual changes in neurocognitive functioning and health-related quality of life in patients with brain oligometastases treated with stereotactic radiotherapy. *J Neurooncol* 2018; 139: 359–368.
44. Minniti G, Capone L, Nardiello B, et al. Neurological outcome and memory performance in patients with 10 or more brain metastases treated with frameless linear accelerator (LINAC)-based stereotactic radiosurgery. *J Neurooncol* 2020; 148: 47–55.
45. van der Meer PB, Habets EJJ, Wiggenraad RG, et al. Individual changes in neurocognitive functioning and health-related quality of life in patients with brain oligometastases treated with stereotactic radiotherapy. *J Neurooncol* 2018; 139: 359–368.
46. Cheng H, Chen H, Lv Y, et al. Prospective memory impairment following whole brain radiotherapy in patients with metastatic brain cancer. *Cancer Med* 2018; 7: 5315–5321.
47. Welzel G, Fleckenstein K, Schaefer J, et al. Memory Function Before and After Whole Brain Radiotherapy in Patients With and Without Brain Metastases. *Int J Radiat Oncol Biol Phys* 2008; 72: 1311–1318.

48. Gotwals P, Cameron S, Cipolletta D, et al. Prospects for combining targeted and conventional cancer therapy with immunotherapy. *Nat Rev Cancer* 2017; 17: 286–301.
49. Sperduto PW, Mesko S, Li J, et al. Survival in Patients With Brain Metastases : Summary Report on the Updated Diagnosis-Specific Graded Prognostic Assessment and Definition of the Eligibility Quotient. *Journal of Clinical Oncology* 2020; 38: 1–13.
50. Roth P, Preusser M, Weller M. Immunotherapy of Brain Cancer. *Oncol Res Treat* 2016; 39: 326–334.
51. Makale MT, McDonald CR, Hattangadi-Gluth JA, et al. Mechanisms of radiotherapy-associated cognitive disability in patients with brain tumours. *Nat Rev Neurol* 2017; 13: 52–64.
52. Le Rhun E, Dhermain F, Vogin G, et al. Radionecrosis after stereotactic radiotherapy for brain metastases. *Expert Rev Neurother* 2016; 16: 903–914.
53. Monje ML, Mizumatsu S, Fike JR, et al. Irradiation induces neural precursor-cell dysfunction. *Nat Med* 2002; 8: 955–962.
54. Raber J, Rola R, LeFevour A, et al. Radiation-induced cognitive impairments are associated with changes in indicators of hippocampal neurogenesis. *Radiat Res* 2004; 162: 39–47.
55. Braun U, Schafer A, Walter H, et al. Dynamic reconfiguration of frontal brain networks during executive cognition in humans. *Proceedings of the National Academy of Sciences* 2015; 112: 11678–11683.
56. Duering M, Gonik M, Malik R, et al. Identification of a strategic brain network underlying processing speed deficits in vascular cognitive impairment. *Neuroimage* 2013; 66: 177–183.
57. Bressler SL, Kelso JA. Cortical coordination dynamics and cognition. *Trends Cogn Sci* 2001; 5: 26–36.
58. Connor M, Karunamuni R, McDonald C, et al. Regional susceptibility to dose-dependent white matter damage after brain radiotherapy. *Radiotherapy and Oncology* 2017; 123: 209–217.
59. Lin J, Lv X, Niu M, et al. Radiation-induced abnormal cortical thickness in patients with nasopharyngeal carcinoma after radiotherapy. *Neuroimage Clin* 2017; 14: 610–621.
60. Nagtegaal SHJ, David S, van der Boog ATJ, et al. Changes in cortical thickness and volume after cranial radiation treatment: A systematic review. *Radiotherapy and Oncology* 2019; 135: 33–42.
61. Seibert TM, Karunamuni R, Kaifi S, et al. Cerebral Cortex Regions Selectively Vulnerable to Radiation Dose-Dependent Atrophy. In: *International Journal of Radiation Oncology Biology Physics*. 2017, pp. 910–918.
62. Simó M, Vaquero L, Ripollés P, et al. Longitudinal brain changes associated with prophylactic cranial irradiation in lung cancer. *Journal of Thoracic Oncology* 2016; 11: 475–486.
63. Nagtegaal SHJ, David S, Snijders TJ, et al. Effect of radiation therapy on cerebral cortical thickness in glioma patients: Treatment-induced thinning of the healthy cortex. *Neuro-Oncology Advances*; 2. Epub ahead of print 2020. DOI: 10.1093/nojnl/vdaa060.
64. Nagtegaal SHJ, David S, Philippens MEP, et al. Dose-dependent volume loss in subcortical deep grey matter structures after cranial radiotherapy. *Clin Transl Radiat Oncol* 2021; 26: 35–41.

65. Simo M, Vaquero L, Ripolles P, et al. Brain damage following prophylactic cranial irradiation in lung cancer survivors. *Brain Imaging Behav* 2016; 10: 283–295.
66. Brown PD, Ballman KV, Cerhan JH, et al. Postoperative stereotactic radiosurgery compared with whole brain radiotherapy for resected metastatic brain disease (NCCTG N107C/CEC-3): a multicentre, randomised, controlled, phase 3 trial. *Lancet Oncology* 2017; 118: 1049–1060.
67. El Shafie RA, Paul A, Bernhardt D, et al. Evaluation of Stereotactic Radiotherapy of the Resection Cavity After Surgery of Brain Metastases Compared to Postoperative Whole-Brain Radiotherapy (ESTRON)-A Single-Center Prospective Randomized Trial. *Neurosurgery* 2018; 83: 566–573.
68. El Shafie RA, Paul A, Bernhardt D, et al. Robotic Radiosurgery for Brain Metastases Diagnosed With Either SPACE or MPRAGE Sequence (CYBER-SPACE)-A Single-Center Prospective Randomized Trial. *Neurosurgery* 2019; 84: 253–260.
69. Grosu A, Frings L, Bentsalo I, et al. Whole-brain irradiation with hippocampal sparing and dose escalation on metastases: neurocognitive testing and biological imaging (HIPPORAD) – a phase II prospective randomized multicenter trial (NOA-14, ARO 2015–3, DTK-ROG). *BMC Cancer* 2020; 20: 1–13.
70. Schimmel WCM, Verhaak E, Hanssens PEJ, et al. A randomised trial to compare cognitive outcome after gamma knife radiosurgery versus whole brain radiation therapy in patients with multiple brain metastases: Research protocol CAR-study B. *BMC Cancer* 2018; 18: 218.
71. Wefel JS, Vardy J, Ahles T, et al. International Cognition and Cancer Task Force recommendations to harmonise studies of cognitive function in patients with cancer. *Lancet Oncol* 2011; 12: 703–708.
72. Wilke C, Grosshans D, Duman J, et al. Radiation-induced cognitive toxicity: Pathophysiology and interventions to reduce toxicity in adults. *Neuro Oncol* 2018; 20: 597–607.
73. Rick O, Dauelsberg T, Kalusche-Bontemps EM. Oncological Rehabilitation. *Oncol Res Treat* 2017; 40: 772–777.
74. Tsai PF, Yang CC, Chuang CC, et al. Hippocampal dosimetry correlates with the change in neurocognitive function after hippocampal sparing during whole brain radiotherapy: A prospective study. *Radiation Oncology* 2015; 10: 253.
75. Lin S-Y, Yang C-C, Wu Y-M, et al. Evaluating the impact of hippocampal sparing during whole brain radiotherapy on neurocognitive functions: A preliminary report of a prospective phase II study. *Biomed J* 2015; 38: 439–449.
76. Brown PD, Pugh S, Laack NN, et al. Memantine for the prevention of cognitive dysfunction in patients receiving whole-brain radiotherapy: A randomized, double-blind, placebo-controlled trial. *Neuro Oncol* 2013; 15: 1429–1437.
77. Mehta MP, Shapiro WR, Phan SC, et al. Motexafin Gadolinium Combined With Prompt Whole Brain Radiotherapy Prolongs Time to Neurologic Progression in Non-Small-Cell Lung Cancer Patients With Brain Metastases: Results of a Phase III Trial. *Int J Radiat Oncol Biol Phys* 2009; 73: 1069–1076.
78. Belderbos J, de Ruyscher D, de Jaeger K, et al. Phase III Randomized Trial of Prophylactic Cranial Irradiation With or Without Hippocampus Avoidance in SCLC. *SSRN Electronic Journal*. Epub ahead of print 2020. DOI: 10.2139/ssrn.3708322.
79. Brown PD, Gondi V, Pugh S, et al. Hippocampal avoidance during whole-brain radiotherapy plus memantine for patients with brain metastases: Phase III trial NRG oncology CC001. *Journal of Clinical Oncology* 2020; 38: 1019–1029.



3

Different profiles of neurocognitive functioning in patients with brain metastases prior to brain radiotherapy

Eva E. van Grinsven, Fia Cialdella, Joost J.C. Verhoeff, Marielle E.P. Philippens,
& Martine J.E. van Zandvoort

Psycho-Oncology (2023)

ABSTRACT

Objective

Patients with brain metastases (BMs) are a heterogeneous population, with almost 50% experiencing cognitive impairment before brain radiotherapy. Defining pre-radiotherapy cognitive profiles will aid in understanding of the cognitive vulnerabilities and offer valuable insight and guidance for tailoring interventions.

Methods

The study population consisted of 58 adult patients with BMs referred for radiotherapy. A semi-structured interview and comprehensive battery including 10 neuropsychological tests were used to assess subjective and objective cognitive performance prior to radiotherapy.

Results

A majority (69%) of patients report decline in cognitive performance compared to their premorbid level (i.e. pre-cancer). Objective testing revealed memory (52%), processing speed (33%) and emotion recognition (29%) deficits were most frequent. 21% of patients had no cognitive deficits while 55% had deficits (-1.5SD) in at least two cognitive domains. Hierarchical cluster analysis based on patient deficit profiles identified four clusters: (I) no or limited cognitive deficits selectively restricted to processing speed or executive function, (II) psychomotor speed deficits, (III) memory deficits and (IV) extensive cognitive deficits including memory. No patient or clinical-related (e.g. age, number of BMs, previous treatment) differences were found between clusters.

Conclusions

Patterns of cognitive performance in patients with BMs are heterogeneous, with most experiencing at least some degree of neurocognitive dysfunction. We identified four meaningful cognitive clusters. Stability of these clusters over time and in different samples should be assessed to advance understanding of the cognitive vulnerability of this patient population.

INTRODUCTION

Brain metastases (BMs) occur in 10-30% of the adult cancer population and this incidence continues to rise.^{1,2} Thereby, BMs are the most common type of brain tumor.³ Median overall survival despite systemic and local treatment is limited, spanning months to several years, depending on factors such as number of BMs, Karnofsky performance status (KPS)⁴, and the primary tumor.⁵⁻⁷ Treatment for BMs consists of different options, including radiotherapy, surgery, chemotherapy, immunotherapy or a combination.⁸ In this vulnerable population, treatment (shared) decisions are tailored toward gaining the best disease control while maintaining acceptable quality of life (QoL) during the remaining life span.

Already before starting BMs-specific treatment, a large percentage of patients experience cognitive problems; half of the patients demonstrate cognitive impairment on minimally one cognitive domain.⁹⁻¹² Multiple cognitive domains can be affected, with impairments reported in memory, executive function, and processing speed. However, substantial variability exists both within and between subjects in terms of cognitive domains of dysfunction. The pathogenesis of this pre-treatment cognitive performance is still incompletely understood, but both tumor-related factors (e.g. primary cancer, number of BMs) as well as treatment-related factors (e.g. previous chemotherapy) seem involved.^{11,13-15}

Previous research predominantly focused on cognitive performance on group-level using a confined set of cognitive tests. However, the heterogeneity of this patient population calls for a more individualized approach using an elaborate test battery. This will aid thorough understanding of the cognitive vulnerabilities and offer valuable insights for tailoring future interventions and optimizing patient-centered care. Therefore, the main aim was to extensively describe and classify the cognitive performance of patients with BMs before brain radiotherapy, using both group- and individual statistics. Additionally, we used hierarchical cluster analysis to provide data-driven comprehensive understanding of the cognitive deficits and their interconnections. Additionally, we assessed the added value of an elaborate versus a core test battery in defining cognitive functioning of this heterogeneous population.

METHODS

Study set-up and population

Data was prospectively collected from the Cohort for patient-reported Outcomes, Imaging and trial inclusion in Metastatic BRAIn disease (COIMBRA, NCT05267158) and Assessing and Predicting Radiation Influence on Cognitive Outcome using the cerebrovascular stress Test (APRICOT) study. The study population consisted of adult patients (≥ 18 years) with either radiographic and/or histologic proof of BMs referred to the University Medical Center Utrecht (UMCU) for radiotherapy. Patients were non-eligible if they were unable to understand the Dutch language or had developmental, psychiatric, or cognitive disorders that hindered the patients' understanding of the informed consent procedure. For both studies, neurocognitive assessments (NCAs) were performed before, 3 months and ≥ 11 months after radiotherapy (see the **Supplementary Materials** for additional study procedures and exclusion criteria). The studies were performed in accordance with the Declaration of Helsinki¹⁶ and the UMCU institutional ethical review approved both the COIMBRA and APRICOT study (#18-642 and #18-747, respectively). Written informed consent was obtained from all participants prior to participation.

Data collection

Subjective cognitive complaints

Prior to the NCA, subjective cognitive experience was assessed using a semi-structured interview regarding complaints on six different cognitive domains (memory, orientation, attention & executive functioning, processing speed, language, emotions), comparable to the structured interview regularly used in neuropsychological settings (**Supplementary Materials**). Based on the answers and reported interference with everyday life, the neuropsychologist rated each domain as cognitive complaints present (yes/no). In order to be classified as present, one complaint per domain sufficed. Additionally, patients rated their subjective cognitive functioning regarding thinking, memory, attention, perception, language and processing speed using visual analogue scales (VAS), similar to Schoo and colleagues.¹⁷ The VAS consisted of a 100 mm vertical line on A3-sized paper, where the top represents perfect and the bottom worst performance. Patients marked the line at their previously experienced premorbid subjective functioning level (i.e. prior to the primary cancer diagnosis) as well as for their current level (i.e. prior to the radiotherapy). This resulted in an estimation ranging from 0 to 100. A difference score was calculated for each cognitive concept to assess change in subjective functioning compared to premorbid levels. This was categorized into stable (± 5), subtle improvement/decline ($\pm 6-25$), substantial improvement/decline ($\pm 26-50$) and

extreme improvement/decline ($\pm > 50$). Patients indicated their current stress levels using the same VAS-methodology, with higher scores indicating more stress, and lower scores indicating lower stress.

Neurocognitive assessment

A comprehensive NCA was used to assess objective cognitive performance. All tests are internationally widely used, standardized psychometric instruments for assessing neurocognitive deficits in the major neurocognitive domains. While neuropsychological tests often tap into more than one neurocognitive domain, tests were classified into different neurocognitive domains based on available literature and clinical experience. In our clinical practice, we assess fatigue by repeating the Digit Span Forward twice during the NCA, once halfway and once at the end. The maximum span reached by the patient at the repeated assessments is compared to the initial maximum span. If the maximum span decreased, this is taken as indication of cognitive fatigue. This approach was also used in this study. NCAs were performed by trained personnel and were planned to be completed within approximately 90 minutes.

The comprehensive battery was compared to the core battery. The core battery represents tests advised by the International Cancer and Cognition Task Force (ICCTF)¹⁸ combined with tests frequently used in previous BMs research⁹. The comprehensive battery encompasses the core battery complemented by additional neuropsychological tests (**Supplementary Table 1**).

For current analyses the cognitive data acquired prior to radiotherapy from October 2020 to January 2023 was used. Each neuropsychological test was scored according to standardized scoring criteria. The uncorrected scores were transformed into z-scores based on the mean and standard deviation of control populations derived from published norm data and corrected for age and education where appropriate (see **Supplementary Table 1** for references of used norm data), with lower z-scores representing worse performance. Overall neurocognitive domain scores were calculated using the mean of the z-scores of the available tests within a domain. Overall neurocognitive domain scores were only calculated if a patient completed at least 50% of the tasks within the domain. Additionally, neurocognitive impairment in each domain was defined as $z\text{-score} \leq -1.5$ on any of the administered tests within the domain to ensure both specificity and sensitivity to cognitive difficulties experienced by patients.

Patient characteristics

Patient characteristics were obtained from the semi-structured interview and electronic patient files (HiX, Chipsoft, The Netherlands). This included sex, age at inclusion, level of education according to the Verhage criteria¹⁹, handedness, KPS⁴, primary tumor, presence of extracranial metastases, time since BMs diagnosis, previous anti-tumor therapy, dexamethasone dose 1-5 days prior to radiotherapy, and symptoms at BMs diagnosis. As part of standard medical care, the pre-radiotherapy MRI scans of each patient were evaluated to determine the number of BMs, hemisphere, and lobe involvement.

Statistical analyses

Analyses were performed using SPSS (IBM SPSS Statistics, 25.0.0). Statistical significance was set at $p < 0.05$, adjusted for multiple comparisons when necessary. Cognitive test scores were analyzed using different methods:

1. *Group-level*: comparison of mean Z-score of the sample with normative performance for each domain ("domain-level") and each task ("task-level") using one-sample t-tests (with the null hypothesis $Z=0$, meaning no difference between patients and expected normative performance) or Wilcoxon-signed rank tests, depending on normality of data distribution.
2. *Individual-level*: the percentage of patients with test performance below the impairment threshold ($Z \leq -1.5$) was calculated for each domain ("domain-level") and each task ("task-level"). To assess the relationship between subjective and objective cognitive performance, subjective complaints were compared between patients with versus without impairment on the domain-level using chi-square tests and Mann-Whitney U tests for categorical and continuous data, respectively. To assess the influence of stress on cognitive performance, correlation analyses were performed between stress and domain-level cognitive performance (see **Supplementary Results**). Additionally, the domain-level impairments were descriptively compared between the comprehensive and the core battery.
3. *Exploratory cluster analysis*: with a data-driven approach patients were clustered based on similarities in deficits at the domain-level using Ward's linkage with squared Euclidean distance. The number of distinguishable clusters was selected by visual inspection of the dendrogram and confirmed by discriminant function analysis. As cluster analysis uses complete cases, only patients with data for all included cognitive domains were considered. To assess how domain-level deficits differed across clusters and whether patient and/or clinical characteristics (see **Supplementary Table 2** for specific variables) differed

across clusters, chi-square tests were performed for categorical data and Mann-Whitney U-test for continuous data.

Results

Clinical characteristics

58 patients (31 men) were included in the analyses. The median age was 66 years. Most patients had two or more BMs (72%) and BMs most often originated from lung cancer (50%). More than half of patients (62%) presented with symptoms at time of the BMs diagnosis which mostly included epilepsy, motor symptoms and/or headache. The majority of patients (74%) was receiving or had received previous anti-tumor therapy (i.e. chemo- or immunotherapy; **Supplementary Materials**).

Subjective cognitive complaints

During the semi-structured interview, the majority of patients reported cognitive fatigue (62%; **Supplementary Table 3**). Additionally, both motor and sensory problems were frequently reported (38% and 22%, respectively). Cognitive complaints were reported across all domains with 59% of patients reporting cognitive problems in at least one domain. Subjective decline compared to previously experienced premorbid functioning was reported in at least one cognitive domain by 69%, with decline in two or more domains reported by 55%. Both subjective complaints and cognitive decline were most frequently reported for memory (38% and 40%, respectively) and attention & executive functioning (38% and 43%, respectively; **Figure 1**). Mean self-reported stress levels were 27 (SD=26), with 11% of patients reporting levels of ≥ 50 . The majority of patients (64%) reported their stress was related to the cancer diagnosis and upcoming treatment.

Neurocognitive data

Neurocognitive functioning

Group-level: On the domain-level, group performance was worse compared to the normative population for memory, processing speed and psychomotor speed. On the contrary, performance on visuospatial functioning was better than the norm population. On the task-level, patients' cognitive performance was significantly lower than the norm data for multiple memory tests (Hopkins Verbal Learning Test – Revised (HVLT-R), semantic fluency), processing speed (STROOP naming), psychomotor speed (Grooved Pegboard dominant and non-dominant hand), and social cognition (FEEST total). Contrarily, mean Z-scores were better than the norm population for tests on attention (Trail Making Test, switching), memory (VAT – delayed), and visuospatial functioning (Hooper Visual Organization Test fragmented).

Group performance for all other (sub)tests were not significantly different from the norm population (**Supplementary Table 4**).

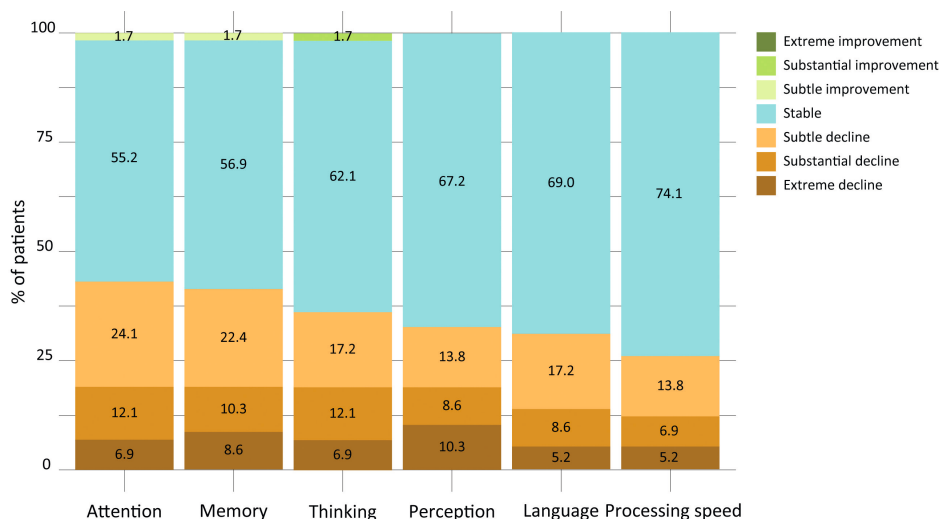


Figure 1. Stacked bar chart comparing pre-radiotherapy to the pre-cancer performance showing the percentage of patients reporting subjective improved, stable or declined performance for each cognitive domain ordered from most decline to least decline. Colors indicate extreme improvement (dark green), substantial improvement (green), subtle improvement (light green), stable performance (blue), subtle decline (light orange), substantial decline (orange) and extreme decline (dark orange). Values shown inside the bar are exact percentages of patients within that category.

Note: stable performance (± 5), subtle improvement or decline ($\pm 6-25$), substantial improvement or decline ($\pm 26-50$) and extreme improvement or decline ($\pm > 50$). Abbreviations: EF, executive functioning.

Individual-level: On the domain-level, severe deficits ($-2.0SD$) were most often observed for memory (35%), psychomotor speed (32%), and processing speed (28%). More subtle deficits ($-1.5SD$ or $-1.0SD$) were found for attention (16% and 40%, respectively) and executive function (22% and 50%, respectively). Deficits in visuospatial functioning were least often found. On the task-level, cognitive impairments were detected across all tests. The percentages of patients with severe cognitive impairments ($-2.0SD$) were highest for HVLt-R (recognition: 32%, immediate 20%, delayed 16%), Grooved Pegboard (dominant: 26%, non-dominant 22%) and STROOP naming speed (19%). More subtle deficits ($-1.5SD$) were observed for the FEEST (29%) and the semantic fluency task (25%; **Figure 2**).

Despite signs of cognitive fatigue in approximately 20% of patients, the current patient sample successfully completed over 90% of the tests of the comprehensive NCA within the intended 90 minutes (**Supplementary Materials**). Comparison of the comprehensive with the core test battery shows that in particular patients with two or more cognitive deficits are 'misclassified' into the group of patients with less cognitive deficits when using the core battery only (**Supplementary Figure 3**). Differences were mostly due to differences in deficits within the domains of attention, executive function and processing speed (based on STROOP performance), while almost no differences were found for memory (**Table 1**).

Table 1. Number and percentage of patients with an impairment within a domain when either determined using the core versus the comprehensive battery.

Cognitive domains	Core, n (%)	Comprehensive, n (%)	Task contributing to difference
Attention	4 (6.9)	9 (15.5)	STROOP IV/III ($n = 5$)
Executive function	12 (20.7)	13 (22.4)	STROOP III/I ($n = 1$)
Memory	28 (49.1)	30 (51.7)	VAT immediate ($n = 2$) ROCFT delay ($n = 1$)
Processing speed	9 (15.5)	19 (33.3)	STROOP I ($n = 8$) STROOP II ($n = 7$)
Psychomotor speed	22 (39.3)	22 (39.3)	NA
Visuospatial functioning	NA	5 (9.1)	Rey Copy ($n = 5$)
Social cognition	NA	10 (29.4)	FEEST ($n = 10$)

Note: Number of patients mentioned behind task names indicate the number of patients this specific task made a difference for when comparing the core with the comprehensive battery. As task deficits are not mutually exclusive, patients can exhibit deficits on more than one task within one domain both contributing to the difference between core and comprehensive. For example, one patient with a memory impairment had deficits on both the VAT immediate recall and the Rey delayed recall. Abbreviations: FEEST, Facial Expressions of Emotion – Stimuli and Tests; ROCFT, Rey Osterieth Complex Figure Test; VAT, Visual Association Test.

Exploratory cluster analysis

Cluster analysis was performed for 56/58 patients using the individual domain-level impairment for the cognitive domains, as two patients were excluded due to missing data regarding psychomotor speed and/or processing speed. Scores for social cognition were not included in this cluster analysis due to a substantial number of patients ($n=24$) with missing data (**Supplementary Figure 2**). The dendrogram provided evidence for two-, three-, four-, and five-cluster solution, with reasonable separation between clusters. A multivariate test of group differences was performed using canonical linear discriminant function analysis, which confirmed a maximum of four clusters could be adequately differentiated with 97% classification accuracy

($\Lambda = 0.03$, $\chi^2(18) = 196.75$, $p < .001$). This indicates that each cluster showed distinct intra-individual profiles regarding the cognitive impairment across domains.

Subsequently, all clusters were compared regarding the proportion of patients with cognitive impairments (**Figure 3**). Attention impairments did not differ between any of the clusters. Cluster IV had significantly more patients with an executive function impairment (55%) compared to both cluster I (14%) and cluster II (0%), but did not differ from cluster III (22%, $p = .032$, $\varphi = .397$). When considering memory impairment, cluster III and IV both had more patients with an impairment (100% and 91%, respectively), than clusters I and II (0% and 17%, respectively, $p < .001$, $\varphi = .936$). Cluster IV had most patients with impairments in processing speed (100%) compared to all other clusters. Additionally, Cluster I had more patients with processing speed impairments (33%) than Cluster III (0%, $p < .001$, $\varphi = .786$). Psychomotor impairments were more frequent among cluster II (100%) than cluster I (0%) and cluster III (33%). Cluster IV also had more patients with psychomotor impairment (73%) than cluster I ($p < .001$, $\varphi = .634$). Lastly, cluster II had significantly more patients with a visuospatial functioning impairment (33%) than cluster I (0.0%; $p = .049$, $\varphi = .375$). There were significant differences between clusters regarding the number of impaired cognitive domains ($p < .001$). Post-hoc tests indicated cluster IV had significantly more impaired cognitive domains compared to all clusters (all $p \leq .001$), and cluster III had more cognitive impairments than cluster I ($p = .008$). Thus, cluster I and II represent the patients with the least number of cognitive impairments.

Based on the different neurocognitive profiles, the clusters were identified as 'no or limited cognitive deficits restricted to processing speed or executive function' (cluster I), 'psychomotor speed impairment' (cluster II) and two clusters with memory impairments (cluster III and IV). Cluster IV exhibited multiple additional cognitive impairments and was therefore named 'Memory + multiple impairments' (**Figure 3**). None of the clusters differed regarding any of the patient or clinical characteristics listed in **Supplementary Table 2**.

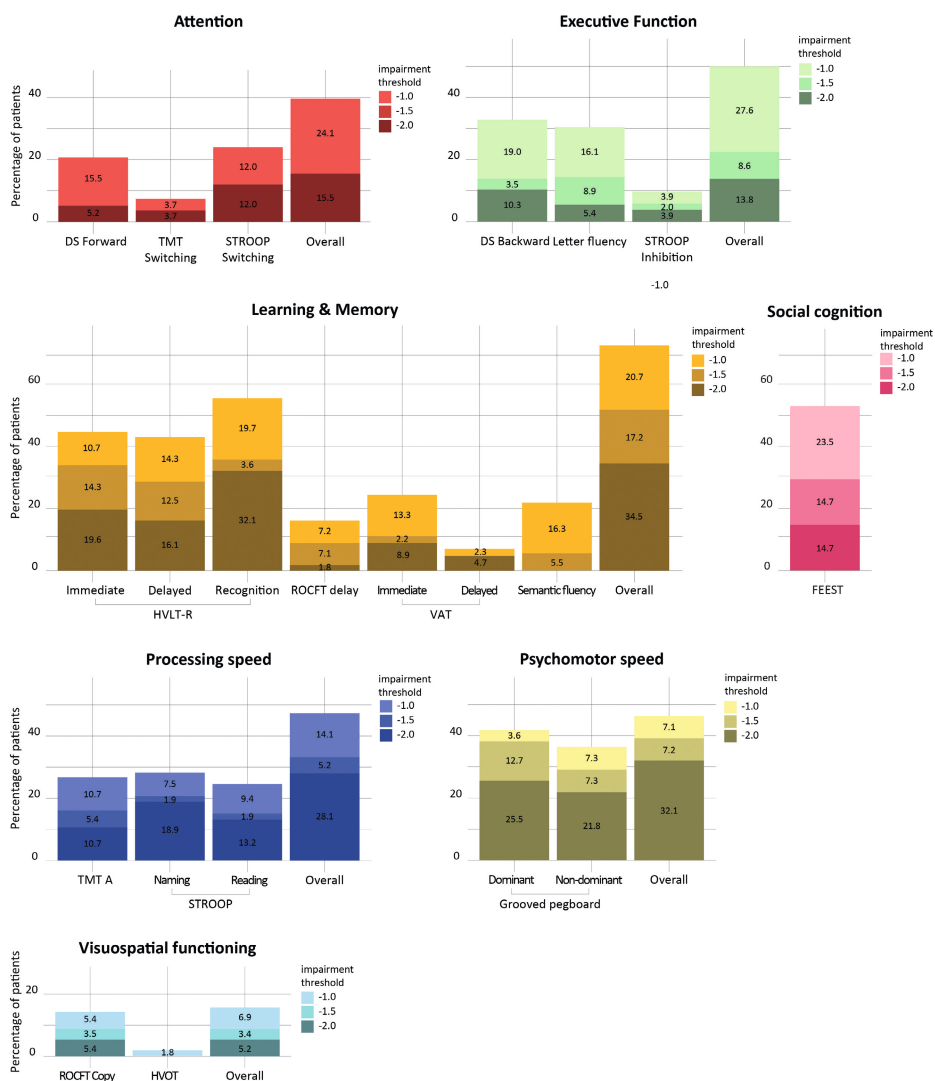


Figure 2. Stacked bar graphs of percentage of patients with a cognitive impairment pre-radiotherapy at certain thresholds grouped per cognitive domain. Each task and overall domain scores are shown. Colors indicate the cognitive impairment at different threshold of ≤ -2.0 (dark colored), ≤ -1.5 (medium colored), and ≤ -1.0 (light colored). Values within the bars represent the exact percentage of patients within an impairment category.

Abbreviations: DS, digit span; FEEST, Facial Expressions of Emotion – Stimuli and Tests; HVLT-R, Hopkins Verbal Learning Test – Revised; HVOT, Hooper Visual Organization Test; ROCF, Rey Osterieth Complex Figure Test; TMT, trail making test; VAT, Visual Association Test.

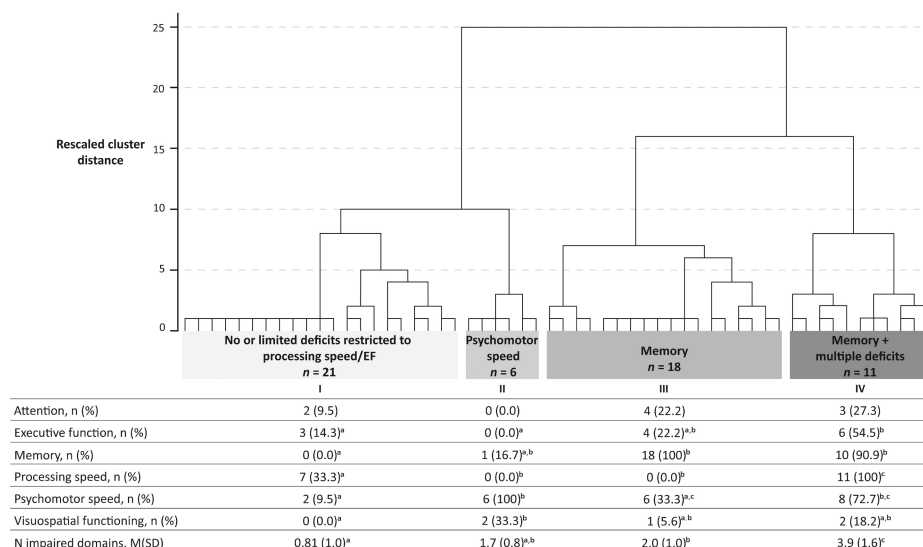


Figure 3. Dendrogram of the cluster analysis performed on the presence/absence of cognitive impairments across all cognitive domains except social cognition. Numbers I-IV indicate the different clusters. The table below shows number and percentage of patients per cluster with a cognitive impairment ($-1.5SD$) on the different cognitive domains. Clusters with different subscripts showed a statistically significant difference ($p < .05$).

DISCUSSION

This prospective study aimed to describe and classify the individual cognitive performance of patients with BMs prior to radiotherapy. Results indicated that impairments in neurocognitive functioning occur frequently; almost 80% of patients had cognitive deficits ($Z \leq -1.5$) in at least one cognitive domain before starting radiotherapy. The most commonly affected cognitive domains included memory, processing speed, psychomotor speed, and social cognition. When applying more stringent thresholds ($Z \leq -2.0$), less than one third of patients were not affected. Thus, nearly all BMs patients referred for radiotherapy experience some degree of neurocognitive dysfunction.

Correspondingly, almost 70% of patients experienced a decline in subjective cognitive functioning compared to their indicated premorbid level, with decline in two or more domains reported by 55%. Decline was reported across all domains, but were most often labelled as attention, memory and thinking. Interestingly, the majority reported stable performance, with some (2%) even reporting improved performance. There could have been a positive bias due to dexamethasone-induced euphoria, which could have led to overall more positive self-reported

cognitive performance.²⁰ While subjective experience was not directly related to the objective cognitive performance, as in the majority of previous studies²¹, both measures did show differentiated profiles across the distinctive neurocognitive domains. Firstly, this indicates that patients are able to differentiate between their premorbid and their current cognitive performance using VAS. Secondly, our results suggest patients have domain-specific self-awareness of their cognitive functioning, similar to participants in a previous study.¹⁷ These findings demonstrate that utilizing domain-specific questions, particularly through the application of VAS, can offer valuable understanding of subjective experiences and serve as a practical tool for psycho-education.

Neurocognitive functioning prior to radiotherapy was characterized by large intra-individual differences. Previous studies have reported 53-67% of BMs patients exhibit cognitive impairments on at least one cognitive test prior to radiotherapy.^{11,12,22,23} While we found 79% of patients had at least one cognitive impairment, this difference is likely due to the more comprehensive NCA performed in the current study, suggesting the reported numbers in the literature may be too low. On some tests patients with BMs, however, outperformed the norm scores, which should be interpreted in term of their motivation and effort to perform well.²⁴ Stress appeared unrelated to their cognitive performance, pointing out that experienced stress cannot explain the differences with the norm population. While cognitive fatigue half-way through the NCA was related to overall slower information processing speed, it was unrelated to deficits within this domain.

Using a data-driven, exploratory hierarchical cluster analysis we examined patterns of cognitive profiles in our BMs sample and found a four-cluster solution providing meaningful cognitive profiles. Separation between clusters was mainly based on the presence or absence of memory deficits. The group of patients with memory deficits ($n=29$) included a subgroup ($n=11$) with impairments across domains and worst overall cognitive performance. In the non-memory group, a substantial number of patients ($n=21$) had either no impairments or impairments restricted to processing speed or executive function. The discerned clusters can contribute to patient-centered care through development of psycho-education for patients and caregivers, thereby enhancing coping mechanisms and managing expectations in line with their profile. Moreover, knowledge of these clusters offers insights into cognitive support strategies for each specific cluster. For example, patients in Cluster III with relatively intact cognitive functions except for memory impairment may require different cognitive strategies (e.g. metacognitive training²⁵) compared to Cluster IV patients with a wide range of cognitive impairments. While our sample

size ($n=56$) may be considered small for cluster analyses, the significant cognitive differences observed and the meaningfulness of these differences, support the value of this exploratory cluster analysis and its potential relevance to reduce the cognitive heterogeneity in this population. No patient- nor clinical factors (e.g. number of BMs, primary tumor, previous treatment) were related to the clusters. In future studies we will assess whether cluster membership has predictive value for the trajectory of cognitive performance after treatment and whether they can be linked to biological substrates. If so, this could improve understanding of the pathophysiology of cognitive performance in these patients.

Clinical implications

Similar to previous studies, memory deficits were prominent in our sample^{11,12,22,23} with severe memory impairment in one out of every three patients. Moreover, in the cluster analysis the presence of memory deficits was a major determining factor. As declines in memory performance have been reported in up to 50% of patients one to four months after radiotherapy^{11,22,26}, this highlights the cognitive vulnerability of this patient population. Additionally, in both the group- and individual analyses processing speed and psychomotor speed deficits were frequent. Processing speed relies on a widespread neural network, which can be altered by the presence of a tumor within that network.^{27,28} Psychomotor slowing is often experienced as a consequence of chemotherapy-induced neuropathy.^{29,30} Accordingly, a significant majority of patients with psychomotor impairment had received chemotherapy (68%), compared to half of those with processing speed impairments. Patients who reported sensory problems were more likely to have psychomotor speed impairments, regardless of whether sensory problems were attributed to neuropathy by patients themselves or not. Overall, this implies it is important to distinguish psychomotor from processing speed deficits within this population.

Almost one third of the BMs patients showed impaired social cognition, specifically emotion recognition. This significantly impacts both patient and caregiver QoL as it enables us to process social information and respond appropriately in social contexts.^{31,32} Stress has been linked to worse emotion recognition^{33,34}, and can also be a side-effect of dexamethasone.²⁰ Nevertheless, neither self-reported stress levels nor dexamethasone use were related to emotion recognition in our sample. Social cognition has not received wide-spread attention yet, and thus only few studies in brain tumor patients exist.³⁵⁻³⁸ A recent study found that before surgery patients with low-grade glioma performed worse on emotion recognition tasks than healthy controls and these deficits remained stable after surgery.³⁵ Further research

is needed on social cognition in the long-term to gain better understanding of the underlying mechanisms and the potential effects of brain radiotherapy.

In the current study we employed an elaborate cognitive test battery comprising 10 neuropsychological tests. While signs of cognitive fatigue were present in about 20% of patients throughout the NCA, the current patient sample was able to complete more than 90% of the tests and most finished within the intended ninety minutes. This illustrates that performing a comprehensive NCA within this vulnerable patient sample is feasible. The comparison between the comprehensive and the core battery indicated that the core battery cannot adequately detect the severity of cognitive deficits. That is, the extent of cognitive deficits (i.e. number of impaired domains) is often underestimated when solely using the core battery. The differences mainly stemmed from performance variations on the STROOP task, which measures attention, executive function, and information processing speed, while minimal differences were observed in the memory domain. Hence, the STROOP task holds significant potential for assessing cognitive performance in this population. Next, we will investigate the value of the comprehensive battery in assessing treatment-related cognitive decline in order to develop a concise yet comprehensive battery for future use in this heterogeneous population.

3

Study limitations

Selection bias may have played a role in our study as only those patients both willing and fit enough to perform a comprehensive NCA were included in the studies. We compared patient and clinical characteristics between the patients included in the less intense COIMBRA versus the APRICOT study. Only KPS was slightly higher in the patients of the APRICOT study, indicating no major differences in patient selection between the studies (**Supplementary Materials**). Additionally, we grouped tests based on their shared conceptual background (“domain”) in order to enhance power and aid interpretation, even though performance on one task relies on more than one cognitive concept. For comparability, we reanalyzed the data using the domain categorization defined by the ICCTF, which indicated that differences between the comprehensive and core battery remained unchanged.

CONCLUSION

In the current study we demonstrated the pre-existing cognitive vulnerability of BMs patients as nearly all patients experienced some degree of neurocognitive dysfunction prior to brain radiotherapy. This neurocognitive dysfunction could be clustered into meaningful cognitive profiles, but future studies with larger samples

should validate these profiles. Advancing our understanding of the vulnerability that results in treatment-related cognitive decline and the origins of the cognitive dysfunction, is likely to facilitate the development of new strategies for patient-centered treatment and rehabilitation.

SUPPLEMENTARY MATERIALS



REFERENCES

1. Gerstenecker A, Nabors LB, Meneses K, et al. Cognition in patients with newly diagnosed brain metastasis: Profiles and implications. *J Neurooncol* 2014; 120: 179–185.
2. Achrol AS, Rennert RC, Anders C, et al. Brain metastases. *Nat Rev Dis Primers*; 5. Epub ahead of print 2019. DOI: 10.1038/s41572-018-0055-y.
3. Lambda N, Wen PY, Aizer AA. Epidemiology of Brain Metastases and Leptomeningeal Disease. *Neuro Oncol*.
4. Oken MM, Creech RH, Tormey DC, et al. Toxicity and response criteria of the Eastern Cooperative Oncology Group. *American Journal of Clinical Oncology: Cancer Clinical Trials* 1982; 5: 649–656.
5. Gaspar L, Scott C, Rotman M, et al. Recursive partitioning analysis (RPA) of prognostic factors in three Radiation Therapy Oncology Group (RTOG) brain metastases trials. *Int J Radiat Oncol Biol Phys* 1997; 37: 745–751.
6. Sperduto PW, Kased N, Roberge D, et al. Summary report on the graded prognostic assessment: An accurate and facile diagnosis-specific tool to estimate survival for patients with brain metastases. *Journal of Clinical Oncology* 2012; 30: 419–425.
7. Sperduto PW, Chao ST, Sneed PK, et al. Diagnosis-specific prognostic factors, indexes, and treatment outcomes for patients with newly diagnosed brain metastases: a multi-institutional analysis of 4,259 patients. *Int J Radiat Oncol Biol Phys* 2010; 77: 655–661.
8. Eichler AF, Loeffler JS. Multidisciplinary management of brain metastases. *Oncologist* 2007; 12: 884–898.
9. Van Grinsven EE, Nagtegaal SHJ, Verhoeff JJC, et al. The Impact of Stereotactic or Whole Brain Radiotherapy on Neurocognitive Functioning in Adult Patients with Brain Metastases: A Systematic Review and Meta-Analysis. *Oncol Res Treat* 2021; 44: 622–636.
10. Mehta MP, Rodrigus P, Terhaard CHJ, et al. Survival and neurologic outcomes in a randomized trial of motexafin gadolinium and whole-brain radiation therapy in brain metastases. *Journal of Clinical Oncology* 2003; 21: 2529–2536.
11. Chang EL, Wefel JS, Maor MH, et al. A pilot study of neurocognitive function in patients with one to three new brain metastases initially treated with stereotactic radiosurgery alone. *Neurosurgery* 2007; 60: 277–283.
12. Habets EJJ, Dirven L, Wiggeraad RG, et al. Neurocognitive functioning and health-related quality of life in patients treated with stereotactic radiotherapy for brain metastases: A prospective study. *Neuro Oncol* 2016; 18: 435–444.
13. Schimmel WCM, Gehring K, Hanssens PEJ, et al. Cognitive functioning and predictors thereof in patients with 1–10 brain metastases selected for stereotactic radiosurgery. *J Neurooncol* 2019; 145: 265–276.
14. Steinmann D, Schäfer C, van Oorschot B, et al. Effects of Radiotherapy for Brain Metastases on Quality of Life (QoL). *Strahlentherapie und Onkologie* 2009; 185: 190–197.
15. Meyers CA, Smith JA, Bezjak A, et al. Neurocognitive function and progression in patients with brain metastases treated with whole-brain radiation and motexafin gadolinium: results of a randomized phase III trial. *Journal of Clinical Oncology* 2004; 22: 157–165.

16. World Medical Association. World Medical Association Declaration of Helsinki: ethical principles for medical research involving human subjects. *JAMA* 2013; 310: 2191–2194.
17. Schoo LA, Van Zandvoort MJE, Biessels GJ, et al. Insight in cognition: Self-awareness of performance across cognitive domains. *Appl Neuropsychol* 2013; 20: 95–102.
18. Wefel JS, Vardy J, Ahles T, et al. International Cognition and Cancer Task Force recommendations to harmonise studies of cognitive function in patients with cancer. *Lancet Oncol* 2011; 12: 703–708.
19. Verhage F. Intelligentie en leeftijd bij volwassenen en bejaarden. *Koninklijke van Gorcum*.
20. Dietrich J, Rao K, Pastorino S, et al. Corticosteroids in brain cancer patients: Benefits and pitfalls. *Expert Rev Clin Pharmacol* 2011; 4: 233–242.
21. Prankeviciene A, Deltuva VP, Tamasauskas A, et al. Association between psychological distress, subjective cognitive complaints and objective neuropsychological functioning in brain tumor patients. *Clin Neurol Neurosurg* 2017; 163: 18–23.
22. Chang EL, Wefel JS, Hess KR, et al. Neurocognition in patients with brain metastases treated with radiosurgery or radiosurgery plus whole-brain irradiation: a randomised controlled trial. *Lancet Oncol* 2009; 10: 1037–1044.
23. van der Meer PB, Habets EJJ, Wiggenraad RG, et al. Individual changes in neurocognitive functioning and health-related quality of life in patients with brain oligometastases treated with stereotactic radiotherapy. *J Neurooncol* 2018; 139: 359–368.
24. Belayachi S, Majerus S, Gendolla G, et al. Are the carrot and the stick the two sides of same coin? A neural examination of approach/avoidance motivation during cognitive performance. *Behavioural Brain Research* 2015; 293: 217–226.
25. Cicerone KD, Goldin Y, Ganci K, et al. Evidence-Based Cognitive Rehabilitation: Systematic Review of the Literature From 2009 Through 2014. *Archives of Physical Medicine and Rehabilitation* 2019; 100: 1515–1533.
26. Brown PD, Jaeckle K, Ballman K V., et al. Effect of radiosurgery alone vs radiosurgery with whole brain radiation therapy on cognitive function in patients with 1 to 3 brain metastases a randomized clinical trial. *JAMA* 2016; 316: 401–409.
27. Hua B, Ding X, Xiong M, et al. Alterations of functional and structural connectivity in patients with brain metastases. *PLoS One* 2020; 15: 1–16.
28. Maesawa S, Bagarinao E, Fujii M, et al. Evaluation of resting state networks in patients with gliomas: Connectivity changes in the unaffected side and its relation to cognitive function. *PLoS One* 2015; 10: 1–13.
29. Miaskowski C, Mastick J, Paul SM, et al. Chemotherapy-Induced Neuropathy in Cancer Survivors. *J Pain Symptom Manage* 2017; 54: 204–218.e2.
30. Wefel JS, Vidrine DJ, Marani SK, et al. A prospective study of cognitive function in men with non-seminomatous germ cell tumors. *Psychooncology* 2014; 23: 626–633.
31. Adolphs R. The social brain: Neural basis of social knowledge. *Annu Rev Psychol* 2009; 60: 693–716.
32. Henry JD, Von Hippel W, Molenberghs P, et al. Clinical assessment of social cognitive function in neurological disorders. *Nat Rev Neurol* 2016; 12: 28–39.

33. Israelashvili J, Sauter D, Fischer A. Two facets of affective empathy: concern and distress have opposite relationships to emotion recognition. *Cogn Emot* 2020; 34: 1112–1122.
34. Hänggi Y. Stress and emotion recognition: An Internet experiment using stress induction. *Swiss Journal of Psychology* 2004; 63: 113–125.
35. Buunk AM, Gerritsen MJJ, Jeltema HR, et al. Emotion Recognition in Patients with Low-Grade Glioma before and after Surgery. *Brain Sci*; 12. Epub ahead of print 2022. DOI: 10.3390/brainsci12091259.
36. Chen P, Wang G, Ma R, et al. Multidimensional assessment of empathic abilities in patients with insular glioma. *Cogn Affect Behav Neurosci* 2016; 16: 962–975.
37. Goebel S, Mehdorn HM, Wiesner CD. Social cognition in patients with intracranial tumors: do we forget something in the routine neuropsychological examination? *J Neurooncol* 2018; 140: 687–696.
38. Campanella F, Shallice T, Ius T, et al. Impact of brain tumour location on emotion and personality: A voxel-based lesion-symptom mapping study on mentalization processes. *Brain* 2014; 137: 2532–2545.
39. John Hugh Court, Raven J. Manual for Raven's Progressive Matrices and Vocabulary Scales. Section 7, Research and References: Summaries of Published Normative Studies, Reliability Studies, Validity Studies, References to All Sections of the Manual. *Oxford Psychologists*.
40. *Wechsler Adult Intelligence Scale Fourth Edition (WAIS-IV-NL) Technische handleiding*. 2013.
41. Bouma A, Mulder J, Lindeboom J SB. *Handboek neuropsychologische diagnostiek*. Amsterdam: Pearson, 2012.
42. Drane DL, Yuspeh RL, Huthwaite JS, et al. Demographic characteristics and normative observations for derived-Trail Making Test indices. *Neuropsychiatry, Neuropsychology and Behavioral Neurology* 2002; 15: 39–43.
43. D.C. Delis EK, Kramer. JH. D-KEFS Color Word Interference Test, Nederlandse bewerking door I. Noens en van der I. Berckelaer-Onnes.
44. Harrison JE, Buxton P, Husain M, et al. Short test of semantic and phonological fluency: Normal performance, validity and test-retest reliability. *British Journal of Clinical Psychology* 2000; 39: 181–191.
45. Schmand B, Groenink SC, Van Den Dungen M. Letterfluency: Psychometric properties and Dutch normative data. *Tijdschrift voor Gerontologie en Geriatrie* 2008; 39: 64–76.
46. Benedict RHB, Schretlen D, Groninger L, et al. Hopkins Verbal Learning Test – Revised: Normative Data and Analysis of Inter-Form and Test-Retest Reliability. *The Clinical Neuropsychologist*, 1998, pp. 43–55.
47. Brandt J, Ralph H B Benedict. Hopkins Verbal Learning Test - Revised Professional Manual.
48. Tremblay MP, Potvin O, Callahan BL, et al. Normative data for the rey-osterrieth and the taylor complex figure tests in Quebec-French people. *Archives of Clinical Neuropsychology* 2015; 30: 78–87.
49. Lindeboom J, Schmand B, Meyer S, et al. Visual Association Test Manual.
50. Van Der Elst W, Van Boxtel MPJ, Van Breukelen GJP, et al. Normative data for the Animal, Profession and Letter M Naming verbal fluency tests for Dutch speaking participants and the effects of age, education, and sex. *Journal of the International Neuropsychological Society* 2006; 12: 80–89.
51. Grooved Pegboard Test User Instructions.

52. Tamkin AS, Rebecca Jacobsen. Age-related norms for the Hooper Visual Organization Test. *Journal of Clinical Psychology* 1984; 40: 1459-1463.
53. Dodich A, Cerami C, Canessa N, et al. Emotion recognition from facial expressions: A normative study of the Ekman 60-Faces Test in the Italian population. *Neurological Sciences* 2014; 35: 1015-1021.
54. Paxton JL, Peavy GM, Jenkins C, et al. Deterioration of visual-perceptual organization ability in Alzheimer's disease. *Cortex* 2007; 43: 967-975.



4

Individualized trajectories in post-radiotherapy neurocognitive functioning of patients with brain metastases

Eva E. van Grinsven, Fia Cialdella, Yoniet Gmelich Meijling, Joost J.C. Verhoeff, Marielle E.P. Philippons, & Martine J.E. van Zandvoort

Neuro-oncology Practice (Submitted)

ABSTRACT

Background

The increasing incidence of brain metastases (BMs) and improved survival rates underscore the necessity to investigate the effects of treatments on individuals. The aim of this study was to evaluate the individual trajectories of subjective and objective cognitive performance after radiotherapy in patients with BMs.

Methods

The study population consisted of adult patients with BMs referred for radiotherapy. A semi-structured interview and comprehensive neurocognitive assessment (NCA) were used to assess both subjective and objective cognitive performance before, 3 months and ≥ 11 months after radiotherapy. Reliable change indices were used to identify individual, clinically meaningful changes.

Results

Thirty-six patients completed the 3-month follow-up, and 14 patients completed the ≥ 11 months follow-up. Depending on the domain, subjective cognitive decline was reported by 1122% of patients. In total, 50% of patients reported subjective decline on at least one cognitive domain. Intracranial progression 3 months post-radiotherapy was a risk factor for self-reported deterioration ($p = .031$). Objective changes were observed across all domains, with a particular vulnerability for decline in memory at 3 months post-radiotherapy. The majority of patients (81%) experienced both a deterioration as well as improvement (e.g. mixed response) in objective cognitive functioning. Results were similar for the long-term follow-up (3- ≥ 11 months). No risk factors for objective cognitive change 3 months post-radiotherapy were identified.

Conclusion

Our study revealed that the majority of patients with BMs will show a mixed cognitive response following radiotherapy, reflecting the complex impact. This underscores the importance of patient-tailored NCAs three months post-radiotherapy to guide optimal rehabilitation strategies.

INTRODUCTION

Brain metastases (BMs) represent a rapidly growing population currently encompassing 10-30% of the adult cancer population.^{1,2} This number is expected to increase due to earlier detection through enhanced imaging techniques and advancements in medical treatment improving survival rates. Overall survival rates currently range from months to several years.²⁻⁹ Treatment consists of different options, including radiotherapy, surgery, chemotherapy, immunotherapy or a combination.¹⁰ However, with prolonged survival comes the increased likelihood of experiencing cognitive side-effects from these treatments, underscoring the urgency of research into the impact of treatment on patients' cognitive function. The ultimate goal of research is to enhance patient-centered care by providing well-informed psycho-education.

Prior to the start of treatment for BMs, a significant proportion of patients already experience cognitive difficulties; at least one out of every two patients demonstrates cognitive impairment on minimally one cognitive domain.¹¹⁻¹⁴ Cancer treatment can lead to further deterioration of neurocognitive functioning with declines observed both after systemic therapy (i.e. chemo- and immunotherapy)¹⁵⁻¹⁸ and local therapies (i.e. brain radiotherapy). Multiple cognitive domains can be affected after brain radiotherapy with impairments reported in memory, executive function, and processing speed.¹¹ On a group level, most patients exhibit a decline in neurocognitive performance during 8 months after whole-brain radiotherapy (WBRT), whereas after stereotactic radiosurgery (SRS), the majority of patients maintain a stable cognitive performance.¹¹ However, substantial variety exists both within and between subjects in terms of which cognitive domains are affected and to what extent. Previous research indicated stable cognitive performance up to 9 months after SRS at group-level, while almost 40% showed declined performance on the individual level.^{19,20}

Despite significant progress, many studies had limited follow-up durations and small sample sizes. Hence, it is crucial to confirm and continue to build upon previous findings. Therefore, the current study evaluated the individual trajectories of both subjective and objective cognitive performance in patients with BMs at the short-term (i.e. 3 months) and at the long-term (i.e. ≥ 11 months) after radiotherapy. By using a reliable change index (RCI)^{21,22} we consider the test-retest reliability of neurocognitive tasks, enabling us to identify individual, clinically meaningful changes in cognitive functioning. This study aims to gain insights into the impact of treatment for BMs on patients' lives by investigating individual cognitive functioning

within this heterogeneous group, considering subjective experiences, and focusing on long-term effects.

METHODS

Study set-up and population

Study procedures have been described previously.²³ Data was prospectively collected from the Cohort for patient-reported Outcomes, Imaging and trial inclusion in Metastatic BRAin disease (COIMBRA, NCT05267158) and the Assessing and Predicting Radiation Influence on Cognitive Outcome using the cerebrovascular stress Test (APRICOT) study. The study population consisted of adult patients (≥ 18 years) with either radiographic and/or histologic proof of metastatic brain disease referred to the University Medical Center Utrecht (UMCU) for brain radiotherapy. For both studies, neurocognitive assessments (NCAs), including semi-structured interviews, were performed before, 3 months and ≥ 11 months after radiotherapy. The studies were performed in accordance with the Declaration of Helsinki²⁴ and the UMCU institutional ethical review approved both the COIMBRA and APRICOT study (#18-642 and #18-747, respectively). Written informed consent was obtained from all participants prior to participation.

Data collection

Semi-structured interview

Prior to each neurocognitive assessment (NCA), subjective cognitive experience was assessed using a semi-structured interview. For the current analyses, the subjective cognitive ratings using the visual analogue scales (VAS) were used. In brief, patients were asked to assess their performance regarding thinking, memory, attention, perception, language and processing speed using VAS, similar to Schoo and colleagues.²⁵ The VAS consisted of a 100 mm vertical line on A3-sized paper, where the top (+) represents perfect performance and the bottom (-) represents worst performance. Patients marked the line at their experienced premorbid performance level (i.e. prior to the primary cancer diagnosis and antitumor treatment) as well as their current experience. This resulted in an intra-individual estimation ranging from 0 (-) to 100 (+). A difference score was calculated for each cognitive concept to assess change in performance. This was categorized into stable performance (± 5), subtle improvement or decline ($\pm 6-25$), substantial improvement or decline ($\pm 26-50$) and extreme improvement or decline ($\pm > 50$).

Neurocognitive assessment

A comprehensive NCA was used to assess objective cognitive performance. All tests are internationally widely used standardized psychometric instruments designed to assess neurocognitive deficits in the major neurocognitive domains. This battery encompasses all tests advised by the International Cancer and Cognition Task Force (ICCTF)²⁶ and supplemented with additional neuropsychological tests (**Supplementary Table 1**). At repeated testing, alternate forms were used to minimize practice effects. Whilst neuropsychological tests often evaluate more than one neurocognitive domain, tests were classified into different neurocognitive domains based on available literature and clinical experience. All NCAs were performed in-person by trained psychologists and were planned to be completed within approximately 90 minutes.

To assess neurocognitive impairment, each neuropsychological test was scored according to standardized scoring criteria. The uncorrected scores were transformed into z-scores based on the mean and standard deviation of control populations derived from published norm data and corrected for age and education where appropriate. Neurocognitive impairment in each domain was defined as a Z-score ≤ -1.5 on any of the administered tests within the domain.

Individual change in neurocognitive performance was assessed using the RCI as formulated by Jacobson and Truax.^{21,22} Using the uncorrected scores, this RCI accounts for the test-retest reliability of the task based on published normative data (**Supplementary Table 2**). RCI values of ≥ 1.645 indicate improvement, ≤ -1.645 decline, and values within ± 1.645 indicate stable cognitive performance.²⁷ Change in neurocognitive performance per domain was defined as improved or declined if at least one task within that domain showed improvement or decline, respectively, as mixed if at least one task indicated improvement and one task indicated decline and as stable when all tasks within that domain demonstrated stable performance.

Patient characteristics

Patient characteristics were obtained from the semi-structured interview and from the hospital's electronic healthrecord (HiX, Chipsoft, The Netherlands). This data included sex, age at inclusion, level of education according to the Verhage criteria²⁸, handedness, Karnofsky Performance Status (KPS)⁶, primary tumor origin, presence of extracranial metastases, time since BMs diagnosis, previous anti-tumor therapy, dexamethasone dose 1-5 days prior to radiotherapy, and symptoms at BMs diagnosis. As part of standard medical care, the pre-radiotherapy MRI scans of each patient were evaluated to determine the number of BMs, hemisphere, and lobe

involvement. Additionally, for those patients who completed follow-up NCAs, the clinical MRI follow-up scans were evaluated to determine intracranial progression during follow-up and new radiotherapy treatments were registered.

Statistical analyses

For this study the subjective and objective cognitive data acquired from October 2020 to May 2023 was used. Analyses were performed using SPSS (IBM SPSS Statistics, 25.0.0). Statistical significance was set at $p < 0.05$, adjusted for multiple comparisons when necessary. We anticipated that the assumption of normally distributed data would be violated due to the sample size and selected non-parametric alternatives for all statistical tests. Differences between patient completing and not completing the follow-up NCAs were assessed using chi-square test for categorical data and Mann-Whitney U-tests for continuous data.

At each time point, the percentage of patients with a cognitive performance below the impairment threshold ($Z \leq -1.5$) was calculated for each task as well as for each domain. Additionally, individual changes in both subjective and objective cognitive performance were calculated for (1) each domain (“domain-level”) and (2) across all domains (“overall-level”). Above-described cut-off scores were used to determine an improvement, deterioration, mixed or stable score. Changes in scores were calculated for baseline versus 3 months, and 3 versus ≥ 11 months.

For the *overall-level*, patients were categorized into four categories for subjective and objective cognitive performance separately: (1) decline, (2) improvement, (3) mixed, and (4) stable performance. Decline and improvement were defined as either a decrease or increase on at least one cognitive domain, respectively. The category “mixed” included patients who showed both declined and improved performance across the domain and/or, for objective cognitive performance only, within one domain. Patients were categorized into “stable” if performance across all domains remained unchanged. Subsequently, age, baseline KPS, primary tumor, presence of extracranial metastases, number of BMs, symptomatic BMs, synchronous diagnosis of BMs, intracranial progression at 3 months as determined by clinical follow-up scans and baseline cognitive impairment were assessed for the four categories, separately for the two time periods and for subjective and objective cognitive performance. As this analysis aimed to explore possible risk factors for cognitive decline, no corrections for multiple comparisons were performed.

RESULTS

Compliance

Thirty-six out of the original 60 (60%) patient were eligible for analysis, having completed the 3-months follow-up NCA (**Figure 1**). Of the 24 patients eligible for ≥ 11 -months follow-up, 14 (58%) patients completed this assessment. Reasons for noncompliance were poor medical condition, death, refusal because testing was considered too burdensome, and time constraints of the patient.

Patients who did not complete the 3-months follow-up had a lower KPS than patients who did complete the 3 months follow-up ($p = .001$). More patient who completed the ≥ 11 -months follow-up had BMs as their first symptom of cancer (i.e. synchronous diagnosis, 57%) than patients who did not complete the ≥ 11 months follow-up (10%; $p = .019$). None of the other characteristics as shown in **Table 1** significantly differed between patient groups. Moreover, there were no differences regarding pre-radiotherapy cognitive performance (domain-level) or number of patients with a cognitive impairment between patients who completed or not-completed the 3-months NCA nor between patients who completed or not-completed the ≥ 11 -months NCA.

Clinical characteristics

Baseline sociodemographic and clinical characteristics are shown in **Table 1**. In total 36 patients (19 male) finished the 3-months follow-up NCA at a median of 16 weeks from baseline (IQR 14-17). Median long-term follow-up time was 61 weeks from baseline (IQR 52-76). The median age was 63 years, and the primary tumor was most frequently lung cancer (47%). Most patients received SRS (94%) for 2-4 BMs (39%).

During the 3-months follow-up, intracranial progression was observed in 13/36 patients (36%) of which 3 patients had received additional radiotherapy for these new BMs before the follow-up NCA. From the 3-months to the ≥ 11 -months follow-up NCA, intracranial progression was observed in 6/14 patients of which 5 patients had received additional radiotherapy for these new BMs before the ≥ 11 -months follow-up NCA.

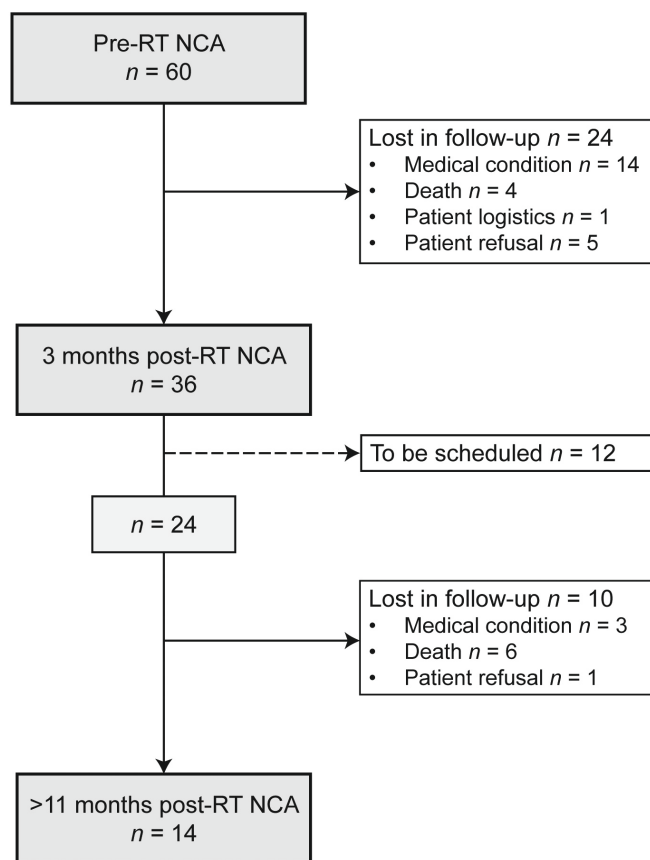


Figure 1. Flow-chart of the patients completing the pre-radiotherapy, 3-months and ≥ 11 -months NCA including reasons for patients lost in follow-up.

Table 1. Pre-radiotherapy sociodemographic and clinical characteristics of the patient population.

	Patients without follow-up	Patients with 3 months follow-up	Patients with ≥ 11 months follow-up
N	24	36	14
Age, years, median (IQR)	68 (63-73)	63 (56-71)	67 (56-73)
Sex (male), <i>n</i> (%)	13 (54)	19 (53)	8 (57)
Educational level ^a , <i>n</i> (%)			
3	0 (0)	3 (8)	2 (14)
4	4 (17)	7 (19)	3 (21)
5	12 (50)	10 (28)	5 (36)
6	5 (21)	10 (28)	3 (21)
7	3 (13)	6 (17)	1 (7)

Table 1. Pre-radiotherapy sociodemographic and clinical characteristics of the patient population. (continued)

	Patients without follow-up	Patients with 3 months follow-up	Patients with ≥11 months follow-up
Ravens matrices ²⁹ , median percentile (IQR)	62.5 (28-75)	69 (38-90)	69 (47-84)
Handedness ^b , <i>n</i> (%)			
Left	5 (21)	3 (8)	2 (14)
Right	18 (75)	32 (89)	11 (79)
Ambidextrous	1 (4)	1 (3)	1 (7)
KPS, median (IQR)	75 (63-80)	80 (80-90)	80 (78-90)
KPS ≥90, <i>n</i> (%)	2 (8)	14 (39)	6 (43)
Missing	5 (21)	0 (0)	0 (0)
No. of BMs, <i>n</i> (%)			
1	7 (33)	11 (31)	5 (36)
2-4	12 (50)	14 (39)	5 (36)
5-10	2 (8)	7 (19)	3 (21)
>10	3 (13)	4 (11)	1 (7)
Hemisphere involvement BMs, <i>n</i> (%)			
Left	7 (29)	9 (25)	2 (14)
Right	5 (21)	7 (19)	4 (29)
Bilateral	12 (50)	20 (56)	8 (57)
Lobe involvement, <i>n</i> (%)			
Frontal	11 (46)	23 (64)	9 (64)
Temporal	5 (21)	8 (22)	4 (29)
Occipital	8 (33)	13 (36)	4 (29)
Parietal	8 (33)	17 (47)	7 (50)
Cerebellum	12 (50)	15 (42)	7 (50)
Brainstem	1 (4)	2 (6)	0 (0)
Primary tumor origin, <i>n</i> (%)			
Lung cancer	13 (54)	17 (47)	9 (64)
Melanoma	4 (17)	9 (25)	3 (21)
Breast Cancer	1 (4)	2 (5)	0 (0)
Renal cell carcinoma	1 (4)	3 (8)	2 (14)
Other	5 (21)	5 (14)	0 (0)
Extracranial metastases, <i>n</i> (%)	15 (63)	21 (58)	9 (64)
BMs as first symptom of cancer diagnosis, <i>n</i> (%)	7 (29)	12 (33)	8 (57)

Table 1. Pre-radiotherapy sociodemographic and clinical characteristics of the patient population. (continued)

	Patients without follow-up	Patients with 3 months follow-up	Patients with ≥11 months follow-up
Previous brain RT, <i>n</i> (%)	2 (8)	7 (19)	2 (14)
Previous BMs resection, <i>n</i> (%)	7 (29)	10 (28)	4 (29)
Previous immuno-/chemotherapy, <i>n</i> (%)	18 (75)	10 (28)	9 (64)
Type of RT			
SRS	19 (79)	34 (94)	14 (100)
WBRT	4 (17)	2 (6)	0 (0)
WBRT + SRS	1 (4)	0 (0)	0 (0)
Dexamethasone use prior to RT, mg/day, median (IQR)	4 (0-4)	0 (0-4)	1 (0-4)
Symptomatic BMs at diagnosis, <i>n</i> (%)	16 (67)	21 (58)	8 (57)
Epilepsy ^c	3 (19)	8 (38)	4 (50)
Motor ^c	5 (31)	7 (33)	3 (38)
Sensory ^c	0 (0)	3 (14)	1 (13)
Balance ^c	5 (31)	4 (19)	2 (25)
Language ^c	0 (0)	2 (10)	1 (13)
Visual ^c	4 (25)	4 (19)	2 (25)
Cognitive ^c	6 (38)	3 (14)	1 (13)
Headache ^c	5 (31)	7 (33)	2 (25)
Other ^c	5 (31)	4 (19)	1 (13)

^aAccording to Verhage classification³⁰; ^bself-reported; ^cPercentage of patients with symptomatic BMS at diagnosis.

Note: Due to rounding, not all percentages add up to 100%. Abbreviations: BMs, brain metastases; IQR, interquartile range; RT, radiotherapy; SRS, stereotactic radiosurgery; WBRT, whole-brain radiotherapy.

Subjective cognitive functioning

Pre-radiotherapy

Pre-radiotherapy subjective performance of a larger sample has been reported previously.²³ Of the currently included sample, 11/36 (31%) reported stable subjective cognitive performance across all domains, while the majority of patients (24/36, 67%), report lower subjective cognitive performance than their premorbid levels on at least one cognitive domain (**Supplementary Figure 1**). Declines were

reported across all domains, but most common for attention, thinking, memory and language (all four domains: 14/36, 39%).

Post-radiotherapy changes

On the domain-level, subjective declines in cognitive performance were reported across all domains 3 months post-radiotherapy (**Figure 2a**). Declines were most frequently reported for attention (22%) and thinking (19%). For most domains, the percentage of patients that reported a decline were balanced out by the percentage of patients that reported an improvement (11-22%). Improvements were most often reported for attention (22%) and memory (22%). A stable score was reported across domains by 56-78% of patients. Stable scores were most often reported for processing speed (78%), language (72%), and thinking (69%).

From 3 to ≥ 11 months after radiotherapy, (further) subjective declines in cognitive performance were reported for memory (29%), perception (21%), attention (14%), and thinking (7%; **Figure 2b**). No declines were reported for processing speed or language. Improvements were also reported across all domains, but most frequently for attention (21%) and perception (21%). Stable scores were again most often observed for processing speed (93%) and language (86%).

Overall, 3 months post-radiotherapy 39% of patients reported a decline, 31% an improvement, 11% mixed performance and 19% stable subjective cognitive performance (**Figure 2c**). In the time period from 3 to ≥ 11 months after radiotherapy similar results were observed, with decline, improvement and stable performance in 29% of patients and mixed in 14%. More patients with intracranial progression showed decline across all cognitive domains 3 months post-radiotherapy compared to patients without intracranial progression ($X^2(3) = 8.896, p = .031$). Age, KPS at baseline, number of BMs, synchronous BMs diagnosis, primary tumor, extracranial metastases, symptomatic BMs and number of cognitive domain impairments at baseline did not significantly differ between the four categories from baseline to 3 months after radiotherapy (**Supplementary Table 3**).

Objective neurocognitive functioning

Pre-radiotherapy

An elaborate evaluation of pre-radiotherapy cognitive performance in a larger sample of this subset has been reported previously.²³ For the currently included sample, 29/36 (81%) showed impairments ($Z \leq -1.5$) in at least one cognitive domain and 18/36 (50%) with impairments in at least two domains. Memory was most

frequently affected (47%), followed by psychomotor speed (36%) and processing speed (31%; **Supplementary Results**).

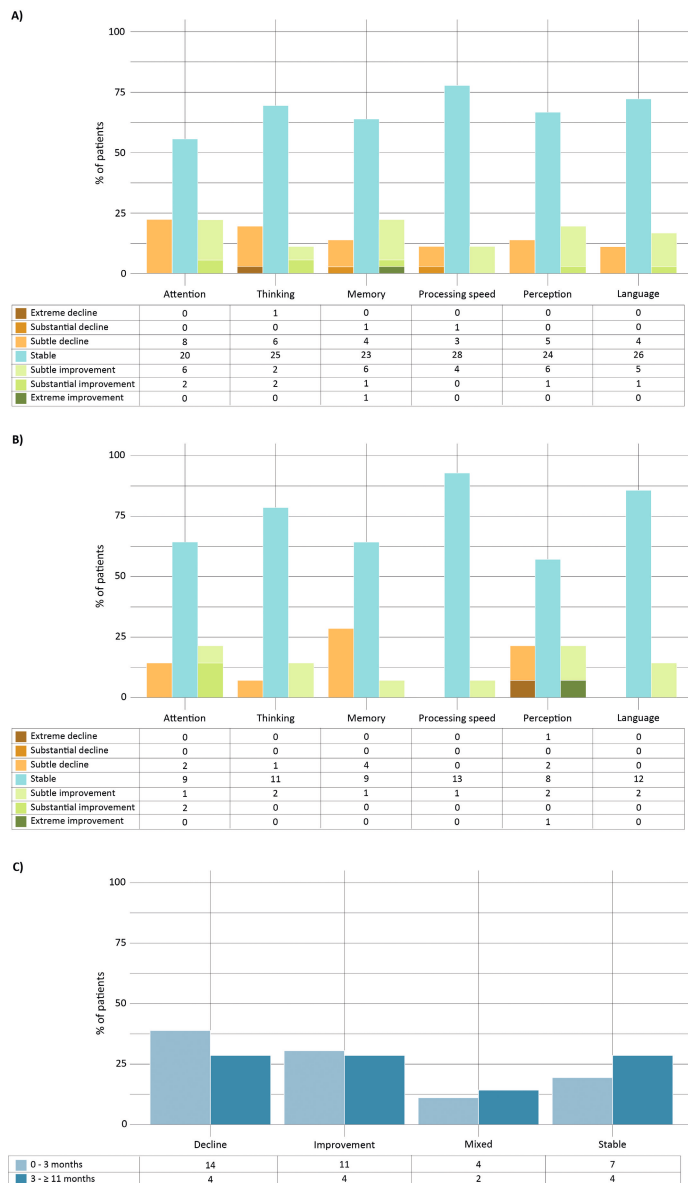


Figure 2. Change in subjective cognitive performance calculated from a) baseline-3 months and b) 3-≥11 months at the domain-level and c) at overall-level. Tables below the graph indicate the number of patients. Note: stable performance (± 5), subtle improvement or decline ($\pm 6-25$), substantial improvement or decline ($\pm 26-50$) and extreme improvement or decline ($\pm >50$).

Short-term post-radiotherapy

Three months after radiotherapy, a cognitive impairment ($Z \leq -1.5$) in ≥ 1 domain was observed for nearly all patients 35/36 (97%), whereby more than half of all patients (68%) showed impaired performance in at least 2 domains. Memory was most often impaired (78%), followed by psychomotor speed (39%) and attention (31%; **Supplementary Materials**).

Using the RCI, decline in cognitive performance was observed across all domains, but most frequently for memory (47%) and processing speed (35%; **Figure 3a**). Improvements were most often observed for executive function and visuospatial functioning (both 31%) and processing and psychomotor speed (both 28%). Mixed cognitive changes across the tests within a cognitive domain were seen for all domains, except visuospatial functioning and social cognition. Memory showed the highest frequency of mixed responses (28%). Stable cognitive performance was most often observed for social cognition (82%) and for visuospatial functioning (61%).

Overall, none of the patients showed stable performance across all domains, with most 29/36 (81%) showing both improvement and decline in different cognitive domains (**Figure 3c**). Solely declined performance was observed in 6/36 (17%). Age, KPS at baseline, number of BMs, synchronous BMs diagnosis, primary tumor, extracranial metastases, symptomatic BMs, intracranial progression and number of cognitive domain impairments at baseline did not differ between the four categories from baseline to 3 months after radiotherapy (**Supplementary Table 5**).

Long-term post-radiotherapy

At least 11 months after radiotherapy, a cognitive impairment ($Z \leq -1.5$) in at least 1 domain was found for 11/14 (79%) of patients, whereby more than half of the patients (71%) showed impaired performance in ≥ 2 domains. Memory was most often impaired (71%), followed by social cognition (43%), and psychomotor speed (39%; **Supplementary Materials**).

The RCI indicated decline in cognitive performance across all domains except social cognition (**Figure 3b**). Declines were most frequently observed for processing speed (54%) and psychomotor speed (39%). Improvements were most often observed regarding memory (57%) and executive function (36%). Mixed responses across the tests within a cognitive domain were seen for all domains, except visuospatial functioning and social cognition, and was most common for memory (29%). Stable cognitive performance was most often observed for social cognition (89%) and

attention (43%). Overall, none of the patients showed declined or stable performance across all domains, with most 13/14 (93%) showing mixed performance (**Figure 3c**). Solely improved performance was observed in 1/14 (7%).



Figure 3. Change in objective cognitive performance calculated from a) baseline-3 months and b) 3-≥11 months at the domain-level and c) at overall-level. Tables below the graph indicate the number of patients.

DISCUSSION

In order to be able to provide patient-tailored cancer care, including personalized psycho-education, we first need individualized research to inform on the effects of cancer treatment on individuals. Therefore, the aim of this study was to evaluate the individual trajectories of subjective and objective cognitive performance after radiotherapy in patients with BMs both at the short-term (i.e. 3 months) and at the long-term (i.e. ≥ 11 months) to provide insight into the cognitive impact of treatment. Our findings demonstrate that on a group-level, the incidence of patients displaying cognitive decline is counterbalanced by those demonstrating improvements within the same cognitive domain. The individualized results reveal a nuanced picture, where the majority of patients who exhibit improvements in one domain also experience a decline in another. Thus, impact of radiotherapy on cognitive performance is complex and multidimensional.

The cognitive impact of radiotherapy was also subjectively reported by the majority of patients. Using VAS, patients were able to provide a differentiated profile of subjective cognitive decline over time. Three months post-radiotherapy, half of the patients experienced a decline in subjective cognitive performance, most frequently involving attention and thinking. In the long-term, memory complaints were more prominent. Considering that intracranial progression emerged as a risk factor for self-reported cognitive decline 3 months post-radiotherapy, these cognitive complaints may primarily reflect new or aggravated symptoms resulting from the presence of new BMs. Based on previous research, it was anticipated that the specific cognitive domains would not fully align with those observed in the objective cognitive assessment.^{23,31} However, there was a consistency between the number of patients reporting subjective cognitive decline and those demonstrating objective cognitive decline. To illustrate, patients may have reported complaints in attention, while these were objectively reflected by worse memory performance. This underlines that while patients may label cognitive complaints differently, it is essential to incorporate subjective assessments to also capture patients' experiences of cognitive difficulties.

Regarding objective cognitive performance, multiple cognitive domains were affected post-radiotherapy, rather than a single domain universally affected in all patients. Nevertheless, memory appeared to be particularly susceptible to the negative effects of treatment, reflected by the 75% of patients exhibiting declined memory performance and 80% of patients with a memory impairment 3 months post-radiotherapy and 75% of patients exhibiting declined memory performance

compared to pre-radiotherapy. After excluding the two patients who received WBRT, these percentages remained unchanged, highlighting the notable prevalence of memory decline within our SRS patient sample. The negative impact of radiotherapy on learning and memory performance has received widespread recognition. As the hippocampus is the primary brain region responsible for learning and memory, a great deal of interest has now been put into hippocampal avoidance WBRT (HA-WBRT)^{e.g. 32-34} and now even HA-SRS³⁵ for the possible preservation of neurocognition. While damage to the hippocampus has indeed been implicated in cognitive decline following brain radiotherapy, recent findings underscore concomitant shrinkage in other subcortical brain structures, as well as damage to both white matter and other cortical territories.³⁶⁻⁴² Moreover, contemporary perspectives on cognitive functioning emphasize its network-based nature, moving beyond mere localization.^{43,44} This recognition complicates the straightforward attribution of cognitive side-effects exclusively to specific radiotherapy-vulnerable brain regions. Further research is needed to better understand the complex interplay between radiotherapy, brain structures, and cognitive functioning in order to optimize treatment outcomes in clinical settings.

In the long-term, slowing of both processing and psychomotor speed was most prominent, while this was not reflected accordingly in self-reported cognitive changes. Multiple factors could have contributed to the observed slowing as processing and psychomotor speed both rely on a widespread neural network.^{45,46} As most patients with BMs receive systemic treatment after brain radiotherapy, the long-term psychomotor slowing could also be a consequence of chemotherapy-induced neuropathy rather than long-term radiotherapy effects.^{47,48}

In our sample, a decline in objective cognitive performance was observed in nearly all patients. Interestingly, for the majority, this decline was accompanied by improvement in another cognitive domain. This pattern of mixed responses persisted in the long-term and was irrespective of patients' pre-radiotherapy cognitive impairment. While not statistically significant, a higher number of BMs and metasynchronous BMs diagnosis appeared more common among patients with cognitive decline 3 months post-radiotherapy, suggesting potential areas for future investigation. As mixed responses were predominant, no other clear risk factors for post-radiotherapy cognitive changes were found. It is important to acknowledge that cognitive improvement does not necessarily indicate the absence of cognitive impairment, as demonstrated by the small percentage of patients without any cognitive impairment at both follow-up times (3-21%). Nonetheless, the RCI enabled us to identify meaningful changes, indicating that both the observed positive and

negative changes are likely to have a significant impact on the daily lives of these patients. The heterogeneity in cognitive outcomes can likely be attributed to a range of factors, including the extent and location of metastases, individual variabilities in treatment response, and pre-existing cognitive or neural vulnerabilities. Future studies incorporating these different variables in large cohorts could advance our understanding of the complex interplay between treatment-related factors and patient-specific factors in shaping cognitive outcomes after radiotherapy.

The current results present a snapshot of the currently available evidence on cognitive trajectories of individual patients with BMs after receiving radiotherapy. It is challenging to discern the effects of radiotherapy from those of other treatments and disease progression, as adjuvant systemic treatments during the study period may have contributed to declines in cognitive performance. Due to the inevitable deterioration in medical condition of this population, results are mainly representative of the group of patients fit enough 3 months post-radiotherapy. Nevertheless, both compliance rates and available patients for follow-up, especially in the long-term, were comparable to or higher than previous studies.^{13,14,20,49-51} Most importantly, these results can be used to design future studies to best capture the complexity of individual cognitive changes in patients with BMs. For example, as memory seems particularly vulnerable, multiple tests each capturing different aspects of this multifaceted cognitive function should be incorporated.

CONCLUSION

The increasing incidence of BMs and improved survival rates underscore the urgent need to investigate the effects of treatments on individuals, because group-level information alone is insufficient when conveying the potential treatment effects to patients and caregivers. Our study revealed a complex impact of radiotherapy on subjective and objective cognitive performance, involving both positive and negative changes across various cognitive domains. Particularly, memory showed vulnerability in the early post-radiotherapy period. The observed within-individual variation emphasizes the involvement of intricate underlying mechanisms, highlighting the need for further investigation. Despite current advancements in treatment patients remain at risk for intracranial progression, which was a clear risk factor for subjective cognitive decline in this study. These findings are specific to patients with BMs who have undergone radiotherapy and should be considered in light of the potential trade-off between cognitive difficulties and survival benefits. Our results show the heterogeneity of cognitive profiles post-radiotherapy,

thereby underscoring the importance of patient-tailored NCAs three months post-radiotherapy to guide optimal rehabilitation strategies.

SUPPLEMENTARY MATERIALS



REFERENCES

1. Gerstenecker A, Nabors LB, Meneses K, et al. Cognition in patients with newly diagnosed brain metastasis: Profiles and implications. *J Neurooncol.* 2014;120(1):179-185. doi:10.1007/s11060-014-1543-x
2. Achrol AS, Rennert RC, Anders C, et al. Brain metastases. *Nat Rev Dis Primers.* 2019;5(1). doi:10.1038/s41572-018-0055-y
3. Nieder C, Spanne O, Mehta MP, Grosu AL, Geinitz H. Presentation, patterns of care, and survival in patients with brain metastases: What has changed in the last 20 years? *Cancer.* 2011;117(11):2505-2512. doi:10.1002/cncr.25707
4. Lanier CM, Hughes R, Ahmed T, et al. Immunotherapy is associated with improved survival and decreased neurologic death after SRS for brain metastases from lung and melanoma primaries. *Neurooncol Pract.* 2019;6(5):402-409. doi:10.1093/nop/npz004
5. Nayak L, Lee EQ, Wen PY. Epidemiology of brain metastases. *Curr Oncol Rep.* 2012;14(1):48-54. doi:10.1007/s11912-011-0203-y
6. Oken MM, Creech RH, Tormey DC, Horton J, Davis TE, McFadden, Eleanor T Carbone PP. Toxicity and response criteria of the Eastern Cooperative Oncology Group. *American Journal of Clinical Oncology: Cancer Clinical Trials.* 1982;5(6):649-656.
7. Gaspar L, Scott C, Rotman M, et al. Recursive partitioning analysis (RPA) of prognostic factors in three Radiation Therapy Oncology Group (RTOG) brain metastases trials. *Int J Radiat Oncol Biol Phys.* 1997;37(4):745-751. doi:10.1016/S0360-3016(96)00619-0
8. Sperduto PW, Kased N, Roberge D, et al. Summary report on the graded prognostic assessment: An accurate and facile diagnosis-specific tool to estimate survival for patients with brain metastases. *Journal of Clinical Oncology.* 2012;30(4):419-425. doi:10.1200/JCO.2011.38.0527
9. Sperduto PW, Chao ST, Sneed PK, et al. Diagnosis-specific prognostic factors, indexes, and treatment outcomes for patients with newly diagnosed brain metastases: a multi-institutional analysis of 4,259 patients. *Int J Radiat Oncol Biol Phys.* 2010;77(3):655-661. doi:10.1016/j.ijrobp.2009.08.025
10. Eichler AF, Loeffler JS. Multidisciplinary management of brain metastases. *Oncologist.* 2007;12(7):884-898. doi:10.1634/theoncologist.12-7-884
11. Van Grinsven EE, Nagtegaal SHJ, Verhoeff JJC, Van Zandvoort MJE. The Impact of Stereotactic or Whole Brain Radiotherapy on Neurocognitive Functioning in Adult Patients with Brain Metastases: A Systematic Review and Meta-Analysis. *Oncol Res Treat.* 2021;44(11):622-636. doi:10.1159/000518848
12. Mehta MP, Rodrigus P, Terhaard CHJ, et al. Survival and neurologic outcomes in a randomized trial of motexafin gadolinium and whole-brain radiation therapy in brain metastases. *Journal of Clinical Oncology.* 2003;21(13):2529-2536. doi:10.1200/JCO.2003.12.122
13. Chang EL, Wefel JS, Maor MH, et al. A pilot study of neurocognitive function in patients with one to three new brain metastases initially treated with stereotactic radiosurgery alone. *Neurosurgery.* 2007;60(2):277-283. doi:10.1227/01.NEU.0000249272.64439.B1

14. Habets EJJ, Dirven L, Wiggenraad RG, et al. Neurocognitive functioning and health-related quality of life in patients treated with stereotactic radiotherapy for brain metastases: A prospective study. *Neuro Oncol.* 2016;18(3):435-444. doi:10.1093/neuonc/nov186
15. Hodgson KD, Hutchinson AD, Wilson CJ, Nettelbeck T. A meta-analysis of the effects of chemotherapy on cognition in patients with cancer. *Cancer Treat Rev.* 2013;39(3):297-304. doi:10.1016/j.ctrv.2012.11.001
16. Joly F, Castel H, Tron L, Lange M, Vardy J. Potential effect of immunotherapy agents on cognitive function in cancer patients. *J Natl Cancer Inst.* 2020;112(2):123-127. doi:10.1093/JNCI/DJZ168
17. Wefel JS, Schagen SB. Chemotherapy-related cognitive dysfunction. *Curr Neurol Neurosci Rep.* 2012;12(3):267-275. doi:10.1007/s11910-012-0264-9
18. Schagen SB, Tsvetkov AS, Compter A, Wefel JS. Cognitive adverse effects of chemotherapy and immunotherapy: are interventions within reach? *Nat Rev Neurol.* 2022;18(3):173-185. doi:10.1038/s41582-021-00617-2
19. Schimmel WCM, Verhaak E, Bakker M, Hanssens PEJ, Sitskoorn MM, Gehring K. Group and Individual Change in Cognitive Functioning in Patients With 1 to 10 Brain Metastases Following Gamma Knife Radiosurgery. *Clin Oncol.* 2021;33(5):314-321. doi:10.1016/j.clon.2021.01.003
20. van der Meer PB, Habets EJJ, Wiggenraad RG, et al. Individual changes in neurocognitive functioning and health-related quality of life in patients with brain oligometastases treated with stereotactic radiotherapy. *J Neurooncol.* 2018;139(2):359-368. doi:10.1007/s11060-018-2868-7
21. Jacobson NS, Roberts LJ, Berns SB, McGlinchey JB. Methods for defining and determining the clinical significance of treatment effects: Description, application, and alternatives. *J Consult Clin Psychol.* 1999;67(3):300-307. doi:10.1037/0022-006X.67.3.300
22. Jacobson NS, Truax P. Clinical Significance: A Statistical Approach to Denning Meaningful Change in Psychotherapy Research. *Journal of Consulting and Clinical Psychology.* 1991;59(1):12-19.
23. van Grinsven E, Cialdella F, Verhoeff J, Philippens M, Zandvoort M. Different profiles of neurocognitive functioning in patients with brain metastases prior to brain radiotherapy. *Journal of Psycho-oncology.* 2023;32(11):1752-1761.
24. World Medical Association. World Medical Association Declaration of Helsinki: ethical principles for medical research involving human subjects. *JAMA.* 2013;310(20):2191-2194. doi:10.1093/acprof:oso/9780199241323.003.0025
25. Schoo LA, Van Zandvoort MJE, Biessels GJ, Kappelle LJ, Postma A. Insight in cognition: Self-awareness of performance across cognitive domains. *Appl Neuropsychol.* 2013;20(2):95-102. doi:10.1080/09084282.2012.670144
26. Wefel JS, Vardy J, Ahles T, Schagen SB. International Cognition and Cancer Task Force recommendations to harmonise studies of cognitive function in patients with cancer. *Lancet Oncol.* 2011;12(7):703-708. doi:10.1016/S1470-2045(10)70294-1
27. Duff K. Current topics in science and practice evidence-based indicators of neuropsychological change in the individual patient: Relevant concepts and methods. *Archives of Clinical Neuropsychology.* 2012;27(3):248-261. doi:10.1093/arclin/acr120
28. Verhage F. Intelligentie en leeftijd bij volwassenen en bejaarden. *Koninklijke van Gorcum.* Published online 1964. <https://research.rug.nl/en/publications/intelligentie-en-leeftijd-bij-volwassenen-en-bejaarden>

29. John Hugh Court, Raven J. Manual for Raven's Progressive Matrices and Vocabulary Scales. Section 7, Research and References: Summaries of Published Normative Studies, Reliability Studies, Validity Studies, References to All Sections of the Manual. *Oxford Psychologists*. Published online 1995.
30. Verhage F. Intelligentie en leeftijd bij volwassenen en bejaarden. *Koninklijke van Gorcum*. Published online 1964.
31. Green HJ, Pakenham KI, Gardiner RA. Cognitive deficits associated with cancer: A model of subjective and objective outcomes. *Psychol Health Med*. 2005;10(2):145-160. doi:10.1080/13548500500093308
32. Popp I, Rau A, Kellner E, et al. Hippocampus-Avoidance Whole-Brain Radiation Therapy Is Efficient in the Long-Term Preservation of Hippocampal Volume. *Front Oncol*. 2021;11(August):1-11. doi:10.3389/fonc.2021.714709
33. Yang WC, Chen YF, Yang CC, et al. Hippocampal avoidance whole-brain radiotherapy without memantine in preserving neurocognitive function for brain metastases: a phase II blinded randomized trial. *Neuro Oncol*. 2020;(August):1-9. doi:10.1093/neuonc/noaa193
34. Wefel JS, Armstrong TS, Tome WA, et al. Sustained Preservation of Cognition and Prevention of Patient-Reported Symptoms with Hippocampal Avoidance during Whole-Brain Radiotherapy for Brain Metastases: Final Results of NRG Oncology CC001. *Int J Radiat Oncol Biol Phys*. Published online 2023. doi:10.1016/j.ijrobp.2023.04.030
35. Burgess L, Nair V, Gratton J, Doody J, Chang L, Malone S. Stereotactic radiosurgery optimization with hippocampal-sparing in patients treated for brain metastases. *Phys Imaging Radiat Oncol*. 2021;17:106-110. doi:10.1016/j.phro.2021.02.001
36. Makale MT, McDonald CR, Hattangadi-Gluth JA, Kesari S. Mechanisms of radiotherapy-associated cognitive disability in patients with brain tumours. *Nat Rev Neurol*. 2017;13(1):52-64. doi:10.1038/nrneurol.2016.185
37. Nagtegaal SHJ, David S, Philippens MEP, Snijders TJ, Leemans A, Verhoeff JJC. Dose-dependent volume loss in subcortical deep grey matter structures after cranial radiotherapy. *Clin Transl Radiat Oncol*. 2021;26:35-41. doi:10.1016/j.ctro.2020.11.005
38. Nagtegaal SHJ, David S, Snijders TJ, Philippens MEP, Leemans A, Verhoeff JJC. Effect of radiation therapy on cerebral cortical thickness in glioma patients: Treatment-induced thinning of the healthy cortex. *Neurooncol Adv*. 2020;2(1). doi:10.1093/nojnl/vdaa060
39. Nagtegaal SHJ, David S, van Grinsven EE, et al. Morphological changes after cranial fractionated photon radiotherapy: Localized loss of white matter and grey matter volume with increasing dose. *Clin Transl Radiat Oncol*. 2021;31(January):14-20. doi:10.1016/j.ctro.2021.08.010
40. Connor M, Karunamuni R, McDonald C, et al. Regional susceptibility to dose-dependent white matter damage after brain radiotherapy. *Radiotherapy and Oncology*. 2017;123(2):209-217. doi:10.1016/j.radonc.2017.04.006
41. Zhu T, Chapman CH, Tsien C, et al. Effect of the Maximum Dose on White Matter Fiber Bundles Using Longitudinal Diffusion Tensor Imaging. *Int J Radiat Oncol Biol Phys*. 2016;96(3):696-705. doi:10.1016/j.ijrobp.2016.07.010
42. Chapman CH, Zhu T, Nazem-Zadeh M, et al. Diffusion tensor imaging predicts cognitive function change following partial brain radiotherapy for low-grade and benign tumors. *Radiotherapy and Oncology*. 2016;120(2):234-240. doi:10.1016/j.radonc.2016.06.021

43. Pessoa L. Understanding brain networks and brain organization. *Phys Life Rev.* 2014;11(3):400-435. doi:10.1016/j.plrev.2014.03.005
44. Sutterer MJ, Tranel D. Neuropsychology and cognitive neuroscience in the fMRI era: A recapitulation of localizationist and connectionist views. *Neuropsychology.* 2017;31(8):972-980. doi:10.1037/neu0000408
45. Hua B, Ding X, Xiong M, et al. Alterations of functional and structural connectivity in patients with brain metastases. *PLoS One.* 2020;15(5):1-16. doi:10.1371/journal.pone.0233833
46. Maesawa S, Bagarinao E, Fujii M, et al. Evaluation of resting state networks in patients with gliomas: Connectivity changes in the unaffected side and its relation to cognitive function. *PLoS One.* 2015;10(2):1-13. doi:10.1371/journal.pone.0118072
47. Miaskowski C, Mastick J, Paul SM, et al. Chemotherapy-Induced Neuropathy in Cancer Survivors. *J Pain Symptom Manage.* 2017;54(2):204-218.e2. doi:10.1016/j.jpainsymman.2016.12.342
48. Wefel JS, Vidrine DJ, Marani SK, et al. A prospective study of cognitive function in men with non-seminomatous germ cell tumors. *Psychooncology.* 2014;23(6):626-633.
49. Chang EL, Wefel JS, Hess KR, et al. Neurocognition in patients with brain metastases treated with radiosurgery or radiosurgery plus whole-brain irradiation: a randomised controlled trial. *Lancet Oncol.* 2009;10(11):1037-1044. doi:10.1016/S1470
50. Brown PD, Jaeckle K, Ballman K V., et al. Effect of radiosurgery alone vs radiosurgery with whole brain radiation therapy on cognitive function in patients with 1 to 3 brain metastases a randomized clinical trial. *JAMA.* 2016;316(4):401-409. doi:10.1001/jama.2016.9839
51. Minniti G, Capone L, Nardiello B, et al. Neurological outcome and memory performance in patients with 10 or more brain metastases treated with frameless linear accelerator (LINAC)-based stereotactic radiosurgery. *J Neurooncol.* 2020;148(1):47-55. doi:10.1007/s11060-020-03442-7
52. *Wechsler Adult Intelligence Scale Fourth Edition (WAIS-IV-NL) Technische Handleiding;* 2013.
53. Bouma A, Mulder J, Lindeboom J SB. *Handboek Neuropsychologische Diagnostiek.* Pearson; 2012.
54. Drane DL, Yuspeh RL, Huthwaite JS, Klingler LK. Demographic characteristics and normative observations for derived-Trail Making Test indices. *Neuropsychiatry Neuropsychol Behav Neurol.* 2002;15(1):39-43.
55. D.C. Delis EK, Kramer. JH. D-KEFS Color Word Interference Test, Nederlandse bewerking door I. Noens en van der I. Berckelaer-Onnes. Published online 2008.
56. Harrison JE, Buxton P, Husain M, Wise R. Short test of semantic and phonological fluency: Normal performance, validity and test-retest reliability. *British Journal of Clinical Psychology.* 2000;39(2):181-191. doi:10.1348/014466500163202
57. Schmand B, Groenink SC, Van Den Dungen M. Letterfluency: Psychometric properties and Dutch normative data. *Tijdschr Gerontol Geriatr.* 2008;39(2):64-76. doi:10.1007/bf03078128
58. Benedict RHB, Schretlen D, Groninger L, Brandt J. Hopkins Verbal Learning Test – Revised: Normative Data and Analysis of Inter-Form and Test-Retest Reliability. *Clin Neuropsychol.* 1998;12(1):43-55. doi:10.1080/13854049508400494
59. Brandt J, Ralph H B Benedict. Hopkins Verbal Learning Test - Revised Professional Manual. Published online 2001.

60. Tremblay MP, Potvin O, Callahan BL, et al. Normative data for the Rey-Osterrieth and the Taylor Complex Figure tests in Quebec-French people. *Archives of Clinical Neuropsychology*. 2015;30(1):78-87. doi:10.1093/arclin/acu069
61. Lindeboom J, Schmand B, Meyer S, Jos de Jonghe. Visual Association Test Manual. Published online 2012.
62. Van Der Elst W, Van Boxtel MPJ, Van Breukelen GJP, Jolles J. Normative data for the Animal, Profession and Letter M Naming verbal fluency tests for Dutch speaking participants and the effects of age, education, and sex. *Journal of the International Neuropsychological Society*. 2006;12(1):80-89. doi:10.1017/S1355617706060115
63. Grooved Pegboard Test User Instructions. Published online 2002.
64. Tamkin AS, Rebecca Jacobsen. Age-related norms for the Hooper Visual Organization Test. *J Clin Psychol*. 1984;40(6):1459-1463.
65. Dodich A, Cerami C, Canessa N, et al. Emotion recognition from facial expressions: A normative study of the Ekman 60-Faces Test in the Italian population. *Neurological Sciences*. 2014;35(7):1015-1021. doi:10.1007/s10072-014-1631-x
66. Paxton JL, Peavy GM, Jenkins C, Rice VA, Heindel WC, Salmon DP. Deterioration of visual-perceptual organization ability in Alzheimer's disease. *Cortex*. 2007;43(7):967-975. doi:10.1016/S0010-9452(08)70694-4
67. Barr WB. Neuropsychological testing of high school athletes - Preliminary norms and test-retest indices. *Archives of Clinical Neuropsychology*. 2003;18(1):91-101. doi:10.1016/S0887-6177(01)00185-8
68. Levine AJ, Miller EN, Becker JT, Selnes OA, Cohen BA. Normative data for determining significance of test-retest differences on eight common neuropsychological instruments. *Clinical Neuropsychologist*. 2004;18(3):373-384. doi:10.1080/1385404049052420
69. Levin BE, Llabre MM, Reisman S, et al. Visuospatial impairment in Parkinson's disease. *Neurology*. 1991;41(3):365-365.
70. Andreotti C, Root JC, Schagen SB, et al. Reliable change in neuropsychological assessment of breast cancer survivors. *Psychooncology*. 2016;25(1):43-50. doi:10.1002/pon.3799
71. Bird CM, Papadopoulou K, Ricciardelli P, Rossor MN, Cipolotti L. Monitoring cognitive changes: Psychometric properties of six cognitive tests. *British Journal of Clinical Psychology*. 2004;43(2):197-210. doi:10.1348/014466504323088051
72. Siciliano M, Chiorri C, Battini V, et al. Regression-based normative data and equivalent scores for Trail Making Test (TMT): an updated Italian normative study. *Neurological Sciences*. 2019;40(3):469-477. doi:10.1007/s10072-018-3673-y





Part II

Using imaging techniques to understand
neurocognitive functioning



5

The impact of etiology in lesion-symptom mapping – A direct comparison between tumor and stroke

Eva E. van Grinsven, Anouk R. Smits, Emma van Kessel, Mathijs A.H. Raemaekers, Edward H.F. de Haan, Irene M.C. Huenges Wajer, Veerle J. Ruijters, Marielle E.P. Philippens, Joost J.C. Verhoeff, Nick F. Ramsey, Pierre A.J.T. Robe, Tom J. Snijders, & Martine J.E. van Zandvoort

NeuroImage: Clinical (2023)

ABSTRACT

Introduction

Lesion-symptom mapping is a key tool in understanding the relationship between brain structures and behavior. However, the behavioral consequences of lesions from different etiologies may vary because of how they affect brain tissue and how they are distributed. The inclusion of different etiologies would increase the statistical power but has been critically debated. Meanwhile, findings from lesion studies are a valuable resource for clinicians and used across different etiologies. Therefore, the main objective of the present study was to directly compare lesion-symptom maps for memory and language functions from two populations, a tumor versus a stroke population.

Methods

Data from two different studies were combined. Both the brain tumor (N = 196) and stroke (N = 147) patient populations underwent neuropsychological testing and an MRI, pre-operatively for the tumor population and within three months after stroke. For this study, we selected two internationally widely used standardized cognitive tasks, the Rey Auditory Verbal Learning Test and the Verbal Fluency Test. We used a state-of-the-art machine learning-based, multivariate voxel-wise approach to produce lesion-symptom maps for these cognitive tasks for both populations separately and combined.

Results

Our lesion-symptom mapping results for the separate patient populations largely followed the expected neuroanatomical pattern based on previous literature. Substantial differences in lesion distribution hindered direct comparison. Still, in brain areas with adequate coverage in both groups, considerable LSM differences between the two populations were present for both memory and fluency tasks. Post-hoc analyses of these locations confirmed that the cognitive consequences of focal brain damage varied between etiologies.

Conclusion

The differences in the lesion-symptom maps between the stroke and tumor population could partly be explained by differences in lesion volume and topography. Despite these methodological limitations, both the lesion-symptom mapping results and the post-hoc analyses confirmed that etiology matters when investigating the cognitive consequences of lesions with lesion-symptom mapping. Therefore, caution is advised with generalizing lesion-symptom results across etiologies.

INTRODUCTION

Topological organization of brain function has been widely studied in patients with brain lesions.¹ It remains the most powerful method to infer causality between brain structures and behavior.² The past decades, lesion analyses methods have evolved³, and lesion-symptom mapping (LSM) is currently performed in large samples and is a frequently utilized method in behavioral neurology.

LSM has most frequently been applied in stroke patients, which raises questions about generalizability. The behavioral consequences of lesions from different etiologies, such as brain tumors or stroke, may vary as a result of how they affect the brain.^{1,4} Firstly, the lesion distribution differs between etiologies, with certain brain areas more likely to be damaged than others. The possible locations for a stroke are confined by the architecture of the vascular system, with a stroke most often occurring in subcortical areas in the territory of the middle cerebral artery.⁵⁻⁷ Primary brain tumors, on the other hand, frequently involve both subcortical and cortical structures in the frontotemporoinsular areas.^{8,9} This nonrandom lesion distribution, which is inherent to each pathology, affects the spatial accuracy of LSM analyses since it limits the possibility to analyze rarely affected brain areas.^{10,11} First, areas that are rarely damaged are often excluded beforehand from the analyses. Second, for the areas that are included in the analysis, statistical power will vary across the brain and power problems arise when areas are very rarely (or very often) damaged.¹² Moreover, if neighboring or downstream areas are always damaged together, the unique involvement of each voxel to a given behavioral deficit cannot be distinguished.

Furthermore, disease-specific characteristics determine the behavioral consequences. An ischemic stroke is defined by an acute event causing immediate cell death, whereas the rate of brain tumor growth is much slower (months to years, dependent on grade), and neural activity can continue to persist after infiltration by tumor cells.¹³⁻¹⁵ This raises the possibility that the brain recruits mechanisms for neural plasticity in different ways when affected by different pathologies, which in turn may lead to different functional outcomes.^{16,17}

The use of etiologies other than stroke in lesion-deficit mapping is a highly discussed and controversial topic.¹⁸⁻²¹ Recently, there has been a rise in lesion studies involving brain tumor patients. The classically theorized neural correlates of behavior, for example the involvement of the posterior perisylvian areas and Broca's area in language, have mostly been corroborated in this population.²²⁻²⁶ In addition, a recent

study investigating neuro-anatomical correlates of neglect in a low-grade glioma population found an association between the medial frontal cortex and neglect, which has not yet been documented in stroke lesion studies.²⁷ This underlines the added value of using different populations in lesion-deficit inferences.

Nevertheless, the stroke population remains the predominant research population in LSM studies, while it is still unclear whether etiology-specific biases limit the generalizability of these results. Therefore, we directly compare LSM for memory and language functions from two populations, a tumor versus a stroke population. We expect that both populations will independently show function-specific neural correlates for memory and language functions, as described in previous literature. The aim of this study is to investigate if brain areas where both stroke and tumor populations have adequate coverage, show topographical overlap in lesion-symptom associations. For this study, data from two different studies were combined: a single-center retrospective study in a cohort of treatment-naïve diffuse glioma patients^{8,28} and a multi-center prospective cohort study in patients with ischemic stroke.^{29,30} With a state-of-the-art machine learning-based, multivariate voxel-wise approach, we produced lesion-symptom maps for memory and verbal fluency tasks for both populations separately.

METHODS

Patient recruitment

The University Medical Center Utrecht (UMCU) institutional ethical review board approved both studies in accordance with the Declaration of Helsinki.³¹ Detailed in- and exclusion criteria are provided in the **Supplementary Materials**.

Tumor patients

The data from the tumor patients was gathered as part of a single-center retrospective study in a cohort of adult treatment-naïve diffuse glioma patients (WHO grade II-IV according to WHO2016 classification³²) who underwent awake brain surgery between January 2010 and July 2019 at the UMCU. As the data of this cohort was previously gathered as part of routine clinical care and was anonymized, informed consent was not required, in agreement with Dutch law. Preoperative neurocognitive assessment and preoperative MRI were part of routine clinical care in preparation for awake craniotomy and used for the current study. Patients who underwent craniotomy under full anesthesia could not be included for the current study, as elaborate preoperative neurocognitive assessment is not part of routine clinical care.

Stroke patients

The data from the stroke patients was gathered as part of the Functional Architecture of the Brain for Vision (FAB4V) study, which is a multi-center prospective cohort study investigating vision and cognition after ischemic stroke. Adult patients with a first-ever symptomatic cerebral ischemic stroke were included in the current study. Written informed consent was obtained from all participants prior to participation. Neurocognitive assessment and an MRI including a T2 FLAIR were performed between three weeks and three months post-infarction. A maximum of one week was allowed between the neurocognitive assessment and the MRI.

Data collection

Neurocognitive assessment

The neuropsychological instruments and corresponding scores for both populations are listed in **Supplementary Table 1**, along with full test descriptions. The uncorrected scores for each test were transformed into z-scores based on the mean and standard deviation of control populations derived from published norm data. For descriptive purposes, a cognitive impairment was defined as a z-score equal to or lower than -1.5. To assess differences between the tumor and stroke group regarding cognitive performance two types of statistics were performed. Firstly, using Pearson's chi-square tests we investigated whether the relative number of patients with a cognitive impairment was higher in the tumor or stroke group for any of the available cognitive tasks. Secondly, using two-samples t-tests we investigated whether the cognitive performance of the tumor group differed from that of the stroke group for the cognitive tasks that were used in subsequent LSM analyses.

For the LSM analyses, we selected two internationally widely used, standardized psychometric instruments: the Rey Auditory Verbal Learning Test (RAVLT), a verbal learning and memory test that taps into multiple aspects of memory (direct recall, delayed recall, and delayed recognition) and the Verbal Fluency Test. The fluency test is separated into a phonemic fluency (Dutch versions of the Controlled Oral Word Association Test) and semantic fluency (animal) part. The phonemic fluency test is thought to rely more heavily on executive control, while the semantic fluency test is more dependent on correct retrieval of semantic knowledge. The RAVLT and Verbal Fluency Test require both overlapping and distinct cognitive concepts, thereby allowing for specificity in lesion-symptom associations.

Patient characteristics

Patient characteristics for the tumor patients were extracted from the electronic patient file. This data included sex, age at time of surgery, level of education,

handedness, and WHO grade. For the stroke patients characteristics were obtained either from the semi-structured interview before the neuropsychological assessment and/or by reviewing the electronic patient file. This data included sex, age, level of education, handedness, stroke location based on MRI, date of stroke onset and medical history.

Image processing

Image Acquisition

A T2 FLAIR sequence was used for lesion delineation in the present study. For the glioma patients this was acquired as part of standard clinical care and the pulse-sequence details of the FLAIR MRI varied between glioma patients. T2 FLAIR scans with a slice thickness >5 mm were excluded in order to maintain adequate quality for lesion segmentation for all included glioma patients. The MRI scan that was closest to the pre-operative neurocognitive testing was chosen.

Depending on the medical center, stroke patients underwent a 3T MRI on a Philips Ingenia R5 (Amsterdam UMC and UMCU) or on the Siemens Magnetom Prisma (Radboudumc and UMCG), using a 32-channel head coil. For the Philips scanner the pulse-sequence details were: 3D T2 FLAIR (TI = 1650ms, TR = 4800ms, TE = 253ms, [FOV] = 250mm, voxel size 1.12×1.12×0.56mm). For the Siemens scanner they were 3D T2 FLAIR (TI = 1650ms, TR = 4800ms, TE = 484ms, [FOV] = 280mm, voxel size 0.9×0.9×0.9mm).

Lesion delineation

Both tumor and stroke lesions were segmented on individual T2 FLAIR images. Both tumor and stroke lesion were first drawn in the axial plane and adjusted accordingly in the sagittal and coronal plane. Tumor lesions were delineated using the Smartbrush implemented in the iPlan v3.0 software (BrainLab AG, Feldkirchen, Germany) and represent the total lesion volume, including both tumor and edema. For the tumor patients, a training set (N = 22) was completed in which all tumor regions were drawn by two researchers (EG & VR) under the supervision of an experienced neurologist (TS). After completing the training set, tumor regions were drawn by one of the two researchers. Through consensus meetings with the neurologist (TS), definitive lesion maps were created. The interrater reliability was calculated as the number of voxels included by both raters, in reference to the mean number of voxels selected per rater.³³ Based on eight different tumor lesions, the interrater reliability was 93.0% (range 88.8-96.7%). Stroke lesions were delineated semi-automatically or manually with the ITK-snap software.³⁴ Stroke lesions were delineated by three researchers and in case of doubt for specific scans, a neurologist

or radiologist was consulted. The interrater reliability was calculated based on eight stroke lesion masks using the same method as for the tumor interrater reliability. The interrater reliability for all three raters was 81.3% (range 69.8-91.1%), as reported previously.²⁹

Pre-processing

Each individual's FLAIR and binary lesion mask (both tumor and stroke) were normalized to an age-specific older adult MNI template using the Clinical Toolbox^{35,36} implemented in SPM12 (www.fil.ion.ucl.ac.uk/spm). For unilateral lesions, enantiomorphic normalization was applied to reduce distortions in the normalization due to the lesion.³⁷ For bilateral lesions normalization with cost function, masking was applied.³⁸ If the normalization results using enantiomorphic normalization was unsatisfactory for the tumor data, the normalization process was repeated using cost-function masking. The superior lesion mask (defined as visually best representing the original lesion location) was used in subsequent analyses. After spatial normalization, each lesion mask in MNI space was visually compared to the lesion in native space, and manually corrected if needed. Subsequently, the lesion mask was smoothed with a Gaussian kernel of 3 mm at FWHM. For stroke patients, normalization was optimized for patients with enlarged ventricles (>1.5 SD above ventricle volume in elderly template) using a warping regularization reduced by one order of magnitude. The resolution of the normalized lesion maps was 2x2x2 mm³. All results are displayed in neurological orientation (left = left hemisphere).

Data analysis

Multivariate lesion-symptom mapping

LSM was applied to test the relationship between lesion status in each voxel and cognitive performance, defined as a Z-score, for each task. For the multivariate LSM we used the support vector regression LSM (SVR-LSM) toolbox running under Matlab2019a (The MathWorks, Inc., Natick, Massachusetts, United States), which is a multivariate regression algorithm based on machine learning (github.com/atdemarco/svrlsmgui).^{39,40} This multivariate method, as opposed to a mass-univariate approach, considers intervoxel correlations and therefore is potentially more sensitive to examine lesion-behavior relationships.^{39,41} It has been successfully used and validated in multiple studies including both real and simulated lesion data.^{e.g.1,22,39,42} As no clear criteria on parameter choice are available yet, the hyperparameter values were kept at a cost of 30 and a gamma of 5, following the original paper.⁴¹ A nonlinear radial basis function kernel was used. A lesion threshold of 3 (i.e. at least 3 patients with lesioned tissue at each voxel) was applied. To test the significance of the beta values, permutation testing was used

with 1000 permutations, and a voxelwise threshold of $p < .005$ without additional correction for multiple comparisons. Since severity of symptoms is often related to lesion size, we performed lesion volume correction by regressing lesion volume on both behavioral scores and lesion data (**Supplementary Table 2**), in line with the recommendations by DeMarco and Turkeltaub.⁴⁰ To assess the effects of this lesion volume correction, all analyses were repeated without correcting for lesion volume (see **Repository** for maps). We ran the SVR-LSM for each cognitive task for the tumor and stroke data separately. For each LSM analyses the area containing most voxels with peak significance was calculated. Additionally, we combined the data of both groups and performed the SVR-LSM analyses for each cognitive task using etiology (tumor or stroke) as a covariate on both the behavioral scores and lesion data (**Supplementary Materials**). The AALCAT atlas was superimposed on the results to relate significant voxels to brain regions. This atlas combines the 116 regions from the AAL atlas⁴³ with 34 white matter regions from the tractography atlas.⁴⁴ Areas with peak significance and/or areas with at least 10% of tested voxels significant are reported in the text.

Univariate lesion-symptom mapping

In LSM statistical testing is performed to identify voxels in which individuals with a lesion perform significantly worse compared to individuals without a lesion in that voxel. With the univariate method this statistical test is independently applied to each voxel in the brain, whereas multivariate LSM considers the effect of all lesioned voxels simultaneously. To substantiate the results from the multivariate LSM, additional univariate LSM was performed for each cognitive task for the tumor and stroke data separately, using the statistical analyses software NiiStat (<https://github.com/neurolabusc/NiiStat>). With continuous behavioral data NiiStat computes statistics using a general linear model. Only voxels damaged in at least 3 patients were considered in the analyses. In line with the multivariate LSM, lesion volume correction was performed. Lesion volume control in NiiStat is based on regressing lesion volume with the behavioral data only. To assess the effects of this lesion volume correction, all analyses were repeated without correcting for lesion volume (see **Repository** for maps). Permutation testing to correct for multiple testing was set to 10,000 permutations and a voxelwise threshold of $p < .05$ was used. Statistical power maps were generated for each LSM using the "nii_power" function of NiiStat, with a critical one-tailed threshold of $p < 0.05$ and a power of 0.6. Power maps hereby represent the number of patients that would be needed to replicate the results in 60% of the studies. A maximum number of 200 patients was chosen as adequate power. Next, for each cognitive task the percentage of voxels with adequate power was calculated relative to three different volumes:

(1) the voxels included in the LSM (minimum threshold of 3 lesions), (2) the voxels included in the LSM for both the stroke and the tumor group (minimum threshold of 3 lesions in both groups), (3) the total MNI brain volume.

Post-hoc analyses

Post-hoc analyses were performed on multivariate LSM results to directly compare cognitive performance between stroke and tumor in specific areas where the LSM findings in stroke and tumor diverged. Therefore, the interaction effect between lesion status and etiology was tested for specific atlas areas. Atlas areas that showed divergent lesion-symptom associations between stroke and tumor, despite sufficient lesion coverage, were selected for post-hoc analyses. For each subject, we recoded voxel counts per atlas area into damaged ($\geq 5\%$ of voxels affected) and not damaged. Next, areas that were damaged in at least 5 subjects of both the tumor and the stroke sample were selected. Post-hoc analyses were performed per atlas area to directly test whether there was an interaction between lesion status (damaged versus not-damaged) and etiology on cognitive performance. We anticipated that the assumption of normally distributed data would be violated in our dataset and selected a non-parametric alternative. A studentized permutation version of the Wald-type statistic (WTS), as implemented in the GFD R package,⁴⁵ was used to test both the main effects of lesion status and etiology as well as their interaction effect. This WTS does not require normally distributed data or variance homogeneity, contrary to the more regular ANOVA statistic.

RESULTS

Clinical characteristics

In the period between January 2010 and July 2019 254 treatment-naïve diffuse glioma patients (WHO grade II-IV) were scheduled for awake brain surgery and included in the retrospective cohort study. Of these 254 patients, a subset of 196 glioma patients could be included for analyses. Of the 222 first-ever cerebral stroke patients, 147 were included for this analysis (**Figure 1**). Average time between ischemic infarct and cognitive assessment was 7.9 weeks (SD = 4.5). Patients from the tumor and stroke group did not differ from each other regarding sex distribution, level of education and hand preference (**Table 1**). On average, the stroke patients were older, despite a comparable age range. Lesion volume was significantly larger in the tumor group (**Supplementary Materials**). While the stroke group had an equal distribution of left and right hemisphere lesions, most tumor patients had a lesion in the left hemisphere. Most tumor patients had a grade IV glioblastoma, IDH-wildtype, followed by grade II + III astrocytoma, IDH-mutant.

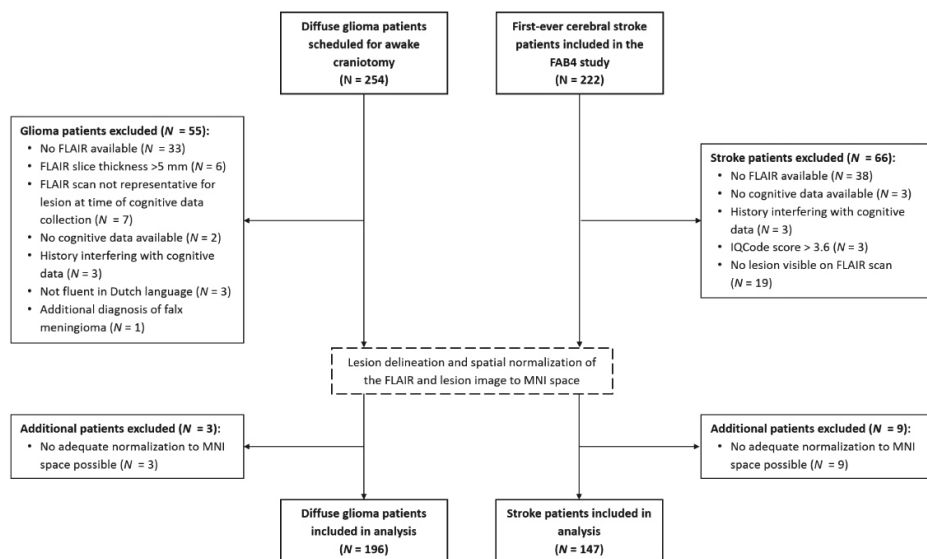


Figure 1. Flow-chart of the in- and exclusion separately for the tumor and stroke population.

Lesion topography

The lesion overlay images of both groups showed a wide distribution of lesions covering both hemispheres (**Figure 2**). Tumor lesions were most often located in the left hemisphere, with the highest frequency of lesions in the insula, operculum and superior temporal gyrus. In the right hemisphere the maximum overlap was located more posterior in the pre- and postcentral gyrus. Most stroke lesions were located within the territory of the right middle cerebral artery, with maximum overlap in the insula, putamen and operculum. In total 46.4% of the voxels were lesioned in at least one patient from both the tumor and stroke group. In 21.8% of the voxels both the tumor and the stroke group had at least 3 patients with a lesion. See **Supplementary Table 4** for an overview of the average percentage of overlap for each atlas structure. For the tumor group, the thresholded lesion overlap map included 125 of the 150 atlas areas. For the stroke group, 98 areas had sufficient coverage. In these lesion maps, the median overlap per area was 12.8% and 4.8% for the tumor and stroke group respectively. The number of areas that had >5% of patients with overlapping lesions in both the tumor and the stroke populations, was limited to 38 out of the 124 atlas areas.

Neurocognitive performance

Fifty-five percent of the tumor patients and 71% of the stroke patients had a cognitive impairment on at least one cognitive task. Letter fluency (30%) and working memory

(26%) were the most frequently affected functions in tumor patients, followed by memory recall (23%), visuoconstructive abilities (23%), and semantic fluency (21%). In the stroke group, visuoconstructive abilities (29%) and letter fluency (24%) were the most often affected domains. Fewer stroke patients experienced impaired working memory (18%) and memory recall (17%) (**Figure 3**). Only for naming abilities and semantic fluency, there was a significant difference between stroke and tumor in the number of patients with cognitive impairments (naming: $\chi^2(1, N = 280) = 8.08$ $p = 0.004$; semantic fluency: $\chi^2(1, N = 277) = 4.20$ $p = 0.04$). Performance on the continuous measures of the cognitive tasks used for LSM (RAVLT and verbal fluency) was not significantly different between tumor and stroke (immediate recall: $t = -0.71$, $p = 0.48$; delayed recall: $t = 0.30$, $p = 0.77$, delayed recognition: $t = 0.90$, $p = 0.37$, letter fluency: $t = -0.85$, $p = 0.40$, semantic fluency: $t = -0.12$, $p = 0.90$).

Table 1. Clinical characteristics for the tumor and stroke patients.

	Tumor	Stroke
N	196	147
Sex (%)		
Male	128 (65.3)	99 (67.3)
Female	68 (34.7)	48 (32.7)
Mean age (SD)	50.9 (14.1)	57.4 (12.9)
Range	21-81	19-82
Mean educational level (SD) ^a	5.4 (1.3)	5.3 (1.3)
Hand preference (%) ^b		
Left	26 (13.3)	18 (12.2)
Right	163 (83.2)	125 (85.0)
Ambidexter	1 (0.5)	2 (1.4)
Unknown	6 (3.1)	2 (1.4)
WHO 2016 classification (%)		N.A.
II + III astrocytoma IDH-M	55 (28.1)	
II + III astrocytoma IDH-WT	12 (6.1)	
II + III oligodendroglioma IDH-M 1p19q	38 (19.4)	
IV glioblastoma IDH-M	4 (2.0)	
IV glioblastoma IDH-WT	72 (36.7)	
Unknown	15 (7.7)	
Median lesion volume in cm ³ (SD)	66.5 (71.9)	5.8 (27.1)
Range	1.2 – 349.1	0.1 – 233.2
Lesion location (%)		
Left	117 (59.7)	66 (44.9)
Right	65 (33.2)	66 (44.9)
Bilateral	14 (7.1)	15 (10.2)

Group differences in clinical characteristics were tested with a Pearson χ^2 test or Kruskal-Wallis test when appropriate. Significant differences ($p < 0.05$) are shown in bold. ^aEducational level was assessed using the Verhage criteria (1964). ^bHand preference was self-reported.

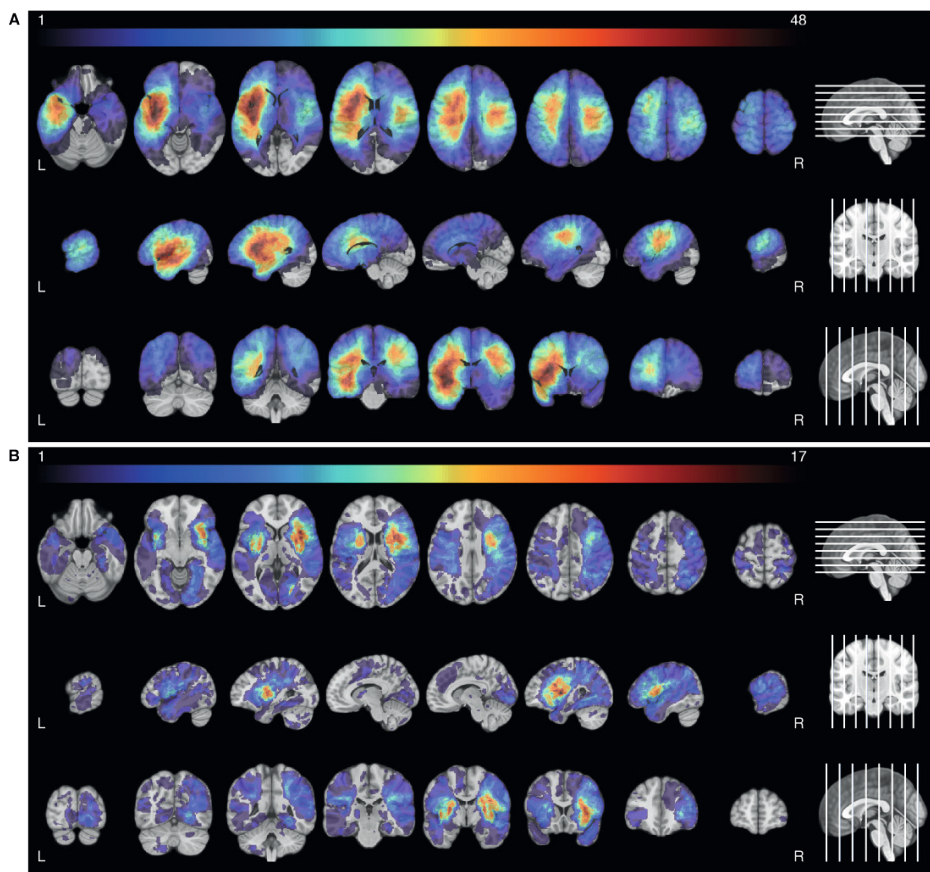


Figure 2. Lesion prevalence maps for the tumor (A) and stroke group (B) are shown superimposed on the MNI brain. Multiple slices are shown in the axial, sagittal and coronal plane. The MNI brain on the right indicates the location of the slices shown in the figure. The legend refers to the number of patients with a lesion at that voxel, with red indicating a higher number of patients. The maximum number of patients with an overlap of lesion damage is 48/196 and 17/147 for the tumor and stroke group, respectively. L = left, R= right.

Multivariate lesion-symptom mapping results

Direct recall verbal memory (Figure 4C)

For tumor patients, SVR-LSM analysis indicated that worse performance on the RAVLT Direct Recall was most strongly associated with lesion in the left cingulum (8.0% of tested voxels in that area were significant). Significant voxels extended into the left hippocampus (60.7%), parahippocampal gyrus (24.8%), lingual gyrus (14.2%) and the fusiform gyrus (9.9%). Besides lesions in grey matter areas, lesions in the optic radiation (14.2%) and the inferior longitudinal fasciculus (ILF; 10.4%) were also significantly associated with worse performance.

For the stroke group, lesions within the putamen were most strongly associated with worse performance (21.0% of tested voxels significant). Additionally, two left-sided white matter tracts, the inferior fronto-occipital fasciculus (IFOF; 13.7%) and the uncinate fasciculus (18.5%) were strongly associated with task performance.

No directly overlapping significant voxels were found, but in both groups, lesions within the left IFOF were related to worse performance on the direct recall albeit with relatively less significant voxels in the tumor group (**Figure 4C** and **Table 2** for a visual representation of all significant voxels and an overview of the percentage of tested voxels that were significant).

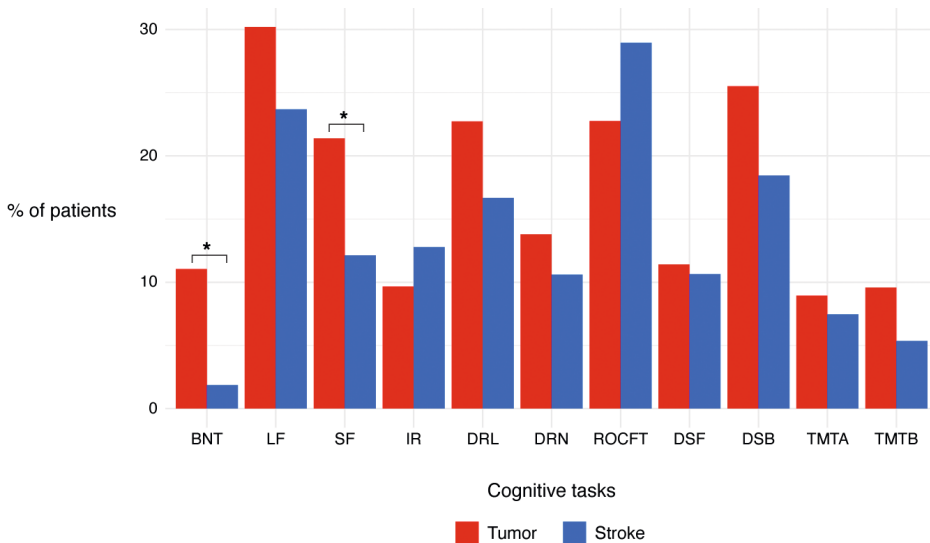


Figure 3. Percentage of patients with a z-score ≤ -1.5 in the tumor (red) and stroke group (blue) for all available cognitive tasks. Asterisks indicate significant difference between the tumor and stroke group. Abbreviations: BNT, Boston Naming Task; LF, letter fluency; SF, semantic fluency; IR, immediate recall (RAVLT); DRL, delayed recall (RAVLT); DRN, delayed recognition (RAVLT); ROCFT, Rey Osterreith Complex Figure Test Copy; DSF, digit span forward (WAIS); DSB, digit span backward (WAIS); TMTA, trail making test part A; TMTB, trail making test part B (ratio score).

Delayed recall verbal memory (Figure 4D)

The SVR-LSM analyses in tumor patients identified a cluster of voxels located within the left ILF (19.6%) that was associated with worse performance on the RAVLT delayed recall. Lesions within the left hippocampus (44.6%), optic radiation (19.3%), parahippocampal gyrus (15.7%), IFOF (12.4%), inferior temporal gyrus (10.6%) and fusiform gyrus (10.0%) were also associated with worse performance.

For stroke patients, lesions within the left putamen (18.7%) were associated most with task performance. For both patient groups the IFOF was associated with task performance, but there were no directly overlapping significant voxels (**Figure 4D** and **Table 2**). Moreover, the relative number of significant voxels was higher in the tumor group than in the stroke group for this area.

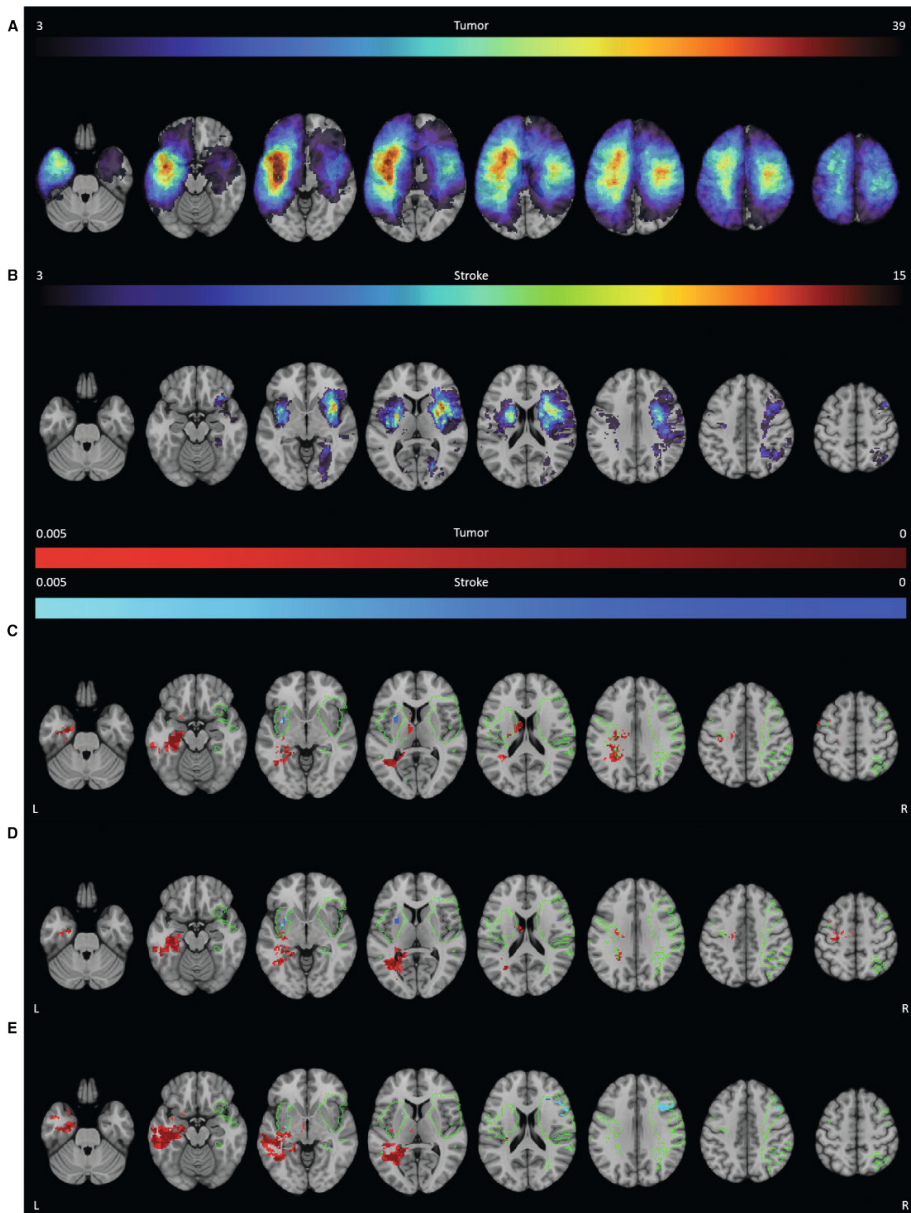


Figure 4. SVR-LSM results for the RAVLT. The thresholded lesion overlap for this task is shown for both the tumor (A) and stroke group (B). The color bar indicates the number of patients with overlapping lesions. Voxels that were significantly associated with worse performance are shown for the tumor group (red) and the stroke group (blue) for the direct recall (C), delayed recall (D) and delayed recognition (E). The colors indicate the p-value for each voxel. The green outline indicates the area within which both groups had a minimum lesion overlap of 3 patients. L = left, R= right.

Delayed recognition verbal memory (Figure 4E)

Tumor lesions within the left middle temporal gyrus (24.6%) were strongly associated with worse performance on the RAVLT delayed recognition. Significant voxels were also found in other grey and white matter areas in the left hemisphere, including the hippocampus (58.5%), ILF (40.3%), optic radiation (23.5%), posterior segment of the arcuate fasciculus (20.8%), parahippocampal gyrus (19.7%), inferior temporal gyrus (17.4%), fusiform gyrus (14.4%) and the IFOF (14.1%).

For stroke patients not only lesions in the left optic radiation (31.1%), but also in the inferior frontal gyrus opercular (24.8%) and middle frontal gyrus (11.7%) in the right hemisphere were associated with recognition performance. Results from both etiologies indicated the left optic radiation to be involved in task performance. The left IFOF was also found in both groups, albeit with a lower number of significant voxels in the stroke group (**Figure 4E** and **Table 2**).

Letter fluency (Figure 5)

The SVR-LSM analyses indicated that tumor lesions within the insula (20.7%) were highly associated with worse letter fluency performance. Significant voxels extended into grey matter in the left inferior frontal gyrus opercular (24.4%) and triangular (12.5%).

Stroke lesions within the left corticospinal tract (9.6%) and putamen (16.5%) were most associated with the task performance. No overlapping region between the tumor and stroke group was found associated with letter fluency performance (**Figure 5** and **Table 2**).

Semantic fluency (Figure 6)

Performance on a semantic fluency task was strongly associated with tumor lesions in the left arcuate fasciculus (16.0%). Additionally, other involved white matter areas included the left long segment of the arcuate fasciculus (32.9%), anterior segment of the arcuate fasciculus (31.3%) and the corticospinal tract (14.9%). Additionally, lesions in the grey matter of the rolandic operculum (16.4%), Heschl's gyrus (15.4%) and the precentral gyrus (14.9%) were associated with worse task performance.

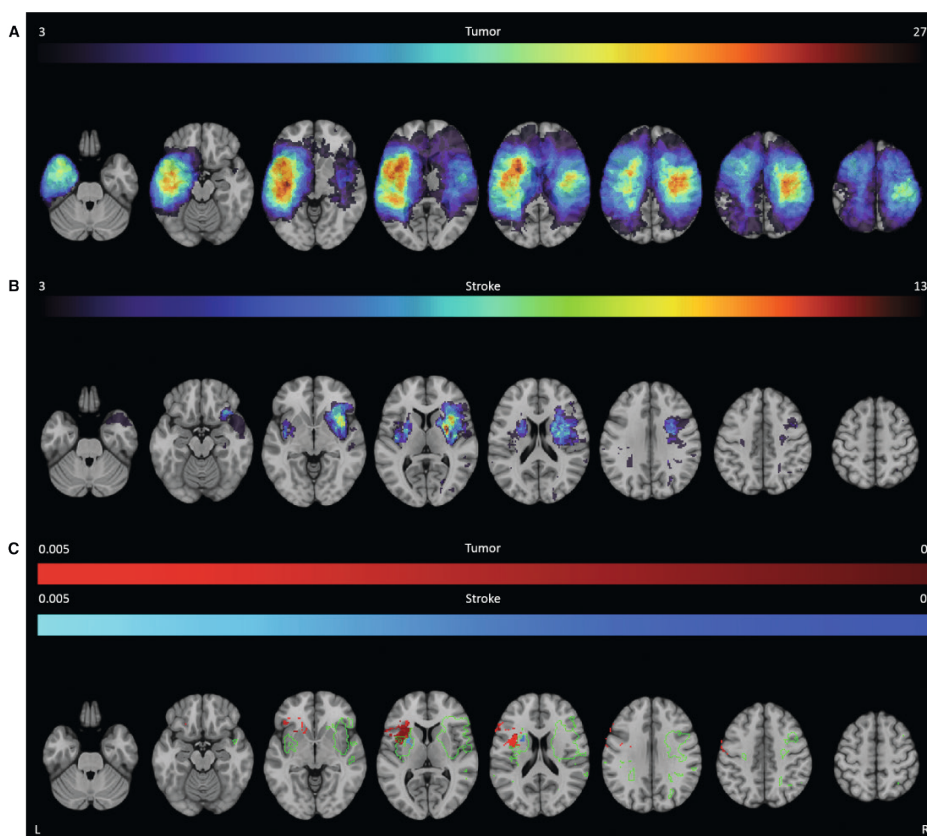


Figure 5. SVR-LSM results for the letter fluency. The thresholded lesion overlap for this task is shown for both the tumor (**A**) and stroke group (**B**). The color bar indicates the number of patients with overlapping lesions. Voxels that were significantly associated with worse performance are shown for the tumor group (red) and the stroke group (blue) for the letter fluency (**C**). The colors indicate the p-value for each voxel. The green outline indicates the area within which both groups had a minimum lesion overlap of 3 patients. L = left, R= right.

Stroke lesions within the left precentral gyrus (1.1%) were most associated with worse semantic fluency scores. In general, most brain areas did not overlap between the tumor and stroke LSM (**Figure 6** and **Table 2**). Nevertheless, lesions in the left corticospinal tract and left precentral gyrus were associated with the task performance in both groups. Of note is that the percentage of significant voxels was lower in the stroke group, even though they contained peak significant values.

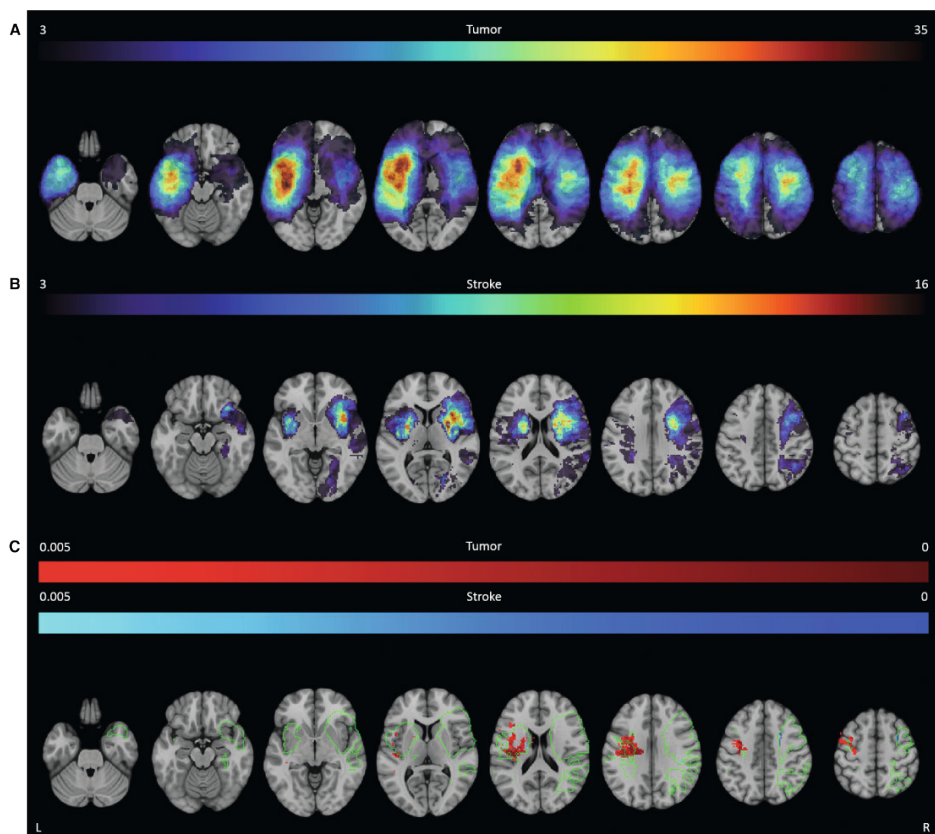


Figure 6. SVR-LSM for the semantic fluency. The thresholded lesion overlap for this task is shown for both the tumor (**A**) and stroke group (**B**). The color bar indicates the number of patients with overlapping lesions. Voxels that were significantly associated with worse performance that were significantly associated with worse performance are shown for the tumor group (red) and the stroke group (blue) for the semantic fluency (**C**). The colors indicate the p-value for each voxel. The green outline indicates the area within which both groups had a minimum lesion overlap of 3 patients. L = left, R= right.

Specificity of lesion-symptom results

Specificity of the lesion-symptom results was assessed by calculating the amount of overlap between voxels that were significantly related to any of the three memory tasks compared to the two fluency tasks. For the tumor group, there was a 2.0% overlap between voxels related to both memory and fluency performance. This overlap was mainly located in and around the left cortico-spinal tract, internal capsule, arcuate fasciculus and corpus callosum. Additionally, some overlapping voxels were found in the left precentral gyrus. 13.9% of voxels associated with all three memory tasks and 33.9% with any two memory tasks. Overlapping areas for all three tasks were located in the left hippocampus, parahippocampal gyrus, the

cingulum, corpus callosum and ILF. For any two memory tasks this extended into the left fusiform gyrus, the temporal gyrus and optic radiations. Between the two different fluency tasks, there was an 8.6% overlap in significant voxels. These were located in and around the left insula, inferior frontal gyrus, rolandic operculum and arcuate fasciculus.

For the lesion-symptom results in the stroke group there was a 4.9% overlap between voxels related to both memory and fluency task performance. Overlapping voxels were mainly located in the left putamen and the cortico-spinal tract. 1.3% of voxels were associated with all three memory tasks and 18.4% with any two memory tasks. For all three memory tasks the overlapping voxels were mainly located in the left IFOF and optic radiations. For any two memory tasks this extended into the left putamen and uncinate fasciculus and the right insula and IFOF. There were no voxels significantly related to both the phonological and semantic fluency task.

Post-hoc analyses (Figure 7)

Post-hoc interaction analyses were performed to further examine atlas areas that showed lesion-symptom associations for only one of the two etiologies, despite sufficient lesion coverage in both. A complete overview of the post-hoc results can be found in **Figure 7**.

For the lesion-symptom associations found in the tumor group only, post-hoc analyses using a permutation version of the Wald-type statistic (WTS) revealed significant interaction effects between lesion status (damaged versus not damaged) and etiology (stroke versus tumor) in 6 out of 9 tested atlas areas. Interaction effects were found for semantic fluency performance in the left insula ($W_T = 5.08$, $p = .033$), left rolandic operculum ($W_T = 9.40$, $p = .01$), left Heschl's gyrus ($W_T = 4.69$, $p = .048$) and white matter areas of the left arcuate fasciculus ($W_T = 6.88$, $p = .016$) (including the long segment ($W_T = 7.39$, $p = .015$) and anterior segment ($W_T = 6.21$, $p = .023$)), with worse performance for tumor lesions. For the association between the left internal capsule and semantic fluency there was only a significant main effect of lesion status ($W_T = 5.43$, $p = .04$). This association was more pronounced in the tumor group, but a similar trend was present in the stroke group. The association between the left corticospinal tract and delayed recall performance was even stronger in stroke than in tumor, leading to a significant main effect of lesion ($W_T = 22.6$, $p < .001$) as well as a significant main effect of etiology ($W_T = 4.88$, $p = .045$). The association between the left caudate and worse direct recall performance was not confirmed in post-hoc analysis.

For the lesion-symptom associations found solely in the stroke group, only the left putamen had sufficient lesion coverage to allow further post-hoc analysis. None of the post-hoc analysis for the left putamen, showed significant main or interaction effects. The variability in cognitive performance was high in the subset of subjects with left putamen lesions, independent of etiology.

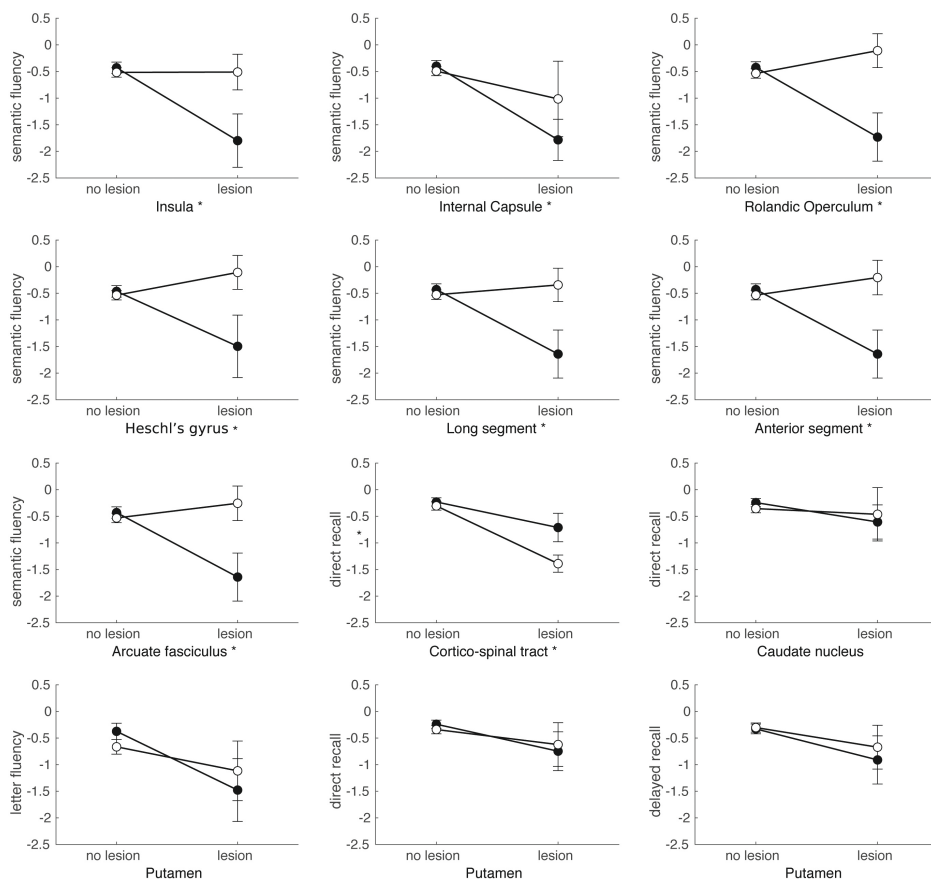


Figure 7. Post-hoc interaction plots based on SVR-LSM results. Plots show the mean and standard error of the cognitive performance per etiology (tumor [black] versus stroke [white]), and lesion status (lesion versus no lesion). All brain areas were in the left hemisphere and their labels are depicted below the individual plots. Cognitive performance on the different tasks (semantic fluency, letter fluency, direct recall RAVLT and delayed recall RAVLT) is shown as z-scores on the y-axis. An asterisk next to the label indicates a brain area for which a significant interaction effect was found.

Table 2. Detailed descriptions of the anatomical location of significant voxels identified by the SVR-LSM analyses

Anatomical location	Hem		Direct recall		Delayed recall		Recognition		Letter fluency		Semantic fluency	
	L	R	T	S	T	S	T	S	T	S	T	S
Grey matter regions												
Precentral gyrus	L				7.2						14.9	1.1
Superior frontal gyrus, dorsolateral	R	a		a			a		a			a
Middle frontal gyrus	R						11.7		a			2.8
Inferior frontal gyrus. opercular	L							24.4	a		7.1	
Inferior frontal gyrus. opercular	R				1.9		24.8					
Inferior frontal gyrus. triangular	L	a		a			a		12.5	a		a
Inferior frontal gyrus. triangular	R						4.6					
Rolandic operculum	L							7.4			16.4	
Insula	L							20.7			7.7	
Hippocampus	L	60.7	a		44.6	a	58.5	a		a		a
Parahippocampal gyrus	L	24.8	a		15.7	a	19.7	a		a		a
Amygdala	L	a					6.6	a		a		a
Calcarine fissure	L	a			6.2	a		a		a		a
Lingual gyrus	L	14.2	a		8.2	a	5.4	a		a		a
Fusiform gyrus	L	10.0	a		10.0	a	14.4	a		a		a
Caudate nucleus	L	9.9										
Putamen	L	21.0			18.7					16.5		
Thalamus	L	7.2	a		a		6.0	a		a		a
Heschl gyrus	L										15.4	
Middle temporal gyrus	L	a			a		24.6	a		a		a

Table 2. Detailed descriptions of the anatomical location of significant voxels identified by the SVR-LSM analyses (continued)

Anatomical location	Hem	Direct recall	Delayed recall	Recognition	Letter fluency	Semantic fluency
Inferior temporal gyrus	L	a	10.6 ^a	17.4 ^a	a	a
White matter regions						
Anterior Segment	L					31.3
Arcuate Fasciculus	L	6.7				16.0
Cingulum	L	8.0 ^a	7.0 ^a	5.9 ^a	a	a
Cortico-ponto-cerebellar tract	L	8.4 ^a	a	9.4 ^a	a	5.6 ^a
Corticospinal tract	L	8.5			9.6	14.9 3.2
Fornix	L	7.7 ^a	6.3 ^a	6.2 ^a	a	a
Inferior Longitudinal Fasciculus	L	10.4 ^a	19.6 ^a	40.3 ^a	a	a
Inferior Fronto-Occipital Fasciculus	L	7.3	13.7	14.1	4.8	8.1
Internal Capsule	L	5.4	5.5	6.2		8.6
Long Segment	L				9.0	32.9
Optic Radiation	L	14.2	19.3	23.6	39.0	a
Posterior Segment	L	8.6 ^a	9.2 ^a	20.8 ^a	a	a
Uncinate Fasciculus	L	18.5	7.2	6.4		

Numbers represent the percentage of significant voxels proportioned to the total of tested voxels for that atlas area in SVR-LSM analyses. Bold values contain the peak z-values in most voxels for each cognitive task. If a task was found to be associated with more than 5 atlas areas, only tested areas containing at least 5% significant voxels are reported. Smaller clusters are included if they contained peak z-values for that task. ^aRegions with less than 5% coverage of that atlas area in that population.

Abbreviations: Hem, hemisphere; L, left; R, right; T, tumor; S, stroke.

Univariate lesion-symptom mapping results

We performed univariate LSM with lesion volume control to corroborate results found in the multivariate LSM analyses. For the tumor population, worse performance on the RAVLT Direct Recall and Delayed Recognition was not related to specific lesion locations when using univariate analyses. For the RAVLT Delayed Recall, letter fluency and semantic fluency voxels related to worse performance on the univariate analyses largely overlapped with those from the multivariate analyses (see **Supplementary Figure 7** and **8**). Regions indicated by multivariate analyses seem to expand from the overlapping regions and encompass larger brain areas.

For the stroke patients, univariate LSM did not indicate a significant relationship between lesion location and cognitive performance for the RAVLT direct recall, delayed recall or delayed recognition. For the two fluency tasks (letter and semantic) voxels related to worse performance on the univariate analyses largely overlapped with those from the multivariate analyses (see **Supplementary Figure 9** and **10**). Regions indicated by multivariate analyses seem to expand from the overlapping regions and encompass larger brain areas. As less voxels were significant in the univariate analyses for both the tumor and stroke group, the minimal overlap that was found with multivariate LSM decreased even further when using univariate LSM results.

Statistical power

To assess possible difference in power throughout the brain, statistical power maps were created for each univariate LSM for the tumor and stroke group separately (see **Supplementary Figure 11**). Adequate power was set at a maximum of 200 patients needed to replicate the results in 60% of the studies. The relative number of voxels with an adequate power was calculated relative to (1) the coverage for the specific cognitive task (minimum threshold of 3 lesions), (2) the overlap in coverage (minimum threshold of 3 lesions in both the stroke and tumor group), and (3) the total MNI brain volume. For each cognitive task, more voxels had adequate power in the tumor than in the stroke group (see **Table 3**).

Lesion volume correction

Both multivariate and univariate LSM were repeated without correcting for lesion volume (maps available in **Repository**). All LSM results were visually compared and no major differences between lesion volume corrected and uncorrected results were found. Corrected LSM tended to encompass smaller, but overlapping, areas with the uncorrected LSM. From the non-corrected LSM, voxels expanded from those regions, thereby indicating more voxels were significantly related to task

performance when lesion volume was not taken into account. Largest differences between corrected and uncorrected LSM results were seen for the tumor group, especially for the RAVLT Delayed recognition and Semantic fluency task.

Table 3. Percentage of voxels with adequate power for univariate LSM (maximum of 200 patients needed to replicate results in 60% of studies) relative to the etiology-specific coverage for the cognitive task, the overlap in coverage between the tumor and stroke group for the cognitive task and the complete MNI volume.

Cognitive task	Coverage		Overlap		Whole-brain	
	Tumor	Stroke	Tumor	Stroke	Tumor	Stroke
Direct recall	31.8	18.2	28.9	19.4	23.7	2.0
Delayed recall	32.2	13.0	26.8	13.7	24.0	1.4
Delayed recognition	20.8	10.5	20.4	11.2	15.5	1.1
Letter fluency	42.6	34.4	30.9	27.7	26.6	2.1
Semantic fluency	42.9	16.0	30.0	17.0	30.2	2.4

DISCUSSION

In this study, we investigated whether etiology-specific biases impact brain-behavior associations in LSM. This study is unique in comparing results from state-of-the-art machine learning-based, multivariate LSM between two large study-populations, a tumor versus a stroke population. We expected overlapping lesion-symptom associations in brain areas affected in both populations and population-specific lesion-symptom associations in brain areas covered per pathology. Despite our large sample sizes, substantial differences in lesion distribution conditioned the degree of lesion overlap between stroke and tumor and hindered direct comparison for most brain areas. Still, both our LSM results as well as the post-hoc analyses suggested that the cognitive effects of damage in certain brain areas depend on the underlying pathology.

Lesion topography

Both study samples showed a wide distribution of lesions covering both hemispheres. Tumors were most prevalent in the left hemisphere, with the highest frequency in the insula, operculum and superior temporal gyrus, while strokes were predominantly located within the territory of the right middle cerebral artery. As patients selected for awake surgery are characterized by tumor localization in eloquent areas, such as language and motor areas, this left-sided predominance was to be expected. Nevertheless, lesion coverage was adequate in both hemispheres. Overall, lesion overlap was both more widespread and higher per brain structure

in the tumor group. Lesion volume was skewed to larger volumes in the tumor group, and to smaller lesions for stroke. These differences in lesion distribution, overlap and volume had repercussions for the statistical power throughout the brain and consequently the ability to compare LSM; only one-fifth of voxels survived the minimal power threshold for direct comparison.

Lesion-symptom mapping

In both samples cognitive impairments were present in more than half of the patients. Despite the clear differences in lesion distribution between tumor and stroke, the cognitive profile was quite similar on a group-level. Importantly, there were no significant group-level differences in performance on the memory and fluency tasks. Lesion volume was correlated with cognitive performance in the tumor group. However, the larger lesion volume in the tumor group did not result in more cognitive impairments compared to the stroke population. Memory and fluency tasks and their neuroanatomical correlates present differentiated cognitive processes, as expected. That is, more resemblance was found in critical neuroanatomical locations within than between cognitive domains. For both populations the overlap between the tasks was mainly located in white matter pathways which have been independently related to memory and fluency performance previously.^{24,46-50} As these white matter tracts have also been related to other cognitive processes, like attention, processing speed and executive functioning,^{24,42,51} it is most likely that these overlapping regions are involved in a wide range of cognitive processes, including memory and fluency. Of note, overlapping lesions for the tumor and stroke group were mostly found in the white matter and subcortical areas. Thereby the power to find overlapping LSM results between our groups was highest in these white matter areas. In addition, lesion volume correction was performed to eliminate the effect of differences in lesion size between the groups on LSM results as much as possible. In the uncorrected LSM we mainly found larger areas associated with task performance for the tumor group, with significant voxels expanding from the regions found with the corrected LSM. Nevertheless, the overlap between the tumor and stroke LSM results only changed slightly for the uncorrected LSM results, indicating lesion volume control was not a great influence in our comparison between etiologies.

Regions associated with memory performance in the tumor group were in both the grey and white matter areas surrounding the left hippocampus. These critical memory-regions are known from literature as part of the core network for episodic memory postulated by Benoit and Schacter⁵² as well as the human memory circuit from Ferguson and colleagues.⁵³ The left hippocampal areas had insufficient

coverage in the stroke group. The majority of memory-regions found in either sample have been identified or are adjacent to regions found previously in tumor and stroke populations.^{24,46,54}

The location of the fluency-related voxels, mainly in the left temporal and frontal lobe, aligns well with previous knowledge of the language system, and fluency in particular.^{26,47} Regions critical for letter fluency performance are located mostly in sensorimotor regions, while regions located around Broca's area were critical for semantic fluency. This distinction in neuroanatomical fluency correlates was also found in a large-scale study in 1231 stroke patients.⁵⁵ Similar to our results, they found lesion-symptom associations between frontotemporal regions and letter fluency, while more posterior temporal regions were crucial for semantic fluency. The importance of white matter to language functions in tumour patients was also found in a recent LSM study in patients suffering from left perisylvian gliomas.²⁶ So, our study shows function-specific neural correlates for the memory and language functions that are corroborated by prior literature, supporting the validity of our LSM results in both populations.

That said, the LSM presents large differences between tumor and stroke. This can partly be explained by the etiology-specific brain coverage that allows for investigation of distinct brain areas in tumor versus stroke. However, also in brain areas affected in both groups the overlap was minimal; we found no directly overlapping voxels between the LSM for tumor and stroke on any task. The similarities we did find mostly involved associated white matter tracts, in accordance with previous literature.^{24,46,55,56} For example, verbal memory tasks were associated with the left IFOF in both populations. Additionally, the left corticospinal tract and precentral gyrus were associated with semantic fluency performance for both populations. These results were confirmed in the combined LSM analyses in which the relation between lesion location and cognitive performance, irrespective of etiology, was tested. Differences did exist, however, between these combined and separate etiology-specific analyses with some brain areas being critical areas in only one of the two analyses. Again, correction for lesion etiology in the combined analyses was only possible in regions where both populations had adequate lesion coverage. Moreover, as was also shown by the statistical power of the univariate LSM, more voxels had adequate power in the tumor group. Thereby, the results of the combined analyses are likely mainly driven by the lesion data available in the tumor population, due to the uneven sample distribution at the voxel level.

Though power inequalities could explain some of the differences, post-hoc analyses in regions with adequate coverage in both groups confirmed that the results of lesion-deficit inference strongly differ. To illustrate, in several brain areas the negative impact of a lesion in this area on semantic fluency performance was only present when this brain area was lesioned by a tumor. This was, however, not the case for all investigated brain areas. For example, all post-hoc analyses in brain regions that were significantly associated with cognitive performance in the stroke group, did not show a similar etiology interaction effect. Here, differences might be better explained by the large variation in cognitive performance, thereby failing to reach significance in the lesion-symptom mapping analyses.

We specifically investigated the effect of etiology on lesion-symptom associations identified by lesion-symptom mapping. In both tumor and stroke, however, the impact of a lesion can extend far beyond local changes in circumscribed tissue visible on standard imaging techniques, and a small lesion can have widespread effects on behavior.^{8,28,57-61} This might also explain the similarity in cognitive profiles between the two samples despite clear differences in lesion location and volume. It is likely that the degree of overlap between both samples is underestimated in terms of structural and functional connections. Nevertheless, this does not explain why we found different cognitive effects in brain areas with overlapping lesion coverage.

Etiology-specific cognitive effects

Few studies discuss the impact of etiology on lesion-behavior associations. Anderson and colleagues matched a small group of brain tumor patients ($n = 17$) to patients with unilateral stroke based on lesion location and compared cognitive outcome.⁶² They showed substantial differences in cognitive performance, with tumor patients outperforming matched stroke subjects and showing relatively mild impairments. Accordingly, it is still often assumed that the location of a tumor bears little explanatory value. This assumption was challenged by Shallice and colleagues⁶³, who did find selective and dissociated visuo-spatial deficits in a series of brain tumor patients.

Two studies of more recent date directly compared the impact of different etiologies on the cognitive sequelae of lesions. Frontal-based functions were compared between tumor and stroke patients and showed no differences in performance.¹⁶ Here, the authors selected patients with frontal lesions, but did not perform further LSM. In a LSM study of apraxia, tumor and stroke patients were included and analyzed both separately and combined.⁶⁴ Critical brain areas for apraxia matched previous literature, but differed in the tumor and stroke group. This is in line with

our findings, since we could relate eloquent functions to areas with an established role in that function.

Tumor patients in lesion-symptom mapping

Different factors could explain the minimal overlap in critical areas, even in brain areas with adequate lesion coverage in both groups. Some factors are inherent to lesion studies in general, others are etiology specific. First, both tumor and stroke have a systematic bias in lesion anatomy. For example, if region A and region B get blood supply from the same artery, a stroke in this artery will likely damage both regions. Suppose that only region A is causally related to the function under investigation, a lesion-symptom association for region B can be found as a mere side-effect.^{11,65,66} The possibility of collateral damage is higher when lesion size increases, irrespective of etiology. Thus, it is possible that some regions are associated with the behavioral deficit in one population but not the other, because of correlated damage occurring in one population only. Hence, the lesion-symptom association in question (region B) is not a causal relation.

Second, several tumor-related factors could cause over- or underestimation of affected tissue. These include the possibility of functional reorganization, tumor invasion of apparently healthy tissue, and vice versa the possibility of functional tissue within the area demarcated by abnormal MRI signal. Both temporal and spatial differences in activity have been observed in glioma-infiltrated cortex compared to healthy cortex during language tasks.¹⁵ This could indicate that glioma-infiltrated cortex also negatively impacts cognitive performance. Since our results indicated that on group level larger tumor lesions did not lead to worse cognitive performance compared to the smaller stroke lesions, this increases the likelihood of functional reorganization in our tumor group. However, in the current tumor sample a large proportion of patients had high-grade gliomas (38.7%), while the chance of functional reorganization or function preservation within the tumor area is highest in slow-growing lesions, like low-grade glioma.¹⁸ Last, mass effect, shift and infiltration of white matter pathways, and increased intracranial pressure may cause noise in lesion-symptom associations. These effects do not always lead to destruction of structures, but impact lesion-symptom associations through spatial displacements that are specific for brain tumors, and may change over time.⁶⁷ These tumor-related factors have been used as arguments against the use of tumor series in function localization. On the other hand, our study also clearly illustrates the advantage of using multiple etiologies. Firstly, the ability to investigate a broader range of brain structures unconstrained by the nonrandom lesion distribution inherent to

each pathology. Secondly, LSM in tumor series may be especially valuable to make assumptions about function localization prior to neurosurgery.

Study limitations and further directions

Methodological choices

LSM tools are used to identify the neural structures critical for a given behavior. However, multiple methodological choices can influence subsequent LSM results. In the current study we performed LSM using two different types of analyses; a univariate and multivariate approach. Previous research has indicated neither method is superior, but rather both have advantages and disadvantages.^{1,10} For example, the multivariate SVR-LSM used in the current study could have been affected by the hyperparameter selection. As no clear criteria on parameter choice are available yet hyperparameter values were kept in line with the original paper. However, this selection was based on a specific stroke sample, with larger lesion sizes (median 76.79 cc) than our current sample.³⁹ Therefore, we corroborated our multivariate LSM results using univariate LSM. However, univariate voxelwise LSM can be conservative due to strict multiple testing corrections. This was also observed in our results with only a small number of voxels surviving significance testing. Nonetheless, most regions related to task performance in the univariate LSM overlapped with those from the multivariate LSM, thereby corroborating our results. Still, we cannot directly compare results from the univariate and multivariate analyses, since the lesion volume correction differed between methods and multiple comparison corrections were only performed for univariate analyses.

Additionally, we chose to perform lesion volume correction in order to eliminate the effect of lesion volume on our comparative analyses as much as possible. The importance of incorporating lesion volume into LSM analyses has been recommended for several years for both multivariate and univariate LSM.^{40,68,69} Nevertheless, for the SVR-LSM this means a double covariate control was performed, thereby possibly further decreasing the power to find overlapping regions between the tumor and stroke group. When comparing uncorrected and corrected LSM results, more areas were related to worse cognitive performance when lesion volume was not taken as a covariate, for both univariate and multivariate analyses. As to be expected, this effect was most pronounced for the tumor population as lesion size was significantly related to task performance (memory and fluency) in the tumor, but not stroke group. However, regardless of the specific LSM method that we used, there was minimal overlap between tumor and stroke LSM results, thereby substantiating our conclusion.

Power across the brain

The power-problem in LSM studies is a heavily discussed topic.^{10,70} Although our patient samples of stroke ($n = 147$) and tumor ($n = 196$) meet the general recommendations of 100-130 for LSM analyses, power does not only depend on the number of participants. Lesion distribution and volume also have a large effect upon the overall power of LSM studies. A sample with an average lesion volume of 3 cm^3 will cover substantially less voxels than a sample with an average lesion volume of 10 cm^3 . Hence, the number of voxels with sufficient power for lesion-symptom analysis will be lower in study samples with smaller lesion sizes. As a result, the number of areas in which we had sufficient overlap to directly compare the LSM between the study samples was only 38 out of the 124 atlas areas. Unfortunately, post-hoc power analyses for multivariate inference cannot be computed, complicating the investigation of the exact effect of power on the multivariate LSM results. However, power analyses for the univariate LSM suggested that also in these areas of overlap, the number of voxels with adequate power to allow for replication was only a quarter to one-third. Overall, the number of voxels with adequate power was higher in tumor than in stroke, especially at a whole-brain level.

These power issues are not unique to our sample. The topography of damage and lesion volume of our stroke sample are comparable to the sample described by Corbetta and colleagues ($n = 132$),⁷¹⁻⁷³ although they included both hemorrhagic and ischemic strokes and relatively small lesions compared to our study. The authors mention the relatively small number of overlapping cortical lesions as one of the main limitations of the study. Even in a large-scale, multi-cohort LSM study ($n = 2950$) with high lesion coverage (average 2.7 cm^3), some brain areas still achieved a maximum lesion overlap of five patients⁷⁴, demonstrating the uneven lesion distribution that is inherent to the stroke population.

Clinical representativeness

Our tumor sample included treatment-naïve diffuse glioma patients who underwent awake brain surgery. Consequently, the tumor population consisted of patients with different tumor grades and molecular markers. As edema, plasticity, lesion momentum and molecular markers are related to tumor grading, different tumor grades could be viewed as distinct (though related) etiologies. Additionally, previous research has indicated that certain molecular markers are independent determinants of cognitive functioning.²⁸ Subgroup analysis stratified by tumor grade or IDH mutation, according to WHO 2021 classification⁷⁵, would be an interesting follow-up study. Stroke populations could also be further subdivided according to time since stroke onset.⁷⁶ Current subgroup sample sizes were too

small to perform this analysis with enough statistical power. Moreover, patients selected for awake surgery differ from patient under general anesthesia in various baseline characteristics.⁸ Additionally, the use of anti-epileptic medication and/or dexamethasone may add noise to the cognitive data of our tumor sample. Nevertheless, this will not lead to gross violations of the internal validity of the lesion-symptom associations. Stroke data was collected in a multi-site research project. Patients with larger infarction and typically also more severe clinical stroke symptoms, participate less frequently in research. Thus, LSM studies that include research participants may be systematically biased towards smaller strokes occurring in less eloquent areas and consequently less severe cognitive deficits. Although we have a large variation of stroke volume in our sample, the left-hemispheric strokes are considerably smaller than those in the right hemisphere. This is probably a direct result of the exclusion of patients who were too aphasic to participate. Still, the lesion-symptom associations that are found with research samples, such as our own, remain valid. Moreover, with a large enough sample size, small lesions will allow for better specificity in lesion-symptom associations than large lesions.

Tumor delineation

We used the hyperintensities on the T2-Flair images to delineate tumor tissue. These hyperintensities are independent of the enhancement of the lesion, and thereby tumor grade, and thus form a widely usable representation of the extent of brain volume potentially hampered in its function. Our tumor lesion masks include tumor core, necrosis, and edema. We implicitly assumed that all visually abnormal tissue on the T2-image is damaged and functionally affected. However, the effect of edema and even tumor infiltration on function may vary within these areas and some function could be preserved. This is probably one explanation for the inconsistent lesion-symptom associations across etiologies in this study. Future research may be aimed at determining the separate effects of edema, infiltration and enhancing tumor core on cognition.

Lesion-network mapping

Recent insights from both structural and functional network studies, have shown the importance of connections between areas when investigating cognitive effects from lesions. The relevance of white matter damage to cognitive outcome is also supported by the current findings even when using an atlas with only 34 fiber bundles.⁷⁷ Future work could use both stroke and tumor lesions as seeds in well-established structural or functional connectomes which can then be used as input for lesion network mapping analysis.^{53,73,78,79} Such studies could elucidate

whether the cognitive effects of damage to critical white matter structures also differ between etiologies.

CONCLUSIONS

In this large-scale, direct comparison of LSM of patients with brain tumors versus ischemic stroke, we found substantial differences in lesion volume and topography between the groups. These differences partly drive the brain-behavior relationships that we found. In contrast to our expectations, the overlap of LSM in brain areas affected in both populations was minimal, though we did find white matter tracts involved in memory and semantic fluency performance across etiologies. Post-hoc analyses confirmed an interaction effect between lesion status and etiology for most brain areas with adequate coverage in both groups. Thus, we conclude that lesion-behavior associations as defined by LSM, are influenced by the etiology causing the lesion. Our findings cannot solely be explained by previous objections to the use of tumor patients in LSM. The pattern shown by tumor patients on the group level is consistent with localizations found in earlier studies using different techniques. In agreement with Shallice and Skrap⁸⁰, we argue that tumor series can be used to provide converging evidence about functional localization, next to evidence from other techniques such as functional imaging and direct electrocortical stimulation. In clinical terms, this study suggests that data from ischemic stroke patients have only limited value for the prediction of behavioral repercussions of specific lesions caused by primary brain tumors, and vice versa. Because of the lack of generalizability of findings across etiologies, we are cautious about grouping different etiologies in LSM, because results are easily driven by one population. Instead, we advocate to test predictions based on one etiology in a second patient population and explore divergent findings. It would be interesting, for example, to test to what extent divergent findings between tumor and stroke result from plasticity or preservation of function using cortical mapping observations during awake surgery.

SUPPLEMENTARY MATERIALS



REPOSITORY

The results from the current study (lesion overlap maps, univariate and multivariate LSM, univariate statistical power maps) are available through the repository (van Grinsven, Eva; Smits, Anouk R. (2022), "Lesion-Symptom Mapping in Brain Tumor and Stroke Patients", Mendeley Data, V1, <https://doi.org/10.17632/k2847vw9gg.1>, <https://data.mendeley.com/datasets/k2847vw9gg>).

REFERENCES

1. Karnath HO, Sperber C, Rorden C. Mapping human brain lesions and their functional consequences. *Neuroimage* 2018; 165: 180–189.
2. Catani M, Stuss DT. At the forefront of clinical neuroscience. *Cortex* 2012; 48: 1–6.
3. Bates E, Wilson SM, Saygin AP, et al. Voxel-based lesion-symptom mapping. *Nat Neurosci* 2003; 6: 448–450.
4. Karnath HO, Berger MF, Küker W, et al. The anatomy of spatial neglect based on voxelwise statistical analysis: A study of 140 patients. *Cerebral Cortex* 2004; 14: 1164–1172.
5. Sperber C, Karnath HO. Topography of acute stroke in a sample of 439 right brain damaged patients. *Neuroimage Clin* 2016; 10: 124–128.
6. Corbetta M, Ramsey L, Callejas A, et al. Common behavioral clusters and subcortical anatomy in stroke. *Neuron* 2015; 85: 927–941.
7. Phan TG, Donnan GA, Wright PM, et al. A digital map of middle cerebral artery infarcts associated with middle cerebral artery trunk and branch occlusion. *Stroke* 2005; 36: 986–991.
8. van Kessel E, Emons MAC, Wajer IH, et al. Tumor-related neurocognitive dysfunction in patients with diffuse glioma: A retrospective cohort study prior to antitumor treatment. *Neurooncol Pract* 2019; 6: 463–472.
9. Kleihues P, Burger PC, Aldape K, et al. WHO Classification of Tumors of the Central Nervous System. *World Health Organization Classification of Tumours* 2007; 33–49.
10. Ivanova M v., Herron TJ, Dronkers NF, et al. An empirical comparison of univariate versus multivariate methods for the analysis of brain–behavior mapping. *Hum Brain Mapp* 2020; 1070–1101.
11. Mah YH, Husain M, Rees G, et al. Human brain lesion-deficit inference remapped. *Brain* 2014; 137: 2522–2531.
12. Kimberg DY, Coslett HB, Schwartz MF. Power in Voxel-based Lesion – Symptom Mapping. *J Cogn Neurosci* 2007; 18: 1067–1080.
13. Krainik A, Lehericy S, Duffau H, et al. Postoperative speech disorder after medial frontal surgery. *Neurology* 2003; 60: 587–594.
14. Kleihues P, Burger PC, Aldape K, et al. WHO Classification of Tumors of the Central Nervous System. *World Health Organization Classification of Tumours* 2007; 33–49.
15. Aabedi AA, Lipkin B, Kaur J, et al. Functional alterations in cortical processing of speech in glioma-infiltrated cortex. *bioRxiv*. Epub ahead of print 2021. DOI: 10.1073/pnas.2108959118/-/DCSupplemental.Published.
16. Cipolotti L, Healy C, Chan E, et al. The impact of different aetiologies on the cognitive performance of frontal patients. *Neuropsychologia* 2015; 68: 21–30.
17. Vaidya AR, Pujara MS, Petrides M, et al. Lesion Studies in Contemporary Neuroscience. *Trends Cogn Sci* 2019; 23: 653–671.
18. Desmurget M, Bonnetblanc F, Duffau H. Contrasting acute and slow-growing lesions: A new door to brain plasticity. *Brain* 2007; 130: 898–914.
19. Duffau H, Capelle L, Denvil D, et al. Functional recovery after surgical resection of low grade gliomas in eloquent brain: Hypothesis of brain compensation. *J Neurol Neurosurg Psychiatry* 2003; 74: 901–907.
20. Plaza M, Gatignol P, Leroy M, et al. Speaking without Broca’s area after tumor resection. *Neurocase* 2009; 15: 294–310.

21. Taphoorn MJB, Klein M. Cognitive deficits in adult patients with brain tumours. *Lancet Neurology* 2004; 3: 159–168.
22. Arbula S, Ambrosini E, Della Puppa A, et al. Focal left prefrontal lesions and cognitive impairment: A multivariate lesion-symptom mapping approach. *Neuropsychologia* 2020; 136: 107253.
23. De Witt Hamer PC, Hendriks EJ, Mandonnet E, et al. Resection Probability Maps for Quality Assessment of Glioma Surgery without Brain Location Bias. *PLoS One* 2013; 8: e73353.
24. Habets EJJ, Hendriks EJ, Taphoorn MJB, et al. Association between tumor location and neurocognitive functioning using tumor localization maps. *J Neurooncol* 2019; 144: 573–582.
25. Hendriks EJ, Habets EJJ, Taphoorn MJB, et al. Linking late cognitive outcome with glioma surgery location using resection cavity maps. *Hum Brain Mapp* 2018; 39: 2064–2074.
26. Fekonja LS, Wang Z, Doppelbauer L, et al. Lesion-symptom mapping of language impairments in patients suffering from left perisylvian gliomas. *Cortex* 2021; 144: 1–14.
27. Herbet G, Duffau H. Contribution of the medial eye field network to the voluntary deployment of visuospatial attention. *Nat Commun*; 13. Epub ahead of print 2022. DOI: 10.1038/s41467-022-28030-3.
28. van Kessel E, Berendsen S, Baumfalk AE, et al. Tumor-related molecular determinants of neurocognitive deficits in patients with diffuse glioma. *Neuro Oncol*.
29. Lugtmeijer S, Geerligs L, de Leeuw FE, et al. Are visual working memory and episodic memory distinct processes? Insight from stroke patients by lesion-symptom mapping. *Brain Struct Funct* 2021; 226: 1713–1726.
30. Lammers NA, Berg NS Van Den, Id SL, et al. Mid-range visual deficits after stroke : Prevalence and co-occurrence. *PLoS One* 2022; 17: e0262886.
31. World Medical Association. World Medical Association Declaration of Helsinki: ethical principles for medical research involving human subjects. *JAMA* 2013; 310: 2191–2194.
32. Louis DN, Perry A, Reifenberger G, et al. The 2016 World Health Organization Classification of Tumors of the Central Nervous System: a summary. *Acta Neuropathol* 2016; 131: 803–820.
33. Neumann AB, Jonsdottir KY, Mouridsen K, et al. Interrater agreement for final infarct mri lesion delineation. *Stroke* 2009; 40: 3768–3771.
34. Yushkevich PA, Piven J, Hazlett HC, et al. User-guided 3D active contour segmentation of anatomical structures: Significantly improved efficiency and reliability. *Neuroimage* 2006; 31: 1116–1128.
35. Crinion J, Ashburner J, Leff A, et al. Spatial normalization of lesioned brains: Performance evaluation and impact on fMRI analyses. *Neuroimage* 2007; 37: 866–875.
36. Rorden C, Bonilha L, Fridriksson J, et al. Age-specific CT and MRI templates for spatial normalization. *Neuroimage* 2012; 61: 957–965.
37. Nachev P, Coulthard E, Jäger HR, et al. Enantiomorphic normalization of focally lesioned brains. *Neuroimage* 2008; 39: 1215–1226.
38. Brett M, Leff AP, Rorden C, et al. Spatial normalization of brain images with focal lesions using cost function masking. *Neuroimage* 2001; 14: 486–500.
39. Zhang Y, Kimberg DY, Coslett HB, et al. Multivariate lesion-symptom mapping using support vector regression. *Hum Brain Mapp* 2014; 35: 5861–5876.

40. DeMarco AT, Turkeltaub PE. A multivariate lesion symptom mapping toolbox and examination of lesion-volume biases and correction methods in lesion-symptom mapping. *Hum Brain Mapp* 2018; 39: 4169–4182.
41. Zhang Y, Kimberg DY, Coslett HB, et al. Multivariate lesion-symptom mapping using support vector regression. *Hum Brain Mapp* 2014; 35: 5861–5876.
42. Zhao L, Biesbroek JM, Shi L, et al. Strategic infarct location for post-stroke cognitive impairment: A multivariate lesion-symptom mapping study. *Journal of Cerebral Blood Flow and Metabolism* 2017; 38: 1299–1311.
43. Tzourio-Mazoyer N, Landeau B, Papathanassiou D, et al. Automated anatomical labeling of activations in SPM using a macroscopic anatomical parcellation of the MNI MRI single-subject brain. *Neuroimage* 2002; 15: 273–289.
44. Catani M, Thiebaut de Schotten M. A diffusion tensor imaging tractography atlas for virtual in vivo dissections. *Cortex* 2008; 44: 1105–1132.
45. Friedrich S, Konietzschke F, Pauly M. GFD: An R package for the analysis of general factorial designs. *J Stat Softw*; 79. Epub ahead of print 2017. DOI: 10.18637/jss.v079.c01.
46. Pisoni A, Mattavelli G, Casarotti A, et al. The neural correlates of auditory-verbal short-term memory: a voxel-based lesion-symptom mapping study on 103 patients after glioma removal. *Brain Struct Funct* 2019; 224: 2199–2211.
47. Na Y, Jung J, Tench C, et al. Language systems from lesion-symptom mapping in aphasia: A meta-analysis of voxel-based lesion mapping studies. *medRxiv* 2021; 2021.06.03.21258096.
48. Dick AS, Bernal B, Tremblay P. The language connectome: New pathways, new concepts. *Neuroscientist* 2014; 20: 453–467.
49. Fridriksson J, Guo D, Fillmore P, et al. Damage to the anterior arcuate fasciculus predicts non-fluent speech production in aphasia. *Brain* 2013; 136: 3451–3460.
50. Thye M, Szaflarski JP, Mirman D. Shared lesion correlates of semantic and letter fluency in post-stroke aphasia. *J Neuropsychol* 2021; 15: 143–150.
51. Bettcher BM, Mungas D, Patel N, et al. Neuroanatomical substrates of executive functions: Beyond prefrontal structures. *Neuropsychologia* 2016; 85: 100–109.
52. Benoit RG, Schacter DL. Specifying the core network supporting episodic simulation and episodic memory by activation likelihood estimation. *Neuropsychologia* 2015; 75: 450–457.
53. Ferguson MA, Lim C, Cooke D, et al. A human memory circuit derived from brain lesions causing amnesia. *Nat Commun* 2019; 10: 1–9.
54. Biesbroek JM, van Zandvoort MJE, Kappelle LJ, et al. Distinct anatomical correlates of discriminability and criterion setting in verbal recognition memory revealed by lesion-symptom mapping. *Hum Brain Mapp* 2015; 36: 1292–1303.
55. Biesbroek JM, Lim JS, Weaver NA, et al. Anatomy of phonemic and semantic fluency: A lesion and disconnectome study in 1231 stroke patients. *Cortex* 2021; 143: 148–163.
56. Li M, Zhang Y, Song L, et al. Structural connectivity subserving verbal fluency revealed by lesion-behavior mapping in stroke patients. *Neuropsychologia* 2017; 101: 85–96.
57. Bowren M, Bruss J, Manzel K, et al. Post-stroke outcomes predicted from multivariate lesion-behaviour and lesion network mapping. *Brain* 2022; 145: 1338–1353.
58. Thiebaut de Schotten M, Forkel SJ. The emergent properties of the connected brain. *Science (1979)* 2022; 378: 505–510.

59. Carrera E, Tononi G. Diaschisis: Past, present, future. *Brain* 2014; 137: 2408–2422.
60. Siegel JS, Shulman GL, Corbetta M. Mapping correlated neurological deficits after stroke to distributed brain networks. *Brain Struct Funct* 2022; 227: 3173–3187.
61. Silvestri E, Moretto M, Facchini S, et al. Widespread cortical functional disconnection in gliomas: an individual network mapping approach. *Brain Commun* 2022; 4: 1–14.
62. Anderson SW, Damasio H, Tranel D. Neuropsychological impairments associated with lesions caused by tumor or stroke. *Arch Neurol* 1990; 47: 397–405.
63. Shallice T, Mussoni A, D'Agostino S, et al. Right posterior cortical functions in a tumour patient series. *Cortex* 2010; 46: 1178–1188.
64. Manuel AL, Radman N, Mesot D, et al. Inter- and intrahemispheric dissociations in ideomotor apraxia: a large-scale lesion-symptom mapping study in subacute brain-damaged patients. *Cereb Cortex* 2013; 23: 2781–9.
65. Sperber C. Rethinking causality and data complexity in brain lesion-behaviour inference and its implications for lesion-behaviour modelling. *Cortex* 2020; 126: 49–62.
66. Lorca-Puls DL, Gajardo-Vidal A, White J, et al. The impact of sample size on the reproducibility of voxel-based lesion-deficit mappings. *Neuropsychologia* 2018; 115: 101–111.
67. van Kessel E, Snijders TJ, Baumfalk AE, et al. Neurocognitive changes after awake surgery in glioma patients: a retrospective cohort study. *J Neurooncol* 2020; 146: 97–109.
68. Sperber C, Karnath HO. Impact of correction factors in human brain lesion-behavior inference. *Hum Brain Mapp* 2017; 38: 1692–1701.
69. de Haan B, Karnath HO. A hitchhiker's guide to lesion-behaviour mapping. *Neuropsychologia* 2018; 115: 5–16.
70. Sperber C, Wiesen D, Karnath HO. An empirical evaluation of multivariate lesion behaviour mapping using support vector regression. *Hum Brain Mapp* 2018; 40: 1381–1390.
71. Ramsey LE, Siegel JS, Lang CE, et al. Behavioural clusters and predictors of performance during recovery from stroke. *Nat Hum Behav* 2017; 1: 1–10.
72. Corbetta M, Siegel JS, Shulman GL. On the low dimensionality of behavioral deficits and alterations of brain network connectivity after focal injury. *Cortex*, 2018. Epub ahead of print 2018. DOI: 10.1016/j.cortex.2017.12.017.
73. Salvalaggio A, de Filippo De Grazia M, Zorzi M, et al. Post-stroke deficit prediction from lesion and indirect structural and functional disconnection. *Brain* 2020; 143: 2173–2188.
74. Weaver NA, Kuijff HJ, Aben HP, et al. Strategic infarct locations for post-stroke cognitive impairment: a pooled analysis of individual patient data from 12 acute ischaemic stroke cohorts. *Lancet Neurol* 2021; 20: 448–459.
75. Louis DN, Perry A, Wesseling P, et al. The 2021 WHO Classification of Tumors of the Central Nervous System: a summary. *Neuro Oncol* 2021; 23: 1231–1251.
76. Karnath HO, Rennig J. Investigating structure and function in the healthy human brain: validity of acute versus chronic lesion-symptom mapping. *Brain Struct Funct* 2017; 222: 2059–2070.
77. de Haan B, Karnath HO. 'Whose atlas I use, his song I sing?' – The impact of anatomical atlases on fiber tract contributions to cognitive deficits after stroke. *Neuroimage* 2017; 163: 301–309.

78. Gleichgerrcht E, Fridriksson J, Rorden C, et al. Connectome-based lesion-symptom mapping (CLSM): A novel approach to map neurological function. *Neuroimage Clin* 2017; 16: 461–467.
79. Boes AD, Prasad S, Liu H, et al. Network localization of neurological symptoms from focal brain lesions. *Brain* 2015; 138: 3061–3075.
80. Shallice T, Skrap M. Localisation through operation for brain tumour: A reply to Karnath and Steinbach. *Cortex* 2011; 47: 1007–1009.
81. de Jonghe JF, Schmand B, Ooms ME, et al. Abbreviated form of the Informant Questionnaire on cognitive decline in the elderly. *Tijdschr Gerontol Geriatr* 1997; 28: 224–229.
82. Bouma A, Mulder J, Lindeboom J SB. *Handboek neuropsychologische diagnostiek*. Amsterdam: Pearson, 2012.



6

Hemodynamic imaging parameters in brain metastases patients – Agreement between multi-delay ASL and hypercapnic BOLD

Eva E. van Grinsven, Jamila Guichelaar, Marielle E.P. Philippens, Jeroen C.W. Siero,
& Alex A. Bhogal

Journal of Cerebral Blood Flow and Metabolism (2023)

ABSTRACT

Background

Arterial spin labeling (ASL) MRI is a routine clinical imaging technique that provides quantitative cerebral blood flow (CBF) information. A related technique is blood oxygenation level-dependent (BOLD) MRI during hypercapnia, which can assess cerebrovascular reactivity (CVR). ASL is weighted towards arteries, whereas BOLD is weighted towards veins. Their associated parameters in heterogeneous tissue types or under different hemodynamic conditions remains unclear.

Methods

Baseline multi-delay ASL MRI and BOLD MRI during hypercapnia were performed in fourteen patients with brain metastases.

Results

In the ROI analysis, the CBF and CVR values were positively correlated in regions showing sufficient reserve capacity (i.e. non-steal regions, $r_{rm}=0.792$). Additionally, longer hemodynamic lag times were related to lower baseline CBF ($r_{rm}=-0.822$) and longer arterial arrival time (AAT; $r_{rm}=0.712$). In contrast, in regions exhibiting vascular steal an inverse relationship was found with higher baseline CBF related to more negative CVR ($r_{rm}=-0.273$). These associations were confirmed in voxelwise analyses.

Conclusion

The relationship between CBF, AAT and CVR measures seems to be dependent on the vascular status of the underlying tissue. Healthy tissue relationships do not hold in tissues experiencing impaired or exhausted autoregulation. CVR metrics can possibly identify at-risk areas before perfusion deficiencies become visible on ASL MRI, specifically within vascular steal regions.

INTRODUCTION

Advances in imaging techniques have made MRI a powerful tool for investigating not only brain function but also brain physiology and auto-regulatory status. One such method, that now sees routine clinical application is Arterial Spin Labeling (ASL). ASL is non-invasive, and can provide diagnostically relevant, quantitative parameters related to hypo- or hyper-perfusion.¹⁻³ Multi post label delay (multi-PLD) methods can even be used to infer the presence of collateral cerebral blood flow (CBF) pathways through their ability to estimate arterial arrival time (AAT) or characterize arterial transit artifacts (ATA). Together these ASL metrics can provide valuable physiological information in healthy subjects and can also identify disease-related auto-regulatory changes in patient populations.

A major cerebral auto-regulatory mechanism responsible for maintaining adequate CBF is cerebrovascular reactivity (CVR). CVR is reflective of smooth-muscle cell mediated blood flow control, and represents a major compensatory mechanism in diseases that compromise cerebral hemodynamics.⁴⁻⁶ The CVR response can be assessed and spatially mapped using Blood oxygenation level-dependent (BOLD) MRI in combination with controlled hypercapnic stimuli. This technique is distinct from resting-state and/or task-based BOLD MRI, where either spontaneous or evoked *neuronal* signals modulate the BOLD signal change, providing information related to brain function. CVR measurements can be interpreted as regional indicators of healthy or disease-impaired vasculature.⁷ Impairments often manifest as negative signal responses, where a vasodilatory stimulus can cause paradoxical decrease in CBF (known as vascular steal) to an area with exhausted dilatory reserve, due to a reduction in vascular resistance in neighboring, non-exhausted regions.⁸ Finally, analysis of dynamic CVR characteristics can provide information on temporal aspects of the CVR response that are encompassed in the hemodynamic response lag.⁹⁻¹¹

Changes in perfusion characteristics and cerebrovascular function have been found in multiple different patient populations, including patients with brain tumors.¹²⁻¹⁴ Growth of intracranial masses, like primary brain tumors or brain metastases, can cause local disruptions of the hemodynamic environment. Metastatic cells have to proceed through a range of developmental steps in order to form macrometastases; (1) cells arrest in the small microvessels, (2) cells extravasate to enter the brain tissue, (3) cells perpetuate into a strict perivascular position, and (4) vascularization is secured through either co-optive or angiogenic growth depending on the tumor type.¹⁵ By vascular co-option, angiogenesis and dilation of blood vessels associated

with brain metastases, the macrometastases subsequently ensure adequate blood supply and thus alter the vascular microenvironment.¹⁶⁻¹⁸ The vasogenic edema often surrounding these brain metastases, caused by the local blood-brain barrier disruption¹⁹, can lead to additional physiological changes. All these brain metastases related physiological changes are likely to be reflected in hemodynamic MRI measurements. ASL and CVR measure associated responses, both describing the status of the vascular network. Thereby they can provide complementary information, however, it remains unclear how ASL and CVR parameters relate in different tissue types or under different hemodynamic circumstances.

In the current exploratory study we test how ASL parameters measured during a physiological steady state relate to functional vascular parameters as measured using CVR in a population of patients with brain metastases. The expected tissue-heterogeneity caused by the brain metastases growth provides a testing ground to answer this question. CBF and AAT were compared to CVR magnitude and hemodynamic lag using two different approaches. Firstly, the inter-modality agreement between ASL and CVR was tested by comparing group values for different tissue types (grey matter (GM), white matter (WM), edema and brain metastases) for both ASL and CVR metrics. Secondly, we assessed the spatial correlation between ASL and CVR metrics throughout the brain using both a ROI and voxelwise approach. Hereby a distinction was made between brain areas showing adequate vascular responses and those exhibiting vascular steal phenomena. Understanding how baseline vascular physiology relates to dynamic vascular processes in cases with brain metastases will aid in interpreting these measures in future research.

METHODS

Study set-up and population

For the current retrospective observational study, MRI datasets were included from the ongoing Assessing and Predicting Radiation Influence on Cognitive Outcome using the cerebrovascular stress Test (APRICOT) study. Participation consists of an elaborate neurocognitive exam and MRI scans, including a BOLD MRI scan during breathing challenges, before radiotherapy and approximately three months after radiotherapy. For the purpose of this study only the MRI data acquired *before* radiotherapy during the period between October 2020 and February 2022 was used. The study population consists of adult patients (≥ 18 years) with either radiographic and/or histologic proof of metastatic brain disease that were referred to the radiotherapy department of the UMC Utrecht for radiation therapy of the brain metastases. Specific in- and exclusion criteria for participation in the APRICOT

study are listed in the **Supplementary Materials**. The study was performed in accordance with the Declaration of Helsinki²⁰ and the UMCU institutional ethical review (Medisch-Ethische Toetsingscommissie (METC) NedMec) approved the study (METC# 18-747). Written informed consent was obtained from all participants prior to participation.

Data acquisition

Imaging protocol

The participants were scanned on a 3 Tesla MRI scanner (Achieva, Philips Medical Systems, Best, The Netherlands) using a 32 channel receive coil. Whole-brain multi-slice single shot FE-EPI BOLD images (TR = 1050 ms, TE = 30 ms, flip angle 65°, resolution 2.292 x 2.292 x 2.5 mm³, acquisition matrix 96 x 96 x 51, 1000 dynamics, multi-band factor = 3) were acquired throughout a computer controlled hypercapnic breathing protocol (described below). Perfusion data was acquired using a multi-PLD ASL sequence. A whole volume was acquired at each of the 4 post-labeling delays (660, 1325, 1989, 2654ms), using a pCASL Look-Locker multi-slice EPI read-out (total scan time = 240 s, labelling train duration = 1650ms, TR = 5s, TE = 12 ms, flip angle 25°, acquired resolution: 3 x 3 x 7 mm³, acquisition matrix: 80 x 80 x 17, 23 averages, SENSE factor = 2, 2 background suppression pulses). A total of 23 label-control pairs were acquired. The first acquired ASL dataset pair here has the labelling, saturation pulses and background suppression turned off and are the M0 images for each post-label delay. An additional dataset pair was acquired for EPI phase (distortion) correction. No breathing challenges were performed during ASL imaging. The ASL was planned using a phase contrast angiography scan, with the labeling plane carefully placed perpendicular to the internal carotid arteries and vertebral arteries. Additionally, a 3D spoiled gradient echo (SPGR) sequence (TR = 8 ms, TE = 3.25 ms, flip angle 10°, isotropic resolution 1 mm, acquisition matrix 240 x 240 x 180), a 3D T2-weighted FLAIR sequence (TR 4800 ms, TE 240 ms, TI = 1650 ms, flip angle 90°, isotropic resolution: 1 mm, acquisition matrix 256 x 256 x 182), as well as a SWI (TR 50 ms, flip angle 17°, inplane slice thickness 2 mm, acquisition matrix 384 x 383 x 63) were acquired as an anatomical reference. A minimum-intensity-projection was constructed from the SWI data, using an in-house developed Matlab script (Matlab R2020a, The MathWorks, Inc., Natick, Massachusetts, United States).

Clinical CT and MRI acquisition

CT and MRI scans were acquired as part of clinical care as usual 1 to 5 days before receiving radiotherapy. CT scans were acquired on a Brilliance Big bore 22 scanner (Philips Medical Systems, Best, The Netherlands) with a tube potential of 120 kVp, matrix size of 512 x 512 and inplane slice thickness of 1 mm. The participants were

scanned on a 1.5 Tesla MRI scanner (Inginia, Philips Medical Systems, Best, The Netherlands) using a 15 channel receive coil. A 3D SPGR sequence after injection of 0.1 ml gadovist/kg was performed (TR = 7.6 ms, TE = 3.4 ms, flip angle 8°, isotropic resolution: 1 mm, acquisition matrix 232 x 232 x 170). The clinician uses this clinically acquired MRI registered to the CT, to plan the radiotherapy and delineate the so-called gross tumor volume (i.e. brain metastases). The CT and corresponding gross tumor volume were extracted for each patient. For the current analysis, a distinction was made between newly treated brain metastases, resection cavities of brain metastases and previously irradiated brain metastases.

Breathing protocol

Hypercapnic stimuli were delivered using a computer-controlled gas blender and sequential delivery system (RespirAct™, Thornhill Research Institute, Toronto, Canada). The breathing mask was sealed to the patients' face using transparent dressings (Tegaderm, 3M, St. Paul, MN, US) to acquire an air tight seal. Before starting the breathing challenges inside the MRI scanner, patients performed a test round with a CO₂ challenge which is similar to the CO₂ block given during the protocol. Only after successful completion of the test round, the breathing challenges inside the scanner were performed (**Figure 1**). The breathing challenges started with a 5-minute baseline period, followed by a block-shaped increase of end-tidal CO₂ (PetCO₂) 10 mmHg relative to a patients' baseline for 90 seconds. After this so-called CO₂-block, PetCO₂ values returned to baseline values for 120 seconds, followed by a PetCO₂ ramp increase of 12 mmHg relative to patients' baseline for 180 seconds after which patients returned to baseline for 90 seconds.

Pre-processing

Pre-processing steps were performed using the Oxford Centre for Functional MRI of the BRAIN (FMRIB) Software Library (FSL – version 6.0; see **Supplementary Figure 1**).²¹ First, both the T1 and T2FLAIR images were brain extracted using BET.²² Tissue segmentation into grey matter (GM), white matter (WM) and cerebrospinal fluid (CSF) was performed on the T1 image using FSL Automated Segmentation Tool (FAST).²³ Additionally, an edema mask was created based on the T1 and T2FLAIR images using the lesion growth algorithm as implemented in the Lesion Segmentation Tool (LST, <https://www.statistical-modelling.de/lst.html>) for SPM.²⁴ Based on previous experience, the initial threshold was set at 0.14. The resulting edema mask was manually adapted to eliminate any false positives or false negatives from the LST edema mask. The CT image was registered to the T1 image using FMRIB's Linear Image Registration Tool (FLIRT).^{22,25}

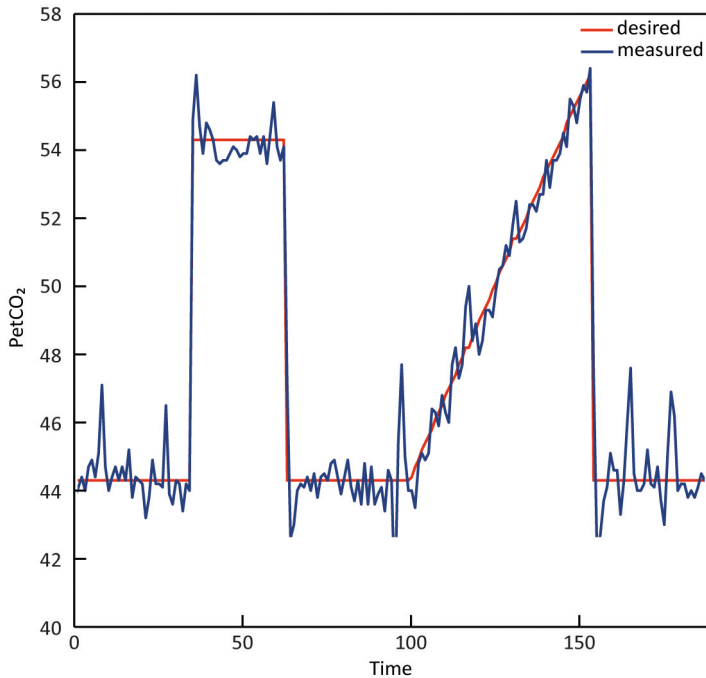


Figure 1. CO₂ breathing trace of a representative subject during the breathing challenge. The blue line indicates the actual measured PetCO₂ values, while the red line indicates the desired values based on the protocol.

Abbreviations: PetCO₂, end-tidal CO₂.

BOLD data was motion corrected (MCFLIRT)²², corrected for geometric distortion using TOPUP^{26,27} and linear spatial co-registered to the T1 image using the 'epi_reg' function.^{22,25} The T1w segmentation masks, edema masks and gross tumor volume masks were translated to the functional (i.e. BOLD) space using the inverse of the matrices output by epi_reg. For the ASL data, the reconstructed T1 (M0) was spatially registered to the pre-TOPUP mean BOLD image. The resulting transformation matrix as well as the distortion-correction fields were then applied to the ASL images in order to move them to functional patient space.

Data analysis

MRI analysis

The pipeline to process and compare the BOLD and ASL data is visually depicted in **Figure 2**. CVR and hemodynamic lag maps were derived using the open-source seeVR toolbox (available at <https://www.seevr.nl/>).²⁸ In brief, in order to remove signal contribution from large veins that might overshadow tissue responses, a

modified whole-brain mask was generated using the 'remLV.m' function of the seeVR toolbox.²⁸ For this, a temporal noise-to-signal (tNSR) map was calculated by taking the inverse of the temporal signal to noise (tSNR) map. Next, voxels showing values higher than the 98th percentile tNSR value were removed from the original whole brain-mask. This modified mask was then used in subsequent analyses.²⁸

Next, a manual bulk alignment was performed between the PetCO₂ and average GM time-series to minimize alignment errors that can occur when using automated correlation methods. Thereby, any bulk delays between end-tidal gas measurements at the lungs and BOLD signal responses in the brain were accounted for. Residual motion signals with a correlation higher than 0.3 with the GM time-series, along with a linear drift term were regressed out using a general linear model. BOLD data was then temporally de-noised using a wavelet-based approach²⁹ and was spatially smoothed using a 3D Gaussian kernel (FWHM: 4 x 4 x 7 mm³). This kernel was chosen in order to best match the effective spatial resolution of the ASL data. BOLD data and corresponding PetCO₂ traces were interpolated by a factor 4 (effective TR: 262.5 ms) to identify sub-TR signal displacements in subsequent hemodynamic lag analysis. A linear regression was performed between the bulk-aligned PetCO₂ trace with each processed BOLD voxel time-series. The slope of this linear regression was taken as the CVR ($\Delta\text{BOLD}/\text{mmHg PetCO}_2$). Hemodynamic lag maps were generated using the Rapidtide^{10,30} approach as implemented in the seeVR toolbox²⁸ and described previously.³¹

The multi-delay ASL was processed using the open-source ClinicalASL toolbox (available at <https://github.com/JSIERO/ClinicalASL>) and FSL BASIL for quantitative CBF maps.³² A T1-weighted image was reconstructed based on the M0 images using the 'ASLT1fromM0Compute.m' function. In short, as we used a Look-Locker read-out, the signal evolution over the multiple PLDs will show a T1-weighted signal response that was used to generate a surrogate T1 weighted image. This image had sufficient T1 contrast to be used for image registration (i.e. improved contrast compared to any single M0 or label/control image). Outlier removal was performed based on the standard deviation and tissue variance. Quantitative CBF and AAT maps were generated using the BASIL tool (**Figure 2.2**).³³

Statistical analysis

The CSF mask and non-brain metastases mask (containing areas of previously resected or irradiated brain metastases) were excluded from the hemodynamic parameter maps (**Figure 2.3**). Thereby, all analyzed tissue consists of either brain matter (GM and WM), edema or non-treated brain metastases. Next, the CVR values

were used to divide brain into regions of vascular steal versus no vascular steal. In this study, steal was conceptualized as voxels containing negative CVR values (i.e. regions in which BOLD signal intensity decreased with increase in PetCO₂; **Figure 2.4**).

The data provided by steps 1-4 were used in the subsequent comparative analyses. First the previously generated masks were used to subdivide the brain into GM, WM, edema and brain metastases regions (**Figure 2.A**). Next, for steal and non-steal regions separately, the mean value per brain regions was calculated for each hemodynamic parameter map. Kruskal-Wallis H-tests were performed to compare the mean hemodynamic values between tissue types. To reduce the false discovery rate due to multiple testing, alpha's were corrected according to the Benjamini-Hochberg method.³⁴ Additionally, Spearman's correlation analyses were performed between the mean values of the different parameter maps within each tissue type.

For a second comparative analysis, the AAT data was sorted based on ascending values. The sorted AAT's were then subdivided into 20 bins, each containing 5 percent of the data. Using the boundaries of these '5%-bins', the AAT map was divided into ROIs. Thereby, each ROI contained 5 percent of the AAT data, where the lowest bin value represented the 5 percent lowest AAT values and the highest bin value the 5 percent highest AAT values (**Figure 2.B**). For each hemodynamic parameter, the mean value for each of these binned ROIs was calculated and used in the subsequent correlation analysis to assess whether the hemodynamic parameters in each AAT bin correlate with other hemodynamic parameters. In order to compare CBF values to the CVR metrics as well, this process was repeated using the CBF maps to bin the data. As this binning resulted in 20 mean values per individual (i.e. for each binned ROI), a repeated-measures correlation was chosen to account for the within-individual variance between these values. The 'rmcorr' package implemented in RStudio (Version 2021.9.1.372) was used to perform this repeated-measures correlation.³⁵ This analysis estimates the common regression slope for repeated measures.

Lastly, a Pearson's correlation coefficient was calculated for the voxelwise association between the ASL and CVR metrics for each individual. This correlation was performed separately for non-vascular steal and vascular steal regions. Next, we performed a nonparametric Wilcoxon-signed rank-test to assess whether the correlation values significantly differed from zero on the group-level (**Supplementary Materials**). For all statistical tests a *p*-value of 0.05 was deemed significant.

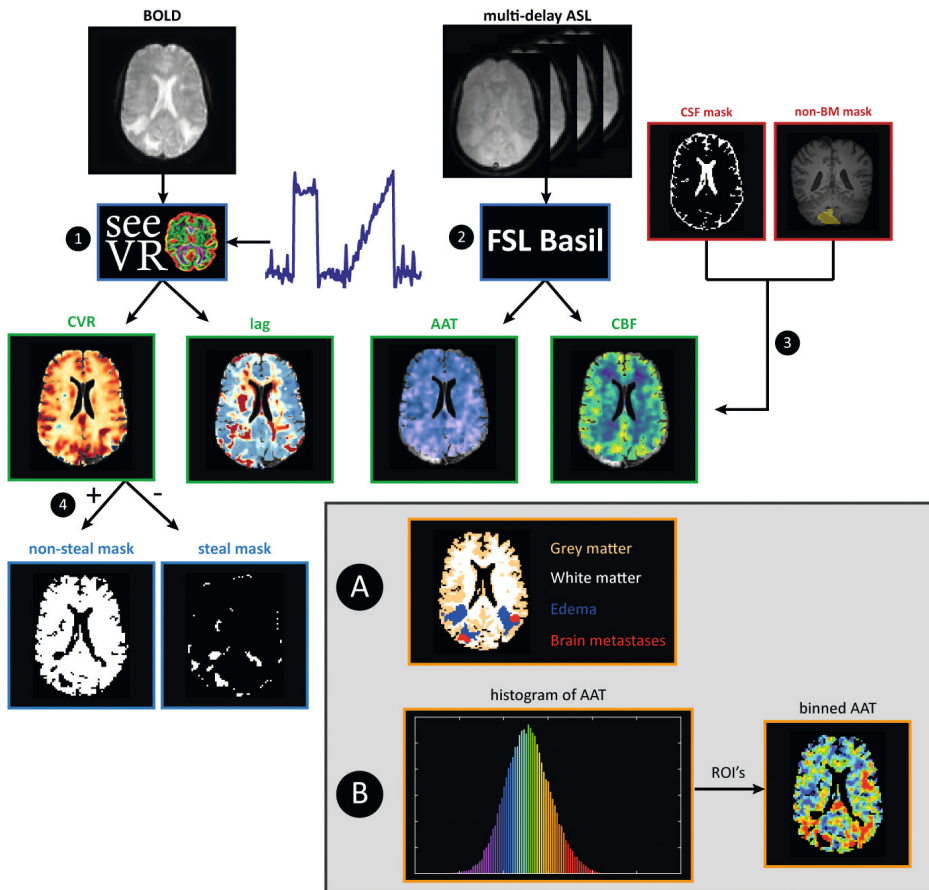


Figure 2. Data analysis steps for the BOLD and ASL MRI data. 1. BOLD time series and PetCO_2 traces were used to generate CVR and hemodynamic lag maps. 2. Quantitative AAT and CBF maps were generated based on Multi-delay ASL data 3. CSF and previously resected or irradiated brain metastases were excluded from all the maps. 4. Based on the CVR values, the brain was segmented into non-steal and steal regions of interest (ROI). Parameter maps were analyzed comparatively (shown in grey). For analysis A, the brain was divided into GM, WM, edema and brain metastases ROIs for each individual and the mean and standard deviation were calculated for each hemodynamic parameter map (CBF, AAT, CVR and hemodynamic lag) for each tissue-ROI. For analysis B, the AAT data were sorted and the AAT maps were divided into ROIs each containing 5% of the sorted data ('5%-bins' - visualized by the colored histogram) for each individual. For each bin-ROI the mean value of each hemodynamic parameter map (CBF, AAT, CVR and hemodynamic lag) was calculated and used in subsequent repeated-measures correlation analysis.

Abbreviations: AAT, arterial arrival time; ASL, arterial spin labeling; BM, brain metastases; BOLD, blood oxygenation level-dependent; CBF, cerebral blood flow; CSF, cerebrospinal fluid; CVR, cerebrovascular reactivity; GM, grey matter; PetCO_2 , end-tidal CO_2 ; ROI, region of interest; WM, white matter.

RESULTS

Participants

In total, 20 patients were included in the APRICOT study in the given time period. Data of 14 of these participants was used in the current analysis and 6 patients were excluded due to various, mostly technical reasons (see **Supplementary Table 1**). The average age of the included patients was 65.1 years and four were female. On average patients had 5.4 brain metastases of which the average volume of the newly treated, non-resected brain metastases was 10.7 cc. Edema encompassed on average 23.93 cc of the brain. Two patients had previous resection of at least one brain metastasis and three patients had received previous brain radiotherapy. On average, 62.30 cc of the brain volume (5.7% of the total brain volume) showed steal phenomena as indicated by negative CVR values (**Table 1**). On average 13.4% (range: 0 – 43.6%) of the brain metastases volume and in 21.9% (range: 0 – 52.3%) of the edema volume showed steal.

Table 1. Patient, treatment and volume information of the included subjects in this study.

Patient number	Age (years)	Sex	Primary tumor	Number of BM	BM volume (cc)	Previous resection	Previous RT	Steal volume (cc)	Edema volume (cc)
APP001	56	F	Gynecological	3	-	Y	Y	37.03	4.36
APP003	57	F	Lung	7	4.32	N	N	33.41	54.27
APP005	66	M	Melanoma	18	0.87	N	Y	57.81	12.46
APP006	81	M	Melanoma	2	7.09	N	N	40.40	17.10
APP007	62	F	Lung	11	11.20	N	N	74.75	19.46
APP008	72	M	Kidney	1	17.56	N	N	105.29	80.14
APP009	67	M	Lung	8	1.17	N	N	77.20	1.48
APP011	52	F	Lung	8	50.64	N	N	61.71	29.41
APP012	58	M	Melanoma	9	0.67	N	N	28.04	0.30
APP013	75	M	Melanoma	2	9.44	N	N	54.61	1.76
APP016	53	M	Melanoma	2	0.13	N	Y	43.71	-
APP018	72	M	Lung	2	1.75	N	N	38.70	13.19
APP019	65	M	Gastro-intestinal	1	23.85	N	N	81.66	84.43
APP020	75	M	Lung	1	-	Y	N	137.79	16.67

Abbreviations: BM, brain metastases; F, female; M, male; N, no; RT, radiotherapy; Y, yes.

Mean group comparison

For each hemodynamic parameter map, the group mean values were compared between steal versus non-steal regions and between different tissue types (GM, WM, edema and brain metastases) using Kruskal-Wallis tests (**Figure 3** and **Supplementary Table 2**). For the AAT, steal regions showed longer AAT than non-steal regions, but only in WM regions ($p = .015$). Additionally, for both non-steal and steal regions AAT values in GM were lower than in WM (non-steal: $p = 0.022$; steal: $p = .004$), edema (non-steal, $p = .006$; steal, $p = .001$) or brain metastases (non-steal, $p = .018$; steal, $p = .007$). AAT values in WM, were lower than in edema in steal regions ($p = .031$), but did not differ from edema in non-steal regions ($p = 0.37$) or brain metastases (non-steal: $p = .111$; steal $p = .143$).

Non-steal regions exhibited significantly higher CBF than steal regions in GM ($p = .010$), WM ($p = .001$) and edema ($p = .034$), but not within brain metastases ($p = .129$). Additionally, GM steal and non-steal regions showed higher CBF than WM (non-steal: $p = .001$; steal: $p < .001$) and edema (non-steal: $p < .001$; steal: $p < .001$). CBF was also higher in WM than edema, but only in the non-steal regions (non-steal: $p = .004$; steal: $p = .136$). While brain metastases showed high variability in CBF values, on average CBF values in brain metastases were higher than in WM (non-steal: $p = .005$; steal: $p = .014$) and edema (non-steal: $p < .001$; steal: $p = .007$), but did not differ from GM values (non-steal: $p = .572$; steal: $p = .953$).

Hemodynamic lag values were shorter in non-steal than steal regions in GM ($p < .001$), WM ($p < .001$) and edema regions ($p = .002$), but not within brain metastases ($p = .056$). For non-steal regions both WM and edema had longer lag times than GM ($p = .010$ and $p < .001$, respectively). Additionally, edema exhibited longer lags than WM ($p = .003$). All of the steal regions exhibited similarly long lags across the tissue types.

As steal regions were defined using the negative CVR values, all steal and non-steal CVR values significantly differed from each other ($p < .001$). In non-steal regions, GM showed a higher reactivity than WM ($p = .002$), edema ($p < .001$) and brain metastases ($p = .009$). WM also had a higher reactivity than edema ($p < .001$). Within steal regions, GM had a larger negative response than both WM ($p = .003$) and edema ($p < .001$), but not brain metastases ($p = 0.61$). Within these steal regions, WM had a more negative response than edema regions ($p = .027$).

Next, Spearman's Rho correlations were performed to test for an association between the different MRI metrics within the tissue types. For the non-steal regions,

in brain metastases only hemodynamic lag significantly negatively correlated with CVR values ($r = -0.73, p = 0.009$). For steal regions, longer AAT was significantly related to lower perfusion ($r = -0.534, p = .048$), but only within GM. See **Supplementary Figure 2** for scatterplots of these associations.

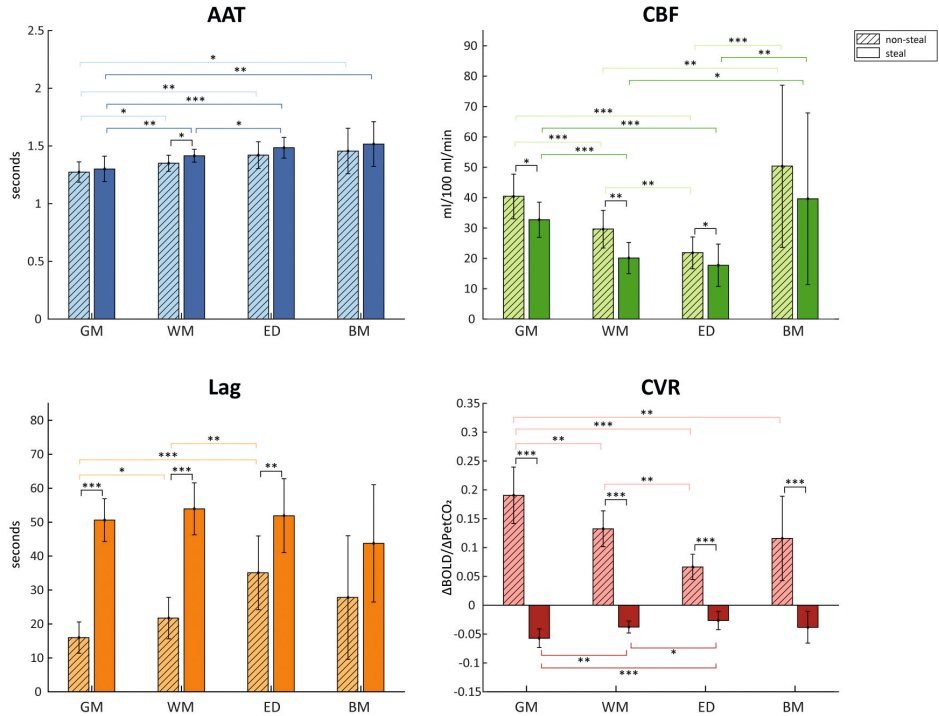


Figure 3. Group mean values per MRI metric (AAT, CBF, hemodynamic lag and CVR) and per tissue type (GM, WM, edema, brain metastases). Error bars represent the standard deviation. Asterisks indicate significant differences between group values with * $p < .05$, ** $p < .01$, *** $p < .001$.

Abbreviations: AAT, arterial arrival time; BM, brain metastases; CBF, cerebral blood flow; CVR, cerebrovascular reactivity; ED, edema; GM, grey matter; WM, white matter.

Repeated measures correlation

Repeated measures correlations were performed between each MRI metric using either the AAT binned or CBF binned ROIs (**Figure 4** and **Supplementary Figure 3**). In non-steal regions, longer hemodynamic lag time was associated with both longer AAT ($r_{rm} = 0.712, p < .001$) as well as lower CBF ($r_{rm} = -0.822, p < .001$). No relationship between either AAT and hemodynamic lag ($r_{rm} = 0.063, p = .308$) or CBF and hemodynamic lag ($r_{rm} = -0.002, p = 0.976$) was found for steal regions. Higher CVR was related to shorter AAT ($r_{rm} = -0.833, p < .001$) as well as higher CBF

($r_{rm} = 0.792, p < .001$) in non-steal regions. Within the steal regions this association flipped with stronger negative CVR (i.e. stronger vascular steal effect) related to shorter AAT ($r_{rm} = 0.320, p < .001$) and higher CBF ($r_{rm} = -0.273, p < .001$). Additionally, similar associations can be visually observed in the representative example patient (Figure 5).

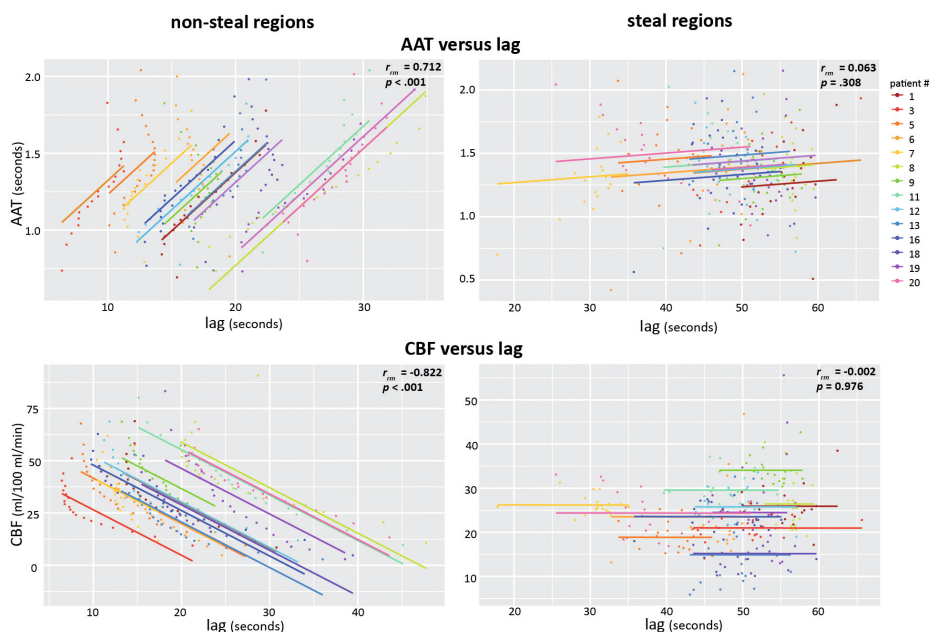


Figure 4A. Repeated measures correlation plots between ASL metrics (AAT, CBF) and CVR metrics (CVR, hemodynamic lag) using AAT-binned or CBF-binned ROIs. Each color represents a different patient and the lines represent the common linear relationship between the MRI metrics when all participants are taken into account. Statistics for each relationship are provided for each plot separately. Correlations between ASL metrics (AAT and CBF) and CVR metrics (CVR and hemodynamic lag) were also performed and are shown in Supplementary Figure 3.

Abbreviations: AAT, arterial arrival time; CBF, cerebral blood flow; CVR, cerebrovascular reactivity; ROI, region of interest.

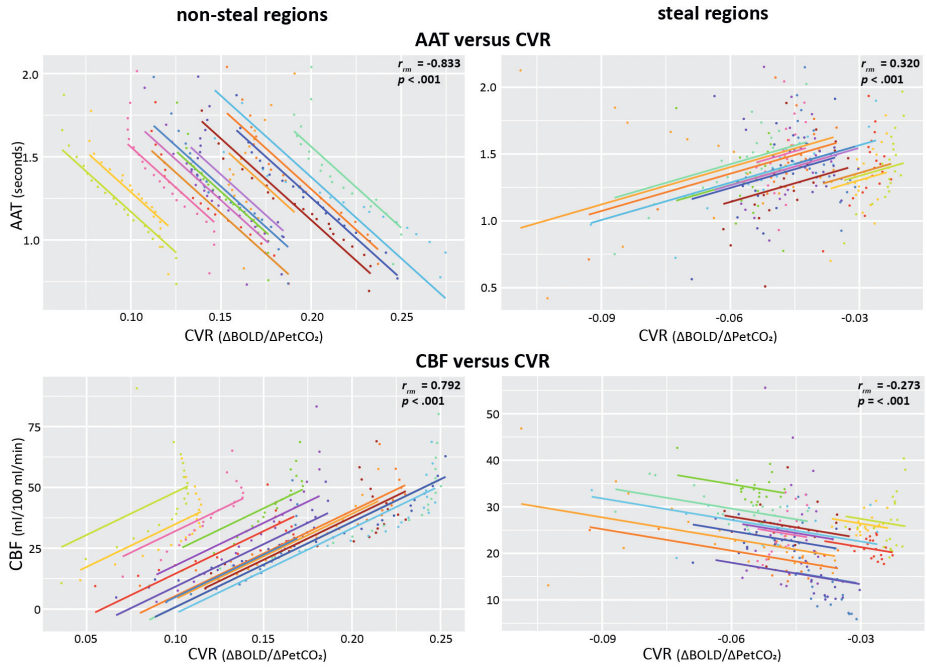


Figure 4B. Repeated measures correlation plots between ASL metrics (AAT, CBF) and CVR metrics (CVR, hemodynamic lag) using AAT-binned or CBF-binned ROIs. Each color represents a different patient and the lines represent the common linear relationship between the MRI metrics when all participants are taken into account. Statistics for each relationship are provided for each plot separately. Correlations between ASL metrics (AAT and CBF) and CVR metrics (CVR and hemodynamic lag) were also performed and are shown in Supplementary Figure 3.

Abbreviations: AAT, arterial arrival time; CBF, cerebral blood flow; CVR, cerebrovascular reactivity; ROI, region of interest.

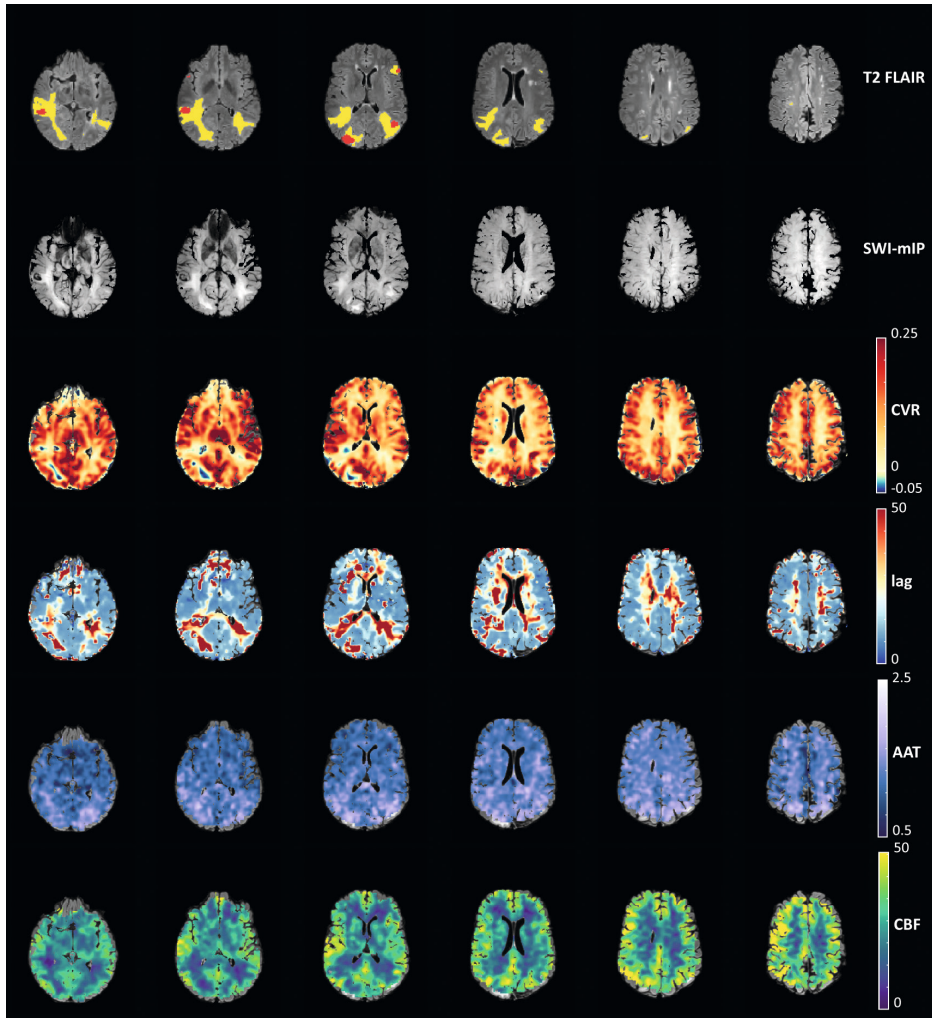


Figure 5. Visual comparison of hemodynamic parameter maps of a representative subject. Red voxels on the T2 FLAIR represent the location of the brain metastases, and yellow voxels are regions with edema. The minimum intensity projection (SWI-mIP) indicates the locations of larger cerebral venous vessels.

Abbreviations: AAT, arterial arrival time; CBF, cerebral blood flow; CVR, cerebrovascular reactivity

DISCUSSION

In the current study, baseline perfusion measurements were compared with functional vascular parameters acquired using CVR in a population of patients with brain metastases. These parameters were compared both spatially, and across

different tissue types (GM, WM, edema and brain metastases), and also tissues exhibiting different hemodynamic characteristics (steal versus non-steal regions). When visually inspecting the MRI data, all vascularly compromised regions visible in the ASL data were also reflected in the CVR metrics. Results indicate a strong, positive relationship between regional baseline CBF and CVR. Additionally, there was a strong positive relationship between the temporal metrics AAT and hemodynamic lag. In both instances, however, these relationships do not hold in brain regions with exhausted cerebral autoregulation (i.e. steal regions). Thus, while ASL may be able to inform on some functional vascular aspects, CVR provides additional information regarding brain tissue at risk as indicated by either vascular steal or increased hemodynamic lag.

Tissue-specific hemodynamic characteristics were observed in our results. WM areas were characterized by lower CBF and longer AAT, which has been previously reported in healthy subjects.³⁶ Additionally, WM areas showed lower reactivity as well as longer hemodynamic lag values than GM. This is consistent with existing literature, and reflects lower WM blood volume, different venous draining architecture and/or potential flow redistribution resulting from the strong GM CO₂ response.^{29,31,37} Our findings suggest that the hemodynamic characteristics of healthy tissue are preserved in the normal appearing brain tissue of patients with brain metastases. On the other hand, large variability in the hemodynamic vascular parameters was seen within tissue containing untreated brain metastases. This was reflected in both the ASL and the CVR parameters. High variability in CBF measurements has previously been shown both between patients with brain metastases as well as between multiple brain metastases within patients.³⁸ The primary tumor (i.e. origin of metastatic cells), might cause some of this heterogeneity as it affects the brain metastases growth pattern.^{15,39,40} Our findings additionally show that edema regions are characterized by lower CBF, lower CVR and both longer AAT and hemodynamic lag times. Previous literature has also found impaired CVR within perifocal edema surrounding diffuse gliomas.¹³ It could be speculated that the local pressure in edematous regions restricts the ability of vessels to dilate and thus cannot maintain adequate perfusion. Additionally, this could limit the vasodilatory reserve capacity, as reflected by the CVR parameters.

GM CBF values varied between 30 and 50 ml/100 ml/min in our patient sample, which is similar to the GM CBF values as measured using PET.⁴¹ CBF and CVR values were strongly correlated within adequately functioning regions, both when performing ROI and voxelwise statistics. That is, regions with lower blood supply also showed lower vascular reactivity. This was to be expected since CVR measurements are

heavily dependent on changes in CBF. Additionally, longer hemodynamic lag times were seen within regions with lower CBF. This has also been observed in healthy subjects and patients with white-matter hyperintensities, where reduced CBF was found alongside lower CVR and longer CVR time to peak.⁴²⁻⁴⁵ In the current study, however, in regions exhibiting vascular steal the negative CVR decreased further with increasing CBF. Even though the effect size of this relationship is considered small,⁴⁶ this result is still striking. Previous research has likewise postulated that the relationship between CBF and CVR may be dependent on the staging of vascular reserve.⁸ This could be explained by the following: within non-steal regions (i.e. adequately responsive regions), the process of cerebral autoregulation ensures CBF is maintained through varying the vasodilation of the vessels. However, in vascular steal regions, vessels are likely to be maximally dilated. When this maximum vascular reserve capacity is able to compensate, adequate CBF could be maintained while CVR is negative. In even more vascularly comprised regions, this maximum vasodilation fails to compensate, leading to both low CBF and CVR values. These different associations could be reflective of the underlying vascular reserve classifications as proposed by both Derdeyn and colleagues⁴⁷ or Kuroda and colleagues⁴⁸.

The timing of the response as measured with CVR was related to the temporal metrics of the baseline CBF (i.e. AAT). In other words, regions in which the arrival time of labeled blood was longer also showed a longer vascular response delay to a hypercapnic stimulus. Since the timing of the CVR is related to the traveling duration of the blood, this positive relationship was to be expected. However, both the correlation analyses as well as visual inspection of the data suggest these two temporal measures are not identical. Within the same region, the hemodynamic lag time is longer than the AAT. This probably reflects the difference in the two temporal metrics. AAT solely reflects the arrival time of labeled blood in a physiological steady state on the arterial side. Hemodynamic lag, on the other hand, is a time measure in reaction to a hypercapnic stimulus, measured at the venous side and influenced by multiple factors like blood redistribution and vascular response speed.²⁹ While prolonged AAT might be able to indicate areas with possible increased vascular collateralization⁴⁹ and thereby also longer hemodynamic lag values, AAT cannot be used to identify regions at risk for decreased vascular response speed.

When comparing ASL with BOLD MRI data, some technical limitations of both techniques should be considered. The main limitation of ASL is the short half-life of the endogenous tracer (~1-2 seconds), leading to possible underestimation of perfusion in areas with long transit delays.⁵⁰ Additionally, the specific ASL

technique may influence the resulting perfusion maps. An example is that too short post-labeling delays can lead to arterial transit artefacts or less accurate CBF measures.^{3,51,52} In the current study, we used a multi post-labeling delay ASL pcASL sequence and did not perform partial volume correction leading to CBF values that are close to the ground truth as measured using PET. A disadvantage of BOLD-metrics, is that the BOLD response is dependent on multiple factors, like changes in cerebral blood volume, cerebral metabolic rate of oxygen consumption, arterial partial pressure of oxygen and baseline parameters like hematocrit, OEF, CMRO₂, and blood volume.^{53,54} This makes it difficult to pinpoint the exact underlying mechanisms and could be viewed as a less pure measure of brain hemodynamics when compared to ASL. Nevertheless, on average the change in BOLD to changes in PetCO₂ seem to be dominated by CBF changes^{43,55,56} Thereby it could be speculated that the BOLD response is mainly affected by changes in CBF and provides a good comparison with ASL MRI.

Additionally, specific analyses choices could have influenced results. In areas with vascular steal, low variability in CVR values in combination with highly variable hemodynamic lag values were observed. As steal regions were defined by any CVR value below zero, these regions could thereby include voxels containing noisy, just below threshold CVR values, thereby influencing the results. Moreover, as the current analysis pipeline is influenced by the time to peak for the hemodynamic lag calculation, it may be difficult to discern the actual lag time of the response. Thereby hemodynamic lag values will not always reflect true underlying temporal characteristics of tissue reactivity. Therefore, we advise not to perform lag analysis within regions indicated by vascular steal as it will possibly lead to spurious lag quantifications.

To further understand the exact hemodynamic mechanisms, oxygen extraction fraction (OEF) would be a valuable additional metric. To illustrate, in regions with exhausted cerebral autoregulation, a further reduction in cerebral perfusion pressure will cause CBF to drop. In order to maintain tissue function, OEF can be increased. The functional consequences of reduced regional CBF will therefore only become apparent when OEF is maximal.⁴ Thus, future studies should add OEF measurements to further understand whether tissue at risk as indicated by either ASL or CVR is also reflective of tissue with maximized OEF. To fully understand the functional consequences of these hemodynamic measure, the MRI metrics should be related to behavioral measures, like cognitive performance.

CONCLUSION

In the current study, we investigated how ASL parameters measured during a physiological steady state relate to functional vascular parameters as measured using CVR in a patient population with brain metastases. When visually inspecting the MRI data, all vascularly compromised regions visible in the ASL data were also reflected in the CVR metrics. This was confirmed by both the regional and voxelwise relationship between on the one hand CBF and CVR measurements and the temporal metrics of ASL and CVR on the other hand. However, the relationship between ASL and CVR measures seems to be dependent on the vascular status of the underlying tissue. That is, relationships do not hold in tissues exhibiting vascular steal. Thus, CVR metrics may be able to flag at-risk areas before they become visible on ASL MRI. However, the downside of using BOLD-metrics is that they are influenced by multiple variables, making it difficult to pinpoint the exact mechanisms underlying this vascular risk. Consequently, to fully understand vascular changes within patients with pathology, combining ASL and CVR will provide a more complete picture.

SUPPLEMENTARY MATERIALS



REFERENCES

1. Alsop DC, Detre JA, Golay X, et al. Recommended Implementation of ASL Perfusion MRI for Clinical Applications. *Magn Reson Med* 2015; 73: 102–116.
2. Detre JA, Rao H, Wang DJJ, et al. Applications of arterial spin labeled MRI in the brain. *Journal of Magnetic Resonance Imaging* 2012; 35: 1026–1037.
3. Telischak NA, Detre JA, Zaharchuk G. Arterial spin labeling MRI: Clinical applications in the brain. *Journal of Magnetic Resonance Imaging* 2015; 41: 1165–1180.
4. Markus HS. Cerebral perfusion and stroke. *J Neurol Neurosurg Psychiatry* 2004; 75: 353–361.
5. Sebök M, Niftrik CHB Van, Wegener S, et al. Agreement of Novel Hemodynamic Imaging Parameters for the Acute and Chronic Stages of Ischemic Stroke: A Matched-pair Cohort Study. *Neurosurg Focus* 2021; 51: 1–8.
6. Václavů L, Meynart BN, Mutsaerts HJMM, et al. Hemodynamic provocation with acetazolamide shows impaired cerebrovascular reserve in adults with sickle cell disease. *Haematologica* 2019; 104: 690–699.
7. Chan ST, Evans KC, Rosen BR, et al. A case study of magnetic resonance imaging of cerebrovascular reactivity: A powerful imaging marker for mild traumatic brain injury. *Brain Inj* 2015; 29: 403–407.
8. Sobczyk O, Battisti-Charbonney A, Fierstra J, et al. A conceptual model for CO₂-induced redistribution of cerebral blood flow with experimental confirmation using BOLD MRI. *Neuroimage* 2014; 92: 56–68.
9. Champagne AA, Bhogal AA, Coverdale NS, et al. A novel perspective to calibrate temporal delays in cerebrovascular reactivity using hypercapnic and hyperoxic respiratory challenges. *Neuroimage*. Epub ahead of print 15 February 2017. DOI: 10.1016/j.neuroimage.2017.11.044.
10. Frederick B de B, Nickerson LD, Tong Y. Physiological denoising of BOLD fMRI data using Regressor Interpolation at Progressive Time Delays (RIPTiDe) processing of concurrent fMRI and near-infrared spectroscopy (NIRS). *Neuroimage* 2012; 60: 1913–1923.
11. Tong Y, Bergethon PR, Frederick B de B. An improved method for mapping cerebrovascular reserve using concurrent fMRI and near-infrared spectroscopy with Regressor Interpolation at Progressive Time Delays (RIPTiDe). *Neuroimage* 2011; 56: 2047–2057.
12. Cai S, Shi Z, Zhou S, et al. Cerebrovascular Dysregulation in Patients with Glioma Assessed with Time-shifted BOLD fMRI.
13. Fierstra J, van Niftrik C, Piccirelli M, et al. Diffuse gliomas exhibit whole brain impaired cerebrovascular reactivity. *Magn Reson Imaging* 2018; 45: 78–83.
14. Sebök M, van Niftrik CHB, Muscas G, et al. Hypermetabolism and impaired cerebrovascular reactivity beyond the standard MRI-identified tumor border indicate diffuse glioma extended tissue infiltration. *Neurooncol Adv* 2021; 3: 1–9.
15. Kienast Y, von Baumgarten L, Fuhrmann M, et al. Real-time imaging reveals the single steps of brain metastasis formation. *Nat Med* 2010; 16: 116–122.
16. Fidler IJ, Yano S, Zhang RD, et al. The seed and soil hypothesis: Vascularisation and brain metastases. *Lancet Oncology* 2002; 3: 53–57.
17. Langley RR, Fidler IJ. The biology of brain metastasis. *Clin Chem* 2013; 59: 180–189.

18. García-Gómez P, Valiente M. Vascular co-option in brain metastasis. *Angiogenesis* 2020; 23: 3–8.
19. El Kamar FG, Posner JB. Brain metastases. *Semin Neurol* 2004; 24: 347–362.
20. World Medical Association. World Medical Association Declaration of Helsinki: ethical principles for medical research involving human subjects. *JAMA* 2013; 310: 2191–2194.
21. Jenkinson M, Beckmann CF, Behrens TE, et al. FSL. *Neuroimage* 2012; 62: 782–790.
22. Jenkinson M, Bannister P, Brady M, et al. Improved optimization for the robust and accurate linear registration and motion correction of brain images. *Neuroimage* 2002; 17: 825–841.
23. Zhang Y, Brady M, Smith S. Segmentation of brain MR images through a hidden Markov random field model and the expectation-maximization algorithm. *IEEE Trans Med Imaging* 2001; 20: 45–57.
24. Schmidt P, Gaser C, Arsic M, et al. An automated tool for detection of FLAIR-hyperintense white-matter lesions in Multiple Sclerosis. *Neuroimage* 2012; 59: 3774–3783.
25. Jenkinson M, Smith SM. A global optimisation method for robust affine registration of brain images. *Med Image Anal* 2001; 5: 143–156.
26. Andersson JLR, Skare S, Ashburner J. How to correct susceptibility distortions in spin-echo echo-planar images: Application to diffusion tensor imaging. *Neuroimage* 2003; 20: 870–888.
27. Smith SM, Jenkinson M, Woolrich MW, et al. Advances in functional and structural MR image analysis and implementation as FSL. *Neuroimage* 2004; 23: S208–S219.
28. Bhogal AA. abhogal-lab/SeeVR: V2.01. 2021; (V2.01).
29. Champagne AA, Bhogal AA. Insights Into Cerebral Tissue-Specific Response to Respiratory Challenges at 7T: Evidence for Combined Blood Flow and CO₂-Mediated Effects. *Front Physiol* 2021; 12: 1–12.
30. Donahue MJ, Strother MK, Lindsey KP, et al. Time delay processing of hypercapnic fMRI allows quantitative parameterization of cerebrovascular reactivity and blood flow delays. *Journal of Cerebral Blood Flow and Metabolism* 2016; 36: 1767–1779.
31. Bhogal AA. Medullary vein architecture modulates the white matter BOLD cerebrovascular reactivity signal response to CO₂: Observations from high-resolution T2* weighted imaging at 7T. *Neuroimage* 2021; 245: 118771.
32. Chappell MA, Groves AR, Whitcher B, et al. Variational Bayesian inference for a nonlinear forward model. *IEEE Transactions on Signal Processing* 2009; 57: 223–236.
33. Chappell MA, Groves AR, Whitcher B, et al. Variational Bayesian inference for a nonlinear forward model. *IEEE Transactions on Signal Processing* 2009; 57: 223–236.
34. Benjamini Y, Hochberg Y. Controlling the False Discovery Rate : A Practical and Powerful Approach to Multiple Testing Author (s): Yoav Benjamini and Yosef Hochberg Source : Journal of the Royal Statistical Society . Series B (Methodological), Vol . 57 , No . 1 (1995), Publi. *Journal of the Royal Statistical Society* 1995; 57: 289–300.
35. RStudio Team. RStudio: Integrated Development for R.
36. Van Osch MJP, Teeuwisse WM, Van Walderveen MAA, et al. Can arterial spin labeling detect white matter perfusion signal? *Magn Reson Med* 2009; 62: 165–173.

37. Bhogal AA, De Vis JB, Siero JCW, et al. The BOLD cerebrovascular reactivity response to progressive hypercapnia in young and elderly. *Neuroimage* 2016; 139: 94–102.
38. Lassen U, Andersen P, Daugaard G, et al. Brain metastases from small cell lung cancer respond to chemotherapy, but response duration is short and the intracerebral concentration of chemotherapy may be too low because of the characteristics of the blood-brain barrier. Positron emission tomography. *Clinical Cancer Research* 1998; 4: 2591–2597.
39. Quattrocchi CC, Errante Y, Mallio CA, et al. Brain metastatic volume and white matter lesions in advanced cancer patients. *J Neurooncol* 2013; 113: 451–458.
40. Berk BA, Nagel S, Hering K, et al. White matter lesions reduce number of brain metastases in different cancers: a high-resolution MRI study. *J Neurooncol* 2016; 130: 203–209.
41. Yamaguchi T, Kanno I, Uemura K, et al. Reduction in regional cerebral metabolic rate of oxygen during human aging. *Stroke* 1986; 17: 1220–1228.
42. Leoni RF, Oliveira IAF, Pontes-Neto OM, et al. Cerebral blood flow and vasoreactivity in aging: An arterial spin labeling study. *Brazilian Journal of Medical and Biological Research* 2017; 50: 1–9.
43. Mandell DM, Han JS, Poubanc J, et al. Mapping cerebrovascular reactivity using blood oxygen level-dependent MRI in patients with arterial steno-occlusive disease: Comparison with arterial spin labeling MRI. *Stroke* 2008; 39: 2021–2028.
44. Lu H, Xu F, Rodrigue KM, et al. Alterations in cerebral metabolic rate and blood supply across the adult lifespan. *Cerebral Cortex* 2011; 21: 1426–1434.
45. Marstrand JR, Garde E, Rostrup E, et al. Cerebral perfusion and cerebrovascular reactivity are reduced in white matter hyperintensities. *Stroke* 2002; 33: 972–976.
46. Cohen J. The effect size. *Statistical power analysis for the behavioral sciences* 1988; 77–83.
47. Derdeyn CP, Videen TO, Yundt KD, et al. Variability of cerebral blood volume and oxygen extraction: Stages of cerebral haemodynamic impairment revisited. *Brain* 2002; 125: 595–607.
48. Kuroda S, Kamiyama H, Abe H, et al. Acetazolamide test in detecting reduced cerebral perfusion reserve and predicting long-term prognosis in patients with internal carotid artery occlusion. *Neurosurgery* 1993; 32: 912–919.
49. Lou X, Yu S, Scalzo F, et al. Multi-delay ASL can identify leptomeningeal collateral perfusion in endovascular therapy of ischemic stroke. *Oncotarget* 2017; 8: 2437–2443.
50. Wang DJJ, Alger JR, Qiao JX, et al. The value of arterial spin-labeled perfusion imaging in acute ischemic stroke: Comparison with dynamic susceptibility contrast-enhanced MRI. *Stroke* 2012; 43: 1018–1024.
51. Alsop DC, Detre JA, Golay X, et al. Recommended Implementation of Arterial Spin Labeled Perfusion MRI for Clinical Applications: A consensus of the ISMRM Perfusion Study Group and the European Consortium for ASL in Dementia. *Magn Reson Med* 2015; 73: 102–116.
52. Fan AP, Guo J, Khalighi MM, et al. Long-Delay Arterial Spin Labeling Provides More Accurate Cerebral Blood Flow Measurements in Moyamoya Patients: A Simultaneous Positron Emission Tomography/MRI Study. *Stroke* 2017; 48: 2441–2449.

53. Hoge RD, Atkinson J, Gill B, et al. Investigation of BOLD signal dependence on CBF and CMRO₂: The deoxyhemoglobin dilution model. *Neuroimage* 1999; 9: 849–863.
54. Petersen ET, Zimine I, Ho YCL, et al. Non-invasive measurement of perfusion: A critical review of arterial spin labelling techniques. *British Journal of Radiology* 2006; 79: 688–701.
55. Shiino A, Morita Y, Tsuji A, et al. Estimation of cerebral perfusion reserve by blood oxygenation level-dependent imaging: Comparison with single-photon emission computed tomography. *Journal of Cerebral Blood Flow and Metabolism* 2003; 23: 121–135.
56. Ziyeh S, Rick J, Reinhard M, et al. Blood oxygen level-dependent MRI of cerebral CO₂ reactivity in severe carotid stenosis and occlusion. *Stroke* 2005; 36: 751–756.



7

Evaluating physiological MRI parameters in Patients with Brain Metastases Undergoing Stereotactic Radiosurgery - A Preliminary Analysis and Case-report

Eva E. van Grinsven, Jordi de Leeuw, Jeroen C. W. Siero, Joost J. C. Verhoeff,
Martine J. E. van Zandvoort, Junghun Cho, Marielle E. P. Philippens,
& Alex A. Bhogal

Cancers (2023)

Special issue "Brain Cancer: Imaging and Radiotherapy"

ABSTRACT

Background

Brain metastases occur in ten to thirty percent of the adult cancer population. Treatment consists of different (palliative) options, including stereotactic radiosurgery (SRS). Sensitive MRI biomarkers are needed to better understand radiotherapy-related effects on cerebral physiology and the subsequent effect on neurocognitive functioning.

Methods

In the current study, we used physiological imaging techniques to assess cerebral blood flow (CBF), oxygen extraction fraction (OEF), cerebral metabolic rate of oxygen (CMRO₂) and cerebrovascular reactivity (CVR) before and three months after SRS in nine patients with brain metastases.

Results

Results showed improvement in OEF, CBF and CMRO₂ within brain tissue that recovered from edema (all $p \leq .04$), while CVR remained impacted. We observed a global post-radiotherapy increase in CBF in healthy-appearing brain tissue ($p = .02$). Repeated-measures correlation analysis showed larger reductions within regions exposed to higher radiotherapy doses in CBF ($r_{rm} = -.286, p < .001$), CMRO₂ ($r_{rm} = -.254, p < .001$), and CVR ($r_{rm} = -.346, p < .001$), but not OEF ($r_{rm} = -.004, p = .954$). Case analyses illustrated the impact of brain metastases progression on the post-radiotherapy changes in both physiological MRI measures and cognitive performance.

Conclusion

Our preliminary findings suggest no radiotherapy effects on physiological parameters occurred in healthy-appearing brain tissue within 3-months post-radiotherapy. Nevertheless, as radiotherapy can have late side effects, larger patient samples allowing meaningful grouping of patients and longer follow-up are needed.

INTRODUCTION

Approximately twenty percent of the basal metabolic rate of the body is consumed by the human brain, making it the most energy demanding organ.^{1,2} The primary sources of energy for the brain include oxygen and glucose, which are delivered by the arterial blood. To ensure the adequate delivery of nutrient necessary for homeostasis, autoregulatory functions serve to maintain stable cerebral blood flow (CBF) in response to changes in perfusion pressure or other hemodynamic events.^{2,3} However, this autoregulatory system can be disturbed by the presence of brain metastases.

Brain metastases represent a distressing aspect of cancer progression and occur in ten to thirty percent of the adult cancer population.^{4,5} To metastasize to the brain, cancer cells sequentially complete a series of processes (e.g. penetration of the blood-brain-barrier)⁶ that may lead to alterations in the surrounding metabolic and vascular microenvironment.⁷⁻¹⁰ Moreover both primary brain tumors and brain metastases are frequently surrounded by vasogenic edema, which is the result of local blood-brain-barrier disruptions, allowing protein-rich fluid to accumulate in the extracellular space.¹¹ A previous study has reported a lower fractional extraction of oxygen in edema surrounding diffuse gliomas and lower regional blood flow in edema surrounding brain metastases.¹² Moreover, impaired cerebrovascular reactivity (CVR) was observed within edema surrounding both diffuse gliomas¹³ and brain metastases¹⁴, which could reflect a local pressure effect restricting the ability of vessels to dilate and maintain adequate perfusion. Treatment and management of edema is aimed at reducing swelling and alleviating symptoms. However, it is unknown whether the metabolic and vascular reserve within these regions also recovers once edema subsides.

Radiotherapy is the cornerstone of (palliative) treatment for brain metastases, in combination with surgery, chemotherapy or immunotherapy.¹⁵ Unfortunately, brain radiation can also damage surrounding healthy tissue, as shown by largely reduced vessel density in the brain after fractionated radiotherapy in rats.¹⁶ Likewise, studies have found vascular damage resulting in reduced blood perfusion in brain areas that received at least 10-15 Gy.¹⁷ Other studies have even shown reduced CBF at radiation doses below 10 Gy.¹⁸ Research on metabolic changes after radiotherapy is rather limited. Hypothetically, radiation damage to vessels could decrease the ability to regulate CBF, leading to increased oxygen extraction fraction (OEF) in order to maintain sufficient cerebral metabolic rate of oxygen (CMRO₂). On the other hand, irradiation of healthy brain tissue can also cause cell damage¹⁹, possibly resulting

in lowered metabolism and need for oxygen. Conclusively, the various metabolic and vascular changes that can occur after radiotherapy highlight the complexity of radiation-induced damage.

These complex and multifaceted changes in the brain may partially explain the large individual differences in radiation-induced cognitive decline experienced by patients with brain metastases.²⁰ Non-invasive, sensitive MRI biomarkers are needed to better understand radiotherapy-related changes in the brain and its subsequent effect on neurocognitive functioning. With this in mind, the main aim of the current study was to assess the added value of using physiological imaging techniques to assess CVR, CBF, OEF and CMRO₂ in both healthy appearing tissue and malignant tissue before and after stereotactic radiosurgery (SRS) in patients with brain metastases. Acquiring both OEF and CBF in the same scan session can provide insight as to whether changes in brain oxygen metabolism (i.e. CMRO₂) occur due to abundant or insufficient blood supply or because the tissue itself has (partly) lost the ability to extract and consume oxygen. The addition of a CVR measurement can give insight into the regulatory state of the tissue at baseline. As a secondary analysis, we investigated cognitive changes after radiotherapy in relation to changes in these physiological MRI parameters on a case-by-case basis. This preliminary study aims to establish a foundational framework for advancing our understanding of radiation-induced brain damage and its relation to cognitive functioning, thereby providing a basis to generate novel hypotheses to guide future research.

METHODS

Study set-up and population

MRI datasets were acquired between October 2022 and February 2023 for the ongoing Assessing and Predicting Radiation Influence on Cognitive Outcome using the cerebrovascular stress Test (APRICOT) study. Participation consists of an elaborate neurocognitive assessment (NCA) and MRI before radiotherapy and approximately three months after radiotherapy. The study population consists of adult patients (≥ 18 years) with either radiographic and/or histologic proof of metastatic disease in the brain that were referred to the radiotherapy department of the UMC Utrecht for radiotherapy of the brain metastases. Specific in- and exclusion criteria for participation in the APRICOT study are listed in the **Supplementary Materials**. The study was performed in accordance with the Declaration of Helsinki²¹ and the UMCU institutional ethical review approved the study (METC# 18-747). Written informed consent was obtained from all participants prior to participation.

Data acquisition

Imaging protocol

The participants were scanned on a 3 Tesla MRI scanner (Achieva, Philips Medical Systems, Best, The Netherlands) using a 32-channel receive coil. The same scanning protocol was used as described before.¹⁴ To acquire CVR measurements, a whole-brain multi-slice single shot gradient-echo EPI BOLD images (TR = 1050 ms, TE = 30 ms, flip angle 65°, voxel size 2.292 x 2.292 x 2.5 mm³, acquisition matrix 96 x 96 x 51, 1000 dynamics, multi-band factor = 3, SENSE factor = 1.8) were acquired throughout a computer-controlled hypercapnic breathing protocol (described below). An additional dataset pair was acquired for EPI phase (distortion) correction. Perfusion data were acquired using a multi-delay ASL sequence. A whole volume was acquired at 4 post-labeling delays (660, 1325, 1989, 2654ms), using a pCASL Look-Locker multi-slice EPI read-out (total scan time = 240 s, labelling train duration = 1650ms, TR = 5s, TE = 12 ms, flip angle 25°, acquired resolution: 3 x 3 x 7 mm³, acquisition matrix: 80 x 80 x 17, 23 volumes of label- control pair, SENSE factor = 2, 2 background suppression pulses. The first volume contains the calibration (M0) images for each post-label delay where the labelling, saturation pulses and background suppression were turned off. No breathing challenges were performed during ASL imaging. The ASL was planned using a fast phase contrast angiography scan, with the labeling plane carefully placed perpendicular to the internal carotid arteries and vertebral arteries. The whole brain SWI was acquired using a multi-echo gradient-echo (ME-GRE) sequence (TE1 = 8.5 ms, TE2 = 17.5 ms, TE3 = 26.5 ms, TE4 = 35.5 ms, TE5 = 44.5 ms, echo spacing 8 ms, TR 50 ms, flip angle 17°, voxels size 0.342 x 0.342 x 2 mm³, acquisition matrix 384 x 383 x 63) was acquired. Additionally, a 3D T1-weighted magnetization prepared rapid gradient echo imaging (MPRAGE) sequence (TR = 8 ms, TE = 3.25 ms, flip angle 10°, isotropic resolution 1 mm, acquisition matrix 240 x 240 x 180) and a 3D T2-weighted FLAIR sequence (TR 4800 ms, TE 240 ms, TI = 1650 ms, flip angle 90°, isotropic resolution: 1 mm, acquisition matrix 256 x 256 x 182) were acquired for anatomical reference.

Clinical CT and MRI acquisition

CT and MRI scans were acquired as part of clinical care as usual 1 to 5 days before receiving SRS. CT scans were acquired on a Brilliance Big bore 22 scanner (Philips Medical Systems, Best, The Netherlands) with a tube potential of 120 kVp, matrix size of 512 x 512 and inplane slice thickness of 1 mm. The participants were scanned on a 1.5 Tesla MRI scanner (Ingenia, Philips Medical Systems, Best, The Netherlands) using a 15-channel receive coil. A 3D SPGR sequence after injection of 0.1 ml gadovist/kg was performed (TR = 7.6 ms, TE = 3.4 ms, flip angle 8°, isotropic resolution: 1 mm, acquisition matrix 232 x 232 x 170). The clinician uses this clinically acquired MRI

registered to the CT, to plan the radiotherapy and delineate the so-called gross tumor volume (GTV; i.e. brain metastases). The prescribed dose was recalculated into equivalent total doses per 2-Gy fractions (EQD2) to aid comparability between and generalizability to different radiation schemes. The CT, dose maps, planned target volume (PTV) and GTV were extracted for each patient. For the current analysis, the GTV was divided into newly treated brain metastases, resection cavities of brain metastases and previously irradiated brain metastases. Analysis were only performed on newly treated brain metastases. If a patient had multiple brain metastases, averages were calculated from all voxels corresponding to the multiple brain metastasis. Dose maps were subdivided into regions of interests (ROIs) with low (<10 Gy), medium (10-15 Gy) and high (>15 Gy) dose, following previous research on vascular damage described above 10-15 Gy (**Figure 1**).¹⁷

Breathing protocol

Hypercapnic stimuli were delivered using a computer-controlled gas blender and sequential delivery system (RespirAct, Thornhill Research Institute, Toronto, Canada). The breathing mask was sealed to the patients' face using transparent dressings (Tegaderm, 3M, St. Paul, MN, US) to acquire an air tight seal. Before starting the breathing challenges inside the MRI scanner, patients performed a test round with a CO₂ challenge which is similar to the CO₂ block given during the protocol. Only after successful completion of the test round the breathing challenges inside the scanner were performed (**Supplementary Figure 1**). The breathing challenges started with a 5-minute baseline period, followed by a block-shaped increase of end-tidal CO₂ (PetCO₂) 10 mmHg relative to a patient's baseline for 90 seconds. After this so-called CO₂-block, PetCO₂ values returned to baseline values for 120 seconds, followed by a PetCO₂ ramp increase of 12 mmHg relative to patients' baseline for 180 seconds after which patients returned to baseline for 90 seconds.

Neurocognitive assessment

An extensive battery of neuropsychological tests was used to assess cognitive performance both before and three months after SRS. All tests are internationally widely used, standardized psychometric instruments for assessing neurocognitive deficits in the major neurocognitive domains (**Supplementary Table 1**).²² Each neuropsychological test was scored according to standardized scoring criteria. Individual change in neurocognitive performance post-radiotherapy was assessed and classified using the reliable change index (RCI) as formulated by Jacobson and Truax.^{23,24} RCI values ≥ 1.645 present improvement, ≤ -1.645 present decline and values not exceeding ± 1.645 indicate stable cognitive performance on the task. Change in neurocognitive performance per domain was defined as improved if at

least one task within that domain showed improvement, as declined if at least one task showed a decline, as mixed if at least one task indicated improvement and one task indicated decline and as stable when all tasks within that domain showed stable performance.

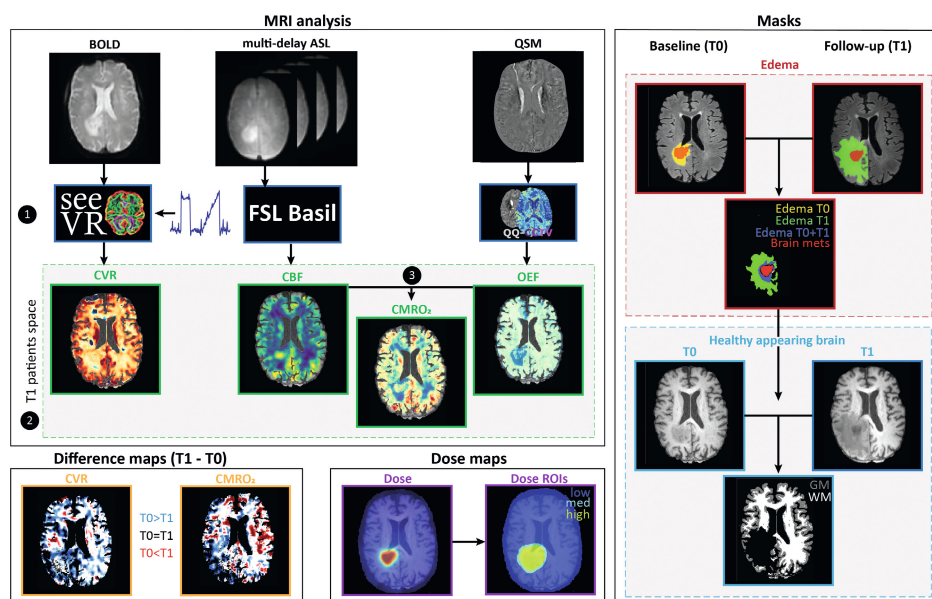


Figure 1. Data analysis steps for the MRI data. MRI analysis was performed for the BOLD, ASL and QSM data. 1) CVR maps were generated with the SeeVR toolbox using the BOLD time series and PetCO₂ traces, quantitative CBF maps were generated based on the multi-delay ASL data using the ClinicalASL toolbox and FSL BASIL, and OEF maps were generated from the QSM data with the QQ-CTV software package. 2) All MRI maps were transformed to the baseline T1 patient space. 3) The CMRO₂ map was generated by multiplying the CBF map with the OEF map. Multiple masks were generated. Edema masks were made based on the T2FLAIR hyper intensities for both baseline (T0) and follow-up (T1). From this, new masks including regions only exhibiting edema at baseline (edema T0), regions only exhibiting edema at follow-up (edema T1) and regions exhibiting edema at both time-points (edema T0+T1) were created. The brain metastases were excluded from the edema regions. Next, the edema and brain metastases mask were excluded from the whole-brain mask to create a mask with healthy appearing brain tissue at both time points. This healthy appearing brain tissue was subdivided into grey matter (GM) and white matter (WM). Difference maps subtracting the follow-up (T1) data from the (T0) were calculated for CVR and CMRO₂. Positive values represent an increase in either CVR or CMRO₂ at follow-up (T0<T1) and negative values represent a decrease in either CVR or CMRO₂ at follow-up (T0>T1). The subtraction process was restricted to pixels that contained values in both the pre- and post-radiotherapy images. Images were masked to exclude CSF. Finally, dose maps were extracted with one map showing the total delivered dose in EQD2 and the other map dividing the dose into ROIs with low (<10 Gy), medium (10-15 Gy) and high (>15 Gy) dose, as described above.

Pre-processing

Pre-processing steps were performed using the Oxford Centre for Functional MRI of the BRAIN (FMRIB) Software Library (FSL – version 6.0).²⁵ First, both the T1 and T2FLAIR images were brain extracted using BET²⁶. Tissue segmentation into grey matter (GM), white matter (WM) and cerebrospinal fluid (CSF) was performed on the T1 image using FSL Automated Segmentation Tool (FAST).²⁷ Additionally, an edema mask was created based on the T1 and T2FLAIR images using the lesion growth algorithm as implemented in the Lesion Segmentation Tool (LST, <https://www.statistical-modelling.de/lst.html>) for SPM.²⁸ Based on previous experience, the initial threshold was set at 0.14. The resulting edema mask was manually adapted to eliminate any false positives or false negatives from the LST edema mask.

BOLD data were motion corrected (MCFLIRT)²⁶, corrected for geometric distortion using TOPUP^{29,30} and linear spatial co-registered to the T1 image using the 'epi_reg' function^{26,31}. QSM maps were calculated from the raw phase and magnitude data of the ME-GRE images using the MEDI toolbox.³² The local field was estimated by the projection onto dipole field (PDF) method³³, and susceptibility values were computed by Morphology Enabled Dipole Inversion (MEDI)³⁴.

Data analysis

MRI analysis

CVR maps were derived using the open-source seeVR toolbox (**Figure 1**).³⁵ In brief, in order to remove signal contribution from large veins that might overshadow tissue responses, a modified whole-brain mask was generated using the 'remLV.m' function of the seeVR toolbox.³⁵ For this, a temporal noise-to-signal (tNSR) map was calculated by taking the inverse of the temporal signal-to-noise (tSNR) map. Next, voxels showing values higher than the 98th percentile tNSR value were removed from the original whole brain-mask to remove the large veins. This modified mask was then used in subsequent analyses.³⁵ Next, a manual bulk alignment was performed between the PetCO₂ and average GM time-series to minimize alignment errors that can occur when using automated correlation methods. Thereby, any bulk delays between end-tidal gas measurements at the lungs and BOLD signal responses in the brain were accounted for. Residual motion signals with a correlation higher than 0.3 with the GM time-series, along with a linear drift term were regressed out using a general linear model. BOLD data was then temporally de-noised using a wavelet-based approach.³⁶ A linear regression was performed between the bulk-aligned PetCO₂ trace with each processed BOLD voxel time-series. The slope of this linear regression was taken as the CVR (% Δ BOLD/mmHg PetCO₂).

The multi-delay ASL was processed using the open-source ClinicalASL toolbox³⁷ and FSL BASIL for quantitative CBF maps³⁸. As described before¹⁴, a T1-weighted image was generated based on the M0 images from each PLD which was used for subsequent image registration and outlier removal. Outlier removal was performed based on the SCORE method by Duloi et al (**Figure 1**).³⁹

ME-GRE data were used to generate OEF maps using the integrative QQ approach of Cho et al (**Figure 1**), with an unsupervised machine learning algorithm, temporal clustering, tissue composition, and total variation (CCTV).⁴⁰⁻⁴⁴ QQ estimates OEF maps based on the QSM processing of the ME-GRE phase and qBOLD modeling of ME-GRE magnitude data. The robustness of QQ against noise was improved substantially by using CCTV⁴⁵, which groups voxels with similar signal evolution and the same tissue type (GM/WM/CSF) into a cluster and assumes that the voxels have similar model parameters including OEF.

All MRIs were registered to the T1 image acquired at baseline using FMRIB's Linear Image Registration Tool (FLIRT; **Figure 1**).^{26,31} Next, CMRO₂ maps were generated by combing the OEF and CBF data according to the following equation:

$$CMRO_2 = OEF \cdot CBF \cdot [H]_{\alpha} \quad (1)$$

in which $[H]_{\alpha}$ is the oxygenated heme molar concentration in the arteriole expressed in $\mu\text{mol/ml}$. In this study, an oxygenated heme molar concentration of $7.377 \mu\text{mol/ml}$ is used in accordance with research by Zhang and colleagues (**Figure 1**).⁴⁶ Difference maps for CVR and CMRO₂ were created by subtracting the follow-up (T1) MRI map from the baseline (T0) MRI map (**Figure 1 - Difference maps**). Hereby positive values represent an increase in either CVR or CMRO₂ at follow-up (T0<T1) and negative values represent a decrease in either CVR or CMRO₂ at follow-up (T0>T1). Lastly, based on previously created edema masks, new masks were generated (**Figure 1**) to incorporate regions only exhibiting edema at baseline (edema T0), regions only exhibiting edema at follow-up (edema T1), and regions exhibiting edema at both time-points (edema T0+T1). The GTV (i.e. brain metastases) were excluded from all edema masks. Next, masks were created that incorporated healthy appearing brain tissue at both time-points. Therefore, the edema mask (edema T0+T1) and PTV were extracted from the whole-brain tissue to make sure any possible malignant tissue was excluded. Then the healthy appearing brain tissue was subdivided into grey matter (GM) and white matter (WM).

Statistical analysis

First, we compared the differences in physiological MRI parameters between various tissue types before SRS. For each physiological MRI map, we calculated the average value per tissue type (GM, WM, edema, and brain metastases) prior to SRS for each patient separately. We used Wilcoxon signed-rank tests to compare the average values across the different tissue types for each physiological MRI map. Secondly, we investigated whether there was a relationship between the extent of edema and the physiological MRI parameters within healthy-appearing brain tissue before SRS. Therefore, we computed the average value within the healthy-appearing brain tissue for each patient and then used Spearman's rank correlations to assess the correlation between this value and the volume of edema (expressed as a percentage of voxels contained within the (extracted) whole brain mask).

Post-radiotherapy changes in the physiological MRI parameters were assessed separately for edematous tissue regions and healthy appearing tissue. Regarding the edematous regions, we divided them into three distinct categories based on their temporal occurrence: 1) regions with edema at either T0 or T1 (i.e. all edema), 2) regions with edema exclusively at T1 (i.e. new edema), and 3) regions with edema exclusively at T0 (i.e. old edema; **Figure 1**). To evaluate the differences between pre- and post-radiotherapy values for each type of edema and each physiological MRI map, we used Wilcoxon signed-rank tests. For healthy-appearing brain tissue, we calculated the mean values of each physiological parameter separately for pre- and post-radiotherapy MRI scans, for each patient. Subsequently, we used Wilcoxon signed-rank tests to determine whether any changes occurred in the healthy-appearing brain tissue after SRS, by comparing the mean pre-radiotherapy values to the mean post-radiotherapy values.

Dose-related changes in healthy-appearing brain tissue were assessed using three different methods. First, we calculated the mean value for each physiological parameter map for each dose ROI (i.e. low, medium, high). Next, Wilcoxon signed-rank tests were performed to compare each of the ROI's to assess whether there was a significant difference between regions receiving either low, medium or high dose. For the second method, the radiotherapy dose map was sorted based on ascending values. The sorted dose values were then subdivided into 20 bins, each containing 5 percent of the data. Using the boundaries of these '5%-bins', the dose map was divided into ROIs. Each ROI contained 5 percent of the dose data, where the lowest bin value represented the 5 percent lowest dose values and the highest bin value the 5 percent highest dose values. For each physiological MRI difference map, the mean value for each of these binned ROIs was calculated and used in the

subsequent correlation analysis to assess whether the mean change in physiological MRI parameters in each bin-ROI correlated with the mean dose received by the tissue within that bin. As this binning results in 20 mean values per individual (i.e. for each binned ROI), a repeated-measures correlation was chosen to account for the within-individual variance between these values. The 'rmcorr' package⁴⁷ implemented in RStudio (Version 2021.9.1.372)⁴⁸ was used to perform this repeated-measures correlation. This analysis estimates the common regression slope for repeated measures. In addition to the two regional dose analyses, voxelwise Spearman's Rank correlations were calculated between the delivered dose and physiological MRI difference maps for each patient separately. We performed Wilcoxon-signed rank tests to assess whether the correlation values significantly differed from zero on the group level for each physiological MRI parameter. For all statistical tests, a p -value < 0.05 was considered statistically significant, corrected for multiple comparisons when necessary.

RESULTS

Participants

In total 17 patients completed both baseline and follow-up MRI and NCA within the given time period. Of these, 9 patients (4 females) were included for the current analysis (**Table 1**), most patients were excluded from the analysis due to artefacts in the MRI data (**Supplementary Figure 2**). Three of the nine patients did not want to perform the breathing challenges during BOLD imaging at follow-up, leading to missing CVR data for those patients.

All nine patients received SRS on a Linear Accelerator (Elekta) with conebeam CT imaging guidance, most commonly 21 Gy delivered in 1 fraction. Median age of patients was 66 years and most patients had a primary lung tumor (all non-small cell lung cancer). The median number of brain metastases was 7 (IQR 2-10) and the total volume was median 4 cc. Before SRS edema volume excluding BMs volumes was median 17 cc and three months after SRS 6 cc, with extensive inter-individual variability. Most patients (6/9) had received systemic therapy during the follow-up period. Response to SRS was evaluated approximately three months after treatment completion and the majority (4/9) showed decreased brain metastases volume on follow-up scans, while 2/9 showed growth of new brain metastases. One patient had a mixed response, indicating some brain metastases had grown and others had shrunk.

Table 1. Patient, treatment and volume information of the included subjects in this study.

#	Age in years	Sex	Primary tumor	#BMs	Total BMs vol in cc	Prescribed SRS dose in Gy/1 fr	Previous RT	In between RT	Post-RT systemic therapy	Edema vol T0 in cc	Edema vol T1 in cc	Dexamethasone dose pre-RT in mg/day	Dexamethasone dose post-RT in mg/day	RT response ^a
3	57	F	Lung	7	4.3	21	N	N	N	54.3	21.4	0.0	1.5	Decrease
5	66	M	Melanoma	18	0.9	21	Y	N	Y	12.5	98.8	0.0	0.0	Stable
6	81	M	Melanoma	2	7.1	21	N	N	Y	17.1	155.3	0.0	0.5	Growth
7	62	F	Lung	11	11.2	21	N	N	Y	19.5	1.4	0.0	0.0	Decrease
8	72	M	Kidney	1	17.6	18	N	N	Y	80.1	5.7	4.0	0.0	Decrease
11 ^b	52	F	Lung	8	50.6	15	N	N	Y	29.4	4.7	4.0	0.0	Decrease
18	72	M	Lung	2	1.8	21	N	N	N	13.2	0.4	2.0	0.0	Decrease
23 ^b	74	F	Lung	1	3.5	18	N	Y	N	16.3	56.4	0.5	2.5	Growth
24 ^b	62	M	Melanoma	10	1.6	24	N	N	Y	3.1	4.5	0.0	0.0	Mixed

^abased on the radiology report of the clinical scan; ^bno post-radiotherapy CVR maps available.

Abbreviations: BMs, brain metastases; F, female; M, male; N, no; RT, radiotherapy; T0, pre-radiotherapy; T1, post-radiotherapy; vol, volume; Y, yes

Baseline Tissue comparison

For each physiological MRI parameter, the group mean values were compared between different tissue (GM, WM, edema, brain metastases) using Wilcoxon signed rank tests (**Figure 2** and **Supplementary Table 2**). A subset of these parameters has been reported previously.¹⁴ In the current analyses, GM had higher CBF and CVR than both WM and edema (all $p = .004$). WM CVR was higher than CVR in edema regions ($p = .008$). For $CMRO_2$, GM values were higher than both WM and edema ($p = .008$ and $p = .004$, respectively), and WM had higher $CMRO_2$ values than edema ($p = .008$). For OEF, GM values were lower than WM ($p = .004$) and WM OEF values were higher than edema ($p = .004$). Brain metastases had lower OEF than in WM ($p = .004$) and higher CBF and $CMRO_2$ than edema regions (both $p = .004$). Excluding subcortical GM areas from the analyses did not lead to changes in these significant differences between tissues (**Supplementary Figure 3**).

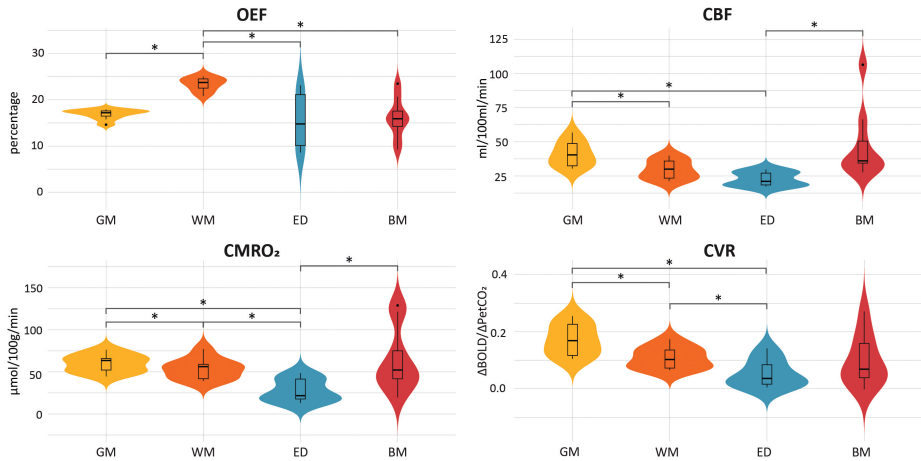


Figure 2. Violin plots displaying the differences in OEF, CBF, $CMRO_2$ and CVR values across different tissue types. Asterisks indicate significant differences using a corrected p-value = .017 for multiple comparisons.

Edema regional comparisons

Edema volume pre-radiotherapy

The relationship between the volume of edema (expressed as percentage of the total brain volume) and the average physiological parameters within the healthy appearing whole-brain pre-radiotherapy was calculated using Spearman's Rank correlations for each MRI metric (**Figure 3**). There were no significant correlations between the pre-radiotherapy edema volume and average whole-brain OEF ($r = .02$, $p = .982$), CBF ($r = .43$, $p = .250$), $CMRO_2$ ($r = .62$, $p = .086$), or CVR ($r = -.45$, $p = .223$).

Post-radiotherapy changes

To assess the influence of the presence of edema on the assessed MRI metric, the average values within edematous regions were compared before and after SRS (**Figure 4**). Within edematous tissue, a distinction was made between regions with edema at both T0 or T1 (i.e. edema), regions with edema exclusively at T1 (i.e. new edema) and regions with edema exclusively at T0 (i.e. old edema). Comparisons were made using Wilcoxon-signed rank tests. For OEF, CBF and $CMRO_2$ values in old edema (T0 edema) regions, were higher post-radiotherapy than pre-radiotherapy (all $p \leq .04$), while CVR did not change in old edema (T0 edema) regions over time. When the outliers as visible in **Figure 4** were removed from the analyses, CBF in old edema regions (T0 edema) was no longer statistically significantly higher post-radiotherapy than pre-radiotherapy ($p = .078$). For OEF and $CMRO_2$ pre-post radiotherapy differences in old edema (T0 edema) remained statistically significant after outlier removal.

Healthy appearing brain tissue

Global post-radiotherapy changes

To assess whether there were global effects of the radiotherapy on the healthy appearing brain tissue, average MRI values were compared pre- and post-radiotherapy using Wilcoxon signed rank tests (**Figure 5**). Only CBF values were significantly higher post-radiotherapy than pre-radiotherapy ($p = .020$). This indicates perfusion throughout healthy appearing brain tissue increased after radiotherapy. None of the other MRI metrics showed significant changes after radiotherapy.

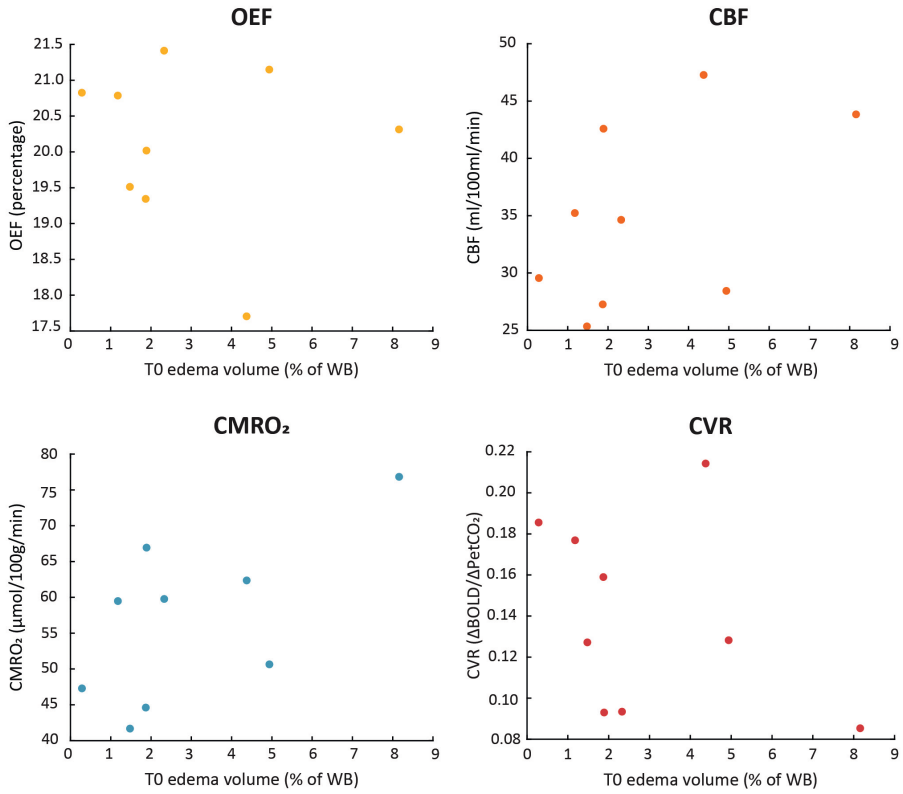


Figure 3. Relationship between the volume of edema pre-radiotherapy and the average physio-logical MRI parameters in healthy appearing whole-brain value.

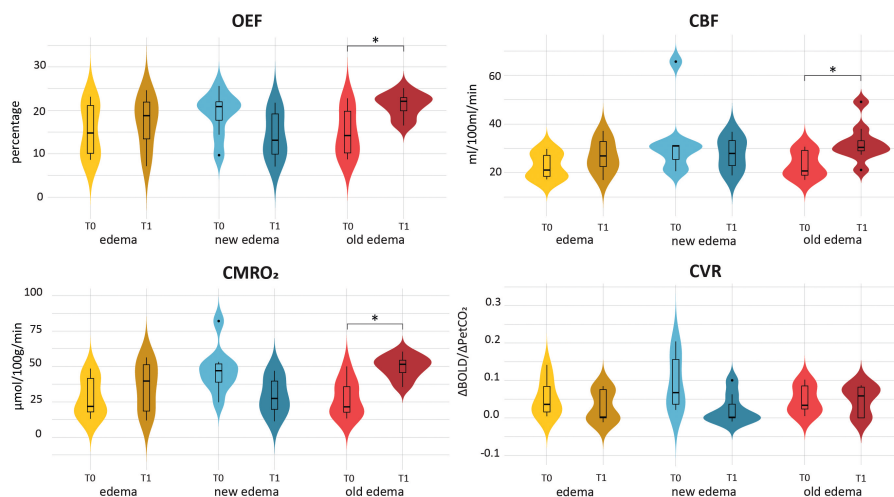


Figure 4. Violin plots of the pre- and post-radiotherapy values within different edema regions. Edema regions encompass any region with edema either pre- or post-radiotherapy. New edema indicates those areas with edema exclusively at post-radiotherapy and old edema indicates those areas with edema exclusively at pre-radiotherapy. Asterisks indicate significant differences.

Dose-related changes

Changes in the MRI metrics from pre- to post-radiotherapy were compared between healthy appearing brain regions that had received low, medium and high radiotherapy dose (**Figure 6**). Differences between dose groups were assessed using Wilcoxon signed-rank tests, which indicated none of the dose regions significantly differed from each other for any of the MRI metrics.

In addition to the ROI dose comparison, repeated measures correlations were performed between the dose and the change each MRI metric post-radiotherapy using the dose binned ROIs (**Figure 7**). The changes in OEF post-radiotherapy were not related to the delivered radiotherapy dose ($r_{rm} = -0.004$, $p = .954$). There was a significant negative relationship between the delivered dose and the post-radiotherapy changes in healthy appearing brain tissue regarding CBF ($r_{rm} = -0.286$, $p < .001$), CMRO₂ ($r_{rm} = -0.254$, $p = .001$) and CVR ($r_{rm} = -0.346$, $p < .001$). This indicates that post-radiotherapy declines in CBF, CMRO₂ and CVR were related to higher delivered radiotherapy dose. Additionally, voxel-wise Spearman Rank correlations between the delivered radiotherapy dose and post-radiotherapy changes in OEF, CBF, CMRO₂ and CVR were performed for each individual (**Supplementary Figure 4**). One-sample Wilcoxon signed-rank tests indicated that the correlation values did not significantly differ from zero on the group-level (all $p > .05$).

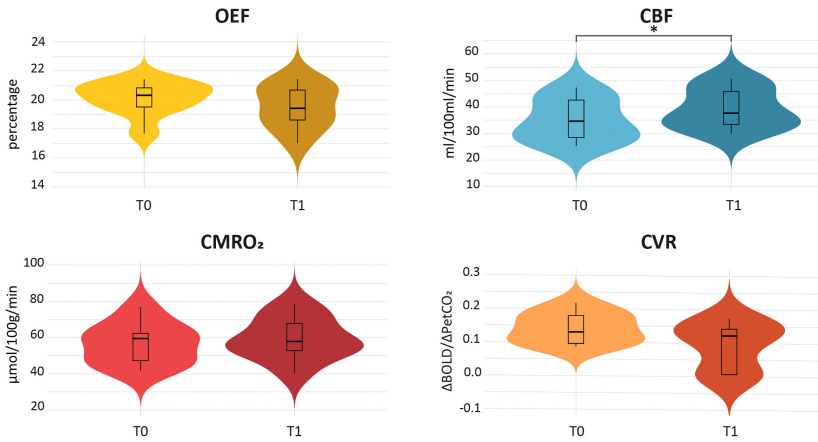


Figure 5. Comparison between global pre- and post-radiotherapy values within healthy appearing brain tissue. Asterisks indicate significant differences.

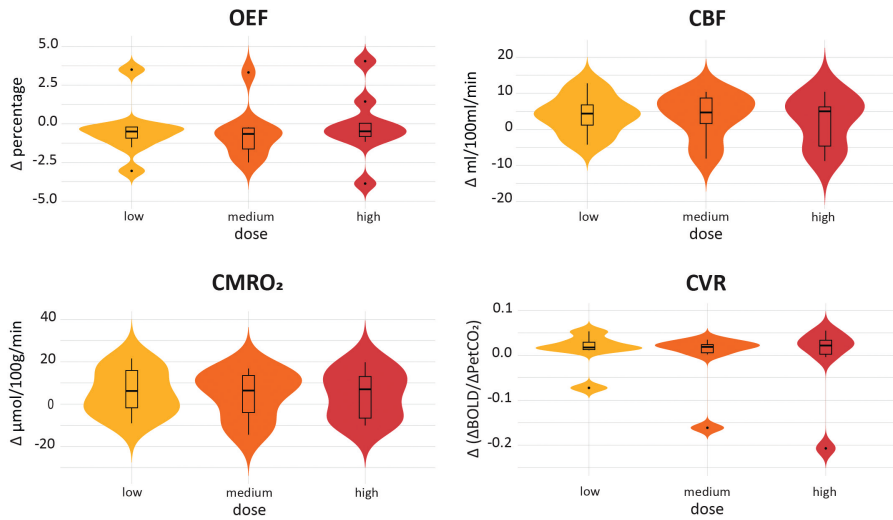


Figure 6. Comparison between the post-radiotherapy changes in the three dose ROIs within healthy appearing brain tissue. Corrected p -value = .025.

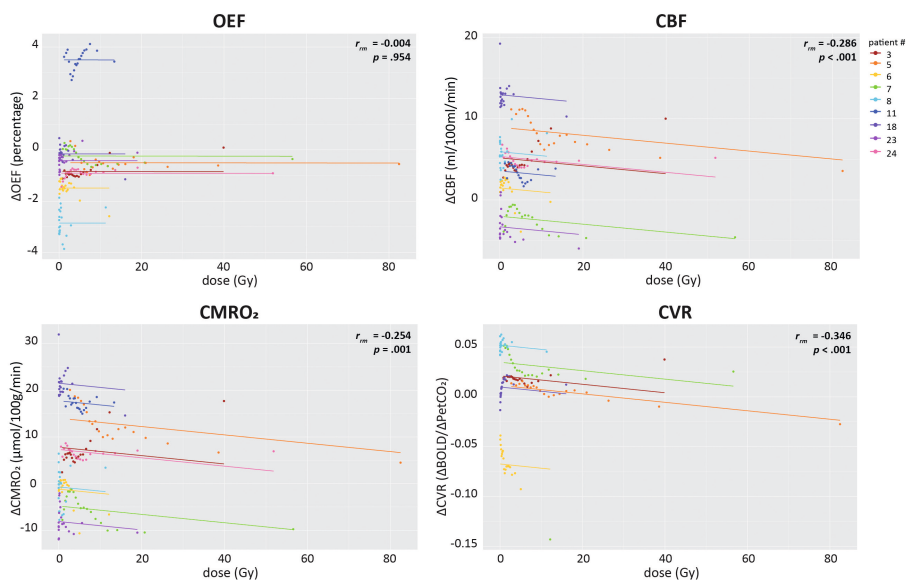


Figure 7. Repeated measures correlations of the post-radiotherapy changes and the dose in the healthy-appearing brain. Each color represents a different patient and the lines represent the common linear relationship between the MRI metrics when all participants are taken into account. Statistics for each relationship are provided for each plot separately.

Case-analysis

As group analysis indicates significant heterogeneity in the post-radiotherapy changes in OEF, CBF, CMRO_2 and CVR, a case-study analysis was performed. Three diverse cases were chosen, based on their response to the radiotherapy: growth of new brain metastases, shrinkage of brain metastases or a mixed response three months after SRS (**Figure 8**). Besides changes in the physiological MRI parameter maps, the cognitive changes post-radiotherapy were assessed. For the patient that had new tumor growth after radiotherapy, the MRI differences and cognitive changes aligned; there was a general worsening of the physiological MRI parameters and cognitive decline in the majority of the cognitive domains. The largest changes in physiological MRI values were near the tumor area. For the patient with tumor shrinkage, the improvement in physiological MRI parameters is most pronounced for OEF where a post-radiotherapy increase of OEF was visible in the areas surrounding the tumor area. This improvement was also reflected in the cognitive changes, with improvement or stability on the majority of the cognitive domains. For the patient with a mixed response after radiotherapy, no clear pattern emerges from the MRI and cognitive data. See **Supplementary Figure 5** for a visual representation of all included patients.

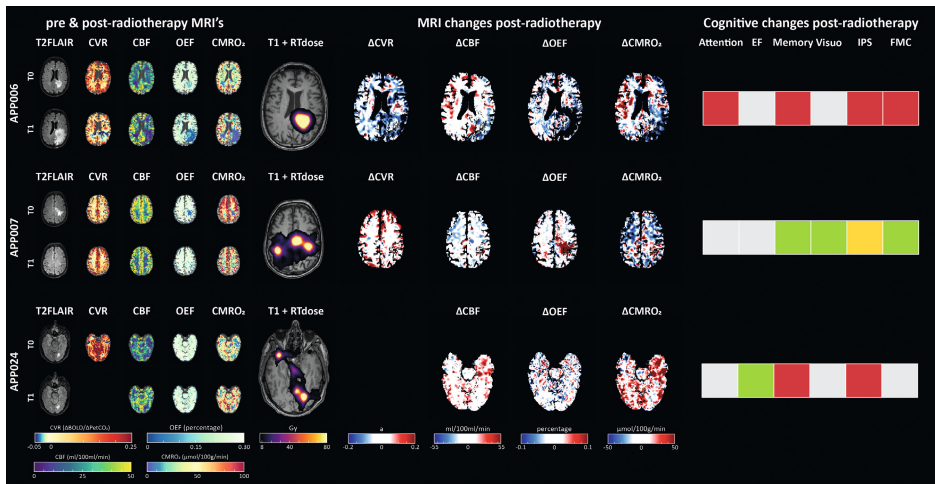


Figure 8. Visual comparison of MRI-related and cognitive changes in three subjects with different radiotherapy responses. Subject 006 had new brain metastases, subject 007 brain metastases shrinkage and subject 024 had a mixed response whereby some brain metastases grew and some shrunk. Pre- and post-radiotherapy MRI maps are shown separately for pre-radiotherapy (T0) and three months post-radiotherapy (T1). Additionally, the delivered radiotherapy dose and difference scores (T1-T0) for the MRI maps are shown alongside the cognitive changes that were observed across the cognitive domains. Hereby grey indicates stable performance, green improvement, red decline and yellow mixed response. As patient 24 did not perform the CVR assessment post-radiotherapy, no difference maps for CVR are available.

DISCUSSION

In this study, we employed state-of-the-art physiological imaging techniques to comprehensively evaluate properties linked to both the metabolic and vascular reserve in patients with brain metastases before and three months after SRS. Our findings revealed a significant improvement in metabolic measures (OEF and $CMRO_2$) within brain tissue that recovered from edema three months post-radiotherapy, while the vascular reserve remained impacted. Additionally, we observed a global post-radiotherapy increase in CBF in healthy-appearing brain tissue. No dose-related changes in any of the MRI metrics were detected when regions were categorized into low, medium, and high delivered dose. Correlation analyses highlighted larger reductions in CBF, $CMRO_2$, and CVR within regions exposed to higher radiotherapy doses, but also indicated considerable variability both among patients and across dose regions. Case analyses suggested that part of this heterogeneity may be attributed to brain metastases progression following SRS. Collectively, our findings

suggest that in this small patient sample no large metabolic or vascular changes occurred in the late-acute phase following SRS in patients with brain metastases.

Tissue-specific differences were observed pre-radiotherapy across both metabolic and vascular parameters. The tissue-differences for CBF and CVR were similar to those reported in our previous study¹⁴ and in healthy subjects⁴⁹, with both WM areas and edema characterized by lower CBF and CVR than GM. $CMRO_2$ values were higher in GM compared to WM, consistent with the higher neuronal density in GM and previous studies.⁵⁰ The OEF in GM was lower than in WM, while previous research has shown relatively homogeneous OEF in GM and WM using either QQ-CCTV⁴² or PET⁵¹. Lower OEF values in deep GM structures due to iron depositions⁵² cannot explain this phenomenon, as restricting the comparison to cortical GM yielded similar results. This may indicate the lower GM OEF is a compensatory auto regulatory response to the increased GM CBF, aiming to sustain stable GM $CMRO_2$. However, due to the smaller number of voxels present in the GM and thereby its heightened susceptibility to extreme values and minor spatial misalignment, this could also potentially account for some of the observed differences.

Large variability in the physiological parameters was seen within tissue containing untreated brain metastases, as was expected based on previous literature.^{12,14,53} The primary tumor (i.e. origin of metastatic cells), might cause some of this heterogeneity as it affects the brain metastases growth pattern, metabolism and vasculature.^{6,10,54,55} As the $CMRO_2$ was not different from that of healthy-appearing tissue, this could be illustrative of the Warburg effect (i.e. less reliant on oxidative metabolism and more on aerobic glycolysis), especially since the OEF was lower than in healthy-appearing WM.⁵⁶⁻⁵⁸ Moreover, we observed low OEF, CBF, $CMRO_2$ and CVR within edema regions. This is in line with previous research^{13,14} and may be reflective of the local pressure in these regions restricting the ability of vessels to dilate and thus maintain adequate perfusion. However, the extent of the edema did not correlate to either the metabolic or vascular reserve in the healthy-appearing brain tissue. This indicates that the edema volume, which is indicative of the pressure exerted on the whole-brain, does not appear to impact the overall vascular and metabolic capacities of the brain. Instead, its effects seem to be primarily localized. As the effect-sizes of these non-significant relationships were moderate to high, future research should further validate these findings in larger samples. As patients with signs of increased intracranial pressure were excluded from participation, the generalizability of these findings to the wider brain metastases population may be limited.

We observed post-radiotherapy changes within edematous regions. Notably, regions that recovered from edema three months after SRS showed increased OEF, CBF, and $CMRO_2$. Contrarily, CVR remained unchanged within these regions, with values lower than those observed in healthy-appearing tissue. These findings suggest that while these resolved edema regions show metabolic recuperation, the vascular reserve continues to be impacted. While there was a trend towards decreased OEF, $CMRO_2$, and CVR in regions with new edema post-radiotherapy, statistical significance for CVR was almost reached ($p = .078$) after removing outliers. This lack of significance may be attributed to the limited number of patients available for analysis, emphasizing the need for further investigation. Altogether, our findings suggest that CVR might be more susceptible to, and serve as a sensitive marker of edema-induced effects, warranting continued exploration in future studies.

We observed a global increase in CBF throughout the brain after SRS, while other physiological measures remained constant. Studies have shown that exposure to radiation leads to an inflammatory response in the tissue.^{59,60} The observed increase in CBF may thereby be either reflective of a restorative mechanism of the brain in response to radiation-induced inflammation or ongoing inflammation. However, as the majority of patients did not use dexamethasone three months after SRS, it is most likely indicative of a restorative mechanism. Previous studies have demonstrated that tissue exposed to a radiation dose exceeding 15 Gy suffers irreversible damage to its vasculature.¹⁷ Surprisingly, our regional analysis did not reveal differences in post-radiotherapy changes among regions exposed to low (<10 Gy), medium (10-15 Gy), or high (>15 Gy) doses. However, it is important to consider all patients in the current study received SRS, which effectively limits the radiation dose to the healthy brain tissue surrounding the tumor. This may have influenced our analysis, particularly in the high dose regions, where the number of voxels available for examination was considerably lower. In order to gain further insights, we therefore conducted regional analysis using equivalently sized ROIs (bins) that corresponded to increasing radiotherapy dose. Our analysis revealed a negative correlation between the dose and CBF, $CMRO_2$, and CVR, but not OEF. This suggests that as the radiotherapy dose increases, the impact on both the metabolic and vascular capacities become more pronounced. While voxel-wise analyses did not support the associations observed in this ROI-based analyses, regional analysis is often more precise in evaluating these association as demonstrated in previous research^{14,61}, due the inherent measurement noise associated with these physiological MRI measures. As our current analyses focused solely on linear relationships, exploring non-linear relationships, especially those seen at low radiotherapy dose, would be valuable for future research. Further investigation

is warranted regarding the potential vascular damage caused by the high fractional doses delivered during SRS, as previous studies have indicated that single fraction doses in particular may contribute to this effect.¹⁷

Importantly, the analyses highlighted substantial variations both among patients and within dose regions. Case analyses suggested that part of this heterogeneity could be attributed to tumor progression following SRS. In our case-study we examined three distinct cases with varying responses to SRS, including tumor growth, tumor shrinkage and a mixed response. In the case of new brain metastases growth, there was a deterioration in both physiological MRI parameters and cognitive function, particularly in areas near the tumor which also showed edema increases. Conversely, for the patient with tumor shrinkage, there was an improvement in physiological MRI parameters, specifically in OEF, which corresponded to positive changes in cognitive performance. In the case of a mixed response, less clear patterns emerged from the MRI and cognitive data with both improvements and declines. These results underscore the complex interplay between physiological changes, tumor response, and cognitive outcomes, highlighting the need for individualized assessment and further research in this domain.

In this research we used state-of-the-art physiological imaging techniques in a heterogeneous patient population with the goal of identifying potential challenges and opportunities for future research. Due to the sensitivity of physiological MRI measures to acquisition artifacts, stringent patient selection was implemented, yet variations in the data could still arise from measurement and calculation discrepancies. For example, the choice of ASL technique can impact perfusion maps and subsequent CMRO₂ calculations. An example is that too short post-labeling delays can lead to arterial transit artefacts or less accurate CBF measures.⁶²⁻⁶⁴ We used a multi post-labeling delay ASL pcASL sequence and found CBF values that are close to the ground truth as measured using PET. The QQ-CCTV method used in this study has been validated against the reference standard 15O-PET with a good scan-rescan reproducibility⁴⁰ and demonstrated sensitivity to detect physiological OEF change, like expected decreased OEF in hypercapnia compared to normoxia⁶⁵. Also, QQ-CCTV has demonstrated OEF abnormalities in neurologic disorders, including multiple sclerosis⁶⁶, ischemic stroke^{67,68}, brain tumor⁶⁹, dementia⁷⁰, and pre-eclampsia⁷¹, and hydrocephalus⁷².

Several limitations should be considered when interpreting the findings of this study. In creating QSM images, the precise positioning of the patients' head in the main magnetic field (B₀) is crucial for accurate dipole inversion, which becomes

challenging when scanning patients at multiple time points due to the inability to reproduce exact head positions. Thereby, subtle changes in QSM, and consequently OEF and $CMRO_2$, may be attributed to variations in head positioning. Additionally, the biophysical model used to estimate OEF is not optimized for regions with edema. Specifically, the prolonged T2 relaxation time (~200 ms) observed in these regions exceeds the maximum echo-time of the ME-GRE sequence (44.5 ms).⁷³ However, as CVR is also affected within edema regions, it is likely other autoregulatory mechanisms, including OEF, play an important role. Furthermore, an inherent limitation of using BOLD-metrics is the dependency of the BOLD response on multiple factors, including changes in cerebral blood volume, cerebral metabolic rate of oxygen consumption, arterial partial pressure of oxygen, and baseline parameters such as hematocrit, OEF, $CMRO_2$, and blood volume.^{74,75} This complex interplay hinders the identification of precise underlying mechanisms, but also underscores the value of integrating multiple physiological MRI measures. Lastly, compared to 7T scanners, the BOLD and ASL signal sensitivity, especially in WM and edema, is notably lower. Combined with the heterogeneous and small patient in this preliminary study, a lack of significant findings could partly be attributed to these factors.

CONCLUSIONS

Our findings suggest that resolved edema regions show metabolic recuperation but ongoing vascular damage, highlighting the sensitivity of CVR as a marker for vascular changes. We also observed a global increase in CBF in healthy-appearing brain regions following SRS, possibly indicating a restorative mechanism against radiation-induced inflammation. While regions exposed to higher doses exhibited larger declines in CBF, $CMRO_2$, and CVR, there was notable heterogeneity among patients and across dose regions. Case analysis demonstrated some of this heterogeneity may be attributed to the tumor response. Overall, our preliminary results suggest that within the 3-month follow-up window no radiotherapy effects on physiological parameters occurred in healthy-appearing brain tissue. Nevertheless, while SRS can lead to local control of the brain metastases it can also have long-term side-effects (i.e. months to years).^{76,77} Continued long-term research with larger patient samples allowing for meaningful grouping of patients will enhance our understanding of the intricate interplay between radiation dose, brain health, and physiological responses.

SUPPLEMENTARY MATERIALS



REFERENCES

1. Rodgers ZB, Detre JA, Wehrli FW. MRI-based methods for quantification of the cerebral metabolic rate of oxygen. *Journal of Cerebral Blood Flow and Metabolism* 2016; 36: 1165–1185.
2. Fantini S, Sassaroli A, Tgavalekos KT, et al. Cerebral blood flow and autoregulation: current measurement techniques and prospects for noninvasive optical methods. *Neurophotonics* 2016; 3: 031411.
3. Murkin JM. Cerebral autoregulation: The role of CO₂ in metabolic homeostasis. *Semin Cardiothorac Vasc Anesth* 2007; 11: 269–273.
4. Gerstenecker A, Nabors LB, Meneses K, et al. Cognition in patients with newly diagnosed brain metastasis: Profiles and implications. *J Neurooncol* 2014; 120: 179–185.
5. Achrol AS, Rennert RC, Anders C, et al. Brain metastases. *Nat Rev Dis Primers*; 5. Epub ahead of print 2019. DOI: 10.1038/s41572-018-0055-y.
6. Kienast Y, Von Baumgarten L, Fuhrmann M, et al. Real-time imaging reveals the single steps of brain metastasis formation. *Nat Med* 2010; 16: 116–122.
7. Fidler IJ, Yano S, Zhang RD, et al. The seed and soil hypothesis: Vascularisation and brain metastases. *Lancet Oncology* 2002; 3: 53–57.
8. Langley RR, Fidler IJ. The biology of brain metastasis. *Clin Chem* 2013; 59: 180–189.
9. García-Gómez P, Valiente M. Vascular co-option in brain metastasis. *Angiogenesis* 2020; 23: 3–8.
10. Eichler AF, Chung E, Kodack DP, et al. The biology of brain metastases—translation to new therapies. *Nat Rev Clin Oncol* 2011; 8: 344–356.
11. El Kamar FG, Posner JB. Brain metastases. *Semin Neurol* 2004; 24: 347–362.
12. Lammertsma AA, Wise RJS, Cox TCS, et al. Measurement of blood flow, oxygen utilisation, oxygen extraction ratio, and fractional blood volume in human brain tumours and surrounding oedematous tissue. *British Journal of Radiology* 1985; 58: 725–734.
13. Fierstra J, van Niftrik C, Piccirelli M, et al. Diffuse gliomas exhibit whole brain impaired cerebrovascular reactivity. *Magn Reson Imaging* 2018; 45: 78–83.
14. Van Grinsven EE, Guichelaar J, Philippens MEP, et al. Hemodynamic imaging parameters in brain metastases patients – Agreement between multi-delay ASL and hypercapnic BOLD. *Journal of Cerebral Blood Flow and Metabolism*; tbp. Epub ahead of print 2023. DOI: 10.1177/0271678X231196989.
15. Eichler AF, Loeffler JS. Multidisciplinary management of brain metastases. *Oncologist* 2007; 12: 884–898.
16. Brown WR, Blair RM, Moody DM, et al. Capillary loss precedes the cognitive impairment induced by fractionated whole-brain irradiation: A potential rat model of vascular dementia. *J Neurol Sci* 2007; 257: 67–71.
17. Park HJ, Griffin RJ, Hui S, et al. Radiation-induced vascular damage in tumors: Implications of vascular damage in ablative hypofractionated radiotherapy (SBRT and SRS). *Radiat Res* 2012; 177: 311–327.
18. Hou C, Gong G, Wang L, et al. The Study of Cerebral Blood Flow Variations during Brain Metastases Radiotherapy. *Oncol Res Treat* 2022; 45: 130–137.
19. Makale MT, McDonald CR, Hattangadi-Gluth JA, et al. Mechanisms of radiotherapy-associated cognitive disability in patients with brain tumours. *Nat Rev Neurol* 2017; 13: 52–64.

20. Van Grinsven EE, Nagtegaal SHJ, Verhoeff JJC, et al. The Impact of Stereotactic or Whole Brain Radiotherapy on Neurocognitive Functioning in Adult Patients with Brain Metastases: A Systematic Review and Meta-Analysis. *Oncol Res Treat* 2021; 44: 622–636.
21. World Medical Association. World Medical Association Declaration of Helsinki: ethical principles for medical research involving human subjects. *JAMA* 2013; 310: 2191–2194.
22. van Grinsven E, Cialdella F, Verhoeff J, et al. Different profiles of neurocognitive functioning in patients with brain metastases prior to brain radiotherapy. *Journal of Psycho-oncology*; Under revision.
23. Jacobson NS, Roberts LJ, Berns SB, et al. Methods for defining and determining the clinical significance of treatment effects: Description, application, and alternatives. *J Consult Clin Psychol* 1999; 67: 300–307.
24. Jacobson NS, Truax P. Clinical Significance: A Statistical Approach to Denning Meaningful Change in Psychotherapy Research. *Journal of Consulting and Clinical Psychology* 1991; 59: 12–19.
25. Jenkinson M, Beckmann CF, Behrens TE, et al. FSL. *Neuroimage* 2012; 62: 782–790.
26. Jenkinson M, Bannister P, Brady M, et al. Improved optimization for the robust and accurate linear registration and motion correction of brain images. *Neuroimage* 2002; 17: 825–841.
27. Zhang Y, Brady M, Smith S. Segmentation of brain MR images through a hidden Markov random field model and the expectation-maximization algorithm. *IEEE Trans Med Imaging* 2001; 20: 45–57.
28. Schmidt P, Gaser C, Arsic M, et al. An automated tool for detection of FLAIR-hyperintense white-matter lesions in Multiple Sclerosis. *Neuroimage* 2012; 59: 3774–3783.
29. Andersson JLR, Skare S, Ashburner J. How to correct susceptibility distortions in spin-echo echo-planar images: Application to diffusion tensor imaging. *Neuroimage* 2003; 20: 870–888.
30. Smith SM, Jenkinson M, Woolrich MW, et al. Advances in functional and structural MR image analysis and implementation as FSL. *Neuroimage* 2004; 23: S208–S219.
31. Jenkinson M, Smith SM. A global optimisation method for robust affine registration of brain images. *Med Image Anal* 2001; 5: 143–156.
32. Chan KS, Marques JP. SEPIA—Susceptibility mapping pipeline tool for phase images. *Neuroimage*; 227. Epub ahead of print 2021. DOI: 10.1016/j.neuroimage.2020.117611.
33. Liu T, Khalidov I, de Rochefort L, et al. A novel background field removal method for MRI using projection onto dipole fields (PDF). *NMR Biomed* 2011; 24: 1129–1136.
34. Liu J, Liu T, De Rochefort L, et al. Morphology enabled dipole inversion for quantitative susceptibility mapping using structural consistency between the magnitude image and the susceptibility map. *Neuroimage* 2012; 59: 2560–2568.
35. Bhogal AA. abhogal-lab/SeeVR: V2.01. 2021; (V2.01).
36. Champagne AA, Bhogal AA. Insights Into Cerebral Tissue-Specific Response to Respiratory Challenges at 7T: Evidence for Combined Blood Flow and CO₂-Mediated Effects. *Front Physiol* 2021; 12: 1–12.
37. Siero J. ClinicalASL toolbox available at <https://github.com/JSIERO/ClinicalASL>.

38. Chappell MA, Groves AR, Whitcher B, et al. Variational Bayesian inference for a nonlinear forward model. *IEEE Transactions on Signal Processing* 2009; 57: 223–236.
39. Dolui S, Wang Z, Shinohara RT, et al. Structural Correlation-based Outlier Rejection (SCORE) algorithm for arterial spin labeling time series. *Journal of Magnetic Resonance Imaging* 2017; 45: 1786–1797.
40. Cho J, Lee J, An H, et al. Cerebral oxygen extraction fraction (OEF): Comparison of challenge-free gradient echo QSM+qBOLD (QQ) with 15O PET in healthy adults. *Journal of Cerebral Blood Flow and Metabolism* 2021; 41: 1658–1668.
41. Cho J, Spincemaille P, Nguyen TD, et al. Temporal clustering, tissue composition, and total variation for mapping oxygen extraction fraction using QSM and quantitative BOLD. *Magn Reson Med* 2021; 86: 2635–2646.
42. Cho J, Kee Y, Spincemaille P, et al. Cerebral metabolic rate of oxygen (CMRO₂) mapping by combining quantitative susceptibility mapping (QSM) and quantitative blood oxygenation level-dependent imaging (qBOLD). *Magn Reson Med* 2018; 80: 1595–1604.
43. Cho J, Zhang J, Spincemaille P, et al. QQ-NET – using deep learning to solve quantitative susceptibility mapping and quantitative blood oxygen level dependent magnitude (QSM+qBOLD or QQ) based oxygen extraction fraction (OEF) mapping. *Magn Reson Med* 2022; 87: 1583–1594.
44. Hubertus S, Thomas S, Cho J, et al. Comparison of gradient echo and gradient echo sampling of spin echo sequence for the quantification of the oxygen extraction fraction from a combined quantitative susceptibility mapping and quantitative BOLD (QSM+qBOLD) approach. *Magn Reson Med* 2019; 82: 1491–1503.
45. Cho J, Zhang S, Kee Y, et al. Cluster analysis of time evolution (CAT) for quantitative susceptibility mapping (QSM) and quantitative blood oxygen level-dependent magnitude (qBOLD)-based oxygen extraction fraction (OEF) and cerebral metabolic rate of oxygen (CMRO₂) mapping. *Magn Reson Med* 2020; 83: 844–857.
46. Zhang S, Cho J, Nguyen TD, et al. Initial Experience of Challenge-Free MRI-Based Oxygen Extraction Fraction Mapping of Ischemic Stroke at Various Stages: Comparison With Perfusion and Diffusion Mapping. *Front Neurosci* 2020; 14: 1–11.
47. Bakdash JZ, Marusich LR. Repeated measures correlation. *Front Psychol* 2017; 8: 1–13.
48. RStudio Team. RStudio: Integrated Development for R.
49. Van Osch MJP, Teeuwisse WM, Van Walderveen MAA, et al. Can arterial spin labeling detect white matter perfusion signal? *Magn Reson Med* 2009; 62: 165–173.
50. Paech D, Nagel AM, Schultheiss MN, et al. Quantitative dynamic oxygen 17 MRI at 7.0 T for the cerebral oxygen metabolism in glioma. *Radiology* 2020; 295: 181–189.
51. Hyder F, Herman P, Bailey CJ, et al. Uniform distributions of glucose oxidation and oxygen extraction in gray matter of normal human brain: No evidence of regional differences of aerobic glycolysis. *Journal of Cerebral Blood Flow and Metabolism* 2015; 36: 903–916.

52. Hatazawa J, Fujita H, Kanno I, et al. Regional cerebral blood flow, blood volume, oxygen extraction fraction, and oxygen utilization rate in normal volunteers measured by the autoradiographic technique and the single breath inhalation method. *Ann Nucl Med* 1995; 9: 15–21.
53. Sebök M, van Niftrik CHB, Muscas G, et al. Hypermetabolism and impaired cerebrovascular reactivity beyond the standard MRI-identified tumor border indicate diffuse glioma extended tissue infiltration. *Neurooncol Adv* 2021; 3: 1–9.
54. Quattrocchi CC, Errante Y, Mallio CA, et al. Brain metastatic volume and white matter lesions in advanced cancer patients. *J Neurooncol* 2013; 113: 451–458.
55. Berk BA, Nagel S, Hering K, et al. White matter lesions reduce number of brain metastases in different cancers: a high-resolution MRI study. *J Neurooncol* 2016; 130: 203–209.
56. Agnihotri S, Zadeh G. Metabolic reprogramming in glioblastoma: The influence of cancer metabolism on epigenetics and unanswered questions. *Neuro Oncol* 2016; 18: 160–172.
57. Tang PLY, Méndez Romero A, Jaspers JPM, et al. The potential of advanced MR techniques for precision radiotherapy of glioblastoma. *Magnetic Resonance Materials in Physics, Biology and Medicine* 2022; 35: 127–143.
58. Feitelson MA, Arzumanyan A, Kulathinal RJ, et al. Sustained proliferation in cancer: therapeutic targets. *Seminars Cancer Biology* 2016; 35: 25–54.
59. Mehnati P, Baradaran B, Vahidian F, et al. Functional response difference between diabetic/normal cancerous patients to inflammatory cytokines and oxidative stresses after radiotherapy. *Reports of Practical Oncology and Radiotherapy* 2020; 25: 730–737.
60. Siva S, MacManus MP, Martin RF, et al. Abscopal effects of radiation therapy: A clinical review for the radiobiologist. *Cancer Lett* 2015; 356: 82–90.
61. Fan AP, Evans KC, Stout JN, et al. Regional quantification of cerebral venous oxygenation from MRI susceptibility during hypercapnia. *Neuroimage* 2015; 104: 146–155.
62. Alsop DC, Detre JA, Golay X, et al. Recommended Implementation of Arterial Spin Labeled Perfusion MRI for Clinical Applications: A consensus of the ISMRM Perfusion Study Group and the European Consortium for ASL in Dementia. *Magn Reson Med* 2015; 73: 102–116.
63. Fan AP, Guo J, Khalighi MM, et al. Long-Delay Arterial Spin Labeling Provides More Accurate Cerebral Blood Flow Measurements in Moyamoya Patients: A Simultaneous Positron Emission Tomography/MRI Study. *Stroke* 2017; 48: 2441–2449.
64. Detre JA, Rao H, Wang DJJ, et al. Applications of arterial spin labeled MRI in the brain. *Journal of Magnetic Resonance Imaging* 2012; 35: 1026–1037.
65. Cho J, Ma Y, Spincemaille P, et al. Cerebral oxygen extraction fraction (OEF): comparison of dual-gas challenge calibrated BOLD with CBF and challenge-free gradient echo QSM+qBOLD. *Magn Reson Med* 2021; 85: 953–961.
66. Cho J, Nguyen TD, Huang W, et al. Brain oxygen extraction fraction mapping in patients with multiple sclerosis. *Journal of Cerebral Blood Flow and Metabolism* 2022; 42: 338–348.
67. Zhang S, Cho J, Nguyen TD, et al. Initial Experience of Challenge-Free MRI-Based Oxygen Extraction Fraction Mapping of Ischemic Stroke at Various Stages: Comparison With Perfusion and Diffusion Mapping. *Front Neurosci* 2020; 14: 1–11.


68. Wu D, Zhou Y, Cho J, et al. The Spatiotemporal Evolution of MRI-Derived Oxygen Extraction Fraction and Perfusion in Ischemic Stroke. *Front Neurosci* 2021; 15: 1–10.
69. Shen N, Zhang S, Cho J, et al. Application of Cluster Analysis of Time Evolution for Magnetic Resonance Imaging-Derived Oxygen Extraction Fraction Mapping: A Promising Strategy for the Genetic Profile Prediction and Grading of Glioma. *Front Neurosci* 2021; 15: 1–13.
70. Chiang GC, Cho J, Dyke J, et al. Brain oxygen extraction and neural tissue susceptibility are associated with cognitive impairment in older individuals. *Journal of Neuroimaging* 2022; 32: 697–709.
71. Yang L, Cho J, Chen T, et al. Oxygen extraction fraction (OEF) assesses cerebral oxygen metabolism of deep gray matter in patients with pre-eclampsia. *Eur Radiol* 2022; 32: 6058–6069.
72. Zhuang H, Cho J, Chiang GCY, et al. Cerebral oxygen extraction fraction declines with ventricular enlargement in patients with normal pressure hydrocephalus. *Clin Imaging* 2023; 97: 22–27.
73. Hattingen E, Jurcoane A, Daneshvar K, et al. Quantitative T2 mapping of recurrent glioblastoma under bevacizumab improves monitoring for non-enhancing tumor progression and predicts overall survival. *Neuro Oncol* 2013; 15: 1395–1404.
74. Hoge RD, Atkinson J, Gill B, et al. Investigation of BOLD signal dependence on CBF and CMRO₂: The deoxyhemoglobin dilution model. *Neuroimage* 1999; 9: 849–863.
75. Petersen ET, Zimine I, Ho YCL, et al. Non-invasive measurement of perfusion: A critical review of arterial spin labelling techniques. *British Journal of Radiology* 2006; 79: 688–701.
76. Greene-Schloesser D, Robbins ME, Peiffer AM, et al. Radiation-induced brain injury: A review. *Front Oncol* 2012; 2 JUL: 1–18.
77. Katsura M, Sato J, Akahane M, et al. Recognizing radiation-induced changes in the central nervous system: Where to look and what to look for. *Radiographics* 2021; 41: 224–248.





Summary and discussion





8

Summary

Brain metastases (BMs) are a common occurrence in adult patients with cancer, affecting approximately 10-30% of patients.¹⁻³ Advances in medical treatments and imaging techniques have led to earlier detection and improved survival rates for patients with BMs, making the population of affected patients only expected to increase in the coming years.⁴⁻⁶ The focus of patient-centered treatment has shifted towards balancing prolongation of life with quality of life (QoL). One of the cornerstones of medical treatment for BMs is radiotherapy. Despite efforts to minimize radiation dose to surrounding healthy tissue, the physical limitations of the radiotherapy technique and necessary safety margins make it impossible to avoid entirely. The dose in the surrounding healthy brain tissue can lead to radiation-induced brain injury and thereby cause cognitive decline, although the exact mechanisms remain unclear.

PART I: NEUROCOGNITIVE FUNCTIONING IN PATIENTS WITH BRAIN METASTASES

The two prominent strategies for radiotherapy in BMs are stereotactic radiosurgery (SRS) and whole-brain radiotherapy (WBRT). SRS employs high-precision localized irradiation to target BMs with minimal harm to surrounding, healthy brain tissue, while WBRT ensures coverage of all brain tissue and thereby sterilizes not-yet visible BMs. A significant disadvantage of WBRT is its potential to inflict radiation-induced tissue damage throughout the brain, which makes SRS preferred option in current clinical practice whenever possible.⁷⁻¹⁰ In **Chapter 2** we compared previous literature on changes in cognitive functioning provoked by either WBRT or SRS in adult patients with non-resected BMs. Based on a systematic literature search and article screening process 20 articles reporting on 14 original datasets were analyzed. The majority of patients who underwent WBRT exhibited a consistent decline in cognitive performance from pre-radiotherapy to short-term follow-up (1-4 months), with a further decrease noted at mid-term follow-up (5-8 months). Only a subset of patients with better prognoses (e.g. those with lower pre-radiotherapy BMs volume and long-term survivors) exhibited stable or improved cognitive performance in the long-term (15 months). Conversely, approximately half of the studies revealed declined cognitive performance in patients during short-term follow-up after SRS. At both mid- and long-term follow-up studies consistently reported cognitive performance to be at pre-SRS levels. Thus, while cognitive-side effects of SRS appear to be transient, significant cognitive deterioration can occur in patients after WBRT. Thereby, the shift in treatment preference towards SRS is further substantiated by a lower risk of persistent cognitive side-effects with SRS.

The findings presented in **Chapter 2** demonstrate that cognitive deficits are prevalent in this population; in roughly one out of every two patients with BMs cognitive deficits can be observed prior to undergoing radiotherapy. Both these pre-treatment deficits and post-treatment declines were not limited to one cognitive domain, but rather span across multiple domains. Thus, in order to fully capture and comprehend the heterogeneity of cognitive functioning of this patient population, a comprehensive cognitive test battery should be used. Therefore, in **Chapter 3** subjective cognitive complaints and neurocognitive functioning of 58 patients with BMs prior to radiotherapy were extensively investigated. Additionally, the added value of an elaborate cognitive test battery versus a core test battery in identifying cognitive deficits was assessed. We used data from the ongoing prospective Cohort for patient-reported Outcomes, Imaging and trial inclusion in Metastatic BRAin disease (COIMBRA) and Assessing and Predicting Radiation Influence on Cognitive Outcome using the cerebrovascular stress Test (APRICOT) study. Both studies include adult patients (≥ 18 years) with either radiographic and/or histologic proof of BMs referred to the University Medical Center Utrecht (UMCU) for radiotherapy. Patients with BMs were able to make differentiated domain-specific judgements of their subjective cognitive functioning when using visual analogue scales (VAS). Moreover, nearly all BMs patients referred for radiotherapy experienced some degree of neurocognitive dysfunction. Both at the group and individual level, significant heterogeneity in cognitive functioning was observed, with a wide variety of cognitive domains affected. The pre-radiotherapy neurocognitive dysfunction could be clustered into four meaningful cognitive profiles, whereby the presence of memory deficits was a major determining factor. No clinical or patient characteristics were found to be related to cluster membership. Employing a 90 minute elaborate cognitive test battery was feasible in this group of cognitively vulnerable patients. When solely using the core battery, the extent of cognitive deficits may be underestimated, demonstrating the value of elaborate testing.

In **Chapter 4** we continued the investigation of neurocognitive dysfunction in patients with BMs at both the short (3 months) and long-term (≥ 11 months) after radiotherapy. Our focus was not solely on objective cognitive deficits, but also included an examination of subjective cognitive functioning. Reliable change indices were used to assess clinically meaningful individual changes. From the COIMBRA and APRICOT study, 36 patients completed short-term follow-up and 14 patients long-term. A considerable number of patients (50%) self-reported cognitive decline in at least one domain, commonly affecting memory and attention. Subjective cognitive decline was more commonly observed in patients with intracranial disease progression within three months post-radiotherapy. Almost all patients suffered from cognitive

impairment in at least one domain at three months post-radiotherapy. Memory was particularly susceptible, as demonstrated both by patients with cognitive deficits and those who experienced a general decline in cognitive performance at short-term follow-up. In the long-term, slowing of processing and psychomotor speed was most prominent. A decline in objective cognitive performance was observed in 97% of patients three months post-radiotherapy. Interestingly, 81% of these patients experienced concurrent improvement in a different cognitive domain. This pattern of both deterioration and improvement persisted in the long-term. No clear risk factors were identified for cognitive decline post-radiotherapy.

PART II: USING IMAGING TECHNIQUES TO UNDERSTAND NEUROCOGNITIVE FUNCTIONING

The presence of within-individual cognitive variation, coupled with the absence of clear risk factors (**Chapter 3** and **4**), suggests a need for further investigation of the underlying mechanisms of cognitive performance in patients with BMs. The location of the BMs in the brain may be a contributing factor to the observed variation. However, lesion-symptom mapping (LSM) studies in the BMs population are complicated by numerous factors, while the generalizability of previous LSM results from other populations remains unclear. **Chapter 5** compared LSM results from patients with ischemic stroke and primary brain tumors. Even with large sample sizes (196 tumor and 147 stroke patients), the limited degree of lesion overlap between stroke and primary brain tumor patients hindered comparison. In brain areas *with* adequate lesion overlap, considerable differences between stroke and tumor patients were found regarding the regions associated with either verbal memory or verbal fluency performance. This confirms that the etiology of focal damage in the brain influences the cognitive consequences of this lesion. Thus, caution is required when generalizing brain-behavior associations from one patient population to another.

In **Chapter 6** we compared physiological imaging parameters derived from either hypercapnic blood oxygenation level-dependent (BOLD) or arterial spin labeling (ASL) imaging in 14 patients with BMs from the APRICOT study prior to radiotherapy. The study focused on cerebrovascular reactivity (CVR), hemodynamic lag, cerebral blood flow (CBF), and arterial arrival time (AAT). There was a positive correlation between BOLD and ASL parameters, whereby areas with higher CVR exhibited higher perfusion and longer hemodynamic lag was found in regions with prolonged AAT. However, these associations were observed only in areas with sufficient vascular reserve capacity. Thus, the relationship between these physiological BOLD and ASL

parameters is dependent on the vascular status of the underlying tissue. Metrics related to CVR exhibited potential to identify vascular risk in tissue prior to visible perfusion deficits on ASL MRI.

Chapter 7 evaluated the impact of radiotherapy on both metabolic and vascular reserve in patients with BMs by assessing CBF, oxygen extraction fraction (OEF), cerebral metabolic rate of oxygen (CMRO₂), and CVR before and three months after radiotherapy in nine APRICOT-patients. Whole-brain CBF increased after radiotherapy, potentially reflecting restorative mechanisms against radiation-induced brain inflammation. Ongoing vascular damage was observed alongside metabolic recuperation in regions with resolved edema. Regional analysis revealed that CBF, CMRO₂, and CVR deteriorated in a dose-dependent manner, with larger deteriorations in regions exposed to higher doses. However, notable patient and dose region heterogeneity was observed, especially at low doses. Case analysis suggests some of the heterogeneity may be linked to tumor response. Though caution must be taken due to the study's preliminary nature and case-analysis, results suggest no substantial radiotherapy-induced brain damage within the three months after treatment, but instead highlight the parameters' possible susceptibility to identify both restoration of or ongoing metabolic or vascular damage following radiotherapy.

REFERENCES

1. Barnholtz-Sloan JS, Yu C, Sloan AE, et al. A nomogram for individualized estimation of survival among patients with brain metastasis. *Neuro Oncol* 2012; 14: 910–918.
2. Achrol AS, Rennert RC, Anders C, et al. Brain metastases. *Nat Rev Dis Primers*; 5. Epub ahead of print 2019. DOI: 10.1038/s41572-018-0055-y.
3. Barnholtz-Sloan JS, Sloan AE, Davis FG, et al. Incidence proportions of brain metastases in patients diagnosed (1973 to 2001) in the Metropolitan Detroit Cancer Surveillance System. *Journal of Clinical Oncology* 2004; 22: 2865–2872.
4. Nieder C, Spanne O, Mehta MP, et al. Presentation, patterns of care, and survival in patients with brain metastases: What has changed in the last 20 years? *Cancer* 2011; 117: 2505–2512.
5. Lanier CM, Hughes R, Ahmed T, et al. Immunotherapy is associated with improved survival and decreased neurologic death after SRS for brain metastases from lung and melanoma primaries. *Neurooncol Pract* 2019; 6: 402–409.
6. Nayak L, Lee EQ, Wen PY. Epidemiology of brain metastases. *Curr Oncol Rep* 2012; 14: 48–54.
7. Tsao MN, Rades D, Wirth A, et al. Radiotherapeutic and surgical management for newly diagnosed brain metastasis(es): An American Society for Radiation Oncology evidence-based guideline. *Pract Radiat Oncol* 2012; 2: 210–225.
8. Pinkham MB, Whitfield GA, Brada M. New developments in intracranial stereotactic radiotherapy for metastases. *Clin Oncol* 2015; 27: 316–323.
9. Yamamoto M, Serizawa T, Shuto T, et al. Stereotactic radiosurgery for patients with multiple brain metastases (JLGK0901): A multi-institutional prospective observational study. *Lancet Oncol* 2014; 15: 387–395.
10. Soliman H, Das S, Larson DA, et al. Stereotactic radiosurgery (SRS) in the modern management of patients with brain metastases. *Oncotarget* 2016; 7: 12318–12330.





9

General Discussion

Development in cancer healthcare has progressed immensely in the last decades, leading to improved survival rates and earlier detection of brain metastases (BMs).¹⁻³ Consequently, the growing population of patients with BMs now survives longer after treatment. This has prompted an increased focus on psychosocial outcomes associated with cancer and cancer treatments. While stereotactic radiosurgery (SRS) is an effective treatment for BMs, there is currently insufficient understanding of its effects on the adjacent healthy brain tissue and resulting cognitive impairment of patients. This paucity of knowledge subsequently limits physicians in their ability to provide patients and their caregivers with clear expectation-management when confronted with the diagnosis and available treatment options. Therefore, the ultimate goal of research is to pinpoint, predict and eventually prevent treatment-related side-effects for optimal patient care.

Patients with BMs inherently present a heterogeneous patient population with diverse medical histories. This calls for an individualized approach. Not only in healthcare management, but in research as well. With the advancements in modern medicine, including faster computers and advanced algorithms, it is now possible to tailor treatments to the specific needs of each patient. At the same time, this ever-evolving healthcare landscape necessitates a constant recalibration of research methodologies. To illustrate, at the outset of this research endeavor the most recent survival data for this patient group indicated a median survival of approximately 7 months.^{4,5} Interestingly, our observations within the COIMBRA cohort have unveiled a more intricate scenario, with median survival spanning between 12 and 33 months, depending upon the primary tumor type [SNO poster, data not shown]. This illustrates the dynamic nature of healthcare and the contextual backdrop against which our investigation unfolded. The purpose of this thesis was to set the initial steps towards investigating radiation-induced brain injury through a multidisciplinary approach, which involved the simultaneous exploration of neurocognitive functioning and potential MRI-biomarkers to provide an integrative and comprehensive view. Consequently, the forthcoming discussion will center on the convergent challenges, both patient and research-related, and the opportunities encountered over the course of this research (**Figure 1**).

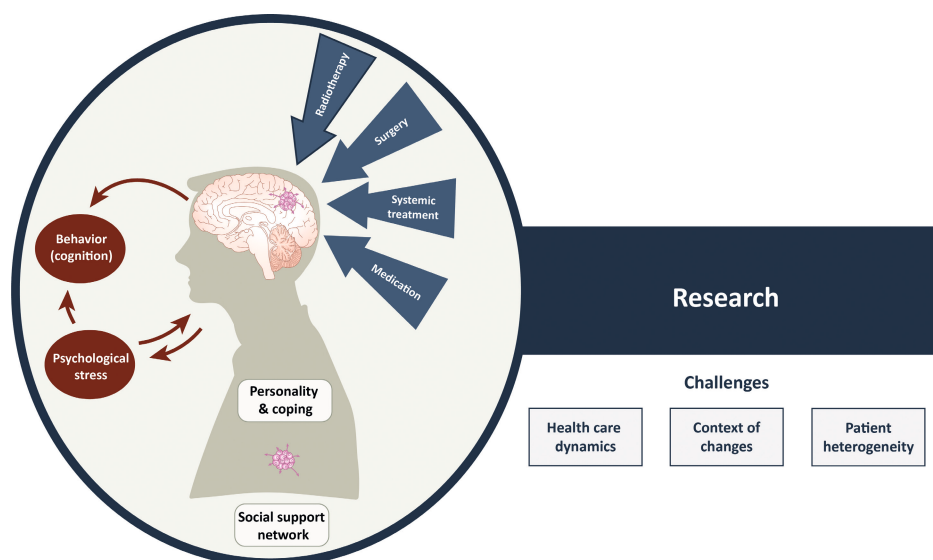


Figure 1. Illustration showcasing the various challenges encountered in studying patients with BMs, including both patient-related and research-related obstacles.

PATIENT-RELATED CHALLENGES

Multifaceted treatment approaches

The focus of the research presented in this thesis was on evaluating the effects of radiotherapy treatment. It is important to consider that treatment of patients with BMs most often requires a multifaceted treatment approach. While radiotherapy is the cornerstone of the medical treatment specifically for the BMs, the primary tumor and sometimes extracranial metastases often require additional systemic treatment and radiotherapy. Most patients with BMs (re)initialize systemic treatment in the weeks following brain radiotherapy, which can include chemotherapy, immunotherapy and targeted therapy or a combination. The significance of systemic treatments for patients with BMs is now underscored by the growing evidence that some systemic treatments also show intracranial efficacy, at least for patient with breast cancer, lung cancer or melanoma.⁶⁻⁸ It has become increasingly difficult to isolate the effect of a single factor, like radiotherapy, in observational studies where patients undergo a variety of treatment at different time points.

Unfortunately, all these anti-cancer treatments can negatively impact cognitive functioning of patients.⁹⁻¹² Cancer-related cognitive impairment is an increasingly recognized phenomena in patients with tumors outside the central nervous system¹², and equally affects patients with BMs undergoing systemic treatment.

Large-scale studies have additionally shown premature brain aging and reduced gray matter volume in specific brain regions in patients with breast cancer who received chemotherapy.¹³ Similar accelerated brain aging has been observed after radiotherapy in patients with gliomas.¹⁴ This highlights the difficulty in interpreting post-radiotherapy brain changes and disentangling the exact contributions of one treatment. Thereby, the results presented in this thesis should be interpreted within the broader context of treatment-related side-effects in patients with BMs.

Additionally, the post-radiotherapy changes presented in this thesis should be considered in light of the trade-off between cognitive difficulties and survival benefits after treatment. It is unclear what the cognitive trajectory would be of patients who do not receive radiotherapy. At the same time, research has shown that median survival is only two months for lung cancer patients with BMs who do not receive any treatment.¹⁵ Ideally, observational research in patients with BMs should include all patients, regardless of treatment choices. However, due to the multidisciplinary nature of BMs' diagnosis, such a study can prove logistically complicated. In particular, locating patients who are not (yet) receiving radiation therapy can be challenging, as they may be under the care of a variety of medical specialties. Large national databases, such as those offered by the Integraal Kankercentrum Nederland (IKNL), possess the potential to facilitate such large-scale studies through their extensive data. However, BMs are not recorded as a distinct entity within the IKNL database. While information regarding the occurrence of BMs is documented on a per-primary cancer basis, there is a lack of comprehensive data on the overall BMs population, including details regarding treatment modalities and survival outcomes specific to this population. Consequently, the utilization of these databases for studying the BMs population becomes challenging. As such, large observational studies on BMs patients encompassing a diverse range of individuals are essential to either allow correction for treatment factors using statistical modeling or the possibility to create subgroups of adequate size for meaningful comparisons. This would allow researchers to piece together the intricacies of treatment-related changes in this patient population.

An alternative option would be to create identical cohort studies including patients with primary tumors that commonly metastasize to the brain, such as breast, lung, and melanoma.¹⁶ The radiotherapy department at the University Medical Center Utrecht (UMCU) has made significant progress in creating extensive patient cohorts in various cancer populations, like the UMBRELLA cohort for breast cancer patients¹⁷ and the U-COLOR cohort for lung cancer patients (NCT05069792)¹⁸. However, these cohorts mainly focus on the medical aspects and quality of life (QoL) of patients,

but do not include specific measures of cognitive functioning. While some other research groups have investigated these populations, cross-study comparisons are hampered by differences in methodological set-up and limited reported data as we observed in **Chapter 2**. Performing identical neurocognitive assessments (NCA) and brain imaging at similar follow-up intervals in cohort studies in these patient populations could be a valuable, yet realistic avenue to further elucidate cancer treatment-related side-effects in patients with BMs. In the first place, the implementation of such long-term cohort studies would provide the chance to capture and evaluate all patients who eventually develop BMs, irrespective of subsequent treatment choices. Moreover, this approach would facilitate insights into the cognitive trajectory of patients with BMs prior to initializing brain radiotherapy. Lastly, it would provide an opportunity to assess the validity and generalizability of cognitive clusters, like those identified in **Chapter 3**, across different patient populations and/or after different treatment regimens.

Various influences on behavior

Countless factors influence neurocognitive functioning in patients with BMs. Thereby the most obvious influence is of course the BMs themselves. The brain can be topologically organized with respect to brain function, whereby lesions in two different locations each have a different effect on subsequent behavior.¹⁹ This probably partly explains the different cognitive profiles that we found in patients with BMs before starting radiotherapy in **Chapter 3**. That is, BMs within the memory network may specifically cause memory problems, while a BMs in the language network may specifically cause language problems. In **Chapter 6** we additionally found out that on top of this, the etiology causing the lesions influences resulting behavior, highlighting the importance of population-specific research.

The influence of systemic treatment on neurocognitive functioning has received more and more attention over the last years. However, it is less well-known that both cognitive and affective disorders are already prevalent in patients with non-central nervous system tumors before starting systemic treatment.²⁰ This indicates that the presence of a primary tumor already exerts an influence on the brain leading to cognitive deficits. On top of that, the psychological distress associated with a cancer diagnosis and treatment has been found to have a detrimental effect on cognition. For example, in patients with BMs who received whole-brain radiotherapy (WBRT), increased psychological distress after WBRT was related to decreased cognitive performance and decreased QoL.²¹ Research has even demonstrated a relationship between stress and structural changes in various brain regions.^{20,22} Together, this illustrates it is crucial for researchers to consider the broader context in which

their studies are conducted and the realization that multifaceted problems ask for a multifaceted research approach. This will eventually aid in deepening the understanding of the research results. For instance, all patients who performed the NCA in our studies also had to indicate their current experienced stress levels. In **Chapter 3** we observed relatively low mean stress levels on the group level, but at the same time found substantial variations at the individual level. The majority of patients primarily attributed their stress to the uncertainties associated with their cancer diagnosis and upcoming treatment. When evaluating the pre-radiotherapy cognitive performance, the addition of a stress measurement provided us with the insight that the observed variety in cognitive functioning was not related to differences in experienced stress levels. Nevertheless, it is worth noting that experienced stress could potentially exert a notable impact on subjective cognitive functioning and QoL, which present intriguing avenues for future investigation.

Subjective patient experiences

When evaluating treatment-related side-effects, it is important to not only capture objectively measured changes, but also include subjective patient experiences. Especially since the goal of treatment is to maintain or even improve a patients' QoL. The difficulty with assessing patient experiences, is that they are a relative and dynamic multidimensional concept influenced by multiple factors like psychosocial aspects (e.g. personality and coping style)²³⁻²⁷, personal expectations²⁸ and the availability of a social support network²⁹. It is challenging to find subjective measures that do justice to the complexity of individuals' experiences. For example, we found that overall patients rated their own cognitive functioning as high when using the Cognitive Failure Questionnaire (CFQ). However, when those same patients were asked to rate their cognitive functioning on different cognitive domains relative to their pre-cancer cognitive functioning using visual analogue scales (VAS), a different picture emerged where patients reported multiple cognitive complaints [Student project, data not shown]. As illustrated in both **Chapter 3** and **4**, these VAS allowed patients to make a differentiated judgment regarding their subjective cognitive functioning and subsequent changes in their subjective cognitive functioning. It could be speculated that VAS as part of a semi-structured interview provides more room for patients to elaborate on their cognitive functioning and thereby fit with their individual experiences, especially when compared to confining cognitive functioning to a restricted set of questions like in the CFQ. In a study on fatigue in patients with rheumatoid arthritis, a single-item VAS even outperformed four longer fatigue questionnaires in terms of sensitivity to change and showed a good correlation with clinical variables.³⁰ This underscores the effectiveness of a VAS as a suitable tool for use in both routine clinical practice and research. Moreover, a VAS

is easy and straightforward to implement in digital tools, making it a practical and efficient method for assessing patients' unique experiences regarding subjective cognitive functioning.

A potential next step in the assessment of subjective patient experiences is to conduct qualitative research, such as (semi-)structured interviews, with patients with BMs. This approach would allow for a more comprehensive exploration of topics that hold significance for them. Currently, only one qualitative study has been conducted to assess treatment expectations in patients with BMs from lung cancer planned to undergo WBRT.³¹ However, given the evolving healthcare landscape and the significant changes in treatment options over the years, it would be highly valuable to conduct qualitative research in a larger cohort of patients with BMs and their caregivers who are planned for SRS. Findings from such qualitative studies could subsequently guide future research into treatment-related side-effects to incorporate these patient-identified factors. Another approach could involve a stepwise qualitative research process. This process aims to determine if existing outcome measures adequately capture the most significant difficulties for patients with BMs. For example, a recent study assessed whether a specific QoL questionnaire captured the most important side-effects as experienced by patients with BMs from lung cancer.³² Ultimately, this can lead to improved alignment between research outcomes and the outcomes of interest to patients and their caregivers. Conclusively, understanding patients' values regarding treatment and their personal goals can help clinicians discuss these issues with patients and provide appropriate information and can aid selection of appropriate outcome measures for research.

It is notoriously difficult to find a good correlation between objective and subjective measures of cognitive performance.^{33,34} The same was observed in our patient sample in **Chapter 3** and **4** where the specific cognitive domains for which patients reported subjective cognitive problems did not completely align with the objectively identified cognitive difficulties in the same sample. However, in **Chapter 4**, we did observe consistency between the number of patients reporting subjective cognitive decline and those demonstrating objective cognitive decline. Patients may have reported subjective difficulties in attention, while these were objectively reflected by worse memory performance. This emphasizes that although patients may use different labels to describe their cognitive performance, they do notice these cognitive changes in their daily lives following cranial radiotherapy. Thus, while we cannot rely on the exact content of cognitive complaints, the mere presence of cognitive complaints or changes in complaints do hold considerable significance.

These findings also highlight an important opportunity for healthcare. That is, patients with BMs may benefit from an elaborate NCA three to four months after radiotherapy, which could provide them with insights into their individual cognitive strengths and weaknesses. Such assessments could help patients and their caregivers understand their cognitive abilities, which in itself could be of great value. Moreover, these individual cognitive profiles could potentially identify specific avenues for cognitive rehabilitation (e.g. memory strategy training), ultimately improving the QoL for these patients.

RESEARCH CHALLENGES

Dynamics of healthcare

As illustrated above, the complexities of the BMs population necessitate careful consideration of multiple factors and influences in research. This research is subsequently conducted within the ever-evolving context of contemporary healthcare. A perfect example of this is the shift in treatment preference from WBRT to SRS, where (Dutch) guidelines advise up to 10 BMs to be treated with SRS.³⁵⁻³⁸ However, unlike WBRT, SRS lacks the ability to sterilize not-yet visible BMS. This has likely led to the increase in retreatments with SRS whereby patients return for subsequent courses of SRS for new BMs in different locations. In 2018 retreatment constituted 12.5% of SRS treatment, which increased to approximately 33% in 2022 in the UMC Utrecht. A wealth of research has demonstrated the feasibility, tolerability and efficacy of multiple courses of SRS for recurrent BMs,^{e.g. 39-44} This research shows that while rates of radiation necrosis are significant, repeated SRS may be indicated for a selected group of patients with local disease recurrence. Consequently, repeated SRS may serve as a means to delay or even avoid WBRT, which would align with the favorable cognitive outcomes after SRS compared to WBRT (**Chapter 2**). However, the impact of these multiple rounds of treatment on the brain in the long-term requires further exploration. It is plausible to speculate that there exists a threshold for brain damage that can be sustained from SRS beyond which clinical manifestations arise, akin to the concept of brain reserve.⁴⁵ This may also explain the absence of apparent changes in vascular or metabolic reserve capacity in patients with BMs after one round of SRS (**Chapter 7**). Future research endeavors should investigate whether the notion of brain reserve extends to repeated rounds of SRS.

Understanding the context of changes

An important part of this thesis has centered around identifying and understanding changes in either cognitive functioning or brain physiology after radiotherapy. To

understand post-treatment changes, it is important to understand the context in which these changes occur. Specifically, it is important to determine whether the observed changes in patients differ from what would be expected in healthy individuals. For assessing change in cognitive test score a reliable change index (RCI) is commonly used.^{46,47} The RCI provides a statistical framework to evaluate the significance of changes in individual scores over time, distinguishing reliable changes from those due to chance, practice effects or measurement error alone. Especially practice effects are a common problem in neuropsychological research, which occur when individuals perform better on a test the second time than individuals who perform the test for the first time. By using normative test-retest data from a control population, an RCI eliminates the need for a control group. However, the RCI calculation is also dependent on the availability of normative data. As I observed calculating RCI's in **Chapter 4**, this normative data is often limited or completely lacking, which consequently limits the possibility of using more sophisticated RCI calculations. Additionally, finding a norm population that matches one's own sample and research setup (e.g., age, test-retest interval) can be challenging.

The investigation of physiological brain changes is confronted with similar challenges. Previous research in healthy subjects indicated that assessing cerebrovascular reactivity (CVR) using a computer-controlled gas system during Blood Oxygenation Level Dependent (BOLD) imaging exhibits good reproducibility.⁴⁸ However, to enhance the ability to detect subtle changes specific to treatment effects (e.g. radiotherapy), such as those observed in **Chapter 7**, it is important to account for natural variation and, again, control for confounding factors (e.g. age). Unfortunately, due to practical constraints, ethical considerations and limited resources a control population is often not included. This while the absence of a control group can limit the ability to draw definitive conclusions. For specific research questions large data repositories like the UK biobank can provide solutions, but ideally research, especially that evaluating treatment effects, should include a matched control population to be sensitive to and better understand the treatment-specific changes. In research grant proposals, allocating budget for control measurements can pose a financial challenge, especially when these costs need to be accommodated in addition to the expenses already incurred for patient data collection and researcher salaries. Consequently, the inclusion of a control population is frequently neglected due to limited available research funding, underscoring the undervaluation of control participants in research. However, a potential solution to this challenge may lie in the combination of control groups across multiple studies, enabling the simultaneous collection of diverse data types. This approach not only offers cost-saving benefits but also presents ethical advantages.

Heterogeneity of patients with brain metastases

Patients with BMs present a heterogeneous group of patients as illustrated by the diverse range of medical histories of patients. This heterogeneity was also reflected in both the cognitive functioning (**Chapter 3** and **4**) and the physiological MRI parameters (**Chapter 6** and **7**). For example, cognitive impairments and post-radiotherapy cognitive decline in the BMs population were not confined to one cognitive domain, but rather spanned the whole range of cognitive domains (**Chapter 3** and **4**). This heterogeneity poses a challenge for research, as we must devise methods to capture and comprehend all the variations.

Capturing the cognitive heterogeneity

Even though patients with BMs pose a vulnerable population, I have shown that a 90-minute comprehensive NCA is feasible in most patients willing to participate in research (**Chapter 3**). Besides its feasibility, this test battery was more adept to provide insights into the extent of cognitive impairment in patients with BMs before radiotherapy. As it remains important to accurately identify cognitive changes, an important avenue for future research is to establish a test battery that is sensitive to these changes, elaborate enough to identify changes across the various cognitive domains, yet as short and efficient as possible. Especially in the context of understanding cognitive changes by investigating a multitude of MRI biomarkers, like I did in **Chapter 7**, utilization of a standardized, yet elaborate cognitive test battery may prove to be the most appropriate approach. One can for example imagine that the Hopkins verbal learning test revised (HVLT-R), which provides measure on immediate recall, learning, delayed recall, recognition as well as response bias, may be a simple yet effective way to capture the multiple aspects of memory functioning with one cognitive test. Another possibility would be to use computerized/online cognitive testing, like the Amsterdam Cognition Scan.⁴⁹ The Amsterdam Cognition Scan has the ability to capture multiple different variables, like response speed and accuracy, at the same time making it an efficient tool for cognitive testing in a heterogeneous patient population. Consistency in methodologies across studies would be beneficial as it would enable the validation of preliminary findings, like those in **Chapter 7**, within larger multi-center studies.

While the International Cancer and Cognition Task Force ICCTF has made an important step in harmonizing the cognitive tests performed in cancer research and advises against the use of screening tests like the Mini-Mental State Examination (MMSE) or Montreal Cognitive Assessment (MOCA) in cancer research⁵⁰, continuous evaluation is warranted. Even though not one cognitive test battery can do justice to the complex interplay of cognitive functions, I firmly believe a test battery aimed

to assess cognitive functioning in a heterogeneous population, should aim to encompass the entire spectrum of potential cognitive disorders. An example is the cognitive domain of social cognition. Social cognition encompasses the cognitive processes involved in the perception, interpretation and understanding of social information. In patients with traumatic brain injury, impairment of social cognition has shown to negatively impact patient QoL and was associated with higher caregiver burden.⁵¹ While highly relevant for daily functioning, social cognition has long been overlooked in both research and clinical practice.⁵² The limited available research in patients with intracranial tumors suggest impairments in social cognition, specifically emotion recognition, occur in a substantial proportion of patients with primary brain tumors^{53,54}, especially when tumors were located in proximity of the insula and anterior temporal lobe^{54,55}. I observed emotion recognition impairment in almost one third of patients with BMs already prior to radiotherapy (**Chapter 3**). This stresses the importance of the incorporation of at least one social cognition measure in routine NCA in both clinical practice and research.

Brain heterogeneity

Cognitive deterioration after cranial radiotherapy cannot yet be predicted at an individual level, and the underlying mechanisms for this so-called radiation-induced cognitive decline are still not fully comprehended. Previous research has illustrated post-radiotherapy changes in white matter microstructure⁵⁶⁻⁶³, as well as in functional brain networks⁶⁴⁻⁶⁸. These changes bear similarities to age-related cognitive decline in healthy individuals, which is associated with structural shrinkage, white matter lesions, and altered functional connectivity.⁶⁹⁻⁷⁴ Notably, a recent study demonstrated that patients with gliomas who underwent radiotherapy exhibited brain tissue atrophy at a rate approximately three times faster than normal aging.¹⁴ In healthy individuals, age-related brain changes extend to changes in hemodynamics. For example, age-related changes in hemodynamics, including reduced whole-brain oxygen metabolism and lower CVR, have been observed in healthy individuals.^{75,76} Moreover, some studies have indicated a relationship between age-related CVR changes and cognitive changes in healthy individuals.^{77,78} Consequently, investigating hemodynamic changes following cranial radiotherapy could offer valuable insights into the mechanisms underlying radiation-induced cognitive decline.

The brain relies on a steady supply of oxygen and glucose for proper functioning, which are delivered through arterial blood. To guarantee healthy functioning, cerebral blood flow (CBF) to the brain must remain relatively constant in response to changes in perfusion pressure or other hemodynamic events. The cerebral

autoregulation system ensures adequate supply of oxygen and nutrients to the brain.^{79,80} CVR is a crucial component of cerebral autoregulation, since it facilitates regulation of CBF by either dilation or constriction of arterial control vessels.⁸¹⁻⁸³ In cases where blood flow compensation is inadequate to meet the metabolic demands of brain tissue (e.g. when dilatory reserve is pathologically exhausted), higher oxygen extraction from the blood, as measured through the oxygen extraction fraction (OEF), serves as an additional regulatory mechanism to maintain oxygen delivery to the tissue. This delicate balance between CBF and OEF supports a consistent cerebral metabolic rate of oxygen (CMRO₂) consumption.⁸⁴ Thus, while CVR can provide information on the vascular reserve capacity, OEF can help gain insight into the metabolic reserve capacity of the brain.

As illustrated above, the brain's reserve capacity is dependent on a balance of both metabolic and vascular factors. This underscores that focusing on solely one of these factors will provide an incomplete picture as each factor provides a separate piece of the puzzle. This was corroborated by the research presented in **Chapter 6**. Thus, the pathophysiology underlying radiation-induced cognitive decline most likely also reflects this multifactorial nature. So far, cerebral hemodynamics have only rarely been investigated in patients with brain tumors. Most of this work has focused on using the hemodynamic status of the BMs to predict their response after radiotherapy.⁸⁵ In the case of gliomas, impaired CVR has been observed both within the glioma tissue itself⁸⁶ and in the whole brain.⁸⁶ Therefore, it has been speculated that whole-brain CVR could potentially serve as an indicator of antitumor treatment efficacy. However, the relationship between hemodynamic changes and cognitive functioning after cranial radiotherapy, remains to be elucidated. In **Chapter 7** I therefore investigated different physiological measures using MRI both before and three months after SRS. In this preliminary analysis, a wide variety of post-radiotherapy changes was observed in both healthy-appearing brain tissue and edematous tissue surrounding the BMs, highlighting the sensitivity of these physiological MRI measures. Moreover, some of these changes seemed related to the received radiotherapy dose and post-radiotherapy cognitive changes, requiring further exploration in larger patient samples. However, in order to comprehensively evaluate the effects of SRS, it is imperative to take into account the temporal aspect of these effects. Given that SRS has been associated with a range of long-term side-effects that can persist for months to several years, the three-months' time window used in the APRICOT study may not have been sufficient to capture the entirety of post-radiotherapy changes. Therefore, it would be advised to extend the observation period beyond three months to encompass potential long-term effects as well.

In **Chapter 6**, our study highlighted the distinction between CBF acquired during Arterial Spin Labeling (ASL) MRI and BOLD-CVR, indicating that they do not convey identical information. Consequently, relying solely on ASL may not be sufficient to comprehensively evaluate subtle post-radiotherapy vascular changes. However, the clinical implementation of BOLD-CVR, particularly with the use of a sequential gas delivery system like that used in the APRICOT study, may encounter limitations due to its restricted availability in hospitals. To enhance clinical applicability, it would be valuable to investigate whether breath holds or resting state CVR can offer similar insights into CVR. Both are less invasive and more feasible techniques in clinical settings, but may not be able to convey the dynamic and rapid changes in CVR. Although some studies in healthy controls have shown the robustness and repeatability of breath holds in healthy volunteers⁸⁷⁻⁸⁹, a comprehensive study in BMs patients is yet to be conducted. Expanding the investigation to include this patient group would further enrich our understanding of the potential utility of BHs as a surrogate marker for assessing post-radiotherapy changes.

BOLD-CVR measurements, like those used in **Chapter 6** and **7**, have been widely used to assess the ability of blood vessels to dilate in response to a hemodynamic stimulus.⁹⁰ It is important to acknowledge that this technique provides an indirect measure of the CVR response. That is, active dilation predominantly occurs in arteries, while veins passively dilate in response to increased blood volume. However, the BOLD response primarily reflects changes in blood oxygenation in veins. In contrast, Vascular-Space-Occupancy (VASO) fMRI can detect changes in arterial cerebral blood volume (aCBV), making it a possible valuable alternative for directly assessing CVR.⁹¹ A recent study illustrated the potential value of VASO fMRI in assessing autoregulatory aCBV and CBF compensation strategies in patients with steno-occlusive disease.⁹² However, VASO fMRI has lower signal-to-noise ratio compared to BOLD fMRI and limited availability due to specific imaging requirements constraining its widespread adoption and clinical application.⁹¹

Another area of interest for future research on vascular and metabolic changes is the capillary transit time, or more specifically capillary transit-time heterogeneity (CTH). In healthy individuals, cerebral perfusion demonstrates a homogenous distribution of capillary transit times. A high CTH indicates a combination of capillaries with low blood flows and long transit times, as well as capillaries with high flows and short transit times. Not only does the low perfusion in some capillaries negatively affect the oxygen delivery to the tissue, but the short transit times in other capillaries also allow less time for oxygen to diffuse into the surrounding tissue, thereby reducing the oxygen extraction fraction.^{93,94} Thereby, a high CTH could decrease the oxygen

availability to the brain tissue, which then could reach a level below the metabolic requirements.⁹⁵ Previous research has shown that patients with steno-occlusive disease who had impaired CVR and elevated CTH indeed had a significant reduction in CMRO₂.⁹⁴ Thus, CTH could aid in understanding the underlying mechanisms for reduced CMRO₂. Thereby, examining CTH can provide additional insights into the relationship between cerebral hemodynamics and cognitive changes following cranial radiotherapy.

Ideally, all research should simultaneously investigate multiple physiological MRI measures. Especially since we know that due to the cerebral autoregulatory processes in the brain, one of these measures may be affected, but then balanced out by another factor. For example, if CBF can no longer increase due to maximized CVR, the OEF of the tissue can increase in order to still maintain adequate supply of oxygen to the underlying tissue. Thereby, radiation-related changes in hemodynamics may only manifest into cognitive decline when the autoregulatory process starts to fail, similar to the brain reserve theory mentioned previously (**Figure 2**).⁴⁵ To investigate this, we could draw parallels from the cluster method I used in **Chapter 3** to identify meaningful subgroups of patients among a heterogeneous pattern of cognitive functioning. Cluster analysis of multiple physiological MRI-measures has the potential to uncover the combined effects of various vascular and metabolic post-radiotherapy changes. Moreover, using this cluster analysis, specific sub-types could be identified which may be related to specific cognitive profiles. Considering the multifaceted nature of radiation-induced cognitive decline, within this cluster framework you can extend beyond physiological MRI measures. Additional valuable MRI biomarkers include changes in white matter microstructure⁵⁶⁻⁶³ and functional brain networks⁶⁴⁻⁶⁸, as demonstrated in previous research. This approach would be in line with the aim of understanding the complex interplay between factors underlying radiation-induced cognitive decline.

Moreover, different brain regions may have varying thresholds, with certain areas, such as the hippocampus, being particularly vulnerable for radiation-damage. In accordance with this notion, the hippocampus is frequently excluded from WBRT in order to mitigate potential adverse effects on cognitive functioning.^{96,97} Recent research has also demonstrated that radiotherapy dose on the neurogenic niches is associated with poorer overall survival in patients with lung cancer BMs.⁹⁸ As age-related decrease in adult neurogenesis have been linked to cognitive performance⁹⁹, radiotherapy-related damage to these neurogenic niches may also be linked to radiation-induced cognitive decline. Future research endeavors should investigate whether distinct brain regions, such as cortical grey matter, white matter and

neurogenic niches, indeed exhibit different thresholds for radiation-induced brain damage.

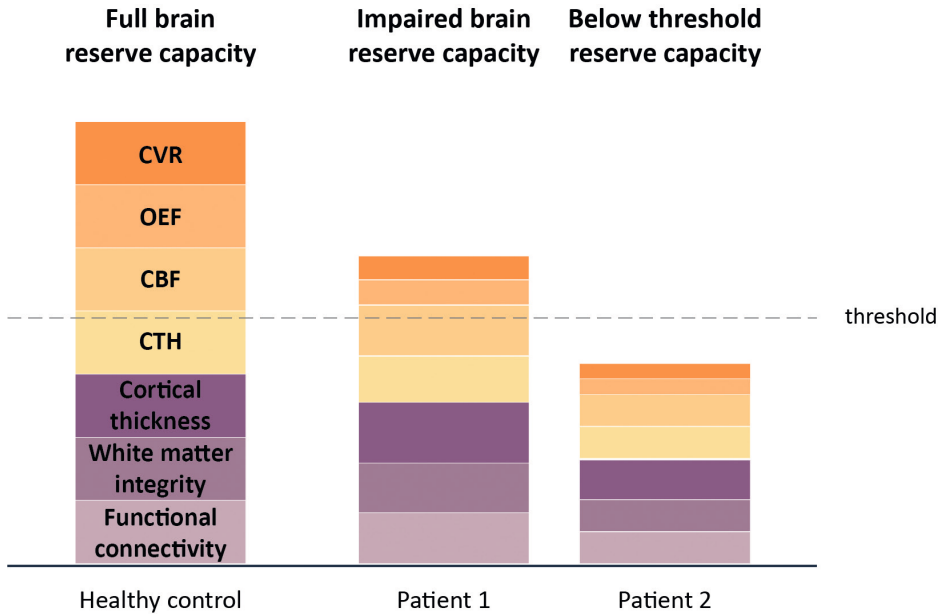


Figure 2. Illustration of how the brain reserve capacity could be buildup of multiple different factors. Depending on the change in all these different factors, the brain reserve capacity can be impacted. When it passes the threshold, these changes will lead to clinical expression (e.g. cognitive decline).

FUTURE RECOMMENDATIONS

While research in the BMs population is complicated by high attrition rates, especially at longer follow-up intervals, we have also learned that we cannot simply generalize results regarding brain-behavior associations from one population to another (**Chapter 5**). This stresses the importance of performing large-scale research in the BMs population itself. Ideally, multi-center or nationwide studies should be started to not only increase the number of patients, but also ensure to capture the diversity of patients with BMs. Throughout this discussion multiple avenues for future research have been mentioned. A summary of the most important points is listed below:

- Use a transdiagnostic approach to incorporate a broad range of cognitive outcome measures throughout multiple different cohorts of cancer patients (e.g. lung and breast cancer) to be able to capture all patients with BMs

regardless of treatment choices and eventually aid in the disentangling of the different treatment effects.

- Performing qualitative research into the topics surrounding treatment-related decision making that are relevant to patients and caregivers in order to guide the selection of patient outcomes in future studies.
- Data-driven design of an efficient cognitive test battery that is sensitive to the wide variety of cognitive changes observed within the BMs population. As online testing may be able to provide multiple cognitive measures at the same time and can be completed from the comfort of the own home, this may be an ideal candidate in this setting. At the same time, such a compact test battery could aid patients in understanding their cognitive strengths and weaknesses and thereby easily provide opportunities for cognitive rehabilitation.
- Increased attention for the inclusion of age and gender-matched healthy controls throughout both cognitive and MRI studies in order to better understand the subtle treatment specific changes.
- Improving our understanding of the complex interplay between different factors underlying radiation-induced cognitive decline by performing a large-scale collection of multifaceted MRI data, both in the short-term and long-term post-radiotherapy. Subsequently, data-driven cluster analysis can be used to identify specific subgroups of patients (e.g. intact brain reserve vs impaired brain reserve) or specifically vulnerable brain regions (e.g. cortical grey matter, white matter, neurogenic niches) which can be related to cognitive functioning.

CONCLUDING REMARKS

In conclusion, the studies presented in this thesis offer a foundation upon which future research endeavors can build, guiding and inspiring further investigations into the cognitive changes experienced by patients with BMs and facilitating a deeper understanding of its pathogenesis. The ultimate objective of this research is to equip clinicians with patient-tailored predictions, empowering patients and their loved ones to make informed decisions about their treatments, optimized for their unique circumstances. However, as illustrated throughout this discussion, the path towards achieving this goal is filled with numerous hurdles and challenges that need to be overcome in the future. The inherent heterogeneity of the patient population and the complexity of the problems calls for an equally complex and multifaceted research approach. Only through a collective integration of all pieces of the puzzle will we be able to achieve the necessary results and make meaningful optimizations in the healthcare for future patients with BMs.

REFERENCES

1. Nieder C, Spanne O, Mehta MP, et al. Presentation, patterns of care, and survival in patients with brain metastases: What has changed in the last 20 years? *Cancer* 2011; 117: 2505–2512.
2. Lanier CM, Hughes R, Ahmed T, et al. Immunotherapy is associated with improved survival and decreased neurologic death after SRS for brain metastases from lung and melanoma primaries. *Neurooncol Pract* 2019; 6: 402–409.
3. Nayak L, Lee EQ, Wen PY. Epidemiology of brain metastases. *Curr Oncol Rep* 2012; 14: 48–54.
4. Jin J, Gao Y, Zhang J, et al. Incidence, pattern and prognosis of brain metastases in patients with metastatic triple negative breast cancer. *BMC Cancer*; 18. Epub ahead of print 19 April 2018. DOI: 10.1186/s12885-018-4371-0.
5. Karlsson AT, Hjermsstad MJ, Omdahl T, et al. Overall survival after initial radiotherapy for brain metastases; a population based study of 2140 patients with non-small cell lung cancer. *Acta Oncol (Madr)* 2021; 60: 1054–1060.
6. Lin X, DeAngelis LM. Treatment of brain metastases. *Journal of Clinical Oncology* 2015; 33: 3475–3484.
7. Alvarez-Breckenridge C, Remon J, Piña Y, et al. Emerging Systemic Treatment Perspectives on Brain Metastases: Moving Toward a Better Outlook for Patients. *American Society of Clinical Oncology Educational Book* 2022; 147–165.
8. Rick JW, Shahin M, Chandra A, et al. Systemic therapy for brain metastases. *Crit Rev Oncol Hematol* 2019; 142: 44–50.
9. Hodgson KD, Hutchinson AD, Wilson CJ, et al. A meta-analysis of the effects of chemotherapy on cognition in patients with cancer. *Cancer Treat Rev* 2013; 39: 297–304.
10. Joly F, Castel H, Tron L, et al. Potential effect of immunotherapy agents on cognitive function in cancer patients. *J Natl Cancer Inst* 2020; 112: 123–127.
11. Wefel JS, Schagen SB. Chemotherapy-related cognitive dysfunction. *Curr Neurol Neurosci Rep* 2012; 12: 267–275.
12. Schagen SB, Tsvetkov AS, Compter A, et al. Cognitive adverse effects of chemotherapy and immunotherapy: are interventions within reach? *Nat Rev Neurol* 2022; 18: 173–185.
13. de Ruyter MB, Dearnorff RL, Blommaert J, et al. Brain gray matter reduction and premature brain aging after breast cancer chemotherapy: a longitudinal multicenter data pooling analysis. *Brain Imaging Behav*. Epub ahead of print 2023. DOI: 10.1007/s11682-023-00781-7.
14. Huisman SI, van der Boog ATJ, Cialdella F, et al. Quantifying the post-radiation accelerated brain aging rate in glioma patients with deep learning. *Radiotherapy and Oncology* 2022; 175: 18–25.
15. Peters S, Bexelius C, Munk V, et al. The impact of brain metastasis on quality of life, resource utilization and survival in patients with non-small-cell lung cancer. *Cancer Treat Rev* 2016; 45: 139–162.
16. Cagney DN, Martin AM, Catalano PJ, et al. Incidence and prognosis of patients with brain metastases at diagnosis of systemic malignancy: a population-based study. *Neuro Oncol* 2017; 19: 1511–1521.

17. Young-Afat DA, van Gils CH, van den Bongard HJGD, et al. The Utrecht cohort for Multiple BREast cancer intervention studies and Long-term evaluation (UMBRELLA): objectives, design, and baseline results. *Breast Cancer Res Treat* 2017; 164: 445–450.
18. Utrecht COhort for Lung Cancer Outcome Reporting and Trial Inclusion (U-COLOR). *ClinicalTrials.gov [Internet]*. 2020; <https://classic.clinicaltrials.gov/ct2/show/NCT050>.
19. Karnath HO, Sperber C, Rorden C. Mapping human brain lesions and their functional consequences. *Neuroimage* 2018; 165: 180–189.
20. Mampay M, Flint MS, Sheridan GK. Tumour brain: Pretreatment cognitive and affective disorders caused by peripheral cancers. *British Journal of Pharmacology* 2021; 178: 3977–3996.
21. Yao S, Zuo H, Li W, et al. The correlations between psychological distress, cognitive impairment and quality of life in patients with brain metastases after whole-brain radiotherapy. *Clinical and Translational Oncology* 2022; 25: 207–217.
22. Yaribeygi H, Panahi Y, Sahraei H, et al. The impact of stress on body function: A review. *EXCLI Journal* 2017; 16: 1057–1072.
23. Siassi M, Weiss M, Hohenberger W, et al. Personality rather than clinical variables determines quality of life after major colorectal surgery. *Dis Colon Rectum* 2009; 52: 662–668.
24. Van Der Steeg AFW, De Vries J, Roukema JA. Anxious personality and breast cancer: Possible negative impact on quality of life after breast-conserving therapy. *World J Surg* 2010; 34: 1453–1460.
25. Whitworth SR, Loftus AM, Skinner TC, et al. Personality affects aspects of health-related quality of life in parkinson's disease via psychological coping strategies. *J Parkinsons Dis* 2013; 3: 45–53.
26. Koleck M, Mazaux JM, Rasclé N, et al. Psycho-social factors and coping strategies as predictors of chronic evolution and quality of life in patients with low back pain: A prospective study. *European Journal of Pain* 2006; 10: 1.
27. Brunault P, Champagne AL, Hugué G, et al. Major depressive disorder, personality disorders, and coping strategies are independent risk factors for lower quality of life in non-metastatic breast cancer patients. *Psychooncology* 2016; 25: 513–520.
28. Carr AJ, Gibson B, Robinson PG. Is Quality of life determined by expectations or experiences? *BMJ* 2001; 322: 1240–1243.
29. Kroenke CH, Kwan ML, Neugut AI, et al. Social networks, social support mechanisms, and quality of life after breast cancer diagnosis. *Breast Cancer Res Treat* 2013; 139: 515–527.
30. Wolfe F. *Fatigue Assessments in Rheumatoid Arthritis: Comparative Performance of Visual Analog Scales and Longer Fatigue Questionnaires in 7760 Patients*, www.jrheum.org (2004).
31. Dorman S, Hayes J, Pease N. What do patients with brain metastases from non-small cell lung cancer want from their treatment? *Palliat Med* 2009; 23: 594–600.
32. Cella D, Wen PY, Ervin C, et al. Understanding the patient experience and treatment benefits in patients with non-small-cell lung cancer with brain metastasis. *Cancer Med*. Epub ahead of print 1 June 2023. DOI: 10.1002/cam4.5975.

33. Prankeviciene A, Deltuva VP, Tamasauskas A, et al. Association between psychological distress, subjective cognitive complaints and objective neuropsychological functioning in brain tumor patients. *Clin Neurol Neurosurg* 2017; 163: 18–23.
34. Poppelreuter M, Weis J, Külz AK, et al. Cognitive dysfunction and subjective complaints of cancer patients: A cross-sectional study in a cancer rehabilitation centre. *Eur J Cancer* 2004; 40: 43–49.
35. Pinkham MB, Whitfield GA, Brada M. New developments in intracranial stereotactic radiotherapy for metastases. *Clin Oncol* 2015; 27: 316–323.
36. Yamamoto M, Serizawa T, Shuto T, et al. Stereotactic radiosurgery for patients with multiple brain metastases (JLGK0901): A multi-institutional prospective observational study. *Lancet Oncol* 2014; 15: 387–395.
37. Soliman H, Das S, Larson DA, et al. Stereotactic radiosurgery (SRS) in the modern management of patients with brain metastases. *Oncotarget* 2016; 7: 12318–12330.
38. Federatie Medisch Specialisten. *Hersenmetastasen Behandelrichtlijn*. 2020.
39. McKay WH, McTyre ER, Okoukoni C, et al. Repeat stereotactic radiosurgery as salvage therapy for locally recurrent brain metastases previously treated with radiosurgery. *J Neurosurg* 2017; 127: 148–156.
40. Minniti G, Scaringi C, Paolini S, et al. Repeated stereotactic radiosurgery for patients with progressive brain metastases. *J Neurooncol* 2016; 126: 91–97.
41. Koffer P, Chan J, Rava P, et al. Repeat Stereotactic Radiosurgery for Locally Recurrent Brain Metastases. *World Neurosurg* 2017; 104: 589–593.
42. Fritz C, Borsky K, Stark LS, et al. Repeated courses of radiosurgery for new brain metastases to defer whole brain radiotherapy: Feasibility and outcome with validation of the new prognostic metric brain metastasis velocity. *Front Oncol*; 8. Epub ahead of print 2018. DOI: 10.3389/fonc.2018.00551.
43. Shultz DB, Modlin LA, Jayachandran P, et al. Repeat Courses of Stereotactic Radiosurgery (SRS), Deferring Whole-Brain Irradiation, for New Brain Metastases after Initial SRS. *Int J Radiat Oncol Biol Phys* 2015; 92: 993–999.
44. Lee WJ, Choi JW, Kong DS, et al. Clinical outcomes of patients with multiple courses of radiosurgery for brain metastases from non-small cell lung cancer. *Sci Rep*; 12. Epub ahead of print 1 December 2022. DOI: 10.1038/s41598-022-13853-3.
45. Stern Y, Arenaza-Urquijo EM, Bartrés-Faz D, et al. Whitepaper: Defining and investigating cognitive reserve, brain reserve, and brain maintenance. *Alzheimer's and Dementia* 2020; 16: 1305–1311.
46. Jacobson NS, Roberts LJ, Berns SB, et al. Methods for defining and determining the clinical significance of treatment effects: Description, application, and alternatives. *J Consult Clin Psychol* 1999; 67: 300–307.
47. Jacobson NS, Truax P. Clinical Significance: A Statistical Approach to Denning Meaningful Change in Psychotherapy Research. *Journal of Consulting and Clinical Psychology* 1991; 59: 12–19.
48. Dengel DR, Evanoff NG, Marlatt KL, et al. Reproducibility of blood oxygen level-dependent signal changes with end-tidal carbon dioxide alterations. *Clin Physiol Funct Imaging* 2017; 37: 794–798.
49. Feenstra HEM, Murre JMJ, Vermeulen IE, et al. Reliability and validity of a self-administered tool for online neuropsychological testing: The Amsterdam Cognition Scan. *J Clin Exp Neuropsychol* 2018; 40: 253–273.

50. Wefel JS, Vardy J, Ahles T, et al. International Cognition and Cancer Task Force recommendations to harmonise studies of cognitive function in patients with cancer. *Lancet Oncol* 2011; 12: 703–708.
51. Maggio MG, Maresca G, Stagnitti MC, et al. Social cognition in patients with acquired brain lesions: An overview on an under-reported problem. *Applied Neuropsychology:Adult* 2022; 29: 419–431.
52. Goebel S, Mehdorn HM, Wiesner CD. Social cognition in patients with intracranial tumors: do we forget something in the routine neuropsychological examination? *J Neurooncol* 2018; 140: 687–696.
53. Buunk AM, Gerritsen MJ, Jeltrema HR, et al. Emotion Recognition in Patients with Low-Grade Glioma before and after Surgery. *Brain Sci*; 12. Epub ahead of print 2022. DOI: 10.3390/brainsci12091259.
54. Chen P, Wang G, Ma R, et al. Multidimensional assessment of empathic abilities in patients with insular glioma. *Cogn Affect Behav Neurosci* 2016; 16: 962–975.
55. Campanella F, Shallice T, Ius T, et al. Impact of brain tumour location on emotion and personality: A voxel-based lesion-symptom mapping study on mentalization processes. *Brain* 2014; 137: 2532–2545.
56. Nazem-Zadeh MR, Chapman CH, Lawrence TL, et al. Radiation therapy effects on white matter fiber tracts of the limbic circuit. *Med Phys* 2012; 39: 5603–5613.
57. Zhu T, Chapman CH, Tsien C, et al. Effect of the Maximum Dose on White Matter Fiber Bundles Using Longitudinal Diffusion Tensor Imaging. *Int J Radiat Oncol Biol Phys* 2016; 96: 696–705.
58. Connor M, Karunamuni R, McDonald C, et al. Regional susceptibility to dose-dependent white matter damage after brain radiotherapy. *Radiotherapy and Oncology* 2017; 123: 209–217.
59. Tibbs MD, Huynh-Le MP, Karunamuni R, et al. Microstructural Injury to Left-Sided Perisylvian White Matter Predicts Language Decline After Brain Radiation Therapy. *Int J Radiat Oncol Biol Phys* 2020; 108: 1218–1228.
60. Chapman CH, Zhu T, Nazem-Zadeh M, et al. Diffusion tensor imaging predicts cognitive function change following partial brain radiotherapy for low-grade and benign tumors. *Radiotherapy and Oncology* 2016; 120: 234–240.
61. Chapman CH, Nagesh V, Sundgren PC, et al. Diffusion tensor imaging of normal-appearing white matter as biomarker for radiation-induced late delayed cognitive decline. *Int J Radiat Oncol Biol Phys* 2012; 82: 2033–2040.
62. Huynh-Le MP, Tibbs MD, Karunamuni R, et al. Microstructural Injury to Corpus Callosum and Intrahemispheric White Matter Tracts Correlate With Attention and Processing Speed Decline After Brain Radiation. *Int J Radiat Oncol Biol Phys* 2021; 110: 337–347.
63. Nagtegaal SHJ, David S, van Grinsven EE, et al. Morphological changes after cranial fractionated photon radiotherapy: Localized loss of white matter and grey matter volume with increasing dose. *Clin Transl Radiat Oncol* 2021; 31: 14–20.
64. Ma Q, Zeng LL, Qin J, et al. Radiation-induced functional connectivity alterations in nasopharyngeal carcinoma patients with radiotherapy. *Medicine* 2016; 95: e4275.
65. Ma Q, Zeng LL, Qin J, et al. Radiation-induced cerebellar-cerebral functional connectivity alterations in nasopharyngeal carcinoma patients. *Neuroreport* 2017; 28: 705–711.
66. Fu G, Xie Y, Pan J, et al. Longitudinal study of irradiation-induced brain functional network alterations in patients with nasopharyngeal carcinoma. *Radiotherapy and Oncology* 2022; 173: 277–284.

67. Ren WT, Li YX, Wang K, et al. Cerebral functional abnormalities in patients with nasopharyngeal carcinoma after radiotherapy: An observational magnetic resonance resting-state study. *Chin Med J (Engl)* 2019; 132: 1563–1571.
68. Qiu Y, Guo Z, Han L, et al. Network-level dysconnectivity in patients with nasopharyngeal carcinoma (NPC) early post-radiotherapy: longitudinal resting state fMRI study. *Brain Imaging Behav* 2018; 12: 1279–1289.
69. Peters R. Ageing and the brain. *Postgraduate Medical Journal* 2006; 82: 84–88.
70. Fjell AM, Westlye LT, Grydeland H, et al. Accelerating cortical thinning: Unique to dementia or universal in aging? *Cerebral Cortex* 2014; 24: 919–934.
71. Grajauskas LA, Siu W, Medvedev G, et al. MRI-based evaluation of structural degeneration in the ageing brain: Pathophysiology and assessment. *Ageing Research Reviews* 2019; 49: 67–82.
72. Bennett IJ, Madden DJ. Disconnected aging: Cerebral white matter integrity and age-related differences in cognition. *Neuroscience* 2014; 276: 187–205.
73. Fjell AM, Walhovd KB. *Structural Brain Changes in Aging: Courses, Causes and Cognitive Consequences*. 2010.
74. Gunning-Dixon FM, Brickman AM, Cheng JC, et al. Aging of cerebral white matter: A review of MRI findings. *International Journal of Geriatric Psychiatry* 2009; 24: 109–117.
75. De Vis JB, Hendrikse J, Bhogal A, et al. Age-related changes in brain hemodynamics; A calibrated MRI study. *Hum Brain Mapp* 2015; 36: 3973–3987.
76. Bhogal AA, De Vis JB, Siero JCW, et al. The BOLD cerebrovascular reactivity response to progressive hypercapnia in young and elderly. *Neuroimage* 2016; 139: 94–102.
77. Peng SL, Chen X, Li Y, et al. Age-related changes in cerebrovascular reactivity and their relationship to cognition: A four-year longitudinal study. *Neuroimage* 2018; 174: 257–262.
78. Catchlove SJ, Parrish TB, Chen Y, et al. Regional Cerebrovascular Reactivity and Cognitive Performance in Healthy Aging. *J Exp Neurosci* 2018; 12: 1–11.
79. Fantini S, Sassaroli A, Tgavalekos KT, et al. Cerebral blood flow and autoregulation: current measurement techniques and prospects for noninvasive optical methods. *Neurophotonics* 2016; 3: 031411.
80. Murkin JM. Cerebral autoregulation: The role of CO₂ in metabolic homeostasis. *Semin Cardiothorac Vasc Anesth* 2007; 11: 269–273.
81. Markus HS. Cerebral perfusion and stroke. *J Neurol Neurosurg Psychiatry* 2004; 75: 353–361.
82. Sebök M, Niftrik CHB van, Wegener S, et al. Agreement of Novel Hemodynamic Imaging Parameters for the Acute and Chronic Stages of Ischemic Stroke: A Matched-pair Cohort Study. *Neurosurg Focus* 2021; 51: 1–8.
83. Václavů L, Meynart BN, Mutsaerts HJMM, et al. Hemodynamic provocation with acetazolamide shows impaired cerebrovascular reserve in adults with sickle cell disease. *Haematologica* 2019; 104: 690–699.
84. Rodgers ZB, Detre JA, Wehrli FW. MRI-based methods for quantification of the cerebral metabolic rate of oxygen. *Journal of Cerebral Blood Flow and Metabolism* 2016; 36: 1165–1185.
85. Digernes I, Grøvik E, Nilsen LB, et al. Brain metastases with poor vascular function are susceptible to pseudoprogression after stereotactic radiation surgery. *Adv Radiat Oncol* 2018; 3: 559–567.

86. Hsu YY, Chang CN, Jung SM, et al. Blood Oxygenation Level-Dependent MRI of Cerebral Gliomas during Breath Holding. *Journal of Magnetic Resonance Imaging* 2004; 19: 160–167.
87. Bright MG, Murphy K. Reliable quantification of BOLD fMRI cerebrovascular reactivity despite poor breath-hold performance. *Neuroimage* 2013; 83: 559–568.
88. Kastrup A, Li TQ, Glover GH, et al. Cerebral blood flow-related signal changes during breath-holding. *American Journal of Neuroradiology* 1999; 20: 1233–1238.
89. Magon S, Basso G, Farace P, et al. Reproducibility of BOLD signal change induced by breath holding. *Neuroimage* 2009; 45: 702–712.
90. Sleight E, Stringer MS, Marshall I, et al. Cerebrovascular Reactivity Measurement Using Magnetic Resonance Imaging: A Systematic Review. *Frontiers in Physiology*; 12. Epub ahead of print 25 February 2021. DOI: 10.3389/fphys.2021.643468.
91. Lu H, van Zijl PCM. A review of the development of Vascular-Space-Occupancy (VASO) fMRI. *NeuroImage* 2012; 62: 736–742.
92. Donahue MJ, Sideso E, MacIntosh BJ, et al. Absolute arterial cerebral blood volume quantification using inflow vascular-space-occupancy with dynamic subtraction magnetic resonance imaging. *Journal of Cerebral Blood Flow and Metabolism* 2010; 30: 1329–1342.
93. Crone C. The Permeability of Capillaries in Various Organs as Determined by Use of the 'Indicator Diffusion' Method. *Acta Physiol Scand* 1963; 58: 292–305.
94. Vestergaard MB, Iversen HK, Simonsen SA, et al. Capillary transit time heterogeneity inhibits cerebral oxygen metabolism in patients with reduced cerebrovascular reserve capacity from steno-occlusive disease. *Journal of Cerebral Blood Flow and Metabolism* 2023; 43: 460–475.
95. Østergaard L, Jespersen SN, Engedahl T, et al. Capillary Dysfunction: Its Detection and Causative Role in Dementias and Stroke. *Current Neurology and Neuroscience Reports*; 15. Epub ahead of print 1 June 2015. DOI: 10.1007/s11910-015-0557-x.
96. Gondi V, Pugh SL, Tome WA, et al. Preservation of memory with conformal avoidance of the hippocampal neural stem-cell compartment during whole-brain radiotherapy for brain metastases (RTOG 0933): A phase II multi-institutional trial. *Journal of Clinical Oncology* 2014; 32: 3810–3816.
97. Brown PD, Gondi V, Pugh S, et al. Hippocampal avoidance during whole-brain radiotherapy plus memantine for patients with brain metastases: Phase III trial NRG oncology CC001. *Journal of Clinical Oncology* 2020; 38: 1019–1029.
98. Cialdella F, Bruil DE, van der Boog A, et al. Investigating the Relationship Between Radiotherapy Dose on the neurogenic niches and Overall Survival in NSCLC Brain Metastases. Epub ahead of print 2022. DOI: 10.1101/2023.05.10.23289385.
99. Artegiani B, Calegari F. Age-related cognitive decline: Can neural stem cells help us? *Aging* 2012; 4: 176–186.





10

Nederlandse Samenvatting

Jaarlijks krijgen ongeveer 150.000 mensen te horen dat ze kanker hebben. Bij 10-30% van hen verspreidt de kanker zich naar de hersenen. Deze uitzaaiingen, zogenoemde hersenmetastasen, kunnen nu dankzij betere medische technologieën eerder worden ontdekt en ook de levensverwachting na diagnose is verbeterd. Hierdoor wordt verwacht dat het aantal patiënten met deze aandoening de komende jaren verder zal toenemen. De belangrijkste behandeling voor hersenmetastasen is radiotherapie, maar zoals bij elke medische behandeling, heeft dit bijwerkingen. Een van deze bijwerkingen is schade aan het gezonde hersenweefsel door de onvermijdbare blootstelling van een deel van het gezonde hersenweefsel aan de straling. Deze zogenoemde stralingsgeïnduceerde hersenschade kan vervolgens leiden tot cognitieve achteruitgang. Hoe dit precies gebeurt, is nog niet helemaal duidelijk. Met een stijgende levensverwachting, is er in de behandeling steeds meer aandacht voor het vinden van een balans tussen het verlengen van het leven en het behouden van de kwaliteit ervan.

DEEL I: COGNITIEF FUNCTIONEREN VAN PATIËNTEN MET HERSENMETASTASEN

Voor de behandeling van hersenmetastasen zijn er twee veelgebruikte radiotherapie technieken: stereotactische radiotherapie (SRT) en totale schedelbestraling. SRT gebruikt zeer nauwkeurige bestraling precies gericht op de hersenmetastasen met daardoor minimale schade aan omliggend gezond hersenweefsel. Totale schedelbestraling behandelt daarentegen het hele brein, waardoor ook kleine, nog-niet-zichtbare hersenmetastasen worden behandeld. Echter, deze aanpak kan ook schade aan het gehele brein veroorzaken, waardoor SRT in de praktijk de voorkeur heeft, als dat mogelijk is. Voorafgaand aan ons onderzoek, heb ik in **hoofdstuk 2** de beschikbare wetenschappelijke studies over veranderingen in de cognitieve functies (i.e. denkfuncties zoals het geheugen) na SRT of totale schedelbestraling bij volwassenen met hersenmetastasen met elkaar vergeleken. Op basis van een systematische zoekopdracht is de relevante literatuur doorzocht en gescreend. Na een strenge selectieprocedure werden de resultaten van 20 artikelen die over 14 verschillende studies rapporteerden geanalyseerd. Uit de resultaten bleek dat patiënten na totale schedelbestraling een achteruitgang in het cognitief functioneren vertoonden op de korte termijn (1-4 maanden), met verdere verslechtering op de middellange termijn (5-8 maanden). Enkel een subgroep van patiënten met een goede prognose (bijv. degene met kleinere hersenmetastasen) lieten stabiele of zelfs verbeterde cognitieve functies zien op de lange termijn (15 maanden). Bij SRT werden wisselende resultaten op korte termijn gezien tussen studies. In vergelijking met totale schedelbestraling was er na SRT minder vaak

een korte termijn achteruitgang. Ook bleef het cognitief functioneren vaak op het oude niveau op zowel de middellange als lange termijn. In conclusie bevestigen de resultaten van dit onderzoek dat, ondanks de beperkingen in de beschikbare studies, SRT vaak de voorkeur krijgt boven totale schedelbestraling in de behandeling van hersenmetastasen vanwege het lagere risico op langdurige en blijvende cognitieve bijwerkingen. Het is echter belangrijk te benadrukken dat de kans op cognitieve bijwerkingen na SRT niet onderschat moet worden. Voor toekomstige studies is het cruciaal om een breed scala aan cognitieve taken af te nemen en resultaten op individueel niveau te interpreteren.

In **hoofdstuk 2** van mijn proefschrift heb ik ontdekt dat veel mensen met hersenmetastasen al voor hun bestraling last hadden van cognitieve problemen; bijna de helft van de patiënten had al cognitieve stoornissen voordat ze starten met hersenbestraling. Daarbij was het niet één specifiek cognitief gebied, ook wel cognitief domein genoemd, dat vaak was aangedaan, maar betrof het verschillende aspecten van het denkvermogen. Daarom heb ik in **hoofdstuk 3** het cognitief functioneren van 58 patiënten met hersenmetastasen grondig onderzocht voordat ze bestraling kregen. Omdat de ervaren kwaliteit van leven niet alleen wordt bepaald door het objectief cognitief functioneren van een individu, maar ook afhankelijk is van de eigen beleving, is ook het subjectief cognitief functioneren meegenomen in dit onderzoek. Ik heb ook onderzocht of een uitgebreide testbatterij beter is dan een kernbatterij om cognitieve problemen bij deze patiënten te ontdekken. Voor dit onderzoek is gebruik gemaakt van gegevens die verzameld zijn binnen de lopende prospectieve studies COIMBRA en APRICOT. De resultaten laten zien dat patiënten met hersenmetastasen goed in staat zijn om hun eigen denkvermogen op verschillende cognitieve domeinen te beoordelen aan de hand van visuele analoge schalen. Daarbij gaven bijna alle patiënten aan enige mate van cognitieve achteruitgang te ervaren sinds de start van de behandeling van de primaire tumor.

Wat betreft het objectief cognitief functioneren zijn er grote verschillen tussen patiënten, zowel op groeps- als individueel niveau. Bijvoorbeeld, sommige patiënten hadden moeite met het onthouden, terwijl anderen problemen hadden met het snel verwerken van informatie. Met behulp van een clusteranalyse is onderzocht of we groepen konden vinden waarin mensen vergelijkbare cognitieve problemen hadden. Hieruit kwamen vier betekenisvolle cognitieve profielen naar voren, waarbij het hebben van geheugenproblemen een belangrijk kenmerk was; in twee van de vier clusters hadden mensen geheugenproblemen, waarbij één cluster ook andere cognitieve problemen vertoonde. Er waren echter geen verbanden tussen verschillende kenmerken van de patiënten (zoals leeftijd of aantal

hersensmetastasen) en de vier cognitieve clusters. Tot slot bleek dat het haalbaar was om een uitgebreide test van 90 minuten te gebruiken bij deze kwetsbare groep patiënten. Als alleen de kern testbatterij werd gebruikt, werd de mate van cognitieve problemen aanzienlijk onderschat, wat aantoont dat de uitgebreide test waardevol is. Kortom, voordat patiënten met hersensmetastasen bestraling krijgen, zien we verschillende cognitieve problemen, zowel zoals ervaren door de patiënten zelf als geobjectiveerd met uitgebreid cognitief onderzoek. Hoewel we enige orde kunnen brengen in deze variatie, is het nog niet duidelijk waarom er zoveel cognitieve verschillen zijn en of deze blijven bestaan na de bestraling.

Met de steeds betere medische zorg neemt de levensverwachting van patiënten met hersensmetastase toe. In **hoofdstuk 4** heb ik daarom onderzoek gedaan naar het cognitief functioneren van patiënten met hersensmetastasen na radiotherapie, zowel op de korte termijn (drie maanden) als op de lange termijn (≥ 11 maanden). Net als in het voorgaande hoofdstuk, heb ik hierbij zowel gekeken naar de eigen beleving van cognitieve veranderingen als objectieve metingen hiervan. In dit onderzoek heb ik me specifiek gefocust op betekenisvolle, individuele cognitieve veranderingen met behulp van zogeheten betrouwbare veranderindices. Vanuit de eerdergenoemde COIMBRA- en APRICOT-studie was data van 36 patiënten beschikbaar voor de korte termijn beoordeling en 14 patiënten voor de lange termijn. Opvallend was dat 50% van de patiënten meldde dat ze na bestraling een achteruitgang in hun denkvermogen ervoeren, vooral op het gebied van geheugen en aandacht. Dit werd vaker gerapporteerd door patiënten met intracraniale progressie (i.e. groei van hersensmetastasen) binnen drie maanden na de behandeling.

Drie maanden na radiotherapie vertoonden bijna alle patiënten cognitieve stoornissen op objectief cognitief onderzoek, waarbij geheugenproblemen het meest voorkwamen. Op de lange termijn zagen we vooral vertraging in de verwerkingssnelheid en psychomotorische snelheid. Opvallend was dat hoewel 97% van de patiënten drie maanden na de behandeling achteruitgang vertoonde in ten minste één cognitief domein, 81% van hen tegelijkertijd verbetering liet zien in een ander cognitief domein. Dit patroon van zowel verslechtering als verbetering bleef ook op de lange termijn bestaan. Er werden geen risicofactoren geïdentificeerd voor cognitieve achteruitgang na radiotherapie. Bij het maken van behandelkeuzes, moeten deze complexe cognitieve veranderingen worden afgewogen tegen langere overleving. Afgestemd neuropsychologisch onderzoek 3 maanden na radiotherapie is belangrijk om patiënten met cognitieve problemen gericht te kunnen begeleiden.

DEEL II: HET GEBRUIK VAN BEELDVORMING OM COGNITIEF FUNCTIONEREN TE BEGRIJPEN

De verschillen in cognitieve prestaties bij mensen met hersenmetastasen, samen met het ontbreken van duidelijke risicofactoren (**hoofdstuk 3 en 4**), benadrukken de noodzaak van verder onderzoek naar de onderliggende oorzaken. De plek van de hersenmetastasen (bijvoorbeeld links of rechts in de hersenen) kan mogelijk bijdragen aan deze variatie in cognitief functioneren. Het verband tussen de locatie van de metastasen in de hersenen en gedragsveranderingen is echter ingewikkeld vanwege verschillende factoren. Veel patiënten hebben meerdere metastasen op verschillende plaatsen in de hersenen, waardoor het onderzoeken van specifieke relaties tussen de locatie van de laesies (i.e. het aangedane gebied) en gedrag bemoeilijkt wordt. Het is onduidelijk of resultaten van eerdere studies over de relatie tussen laesies en symptomen (laesie-symptoom mapping, LSM) bij andere patiëntengroepen kunnen worden toegepast op mensen met hersenmetastasen. Daarom heb ik in **hoofdstuk 5** LSM-resultaten vergeleken tussen twee verschillende groepen patiënten: 196 mensen met primaire hersentumoren en 147 mensen met een ischemisch herseninfarct. Ondanks grote aantallen patiënten, maakte een beperkte ruimtelijke overlap in laesies een precieze vergelijking lastig. In hersengebieden waar wel voldoende laesie overlap was, werden aanzienlijke verschillen gevonden in hersen-gedrag relaties tussen de twee groepen wat betreft verbaal geheugen en verbale vloeiendheid. Dit bevestigt dat de oorzaken van schade aan specifieke hersengebieden de cognitieve gevolgen hiervan beïnvloeden. Bij het onderzoeken van de relatie tussen hersenen en gedrag kunnen we resultaten van andere groepen patiënten gebruiken om hypothesen te bedenken, maar het is altijd nodig om deze bevindingen te bevestigen in de specifieke groep die we bestuderen.

De variatie in cognitieve veranderingen na bestralingen kan mogelijk ook verklaard worden door verschil in kwetsbaarheid van de hersenen voor de negatieve effecten hiervan. Eerdere onderzoeken hebben laten zien dat bestraling schadelijk kan zijn voor de bloedvaten in de hersenen. Aangezien zuurstof en belangrijke voedingsstoffen via het bloed aan de hersenen worden afgeleverd, zou schade aan de vaten impact kunnen hebben op het denkvermogen. Patiënten die voorafgaand aan de bestraling al vaatschade hebben, zouden daarmee extra gevoelig kunnen zijn voor verdere beschadiging door de bestraling. Met de recente technologische ontwikkelingen kunnen geavanceerde MRI-scans worden gebruikt om zowel de structuur als het functioneren van de bloedvaten in de hersenen in kaart te brengen. In **hoofdstuk 6** van mijn proefschrift beschrijf ik hoe we met twee verschillende MRI-technieken, namelijk 'blood oxygenation level-dependent' (BOLD) en 'arterial

spin labeling' (ASL) MRI, hebben gekeken naar het functioneren van de bloedvaten in de hersenen voordat patiënten met hersenmetastasen bestraling kregen. Dit heb ik gedaan bij 14 deelnemers van de APRICOT-studie. Het doel was om beter te begrijpen hoe verschillende metingen van de MRI (BOLD en ASL) samenhangen. We hebben gekeken naar twee BOLD-parameters (1 & 2) en twee ASL-parameters (3 & 4):

1. Cerebrovasculaire reactiviteit (CVR): Dit vertelt ons of de bloedvaten goed kunnen verwijden en vernauwen, zodat ze zich kunnen aanpassen aan verschillende situaties.
2. Hemodynamische vertraging: Dit vertelt ons hoe snel de bloedvaten deze aanpassingen kunnen maken.
3. Perfusie: Dit geeft aan hoe goed het hersenweefsel wordt voorzien van bloed en daarmee van zuurstof en voedingsstoffen.
4. Arteriële aankomsttijd (AAT): Dit vertelt ons hoelang het duurt voordat zuurstofrijk bloed in de hersenen aankomt.

De resultaten lieten zien dat gebieden in de hersenen met betere CVR ook beter doorbloed waren. Ook zagen we dat gebieden met een langere hemodynamische vertraging ook een langere AAT hadden. Maar deze verbanden waren alleen zichtbaar in gebieden waar de bloedvaten nog goed konden aanpassen aan verschillende omstandigheden, oftewel in die gebieden waar de hersenen nog voldoende vasculaire reservecapaciteit hadden. Belangrijk was ook dat CVR-parameters mogelijk gebieden in de hersenen kunnen identificeren die kwetsbaar zijn voor vaatproblemen voordat dit zich vertaalt in een verminderde doorbloeding en dus zichtbaar wordt op ASL-MRI. Dit betekent dat CVR misschien gevoeliger is om subtiele veranderingen na bestraling in kaart te brengen.

Hoewel de eerdergenoemde BOLD-parameters waardevolle maatstaven zijn om het functioneren van de bloedvaten, met name de capaciteit van de bloedvaten om zich aan te passen (vasculaire reservecapaciteit), te onderzoeken, gebruikt ons brein verschillende compensatietechnieken. De zuurstofextractiefractie, wat aangeeft hoeveel zuurstof door het weefsel wordt opgenomen wanneer het bloed door de haarvaten stroomt, kan bijvoorbeeld worden verhoogd. Ook biedt het cerebraal metabool zuurstofverbruik inzicht in de snelheid waarmee de hersenen zuurstof verbruiken, en wordt het beschouwd als een directe indicator van de energiebalans en gezondheid van de hersenen. In **hoofdstuk 7** onderzocht ik daarom de impact van radiotherapie op zowel de metabole als vasculaire reserve bij negen patiënten


met hersenmetastasen uit de APRICOT-studie door de beoordeling van perfusie, zuurstofextractiefraction, cerebraal metabool zuurstofverbruik en CVR vóór en drie maanden na radiotherapie.

Na de bestraling was er een toename van de bloeddorstrooming in het gehele brein. Dit kan wijzen op herstellende mechanismen tegen ontstekingen die bestraling kan veroorzaken. In gebieden waar de zwelling (oftewel oedeem) na de bestraling was afgenomen, zagen we herstel van de stofwisseling maar ook blijvende schade aan de bloedvaten. Door gedetailleerder te kijken, ontdekten we dat de perfusie, zuurstof extractie fractie, cerebraal metabool zuurstofverbruik en CVR verslechterden, vooral in hersengebieden die meer bestraling hadden gekregen. Opvallend was dat er veel verschillen waren tussen patiënten en de bestralingsdosis, vooral bij lagere doses. Uit analyse van individuele gevallen bleek dat dit mogelijk te maken heeft met hoe de hersenmetastasen reageren op de bestraling. Oftewel, we zagen verslechtering in zowel metabole als vasculaire maten bij een patiënt waar de hersenmetastasen drie maanden na bestraling waren gegroeid, terwijl we verbetering zagen bij patiënt waar de hersenmetastasen door de behandeling waren gekrompen. Deze veranderingen leken ook parallel te lopen aan de cognitieve veranderingen. Hoewel het onderzoek nog voorlopig is en deels berusten op individuele analyses, suggereren de resultaten dat er binnen drie maanden na bestraling geen grote schade aan de bloedvaten of stofwisseling was. Desalniettemin bleken de verschillende gebruikte MRI-parameters gevoelig te zijn voor het identificeren van herstel van metabole of vasculaire schade na radiotherapie. Het blijkt dus waardevol om deze MRI-parameters te gebruiken bij het opsporen van veranderingen na bestraling van de hersenen, vooral wanneer we inzichten vanuit verschillende MRI-technieken combineren.

In dit proefschrift wordt duidelijk dat patiënten met hersenmetastasen verschillen in hun cognitieve, vasculaire en metabole kenmerken. Zelfs vóór bestraling ervaren velen cognitieve problemen, en bij sommigen verslechtert het cognitief functioneren in de 12 maanden na de behandeling. Er zijn voorzichtige aanwijzingen dat de variatie in cognitief functioneren gerelateerd is aan verschillen in vaat- en stofwisselingscapaciteit. Geavanceerde MRI-metingen laten niet alleen zien dat deze technieken bruikbaar zijn in het identificeren van subtiele veranderingen, maar bieden ook nieuwe inzichten in deze complexe patiëntengroep. Toekomstig onderzoek zou niet alleen naar afzonderlijke MRI-maten moeten kijken, maar juist de combinatie van inzichten uit verschillende technieken moeten benutten. Hierdoor kan worden onderzocht of de ophoping van hersenschade of de afname van de reservecapaciteit van de hersenen voorspellend is voor cognitieve achteruitgang na radiotherapie. Het uiteindelijke doel is dat deze cognitief kwetsbare en snelgroeiende

patiëntengroep op basis van goed onderbouwde informatie een beslissing kan nemen over hun behandeling in de laatste fase van hun leven.





Appendices

List of publications
Educational portfolio
Dankwoord (Acknowledgements)
About the author

LIST OF PUBLICATIONS

Published and submitted journal articles

1. van der Voort, E. C., Tong, Y., **van Grinsven, E. E.**, Zwanenburg, J. J. M., Philippens, M. E. P., & Bhogal, A. A. (2024) CO₂ as an engine for neurofluid flow; exploring the coupling between vascular reactivity, brain clearance and changes in tissue properties. *Accepted*.
2. van der Boog, A. T. J., **van Grinsven, E. E.**, Rados, M., Snijders, T. J., Verhoeff, J. J. C., & Robe, P. A. (2023). Postoperative ischemia and neurological deficits after glioma resection: A systematic review and meta-analysis. *Submitted*.
3. **van Grinsven, E. E.**, de Leeuw, J., Siero, J. C. W., Verhoeff, J. J. C., van Zandvoort, M. J. E., Cho, J., Philippens, M. E. P., & Bhogal, A. A. (2023). Evaluating physiological MRI biomarkers and cognitive performance in patients with brain metastases after stereotactic radiosurgery - a preliminary analysis and case-report. *Cancers*, 15(17), 4298. DOI: 10.3390/cancers15174298.
4. **van Grinsven, E. E.**, Cialdella, F., Gmelich Meijling, Y. A., Verhoeff, J. J. C., Philippens, M. E. P., & van Zandvoort, M. J. E. (2023). Individualized trajectories in post-radiotherapy neurocognitive functioning of patients with brain metastases. *Submitted*
5. **van Grinsven, E. E.**, Cialdella, F., Verhoeff, J. J. C., Philippens, M. E. P., & van Zandvoort, M. J. E. (2023) Different profiles of neurocognitive functioning in patients with brain metastases prior to brain radiotherapy. *Psycho-Oncology*, 32(11), 1752-1761. DOI: 10.1002/pon.6229.
6. **van Grinsven, E. E.**, Guichelaar, C. J., Philippens, M. E. P., Siero, J. C. W., & Bhogal, A. A. (2023). Hemodynamic imaging parameters in brain metastases patients – Agreement between multi-delay ASL and hypercapnic BOLD. *Journal of Cerebral Blood Flow & Metabolism*, 43(12), 2072-2084. DOI: 10.1177/0271678X231196989.
7. **van Grinsven, E. E.**, Smits, A. R., van Kessel, E., Raemaekers, M. A. H., de Haan, E. H. F., Wajer, I. H., ... & van Zandvoort, M. J. E. (2023). The impact of etiology in lesion-symptom mapping–A direct comparison between tumor and stroke. *NeuroImage: Clinical*, 37, 103305. DOI: 10.1016/j.nicl.2022.103305.
8. **van Grinsven, E. E.**, Nagtegaal, S. H., Verhoeff, J. J., & van Zandvoort, M. J. (2021). The impact of stereotactic or whole brain radiotherapy on neurocognitive functioning in adult patients with brain metastases: a systematic review and meta-analysis. *Oncology Research and Treatment*, 44(11), 622-636. DOI: 10.1159/000518848.
9. Nagtegaal, S. H. J., David, S., **van Grinsven, E. E.**, van Zandvoort, M. J. E., Seravalli, E., Snijders, T. J., ... & Verhoeff, J. J. C. (2021). Morphological changes after cranial fractionated photon radiotherapy: Localized loss of white matter and grey matter volume with increasing dose. *Clinical and Translational Radiation Oncology*, 31, 14-20. DOI: 10.1016/j.ctro.2021.08.010.

Conference proceedings

1. **van Grinsven, E. E.**, Cialdella, F., Vrolijk, T. G. G., Philippens, M. E. P., Verhoeff, J. J. C., & van Zandvoort, M. J. E. (2023). Quality of life in patients and caregivers following radiotherapy for brain metastases: lower health status and more symptoms of anxiety. *Oral presentation, EANO.*
2. **van Grinsven, E. E.**, Gmelich Meijling, Y. A., Cialdella, F., Verhoeff, J. J. C., Philippens, M. E. P., & van Zandvoort, M. J. E. (2023). Evolution of neurocognitive functioning after radiotherapy in patients with brain metastases. *Poster presentation, EANO.*
3. **van Grinsven, E. E.**, Verhoeff, J. J. C., Philippens, M. E. P., & van Zandvoort, M. J. E. (2023). Neurocognitive dysfunction in patients with brain metastases prior to radiotherapy. *Oral presentation, FESN.*
4. Cialdella, F., **van Grinsven, E. E.**, van der Boog, A. T. J., Nagtegaal, S. H., Smid, E. Claes, A., Kleynen, K., Seravelli, E., Philippens, M. E. P., van Zandvoort, M. J. E., & Verhoeff, J. J. C. (2023). Redefining boundaries: Stereotactic Radiosurgery for Enhanced Quality of Life and Survival in Patients with 5-20 Brain Metastase. *Poster presentation, SNO.*
5. Cialdella, F., **van Grinsven, E. E.**, van der Boog, A. T. J., Nagtegaal, S. H., Smid, E. Claes, A., Kleynen, K., Seravelli, E., Philippens, M. E. P., van Zandvoort, M. J. E., & Verhoeff, J. J. C. (2023). A Prospective Cohort Study on the Impact of Radiotherapy on Quality of Life and Disease Progression in Patients with Brain Metastases and Their Caregivers. *Poster presentation, SNO.*
6. **van Grinsven, E. E.**, Verhoeff, J. J. C., Philippens, M. E. P., & van Zandvoort, M. J. E. (2023). Neurocognitive dysfunction in patients with brain metastases prior to radiotherapy. *Oral presentation, LWNO wetenschappelijke dag.*
7. **van Grinsven, E. E.**, Guichelaar, C. J., Philippens, M. E. P., Siero, J. C. W., & Bhogal, A. A. (2023). Hemodynamic imaging parameters in brain metastases patients – Agreement between multi-delay ASL and hypercapnic BOLD. *Poster pitch, ISMRM Benelux chapter.*
8. de Leeuw, J., **van Grinsven, E. E.**, Siero, J. C. W., Philippens, M. E. P., Cho, J., & Bhogal, A. A. (2023). Effects of radiotherapy on tissue in patients with brain metastases in terms of OEF and CMRO2. *Digital poster, ISMRM.*
9. Zwanenburg, J., Tong, Y. **van Grinsven, E. E.**, Philippens, M. E. P., & Bhogal, A. A. (2023). CO2 as an engine for neuro-fluid flow. *Digital poster, ISMRM.*
10. van Zandvoort, M. J. E., **van Grinsven, E. E.**, Hinkert, C., Siero, J. C. W., & Philippens, M. E. P. (2023). The effect of radiotherapy on resting-state networks and cognitive functioning in patients with brain metastases – an exploratory study. *Poster presentation, ICCTF.*
11. **van Grinsven, E. E.**, Smits, A. R., van Kessel, E., Raemaekers, M. A. H., de Haan, E. H. F., Wajer, I. H., ... & van Zandvoort, M. J. E. (2022). Lesion-symptom mapping based on stroke or glioma: etiology matters! *Pitch and poster, EANO.*
12. **van Grinsven, E. E.**, Bhogal, A. A., Guichelaar, C. J., Siero, J. C. W., Hoogduin, J. M., van Zandvoort, M. J. E., Verhoeff, J. J. C., & Philippens, M. E. P. (2021). Feasibility of the APRICOT-trial: identifying MRI biomarkers for radiation-induced cognitive changes. *Online poster presentation, ESTRO.*
13. **van Grinsven, E. E.**, Smits, A. R., van Kessel, E., Raemaekers, M. A. H., de Haan, E. H. F., Wajer, I. H., ... & van Zandvoort, M. J. E. (2021). Can different etiologies provide converging evidence regarding the neural correlates of cognitive performance? Tumor versus stroke. *Poster presentation, ISMRM.*

14. **van Grinsven, E. E.**, Smits, A. R., van Kessel, E., Raemaekers, M. A. H., de Haan, E. H. F., Wajer, I. H., ... & van Zandvoort, M. J. E. (2021) . Can different etiologies provide converging evidence regarding the neural correlates of cognitive performance? Tumor versus stroke. *Oral presentation, LWNO wetenschappelijke dag.*
15. **van Grinsven, E. E.**, Champagne, A. A., Philippens, M. E. P., & Bhogal, A. A. (2020). Investigating the Optimal Vasoactive Stimulus to Extract Dynamic Cerebrovascular Reactivity Information: Breath holding versus CO2 Challenge. *Poster presentation, ISMRM.*
16. **van Grinsven, E. E.**, Champagne, A. A., Philippens, M. E. P., & Bhogal, A. A. (2020). Investigating the Optimal Vasoactive Stimulus to Extract Dynamic Cerebrovascular Reactivity Information: Breath holding versus CO2 Challenge. *Oral presentation, ISMRM Benelux chapter.*
17. **van Grinsven, E. E.**, Nagtegaal, S. H., Verhoeff, J. J., & van Zandvoort, M. J. (2019). The impact of radiotherapy on neurocognitive functioning in adult patients with brain metastases – A systematic review. *Poster presentation, FESN.*

Dutch Video Overview of Dissertation Chapters

<https://youtu.be/Cb7uFh32kxM>



EDUCATIONAL PORTFOLIO

	Year
Discipline-specific educational activities	
Introduction to the program	2018
CEN Summer School	2019 & 2021
Annual BCMR research symposium (including pitch presentation)	2021 & 2022
Utrecht Brain Conference	2022
Attendance at ≥8 X-Talks (CEN)	2018 - 2023
3 rd FESN Autumn School "A Toolbox for Neuropsychological Research and Practice"	2018
<i>Awarded with a travel grant</i>	
Functional Neuroanatomy (ONWAR)	2019
Cognitive Neuroscience (ONWAR)	2019
Neuro-onco / Neuro-RT journal club	2018-2022
General educational activities	
Basic Course for Clinical Investigators (BROK), including reregistration (EMWO)	2018 & 2022
Supervising master students	2019
Data management	2019
Time management	2019
Data Science: Statistical Programming with R (Summer School Utrecht)	2019
Best Practices for Writing reproducible code	2020
Adobe Illustrator Course	2020
Achieving your Goals and Performing more Successfully in your PhD	2020
Writing a Scientific Paper - Online	2020
Selling your Science	2021
The Power of a Compliment/Appreciation	2021
Effective Meetings	2021
Online Flirting	2021
Improve Your Online Presence	2021
The Art of Presenting Science	2022
(Inter)national meetings and conferences	
5 th EORTC Quality of Life Cancer Clinical Trials Conference, Belgium	2019
7 th meeting of the FESN, Italy, <i>poster presentation</i>	2019
ISMRM Beneluxe Chapter, The Netherlands, <i>oral presentation</i>	2020
LWNO wetenschappelijke dag, <i>oral presentation</i>	2021
ISMRM, online, <i>poster presentation</i>	2021

ESTRO, online, <i>poster presentation</i>	2021
EANO conference and educational day, Austria, <i>pitch and poster presentation</i>	2022
ISMRM Benelux Chapter, Belgium, <i>pitch and poster presentation</i>	2023
ISMRM, Canada, <i>oral presentation</i>	2023
LWNO wetenschappelijke dag, <i>oral presentation</i>	2023
EANO, The Netherlands, <i>oral and poster presentation</i> <i>Awarded with the Young Investigator Scholarship</i>	2023
8 th meeting of the FESN, Greece, <i>oral presentation</i>	2023

Education

Lisa van 't Schip (Master thesis, Vrije Universiteit Amsterdam) " <i>The Feasibility and Utility of Combining an Activity Tracker and the Experience Sampling Method to Measure Fluctuations in Physical Activity, Cognition and Mood and Their Coherence: a Pilot Study in Healthy Participants</i> "	2020
Eline van Daele (Master thesis, University Utrecht) " <i>The influence of Cerebellar Brain Metastases on Cognitive functioning</i> "	2022
Gelena Mahmoud (Master thesis, University Utrecht) " <i>Depressive Symptoms in Patients with Brain Metastasis: Predictive Factors</i> "	2022
Charlotte Doll (Master thesis, Utrecht University) " <i>The volume of brain metastases and cognitive performance in patients receiving radiotherapy</i> "	2022
Charlotte Doll (Innovation internship, Utrecht University) " <i>Cognitive performance and cerebral microbleeds in patients with brain metastases receiving radiotherapy</i> "	2022
Manon Kraaij (Master thesis, Utrecht University) " <i>Caregiver Burden and Depressive Symptoms; The Relationship with Cognitive Performance of Patients with Brain Metastases</i> "	2022
Celeste Hinkert (Master thesis, University Utrecht) " <i>The Effect of Radiotherapy on Resting State Networks and Cognitive Functioning in Patients with Brain Metastases</i> "	2022
Thirza Vrolijk (Master thesis, Utrecht University) " <i>Wellbeing of Patients with Brain Metastases receiving Radiotherapy and their Caregivers</i> "	2023
Yoniet Gmelich Meijling (Master thesis, Utrecht University) " <i>Changes in Neurocognitive Functioning After Radiotherapy in Individual Patients with Brain Metastases</i> "	2023
Janneke Verhoeven (Utrecht University) " <i>Social Cognition in Patients with Brain Metastasis or Ischemic Stroke</i> "	2023

DANKWOORD

Vijf jaar geleden kreeg ik de kans om mijn proefschrift te schrijven op dit mooie onderzoeksproject. Ik was direct enthousiast, maar deze reis was ongetwijfeld niet zonder uitdagingen. Het was een periode van hard werken, waarbij er af en toe tranen vloeiden, maar waarin ook veel werd gelachen en plezier werd gemaakt. Ik had dit nooit alleen gekund.

Allereerst wil ik alle **patiënten van de APRICOT- en COIMBRA-studie** bedanken. Zonder jullie onzelfzuchtige beslissing om deel te nemen en jullie kostbare tijd te investeren, was dit proefschrift nooit tot stand gekomen. Dank voor jullie openheid en de inspirerende, soms ontroerende gesprekken die we hebben gevoerd. Ondanks dat het tijdsintensief was om alle cognitieve en MRI-data te verzamelen, herinnerden onze gesprekken me altijd aan mijn motivatie voor dit onderzoek en gaven ze me weer energie en inspiratie om door te gaan.

Lief **promotieteam**, ook al was het soms een uitdaging was om jullie met vier volle agenda's daadwerkelijk bij elkaar te krijgen, wil ik jullie bedanken voor de prettige begeleiding gedurende dit project. Jullie uiteenlopende kennis, eigenschappen en persoonlijkheden vulden elkaar aan, wat soms voor uitdagende, maar vooral waardevolle begeleiding zorgde. En wat een eer om dit traject te doorlopen met twee ambitieuze en sterke vrouwen aan het hoofd van mijn promotieteam. **Prof. dr. van Zandvoort, beste Martine**, vanaf mijn allereerste college tijdens de bachelor wist je jouw enthousiasme voor de neuropsychologie op me over te brengen. Ik ben enorm blij dat ik al vanaf de Creative Challenge van jou heb mogen leren en me onder jouw vleugels verder heb mogen ontwikkelen, zowel als neuropsycholoog als onderzoeker. Onze meetings waren soms een hele onderneming, niet alleen qua planning, maar ook om jouw razendsnelle denktempo bij te benen. Gelukkig werden onze meetings altijd vergezeld van eten, van mandarijtjes tot chocola, en verliet ik jouw kantoor daardoor altijd met een gevulde buik en mijn hoofd vol nieuwe ideeën. Dankjewel voor alle kansen die je me hebt geboden en het altijd blijven zoeken naar creatieve oplossingen. Ik bewonder jouw tomeloze inzet om de medische neuropsychologie op de kaart te zetten en kijk er naar uit om in de toekomst met je te blijven samenwerken.

Dr. ir. Phillippens, beste Marielle, wat een voorrecht om met jou te hebben mogen samenwerken. Jouw betrokkenheid, gedrevenheid en toegankelijkheid waren van onschatbare waarde. Jij staat altijd open voor nieuwe ideeën en draait jouw hand niet om voor een uitdaging. Jouw deur stond altijd open voor vragen of een praatje,

maar ook zelf kwam je vaak langs om gewoon even te kijken hoe het met me ging en een dropje uit mijn snoepje te pakken. Het was dan ook geen verrassing van wie ze afkomstig waren wanneer er weer een nieuwe voorraad lekkere dropjes op mijn bureau verscheen. Ik heb ook goede herinneringen aan onze tweewekelijkse lunchwandelingen op vrijdagmiddag. Ze boden niet alleen een moment om over van alles en nog wat te praten, maar jij liet mij door jouw openheid zien dat promotoren “ook maar mensen zijn”. Ik bewonder hoe je je in de afgelopen jaren eigen hebt gemaakt in de neuropsychologie, want je stelt ondertussen niet alleen lastige vragen over imaging en de bijbehorende analyses, maar ook kritische vragen over de cognitieve analyses. Ik kijk uit naar mogelijke toekomstige samenwerkingen en gesprekken, waarvan ik weet dat ze even waardevol zullen zijn als deze afgelopen jaren.

Prof. dr. Verhoeff, beste Joost, wat fijn om jou als echte clinicus in mijn promotieteam te hebben gehad. Tijdens de vele momenten waarop we gezamenlijk de patiëntenlijst doornamen voor de screening van de studie, heb je mij veel geleerd over de behandeling van patiënten met hersenmetastasen en de impact hiervan. Dank voor het altijd vrijmaken van tijd en ruimte voor mijn nieuwsgierigheid hierover. Jouw voortdurende inzet om onderzoek naar de praktijk te vertalen, is bewonderenswaardig en hield mij scherp. Bovendien ben jij, als ware out-of-the-box denker, van mening dat er geen problemen bestaan, maar slechts oplossingen. Dit samen met jouw altijd snelle, kritische reacties en enorme enthousiasme voor onderzoek, maakte de samenwerking met jou zeer waardevol.

Dr. Bhogal, dear Alex, I will try to not be too wordy, but I do want to thank you for all your support during this project. From explaining all the ins and outs of the RespirAct to very early morning scanning sessions (sorry again!) and sharing and explaining your Matlab code. As we (luckily) are both visual thinkers, I always left your office with lots of sketches in my notebook after you (again) patiently explained everything about brain hemodynamics. Your competence as a researcher is truly admirable; your ability to conceive new ideas using innovative techniques and present them in an accessible manner is a rare talent. Over the years, I have not only gained profound knowledge from you, but have also learned the art of creating compelling visuals for manuscripts. Your feedback has been a constant source of positivity and guidance, keeping me motivated throughout the sometimes tough-to-write imaging papers. I have enjoyed our conversations, your humor, and your sincere interest and time for me as a person. Thanks for looking out for me all those years.

Leden van de beoordelingscommissie en opponenten, **prof. dr. Verkooijen, prof. dr. Schagen, prof. dr. Biessels, dr. de Vos, dr. Deprez en prof. dr. Hendrikse**, graag wil ik u bedanken voor de tijd en moeite die u in het beoordelen van dit proefschrift heeft gestoken. Ik kijk er naar uit om met jullie van gedachten te wisselen tijdens de verdediging. Ook veel dank aan alle **co-auteurs** voor de kritische blik en waardevolle suggesties bij het onderzoek in dit proefschrift.

Alle MRI-data voor de APRICOT-studie was nooit verzameld zonder de enorme inzet van de **MRI-laboranten** van de afdeling radiotherapie. Jullie interesse in zowel het onderzoek als mij en de goede gesprekken gedurende de scansessies heb ik altijd enorm gewaardeerd. **Tuan Nguyen** en **Teun Coolen**, jullie zijn van begin af aan onmisbaar geweest bij de studie. Jullie hebben altijd meegedacht en in oplossingen gedacht om de studie mogelijk te maken. **Amy Zomer**, bedankt dat je het stokje van Teun zo soepel hebt overgenomen.

Aan al mijn **(oud) collega's op de afdeling radiotherapie**: hoewel ik als neuropsycholoog wellicht een vreemde eend was in de bijt te midden van alle medici en fysici, voelde ik me op de radiotherapie afdeling uiteindelijk toch echt thuis. Hartelijk dank voor de aangename en inspirerende werkomgeving. Het uitvoeren van onderzoek is een onmogelijke taak zonder de bijdrage van de medewerkers van het **trialbureau** van de divisie Beeld en Oncologie. Specifiek wil ik **Saskia Amelsvoort-van der Vorst, Rosalie van den Boogaard** en **Annette van Dijk** bedanken, die onmisbaar waren bij het opzetten, aanpassen en in stand houden van zowel de COIMBRA- als de APRICOT-studie. Daarnaast wil ik alle collega's van het **secretariaat**, de **ICT**, het **datamanagementteam**, de **stafleden** en de **AIOS** van de radiotherapie bedanken, die allen hebben bijgedragen aan de succesvolle uitvoering van mijn onderzoek. Een speciaal woord van dank aan **Kitty Giezen**, die altijd paraat stond met een VVV-bon voor mijn patiënten en samen met mij op zoek ging naar geschikte werkplekken voor mijn talloze studenten. Ik wil tevens **Ernst Smid, Karin Kleynen** en **An Claes** bedanken voor de vlotte communicatie en ontelbare telefoontjes en e-mails wanneer er potentiële COIMBRA- en APRICOT-patiënten op de radiotherapie poli kwamen. Jullie inzet en samenwerking hebben zowel het onderzoek als mij enorm geholpen.

Gedurende de afgelopen jaren hebben er talloze (digitale) vergaderingen plaatsgevonden, ideeën zijn ontstaan en weer verworpen, alles met als doel de studie optimaal te laten verlopen en flexibel in te spelen op alle ontwikkelingen binnen een academisch ziekenhuis. Dit heb ik niet alleen gedaan, en daarom wil ik ook de volledige **APRICOT-onderzoeksgroep** bedanken. **Jeroen Siero**, telkens als

ik je in de gang tegenkwam, was er ruimte voor een praatje en oprechte interesse in mijn promotietraject. Je dacht altijd mee en stond klaar om te helpen. Jouw kennis en hulp waren onmisbaar bij het bedenken en vervolgens updaten van het scanprotocol voor de studie. Hartelijk dank ook voor jouw kritische blik op mijn imaging manuscripten; dit heeft de kwaliteit ervan aanzienlijk verbeterd. **Hans Hoogduin** en **Fredy Visser**, mijn dank voor jullie bijdrage aan het opzetten van het scanprotocol voor de studie. Dank ook voor de geduldige uitleg over het scannen van frietjes of patatjes. **Steven Nagtegaal**, jouw harde werk legde het fundament van de APRICOT-studie, waardoor ik vervolgens met een vliegende start verder kon om het protocol dan uiteindelijk toch goedgekeurd te krijgen.

Ik heb ook veel geleerd tijdens de meetings van de NeuroRT/Onco groep, met onder andere **Tom Snijders**, **Szabolcs David**, **Hema Venugopal**, **Christina Flies** en **Sjo van Rooij**. Tijdens de bijeenkomsten werden updates gedeeld over ieders werk, werden presentaties voor congressen geoefend, en was er ruimte voor discussie met andere enthousiaste neuro-onderzoekers. Ook voor de vele studenten die hier hun proposal- en eindpresentatie hebben mogen doen, was dit een enorm leerzame plek.

In de laatste anderhalf jaar van mijn promotietraject kreeg ik de kans om enkele studenten van de master Neuropsychologie te begeleiden tijdens hun thesis. **Charlotte Doll**, **Eline van Daele**, **Gelena Mahmoud**, **Manon Kraaij**, **Celeste Hinkert**, **Yoniet Gmelich Meijling**, **Thirza Vrolijk**, **Janneke Verhoeven**, hartelijk dank voor al jullie hulp bij de dataverzameling, jullie enthousiasme voor het onderzoek, en de plezierige begeleidingsmomenten. Het was een eer om jullie te zien groeien gedurende jullie onderzoeksstage en ik hoop dat ik mijn passie voor onderzoek een beetje op jullie heb kunnen overbrengen. **Celeste**, jouw inzet als onderzoeksassistent voor zowel de APRICOT- als COIMBRA-studie was onmisbaar. Ik hoefde jou altijd maar één keer om hulp te vragen en dan was het al geregeld of werd het direct gedaan. Daarnaast ben je ook nog eens een bijzonder fijn mens om mee samen te werken en heb je een groot hart voor het onderzoek. Ik kijk er naar uit om over een aantal jaar hopelijk ook op jouw promotie te kunnen proosten.

Charisma Hehakaya, mijn paranimf, PhD-partner in crime en lieve vriendin, wat was ik blij dat ik mijn eerste dag als promovenda bij jou op de kamer terecht kwam en dat we onze promotietrajecten vrijwel parallel doorliepen. We waren allebei de vreemde eend tussen de medici en fysici, en dat schiep direct een band. Beiden waren we in onze multidisciplinaire projecten druk met bruggen bouwen en de uitdagingen die hier soms bij komen kijken. Wat fijn om iemand te hebben die in

hetzelfde schuitje zat, en dan ook nog eens zo'n lief en mooi mens als jij. Ik bewonder jouw enorme doorzettingsvermogen en drive om de (academische) wereld voor iedereen toegankelijk te maken. In de afgelopen jaren hebben we vele mooie gesprekken gehad over de grote en kleine dingen in het leven. Je was er altijd voor me en zorgde ervoor dat ik mijn successen niet zomaar voorbijliep. Ik ben enorm blij dat jij mijn paranimf wilde zijn en hoop dat we samen nog vele mooie herinneringen zullen maken.

Fia Cialdella, mijn paranimf, onderzoeks-partner en lieve vriendin, bijna drie jaar geleden begon jij aan jouw promotieonderzoek op de afdeling en wat ben ik daar dankbaar voor. Je was niet alleen een onschatbare aanwinst voor het neuro-team, maar ook tussen ons ontstond al snel een hechte band. Het is maar goed dat we al snel niet meer op dezelfde kamer zaten, want wij kunnen urenlang kletsen over zowel werk als persoonlijke zaken. Jouw kritische instelling komt altijd goed van pas; je stelt me uitdagende vragen en zorgt hiermee er niet alleen mee dat mijn onderzoek beter wordt, maar ook dat ik als persoon groei. Je hebt een enorm groot hart voor de zorg van jouw patiënten. Ik hoop nooit een dokter nodig te hebben, maar als dat toch het geval is, zou ik willen dat jij het bent. Bedankt dat je mijn paranimf wilde zijn en ook tijdens dit laatste traject een immense steun bent.

Lieve kamergenootjes van de Q.02.2.314, **Anita Werensteijn-Honingh**, **Eline Huele** en **Renée Hovenier**, dank voor al jullie gezelligheid op de kamer, de slingers bij verjaardagen en de leuke tekeningen op het whiteboard. Samen slaagden we er altijd in een goede balans te vinden tussen hard werken en even ontspannen. Door jullie was de uitspraak "Promoveren is leuk", die boven onze kamerdeur hing, ook daadwerkelijk waar. **Anita**, jij was er vanaf het allereerste moment van mijn promotietraject en hebt me met jouw rust, luisterend oor en goede adviezen over vele hobbels geholpen. Ik bewonder hoe je jouw privéleven wist te combineren met het werk als onderzoeker, en je hielp me altijd om ook mijn eigen werktijden in de gaten te houden. **Renée**, wat gezellig dat je bij ons op de kamer kwam! Jij bent een attente en lieve collega die nooit een belangrijk moment voor een ander vergeet (waar de vele leuke kaartjes een bewijs van zijn). Bovendien heb ik meermaals mogen genieten van jouw bakkunsten als je weer iets lekkers meebracht naar het werk. **Eline**, jij maakte onze kamer weer compleet. Wat was het fijn om al die schrijffuren met zo'n gezellige en lieve collega door te brengen en onze werkuitdagingen en -overwinningen met elkaar te kunnen delen. Zeker in het laatste halfjaar hadden we een perfect werk-klets ritme en zorgden we ervoor dat we allebei aan het einde van de dag ook weer samen op de fiets naar huis gingen. Dank voor die stok achter de deur.

Arthur van der Boog, ik ontmoette je tijdens de Neuroscience master en later deden we beiden ons promotieonderzoek op dezelfde afdeling. Regelmatig verscheen jouw hoofd om de hoek van mijn deur voor een dropje en een goed gesprek. Ik snap nog steeds niet hoe het je is gelukt om alle ballen van jouw ontelbare studies in de lucht te houden. In de hectiek van jouw huidige baan als ANIOS-neurochirurgie zie ik je met name met een wapperende witte jas door de gangen rennen, maar wie weet dat we in de toekomst wel weer de mooie kans hebben om samen te werken.

Freek Teunissen, Dieuwke Mink van der Molen, Jasmijn Westerhoff en **Tariq Lalmahomed**, lieve buurvrouwen en -mannen, dank voor alle gezelligheid. Ondanks dat we allemaal druk waren, kon ik altijd bij jullie aankloppen voor een praatje of om te sparren over mijn onderzoek. **Maureen Groot-Koerkamp**, al bevond jouw kantoor zich enkele deuren verderop, bij ontmoetingen in de gang was er altijd ruimte om bij te praten over ons onderzoek. En niet te vergeten zijn ook alle andere geweldige mede-PhD'ers en voormalig Qamer-genoten, waaronder **Jikke Rutgers, Floris Reinders, Hilde Smits, Osman Akdag, Anouk de Jong, Maaïke Verweij, Thomas Willigenburg, Robin de Boer, Guus Grimbergen, Hidde Eikelenkamp** en **Katrinus Keijnemans**. Ondanks het vele thuiswerken door de pandemie en mijn verhuizing naar Q-nieuw, was er altijd een plekje op de Qamer voor een koffiemoment of gezellige lunchpauze waarbij uiteenlopende onderwerpen werden besproken, variërend van badkamerschoonmaakfrequenties tot updates uit ieders datingleven. En niet te vergeten zijn natuurlijk het fantastische onderzoekersweekend op Texel en de gezellige borrels in de stad.

Lieve collega's van de neuropsychologie, **Irene Huenges Wajer, Carla Ruis, Mariska Mantione, Josje Kal, Anouk Smits, Suzanne Hartung** en **Dilara Ozturk**, wat fijn om na mijn promotie weer met jullie te mogen samenwerken. Jullie inzet om de medische neuropsychologie op de kaart te zetten, zowel in de zorg als in het onderzoek, is enorm inspirerend en wat ben ik blij dat ik van jullie mag leren. **Anouk**, van mijn begeleider tijdens mijn masterthesis naar collega en co-auteur. Wie had dat gedacht? Hoewel het stroke vs tumor stuk ons beiden soms de neus uit kwam en we meer opgelucht dan blij waren toen het eindelijk gepubliceerd was, heb ik jouw kritische en precieze manier van werken in onze samenwerking enorm gewaardeerd. Lieve **Suzanne**, samen hebben we eindeloos gewerkt aan de CASTOR databases om het vervolgens toch weer helemaal om te gooien, konden we sparren over analyses voor onze manuscripten en gaven we feedback op elkaars presentaties en posters voor congressen. Daarnaast was er altijd ruimte voor zowel de leuke als verdrietige aspecten van het leven. Ik waardeer het enorm om een vriendin te hebben waarmee ik op zoveel niveaus herkenning vind.

Wat een rijkdom om daarnaast nog meer lieve vrienden en familie te hebben die zorgden voor de nodige afleiding tijdens dit traject. Lieve **Wietske** en **Johannes**, soms gaan er weken voorbij zonder dat we elkaar zien, en dan treffen we elkaar plotseling drie keer achter elkaar. Het maakt niet uit; het is altijd gezellig met jullie, of het nu gaat om een lekker etentje, een avondje Drunken Cinema, of gewoon een biertje in de stad. Jullie slagen er altijd in om ervoor te zorgen dat ik mijn gedachten even opzij kan zetten.

Anouck, lieve Nouckie, zonder jou was ik nooit heelhuids door de researchmaster gekomen. Jouw enorme doorzettingsvermogen en de altijd aanwezige glimlach op je gezicht zijn een enorme inspiratie. We hebben samen veel gelachen, soms gehuild en prachtige gesprekken gevoerd. Je was altijd bereid om mooie voors- en tegenslijstjes te maken, en samen met onze mede-stagiaires hebben we vele leuke momenten beleefd. Ondertussen nadert ook jouw promotietraject zijn einde, en ik kan niet wachten om te zien welke prachtige stappen jij hierna gaat zetten.

Lieve **Kalijn** en **Fanny**, studiemaatjes vanaf de allereerste dag in Utrecht, wat hebben wij samen veel uren op de uni doorgebracht om te studeren of gezellig samen te koken in een van onze studentenhuizen. Wat had ik dit moment graag met jullie allebei willen delen. Des te meer besef ik dat Fan helemaal gelijk had met de quote bij haar bureau: "Life isn't about waiting for the storm to pass, it's about learning how to dance in the rain."

Lobke, liefste buuffie, beste vriendin en maatje vanaf het allereerste moment. Tijdens alle belangrijke momenten in mijn leven ben jij erbij geweest en heb je (vaak ook letterlijk) naast me gestaan. Ondanks dat we allebei totaal verschillende dingen doen en jij nu in het prachtige Engeland woont, vinden we altijd weer de weg naar elkaar. Wij kunnen urenlang FaceTimen (dankjewel dat ik jouw vriendin steeds mag lenen, Rory!), waarbij we na het bespreken van alle belangrijke hoogte- en dieptepunten vaak belanden in heerlijke koetjes-en-kalfjes gesprekken waarvan we zelf uiteindelijk niet meer weten hoe we op dat onderwerp zijn gekomen. Ik bewonder jouw doorzettingsvermogen, flexibiliteit en durf. Je staat altijd voor iedereen klaar, weet precies wanneer iemand je nodig heeft en verraste me bijvoorbeeld door op de stoep te staan voor mijn masterdiploma-uitreiking of afgelopen zomer toen ik er even doorheen zat. Bedankt voor onze dierbare vriendschap. **Rory**, even though you made my best friend move across the sea, I am happy she found such a wonderful guy. I'm looking forward to spending many more evenings and weekends together in both England and the Netherlands.

Francisco, our paths crossed during my internship at the RIBS-group, and from there, our friendship continued to grow. Throughout my internship, I would often walk into the office to find a surprise on my desk, whether it was a sweet note wishing me a good morning, a chocolate bar, or my pens artfully arranged in the shape of a heart. Then, you met the incredible **Lieke**, and our friendship grew. Working together at the UMCU meant numerous shared coffees and lunches together discussing the challenges of our PhD, and our friendship quickly expanded outside of the workplace. Over these past few years, we have enjoyed countless dinners, engaged in lengthy discussions, played spirited Mario Kart games, created precious memories during weekends in the Ardennes or Lisbon, and so much more. I am blessed to have you both as integral members of my chosen family, and I couldn't have envisioned navigating these years without you. Your unwavering support, whether it's showing up and just being there, bringing us food, or taking care of our bunnies, has meant the world. Thank-you.

Lieve **Gerda**, ruim dertien jaar geleden leerde ik Jordy kennen, en direct stond jouw deur ook voor mij open. Toen ik nog in Enkhuizen woonde, heb ik vele uren bij jullie op de bank doorgebracht, en was er altijd tijd om even samen een kopje thee te drinken. Lieve **Opa** en **Oma Schuitemaker**, ondanks dat jullie soms geen idee hebben waar ik allemaal druk mee ben, zullen jullie altijd vragen hoe het met me gaat en me op het hart drukken dat ik wel een beetje op mezelf moet letten. Dankjewel dat jullie mijn extra opa en oma zijn. Jullie warmte en zorgzaamheid waardeer ik enorm, en ik koester de momenten die we samen delen.

Lieve **Oma**, ook al ben je er niet meer om het te vieren, jij was altijd mijn grootste supporter en brandde ontelbare kaarsjes voor tentamens, presentaties, of belangrijke afspraken. Ik weet zeker dat er tijdens mijn verdediging ergens daarboven ook een kaarsje zal branden.

Lieve **Irene**, lieve pinguïnpoot, lief letje, wat een voorrecht om iemand nabij te hebben die exact begrijpt wat het betekent om in mijn schoenen te staan en de uitdagingen van een promotietraject te doorgronden. Ik kon altijd bij je terecht voor een kritische blik op mijn figuren of hulp bij het verfijnen van ingewikkelde teksten. Als echte visuele denker heb je meermaals jouw talenten ingezet om mijn figuren nog mooier te maken of ons huis nog slimmer in te richten, en wist je me steeds weer handige, nieuwe tips voor Adobe Illustrator bij te brengen. Ik bewonder jouw veerkracht en vastberadenheid tijdens jouw eigen PhD-traject, wat heeft geleid tot een prachtig proefschrift en een geweldige verdediging. Ik kijk ernaar uit om me op 11 april naast papa en jou aan te sluiten in het rijtje van Dr. van

Grinsven-en. Lieve **Lotte**, zo'n vijf jaar geleden leerde jij Irene kennen en sindsdien maak jij haar ontzettend gelukkig. Ik hoop dat we in jullie mooie huis in Bilthoven nog vele spelletjesavonden kunnen doorbrengen met jullie enorme collectie spelletjes. Dank ook voor het verwelkomen van **Stine** in de harige van Grinsven-familie; haar gekke acties en bijzondere slaaphoudingen maken het altijd weer een feestje om de gezinsapp te openen.

Ongeveer een jaar geleden vroeg iemand me of mijn vader nog steeds een grote rol speelde in mijn leven. Na even nadenken kon ik trots antwoorden dat dit zeker zo was. Lieve **papa**, dankjewel voor wie je was en voor het fijne thuis en alle kansen die jij en mama ons hebben gegeven. Op de ijsbaan wist je me altijd te pushen om nog een rondje te schaatsen, zelfs als ik al helemaal kapot was of geen zin meer had en dit neem ik altijd met me mee. Ook koester ik de herinneringen aan heerlijke zelfgemaakte pasta, mooie muziek, dansen in de woonkamer en lange discussies aan de eettafel, die zeker weten mijn kritische houding en nieuwsgierigheid hebben gevoed. Veertien jaar is en blijft veel te kort, maar wat ben ik immens blij dat ik jouw dochter ben en zoveel van jou als mens heb mogen leren.

Lieve mama, ervaringsdeskundige in het ondersteunen van van-Grinsven-PhD-ers, allerliefste **mamsie**, dankjewel dat jij mijn mama bent. Bedankt voor het warme thuis, waar altijd een plek is om naar terug te keren, niet alleen voor mij maar ook voor Jordy. Onderweg van school naar huis kon ik al hele gesprekken met jou voeren over de dagelijkse stand van zaken in mijn klas. Later belde ik je direct op na mijn allereerste college van Martine om te vertellen dat ik iets had gevonden waar ik echt heel erg blij van werd. Waar het ook over gaat, jij staat altijd klaar met een luisterend oor, kritische vragen en advies. Dankjewel voor alles. Zonder jouw steun, knuffels en heerlijke restjes, waren deze jaren een stuk moeilijker geweest. Ook al worden we allebei ouder en veranderen onze rollen langzaam, jij bent en blijft altijd mijn mama en ik zou het niet anders willen. Jij bent mijn voorbeeld van een sterke, onafhankelijke, zorgzame vrouw. Hoe uit het veld geslagen ons gezin 14 jaar geleden ook was en wat we onderweg ook nog verder zijn tegengekomen, het is ons met z'n drieën gelukt bij elkaar te blijven, en daar ben ik ontzettend trots op. Onze allerbeste beslissing ooit als gezin was onze allerliefste harige vriendje, **Juno**. Ondertussen heeft hij een witte snoet gekregen, maar in al deze jaren heeft hij voor zoveel liefde, warmte en afleiding gezorgd.

Lieve **Jordy**, mijn maatje, beste vriend en rotsvaste thuis. Wie had dat dertien jaar geleden gedacht dat wij hier nog steeds samen zouden staan? Jij bent mijn thuis en veilige haven. Bij jou kom ik tot rust en mag ik 100% mezelf zijn. Samen doorstaan

we de rollercoaster van het leven en proberen we van iedere dag iets moois te maken. Wat ben ik dankbaar voor de mooie avonturen die we samen mogen beleven en dat jij mij altijd de zekerheid en moed geeft om nieuwe dingen uit te proberen. Jouw mentaliteit “als het niet lukt, dan bedenken we wel weer een oplossing”, maakt dat alles kan en niets te gek is. Bovendien tover je altijd wel weer een lach op mijn gezicht met jouw humor, flauwe grappen en eeuwige plagerijtjes. Dankjewel voor jouw engelengeduld, de dansjes in de keuken, en de ontelbare kopjes thee die je me hebt gebracht. Jij en ik, voor altijd. En natuurlijk kan ik dan als laatste onze eigen harige vriendjes niet vergeten, **Reyes** en **Yosie**, met jullie lieve snoetjes en gekke capriolen hebben jullie vaak een lach op mijn gezicht getoverd.

Hoewel een PhD soms eenzaam kan voelen, blijkt maar weer uit dit dankwoord dat je onderzoek nooit alleen doet. Het is het samenkomen van verschillende mensen, met verschillende kennis, verschillende invalshoeken en verschillende achtergronden. En juist dat is wat onderzoek doen zo mooi maakt. Bedankt aan iedereen die op zijn of haar manier een steentje heeft bijgedragen aan mijn onderzoek.

Eva van Grinsven
December 2023
Utrecht

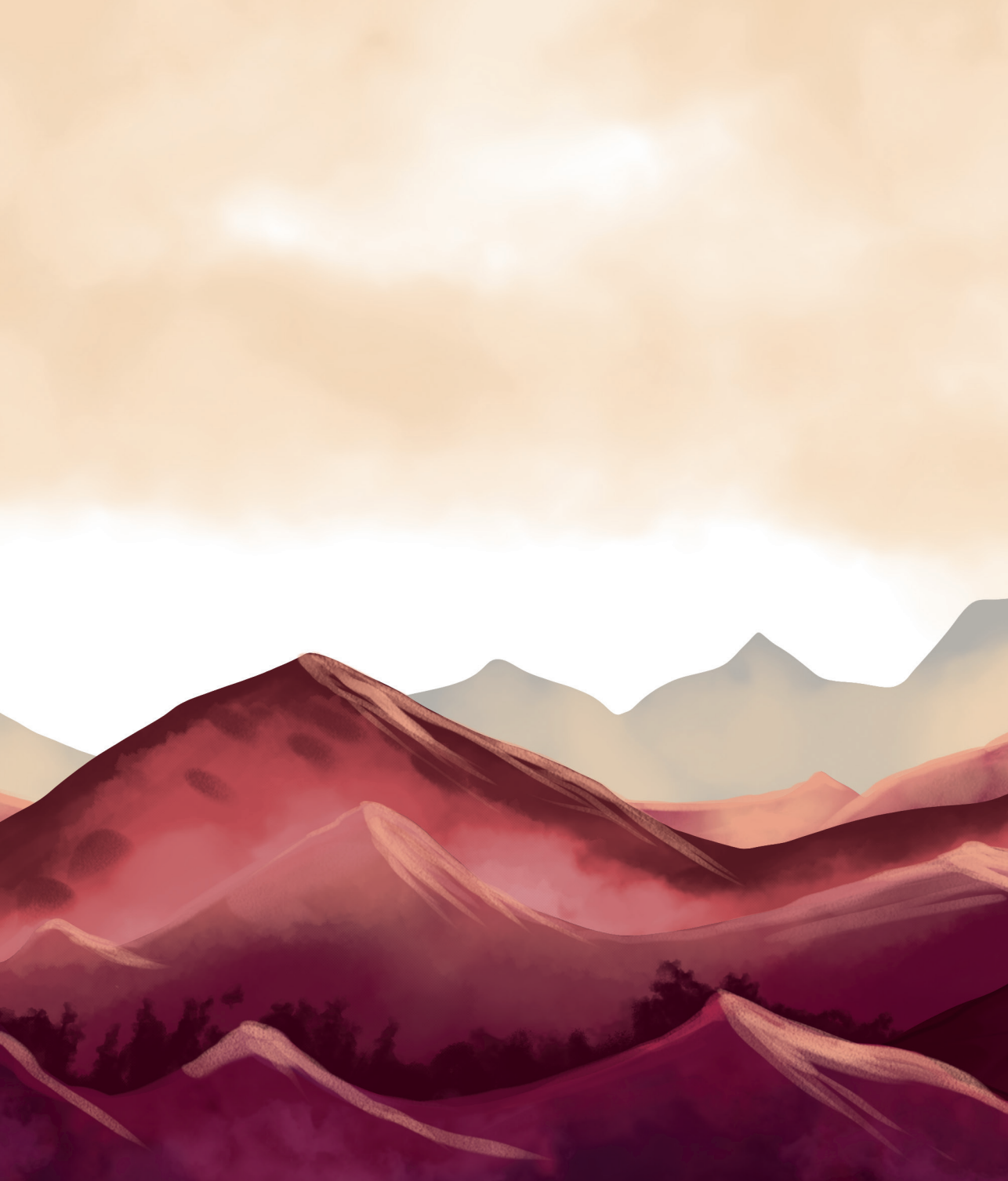
ABOUT THE AUTHOR

Eva Elisabeth van Grinsven was born in May 1994 Enkhuizen, the Netherlands. Growing up in a loving family alongside her father, mother, and sister, Eva's early experiences included a year in Santa Cruz (USA) at the age of three, during which life-long friendships were forged. The remainder of her childhood unfolded in Enkhuizen where she graduated high school in 2012. After this she embarked on a half-year adventure in Peru with her best friend before pursuing her Bachelor's in Psychology at Utrecht University. Captivated by the intricate interplay between the brain and behavior, she specialized in neuropsychology with a minor in cognition, complemented by an enrollment in the interdisciplinary honors program of the Faculty of Social Sciences. Graduating cum laude, she pursued a dual master's in Neuropsychology and researchmaster Neuroscience & Cognition.



After graduating cum laude from both master programs, Eva commenced with her PhD thesis at the University Medical Center Utrecht (UMCU) in October 2018 under the supervision of a multidisciplinary team. Throughout her doctoral research, Eva spearheaded the APRICOT-study, a prospective exploration into short- and long-term cognitive and brain changes following brain radiotherapy for brain metastases. Furthermore, she actively contributed to the COIMBRA-study, an observational cohort study exploring the quality of life among patients with brain metastases. Collaboratively with her fellow PhD candidate, she introduced both a cognitive and caregiver component to enhance the depth of the COIMBRA research project. Concurrently, Eva supervised numerous students from the master Neuropsychology through their thesis.

Eva's commitment to bridge research, clinical practice, and education, lead to the combined role of neuropsychologist at the UMCU and junior teacher for the Neuropsychology Master at the University Utrecht from June 2023. Following a 7-week adventure in Ecuador and a relocation to Amersfoort, Eva continued her journey in February 2024, concurrently fulfilling roles as a postdoc and neuropsychologist at the Department of Neurology and Neurosurgery at the UMCU, along with teaching responsibilities at the University Utrecht.



UMC Utrecht



Universiteit Utrecht

ISBN 978-94-6483-766-7